Keratin Adsorbent Material for Chemical Protective Clothing

Ross Ritchie Ward

Submitted in accordance with the requirements for the degree of
Doctor of Philosophy

The University of Leeds

School of Design

September 2017

The candidate confirms that the work submitted is his own and that appropriate credit has been given where reference has been made to the work of others.

Acknowledgements

Abstract

Wool is potentially a valuable adsorbent that has been used for the depletion of air-borne gas molecules. The aim of the research is to modify the complex hierarchical structure of wool fibres to form a reticulated internal porous structure within the fibre in order to ultimately enhance the adsorption capacity of wool and/or its composite fibres.

In this study, the effects of several chemical treatments and their combinations on the formation of porous microstructure within wool fibres are studied. The techniques studied include oxidation (Formic acid treatment), oxidation/swelling (Ozone treatment in urea hydrogen peroxide solution) and reduction treatments (Sodium hydroxide treatments) and their combinations. Mesopore and macropore formations were evident after wool fibres and fabrics were treated with individual and consecutive chemical treatments. However, the pore formations after these chemical treatments did not produce materials with specific surface areas comparable to activated carbon. Despite this shortcoming there was evidence of both accessible and inaccessible pore formations within wool fibres.

Additional physical selective degradation of raw and chemically modified wool fibres by using both electron beam irradiation using SEM and low pressure oxygen plasma irradiation treatments were identified to expand accessible pores or expose inaccessible pores formed within wool fibres after chemical treatment. Porous wool fibres with reticulated pore structures were evident after exposing the chemical pre-treated wool fibres to low pressure plasmas.

To enhance the adsorption capacity of the porous wool fibres formed, novel wool-aerogel composite wool fibres have been developed. The resultant composite fibres were capable of adsorbing cyclohexane with up to 2.5 w/w% uptake. Also, similar uptakes were evident after testing without any sample pre-heating process. This demonstrates that wool-aerogel composite fabrics are capable of adsorbing VOCs at conditions similar to environments present during the use of CPC.

Table of Contents

List of Figures

List of Tables

List of Abbreviations

AC	Activated carbon
CF	Activated carbon fibres
ACCs	Activated carbon cloths
Ach	Acetylcholine
AChE	Acetyl cholinesterase
AD	Apparent density
Au	Gold
B	British black colour wool fibres
BET	Brunauer–Emmett–Teller
C	British cross wool fibres
CC	Carboxymethyl cellulose
C_6H_{12}	Cyclohexane
$CHCL_3$	Chloroform
CMC	Cell membrane complex
CMS	Carboxy Methyl Starch
CNCl	Cyanogen chloride
CO_2	Carbon dioxide
CPC	Chemical protective clothing
CWAs	Chemical warfare agents
CX	Phosgene oxime
DFT	Density functional theory
DMF	Dimethylformamide
DSTL	Defence Science and Technology Laboratory
DVS	Dynamic vapour sorption
EDX	Energy-dispersive X-ray spectroscopy
FA	Formic acid
FTIR	Fourier transform infrared spectra
GA	Tabun
GB	Sarin
GCMC	Grand canonical Monte Carlo simulations (page 18)
GD	Soman
H	British hill wool fibres
H_2O	Water
HCN	Hydrogen cyanide
HD	Sulfur mustard
HN	Nitrogen mustard
IUPAC	International Union of Pure and Applied Chemistry
JSLIST	Joint Service Lightweight Integrated Suit Technology
K_2CO_3	Potassium carbonate
L	British lustre wool fibres
LEMAS	Leeds Electron Microscopy and Spectroscopy Centre

M	British mountain wool fibres
MeOH	Methanol
MFH	British medium fine hill wool fibres
MFL	British medium fine lowland wool fibres
MOFs	Metal organic frameworks
MTMS	Methyltrimethoxysilane
MWov	Australian worsted woven merino wool fabrics
NaOH	Sodium hydroxide
NBC	Nuclear, biological and chemical
NRBC	Nuclear, radiological, biological and chemical
OP	Organophosphate
PA	Polyacrylate
PA66	Nylon 66
PET	Polyethylene terephthalate
PFIB	Perfluoroisobutylene
PIM	Polymers of intrinsic microporosity
Pt	Platinum
PTFE	Polytetrafluoroethylene
PVC	Polyvinyl alcohol
RESS	Rapid extraction of supercritical solutions
RT	Room temperature
SCCO$_2$	Supercritical carbon dioxide
SEM	Scanning electron microscope
SPMs	Selective permeable materials
TD	True density
TFTPN	2,3,5,6-tetrafluoroterephthalonitrile
THF	Tetrahydrofuran
TTSBI	5,5',6,6'-tetrahydroxy-3,3,3',3'-tetramethylspirobisindane
UHP	Urea hydrogen peroxide
UK	United Kingdom
VOCs	Volatile organic compounds
VX	O-ethyl S-(2-diisopropylaminoethyl) methylphosphonothioate
WWI	World War I
WWII	World War II

Chapter 1 Introduction

1.1 Background

Concerns over the use of chemical weapons have prompted the introduction of programs and countermeasures against such agents (Cameron and Clegg, 2010). Chemical protective clothing (CPC) is widely used to protect personnel from various chemical hazards on the battlefield, during chemical industry production or accidents, riots and counter terrorism activities. These applications often require intense physical activities. Therefore, in addition to the primary protection function, the CPC when worn for long time durations may be required to manage both the thermo-regulation of human homeostasis and the perspiration generated from the body so that the thermo-physiological comfort of the wearer is maintained. Thermal strain can be caused by a combination of heavy garments, poor breathability and high temperature environments. Insufficient protection or high levels of thermal strain caused by the CPC can be dangerous to the wearer and potentially fatal.

In addition to moisture management and natural flame resistant properties, keratin wool fibres have been proven to be effective sorbents of sulphuric acid, sodium hydroxide, hydrochloride acids within early CPC (Metha, 1980) and have the capacity to adsorb volatile organic compounds (VOCs), such as formaldehyde (Sou et al., 2001), nitrogen dioxide (Spicer et al., 1989; Causer, 1993) and sulphur dioxide (Walsh et al., 1977). It contains reactive groups, that provide potential binding sites for chemical and biological agents, including carboxylate, amine, amide, disulphide and thiol functional groups, that are proven binding sites for metal ions and VOCs (Mao, 2013). Consequently, the wool fibres have the potential to be used as a type of adsorbent material in chemical protective clothing.

The proposed adsorbent material will be developed with the objective of being used in air-permeable CPC. Current permeable CPC garments (Wilusz, 2008; JSLIST Military Specification, 2002) were developed to provide better clothing thermo-physiological properties and extending wearing durations than impermeable CPC, which form a continuous barrier between the human body and the external environment. Consequently, impermeable CPC provides an advanced protection capability, but prevent the evaporation of perspiration released from the body, which restricts the wearing durations due to additional thermal stress. Generally, permeable CPC comprises of an air-permeable liquid repellent textile outer layer and a permeable adsorbent layer to adsorb hazardous gases, additional protective layers may also be included. Most of the weight and volume of the CPCs are from the large amount of materials being used in the adsorbent layer. Activated carbon (AC) is the only adsorbent materials used in existing protective clothing and it has great capacity for adsorbing chemical liquids and vapours (Abbott, 1962) in chemical protective clothing (Boucher et al., 1970). The unique porous micro-structure with large surface areas up to 2500 $m^2.g^{-1}$, pore volumes up to 1 $cm^3.g^{-1}$ and the combination of open or accessible micropores (less than 2 nm) and mesopores (2 to 50 nm) makes the carbon an effective adsorbent material. To increase the thermal comfort properties of CPC, AC is often combined with other porous fibrous materials to form an air-permeable inter-liner. However, these shell materials incorporating with AC materials often have low levels of air permeability and lack of thermal and moisture management properties. Therefore, if the modified wool fibres exhibit adsorbent properties as well as have sufficient strength, moisture management properties, this material could compromise part of the shell textile, reducing or even removing altogether, the need for activated carbon materials. Additional disadvantages associated with using AC in CPC are the absence of moisture management properties and the high volumetric density of AC (1800-2000 $kg.m^{-3}$), which makes the garments heavy. Also, the adsorption capacities of carbon materials degrade with time, especially in humid environments, and so the garments

have a short shelf-life once removed from the packaging. This factor is important when considering logistical efficiencies and costs.

The development of adsorbent fibres, particularly by trying to convert the bulk of the fibre itself, for protective clothing is a completely new field and desirable in industries. So, the approach in this research is to consider multiple options including introducing micro-, meso- and macro-pores in the wool and the incorporation of meso- and microporous additives to lay the foundations for future work.

Adsorbent wool could be used either by itself or in conjunction with other fibres to produce woven, nonwoven or knitted textiles that could be used to make a chemically protective garment. Incorporating these materials into CPC could improve moisture management properties. Also, to reduce weight, these wool fibres should also retain strength so that the adsorbent material is not in addition to CPC structural materials, but is the structural material or part of it. In terms of adsorption capability, the wool may not need to be as effective as activated carbon garment. Truong, Q and Wilusz (2006) reported that a 'lightweight' garment with lower levels of protection is a useful equipment in militarily.

Various technical routes of chemical and physical treatments have been investigated, as well as, the incorporation of micro-porous materials inside macropores formed within the keratin wool fibres. Also, characterisation techniques used for porous materials have been adapted to quantify and differentiate between pores formed within resultant wool fibres.

1.2 Aims and research scope

This project aims to develop a novel keratin wool adsorbent material by introducing micro-, meso- and macroporosity to wool fibres by selectively degrading some components of complex hierarchical morphology in wool. Chemical and physical modification techniques will be considered, as well as, the incorporation of nanoporous materials into the porous wool fibres formed.

Chapter 2 Literature Review

The purpose of the literature review is to establish both the theoretical framework and relevant research in the modification of wool fibres to form reticulated pore structures and explore the methods suitable for the characterisation and quantification of the changes of the porous structure of resultant wool fibres.

Furthermore, principles and mechanisms associated with physisorption, and chemical and physical modification techniques to enhance the adsorption capacity of keratin wool fibres are covered within this literature review.

2.1 Key research topics that define the framework of the study

2.1.1 Chemical warfare agents and other dangerous chemicals

Chlorine gas was first used in chemical warfare in World War I (WWI), due to its wide-spread industrial production in combination with its volatility and toxicity. This prompted the development of first-generation chemical agents became a major focus, these included the vesicant sulfur mustard, the blood agents hydrogen cyanide and cyanogen chloride and choking agents phosgene and diphosgene (Karasik, 2002; Talbot et al., 2008). Since then the threat of chemical warfare agents to military, civilians and industrial personnel has continued to evolve (Szinicz, 2005).

CWA stockpiles developed during WWI and World War II (WWII) are still being de-militarised in accordance with the Chemical Weapons Convention of 1993 (OPCW, 1993). More recently, concerns over the use of chemical weapons have prompted discussions over the need for the introduction of programs and countermeasures against such agents (Cameron and Clegg, 2010).

CWAs have direct toxic effects to organisms, causing incapacitation or death. They are defined as natural or synthesised chemical substances and are classified according to

their effect on the organisms; including, nerve, blister, blood, choking, vomiting, incapacitating and tear agents (Truong, Q and Wilusz, 2005). According to the Centres of Disease Control and Prevention (UK), CPC incorporating adsorbent carbon materials are developed to deal with CWAs in gaseous or liquid state (CDC, 2014), although Truong, Q and Wilusz (2005) identified additional solid state CWAs.

Table 2.1 summarises some of the chemical hazards posed on both military and industrial personnel, including their wide range of removal chemistries.

Table 2.1 - Target chemical groups/ functionalities (DeCoste and Peterson, 2014)**. Only nerve and blister agents are relevant for dermal protection and the remaining groups are not classed as CWA**

Group	Examples	Chemistry/ removal mechanism required
Nerve/ blister agents	GA, GB, GD, VX, HD	Physical adsorption; nucleophilic attack
Acidic/ acid-forming gases	Chlorine, hydrogen halides, phosgene	Nucleophilic attack; acid-base reactions
Basic/ base-forming gases	Ammonia, amines, hydrazines	Oxidation; acid-base reactions
Oxidised gases	Sulfur dioxide, nitric oxide, nitrogen dioxide	Reduction; further oxidation
Reduced gases	Arsine, phosphine, hydrogen sulphide	Oxidation
Aldehydes	Formaldehyde, acrolein	Oxidation; polymerisation
Simple organics	Cyclohexane, alkyl halides	Adsorption; nucleophilic attack

Nerve agents affect the transmission of nerve impulses in the nervous system. All nerve agents belong chemically to the group of organophosphate (OP) compounds, which are highly toxic and generally inexpensive to synthesise. They have rapid effects both when absorbed through the skin and via respiration and can cause death within minutes depending on the dose. G-agents such as Tabun (GA), Sarin (GB) and Soman (GD) were developed by Germany during WWII; however, these agents were never used despite the extensive stockpiles (López-Muñoz et al., 2008). V-agents were developed post WWII, these are sulfur containing OP compounds. These compounds are more toxic and stable, but less volatile and water soluble than G-agents. Also, they

are active in an environment for up to two weeks (Ganesan et al., 2010). The chemical structure of GA, GB, GD and VX are illustrated within Figure 2.1.

O-Ethyl N,N dimethyl-phosphoramidocyanate
Tabun (GA)

Isopropyl methylphosphonofluoridate
Sarin (GB)

O-1,1,2-trimethylpropylmethyl
phosphonofluoridate
Soman (GD)

O-ethyl S-diisopropylaminoethyl methylphosphonothiolate (VX)
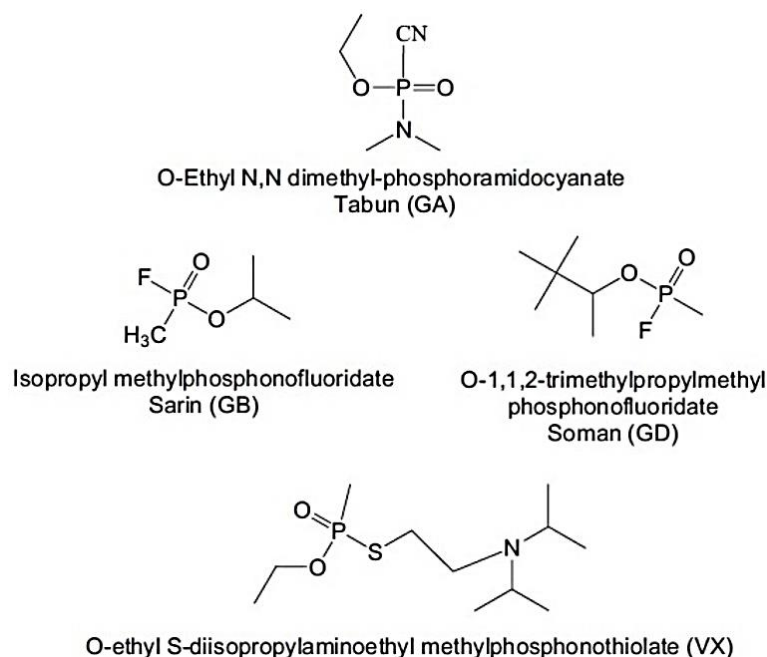
Figure 2.1 - Chemical structure of nerve agents (Hoenig, 2007)

These agents inhibit the enzyme acetyl cholinesterase (AChE), which is responsible for hydrolysing the neurotransmitter acetylcholine (ACh). If ACh is allowed to accumulate then over excitation or convulsions can occur, eventually causing death (Somani, 1992; Bajgar, J. et al., 2009; Bajgar, J. , 2004; Bajgar, J., 2005).

Blister agents, such as sulfur mustard (HD), nitrogen mustard (HN) and lewisite are some of the most common CWA. They cause large skin blisters which resemble severe burns, cause eye irritation, respiratory tract and eventually cell poison. Mustard agents are extremely toxic to dividing cells as they are lipophilic and imitate the effects of radiation (radiomimetic). Sulfur mustard is converted into highly reactive sulphonium ion (see Figure 2.2) after passing through the cellular membrane (Ganesan et al., 2010) and is known to irreversibly alkylate DNA, RNA and proteins (Shakarjian et al., 2010).
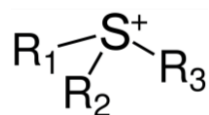
Figure 2.2 - Sulfonium ion features three organic substituents attached to sulfur

Plowman et al. (2003) conducted a study to investigate the effect of alkylation on the separation of wool keratin proteins using iodoacetamide (1 M, pH 8) for periods ranging from 10 min to 48 h. This study determined that high proportions (70-95%) of the cysteines in the keratin proteins were alkylated within the first 10 min. Also, non-cysteine alkylation was evident within the proteins containing high concentrations of glycine-tyrosine. Therefore, it is possible the mustard agents, once converted into a sulphonium ion, could alkylate with both the cysteine and noncysteine residues within the keratin wool fibres.

Blood agents are poisons that effectively cause the body to suffocate and are distributed via the blood and enter the body via inhalation (OPCW, 2014). Hydrogen cyanide (HCN) and cyanogen chloride (CNCl) are examples of blood agents. Cyanide has an affinity for iron in the ferric (Fe^{+3}) state and reacts with trivalent iron of cytochrome oxidase, which is an end-chain enzyme of cellular respiration. This complex impairs the utilisation of oxygen in the tissues, leading to respiratory failure and eventually death (Raza and Jaiswal, 1994; Ganesan et al., 2010).

Choking agents were produced in large quantities and used extensively during WWI. They are capable of causing damage to the respiratory tract, which contains the nose, throat and the lungs. These agents are capable of swelling membranes within the lungs, which cause the lungs to fill with excess liquid. The liquid inhibits the exchange of oxygen within the lungs, causing the unprotected individuals to 'choke'. Fatalities of this type are called 'dry-land drownings' (Compton, 1987). Chlorine, phosgene and diphosgene are examples of choking agents. Chlorine and phosgene are acid forming gases (DeCoste and Peterson, 2014), which are used in many chemical industrial processes. Consequently, due to their accessibility they are hard to control and can be

obtained and adapted to form devastating CWAs (Croddy et al., 2002). Poisoning by phosgene is mainly attributed to acylation of thiol (–SH), amino (–NH$_2$), and hydroxyl (–OH) groups of biological macromolecules, including enzymes, and increased permeability of the alveolar mucous membrane. These toxic effects are responsible for pulmonary edema, which causes anoxia and eventually death (Buckling, 1943; Cucinell, 1974; Glass et al., 1971). Thiol, amino and hydroxyl functional groups are present within cysteines residues (see Figure 2.3), which are known to exist within keratin wool fibres (Kozlowski, 2012).
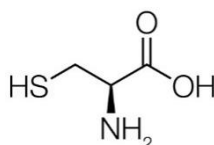
Figure 2.3 - Cysteine molecule

Due to the extensive range of CWA, there is an extensive need for highly efficient materials capable of protecting personnel.

2.1.2 Structure of permeable chemical protective clothing

In addition to the primary protection function, modern chemical protective clothing (CPC) require thermal and moisture management properties to regulate thermo-physiological comfort, especially when various intense activities are carried out. Therefore, the keratin wool adsorbent material to be developed in this project will be intended to be integrated into permeable CPC.

Impermeable CPC has thermo-physiological limitations in terms of thermal comfort, which impedes the wearing duration, thus air-permeable CPC is necessary for many purposes and studied in this project. Impermeable CPC, such as Tychem (DuPont, 2014), butyl, halogenated butyl rubber and neoprene (Wilusz, 1996) provide superior protection against CWAs compared to the permeable materials discussed previously. However, these materials impede the transition of heat and water vapour caused by homeostasis. This eventually leads to thermal discomfort and significantly increases

the chances of heat stress. Consequently, these materials and garments are only suitable for wearing for shorter periods of time (30 to 120 min) and depend upon the activity level of the user. Many impermeable CPC systems incorporate temperature regulating devices to compensate for the materials inability to allow moisture permeation (Truong, Q and Wilusz, 2005).

Permeable CPC usually consists of an external textile layer treated with liquid repellents that, along with additional protective layers that are for construction and comfort purposes, enclose a permeable adsorbent inter-liner for adsorbing or containing hazardous chemicals or vapours. There are four types of CPC (Truong, Q and Wilusz, 2005) based on the barrier materials used, which includes permeable, semi-permeable, impermeable and selective permeable materials (SPMs). Both the materials used and their functionalities in the four types of CPC are compared in Figure 2.4. Mark IVa NBC Suit (UK), Paul Boye's NRBC Protective Suit (France) and Joint Service Lightweight Integrated Suit Technology (JSLIST) Overgarment (USA) (JSLIST Military Specification, 2002) are all examples of permeable CPC currently used by international military forces, designed to enable soldiers to wear them for up to 24 hours.
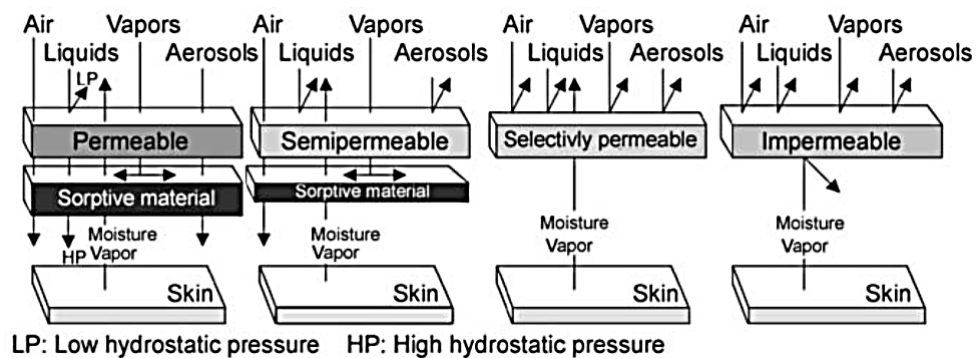
Figure 2.4 - Permeable, semi-permeable, impermeable and selective permeable materials and their capabilities for CPC (Truong, Q and Wilusz, 2005)

Truong, Q. and Rivin (1996) and Ho and Sircar (1992) describe semi-permeable materials as either porous or solution-diffusion materials. Generally, the pore sizes

within these materials enable the level of permeability or what is able to permeate the material.

Larger pore sizes may allow convection flow of air, aerosols and vapours; whereas materials containing smaller pores may support preferential diffusion of gas molecules through their pores on the basis on their physical size. Throughout this study, the former is described as air-permeable membranes systems, whereas the later description is referred to as either semi-permeable or selectively permeable systems.

Nonporous or monolithic membranes relate to solution-diffusion materials that follow Fickian permeation. These materials allow gases to dissolve into and travel through the membrane, before being desorbed on the other side. Parameters associated with this theory include concentration gradient, time and membrane thickness (Truong, Q and Wilusz, 2005).

SPMs used in CPC are non-porous and combine the properties of impermeable and semi-permeable materials. They allow the selective permeation of moisture vapour from the body to escape through the garment layers. Unlike impermeable and semi-permeable clothing systems, SPMs do not require sorption layers such as activated carbon, which can be heavy and restrict movement. However, occasionally activated carbon layers are positioned at the garment interfaces for extra protection and to adsorb any compounds present within that passage. The protection mechanism relies upon the selective diffusion of molecules and compounds through the SPM layer, while restricting the passage of CWAs in liquid, vapour or aerosol form (Ramkumar et al., 2008). Figure 2.5 depicts the SPM material concept, developed for military applications, gas separation within the chemical industry, medical filtration and water purification (Koros and Fleming, 1993).
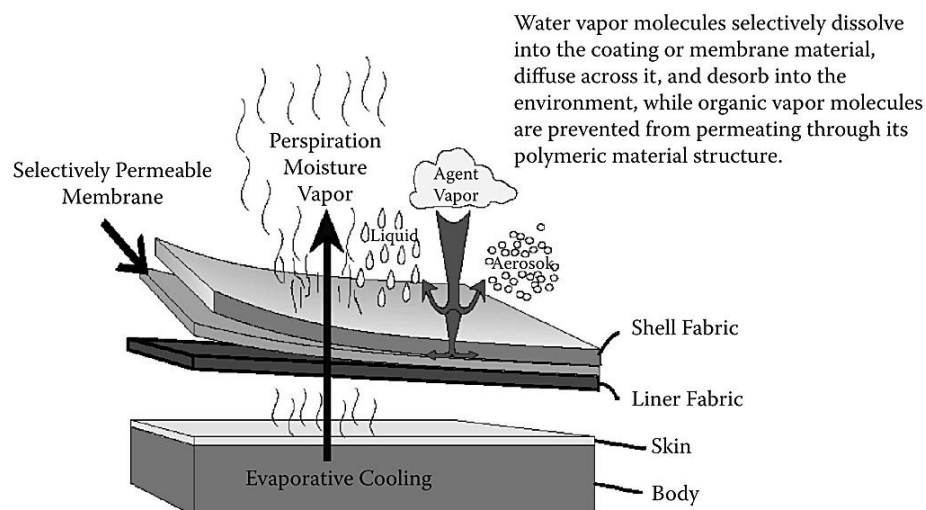
Figure 2.5 - The concept of SPMs (Wilusz, 2008)

Desorption of gas within SPMs depends upon exposure time, thickness of the garment and, according to Fick's Law, the concentration gradient of the CWA. Also, far less water vapour can be transported by a membrane (SPM and semi-permeable as described by Wilusz (2008), (see Figure 2.4) than is enabled by having an air-permeable system, which has a large impact on the physiological burden.

Recent and current research has focused on functionalising SPM materials with agent specific catalysts , anti-microbial finishes and self-detoxifying capabilities (Truong, Q and Wilusz, 2006; Wilusz, 2007; Lamprou et al., 2010; A. Brewer et al., 2007; Stachewicz et al., 2012; Yildiz et al., 2015; Brewer et al., 2004)

2.1.3 Adsorption and adsorsorptive materials

Despite often being confused, the terms adsorption and absorption are two very two different phenomenon. Adsorption is described by International Union of Pure and Applied Chemistry (IUPAC) as "*an increase in the concentration of a dissolved substance at the interface of a condensed and a liquid phase due to the operation of surface forces*" (IUPAC, 1997); whereas, absorption is described as "*the take up of a gas by a solid or liquid, or the take up of a liquid by a solid. Absorption differs from adsorption in that the absorbed substance permeates the bulk of the absorbing*

12

substance" (Rennie, 2016). The term absorption is used when molecules of the adsorptive penetrate the surface and enter the structure of the bulk solid. However, the term sorption is used when it is necessary or difficult to differentiate between adsorption and absorption. The main parameters that promote adsorption and absorption are surface area and volume, respectively. Desorption is the term used to describe the opposite effect of adsorption and is the process in which the amount of adsorbed material decreases (Klobes et al., 2006).

Adsorption has been defined as the interaction and attraction of components, such as, ions, atoms and molecules to a solid interface (Gregg and Sing, 1982). The absorbing phase is called the absorbent while the accumulating material is called the adsorbate (Ruthven, 1984). Adsorption is a consequence of intermolecular surface energy. Incomplete binding of surface atoms attracts gases, vapour and liquids to satisfy the imbalance of atomic forces (Micromeritics, 2014a).

As early as the late 18th century, Fontana (1777) documented that calcinated charcoal had the capability of adsorbing several times its own volume of various gases. However, it was not until the next century that exposed surface area (de Saussure, 1982) and the porous morphology of materials (Mitscherich, 1843) was documented as a characteristic of adsorption efficiency. Silica gel, zeolites, activated alumina, activated carbon, activated carbon fibres, carbon molecular sieves, metal organic frameworks (MOFs), and polymers of intrinsic microporosity are examples of materials that have been investigated as adsorptive materials within CPC due to their unique porous structures and high surface areas.

Keratin wool fibres have been proven to be effective sorbents of sulphuric acid, sodium hydroxide, hydrochloride acids within early CPC (Metha, 1980) and have demonstrated sorption capacity for VOCs, such as formaldehyde (Sou et al., 2001), nitrogen dioxide (Spicer et al., 1989; Causer, 1993) and sulphur dioxide (Walsh et al., 1977). Keratin has a complex physical and chemical structure that supports an attractive combination of properties and performance attributes. Keratin fibres contain reactive groups, that

provide potential binding sites for chemical and biological agents, including carboxylate, amine, amide, disulphide and thiol functional groups, that are proven binding sites for metal ions and volatile organic compounds (VOCs) (Mao, 2013). Consequently, if porous structures are introduced to these fibres they may have the potential to be used as a type of adsorbent material in chemical protective clothing. Therefore, technical routes will be investigated to modify the wool keratin fibres to open the pore structures in the fibre surface to maximise the adsorption capacities to targeted chemical agents.

2.1.3.1 Mechanisms of adsorptions

To improve the adsorption capability of wool keratin fibres it is important to understand the principles associated with adsorbent materials. Adsorption occurs when a foreign substance accumulates at an interface or interfacial region of a material. Physisorption and chemisorption are two processes associated with adsorption.

2.1.3.1.1 Physical adsorption

Physical adsorption (or physisorption) is the molecular adhesion of matter in a gaseous/fluid phase to a solid interface, caused by van der Waals forces. Foreign adsorbate molecules are physically attracted to the adsorbent surface by molecular electronic fields. The matter accumulates on the solid surface, forming a thin layer. The transfer of adsorbate molecules from a gaseous/fluid phase onto a solid surface is a reversible process and adsorption equilibrium is achieved when the rate of these processes are equal (Johnson et al., 1999).

2.1.3.1.2 Chemical adsorption

Unlike physisorption, chemisorption changes the electronic orbital states of the interacting atoms and significant chemical bonds are formed at the interface or in the interfacial region (Klobes et al., 2006).

2.1.3.2 **Adsorption isotherm**

The adsorption process or the adsorption capability of a material is often described by an adsorption isotherm, which is a graph expressing the amount of adsorbate adsorbed onto the surface of an adsorbent at a constant temperature. When an adsorbent is exposed to a gas or vapour in a closed space at a definite partial pressure, the adsorbent begins to adsorb the adsorbate. Standard systems usually maintain a constant partial pressure and calculate the amount of mass adsorbed; however, there are some more complex systems that calculate the pressure within the closed space, which decreases as the mass of the adsorbate begins to increase.

After a time the mass of the adsorbate ceases to increase and the pressure becomes constant. Therefore, if n is the quantity of gas adsorbed expressed in moles per gram of solid then n is a function of the pressure (p), temperature (T), and solid (see Equation (1)). This is because the quantity of gas adsorbed by the solid is proportional to the mass of the sample. Also, the quantity of gas adsorbed by the solid depends upon the temperature, the pressure of the gas and the nature of both the gas and the solid (Gregg and Sing, 1982). Also, it is worth noting that this measurement is a thermodynamic and not kinetic.

$$n = f(p, T, gas, solid) \qquad (1)$$

If the temperature, the type of gas and solid are maintained then Equation (1) can be expressed as:

$$n = f(p)_{T, gas, solid} \qquad (2)$$

Furthermore, if the temperature is below the critical temperature, the Equation can be expressed as:

$$n = f\left(\frac{p}{p_0}\right)_{T, gas, solid} \qquad (3)$$

with p^0 being the saturation vapour pressure of the adsorbate.

By applying Equations (2) and (3), the amount of gas adsorbed can be calculated and expressed as an adsorption isotherm.

The classification of standard physisorption isotherms, according to the International Union of Pure and Applied Chemistry (IUPAC) are detailed within Figure 2.6 (SING et al., 1985) and the various isotherm descriptions are detailed below (BSISO15901-2, 2006):

- Type I - indicates the solid is micro-porous. Micro-pore filling is characterised by the rapid increase in the amount of gas adsorbed over the low relative pressure range. Once these pores are filled and no further adsorption takes place the isotherm plateaus. Examples of micro-porous materials include activated carbons and molecular sieve zeolites.

- Type II - indicates the solid is non-porous or macro-porous.

- Type III - indicates the material is a non-porous solid. These isotherms are relatively uncommon and occur when weak gas-solid interactions occur on non-porous or macro-porous solids.

- Type IV - indicates the solid is meso-porous. A hysteresis loop is observed and the adsorption portion of the isotherm is not the same as the desorption portion of the isotherm. Also, a plateau region is observed at higher p/p_0 values, which occasionally concludes with a final upward turn of the isotherm.

- Type V – These isotherms are relatively uncommon and result from weak gas-solid interactions on microporous and mesoporous solids. The isotherm point of inflection is at higher relative pressures.

- Type VI – These isotherms are the result of sequential multilayer adsorption of uniform non-porous surfaces and are characterised by a step-like trend.
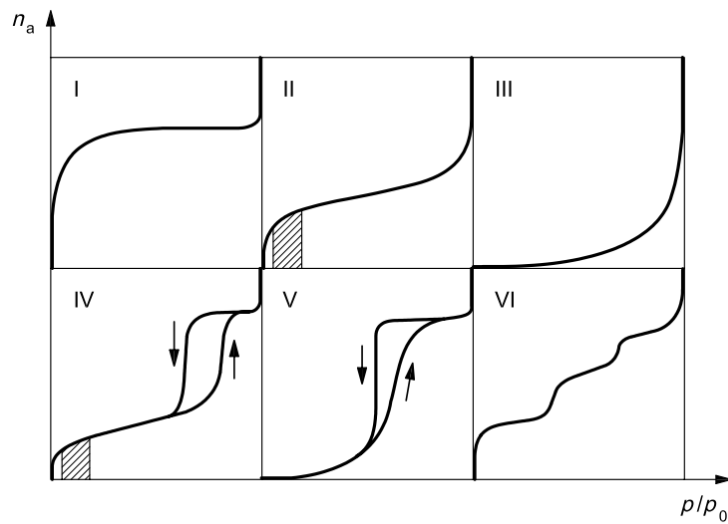
Figure 2.6 - Types of adsorption isotherms (*BS ISO 9277*, 2010)

2.1.3.3 **Porosity and specific surface area**

The area of a solid surface per unit mass of a material is described as the "specific surface area" (Klobes et al., 2006). The distinction between "surface area" and "specific surface area" is important as the latter is determined by the accessible area of the solid surface per unit mass of material, which in practice is often measured by the experimental method employed. The validity of the method is often dependant on the experimental conditions, the size of the probe, for example the molecular size of the adsorbate gas or the wavelength of radiation, and assumptions used in model.

Furthermore, the shapes of pores are often irregular and variable, which is an additional complication for the characterisation of porous materials. Klobes et al. (2006) categorised pores types as described in Figure 2.7. Many systems are unable to differentiate between the different pore types and in some cases certain pore types are not able to be detected.
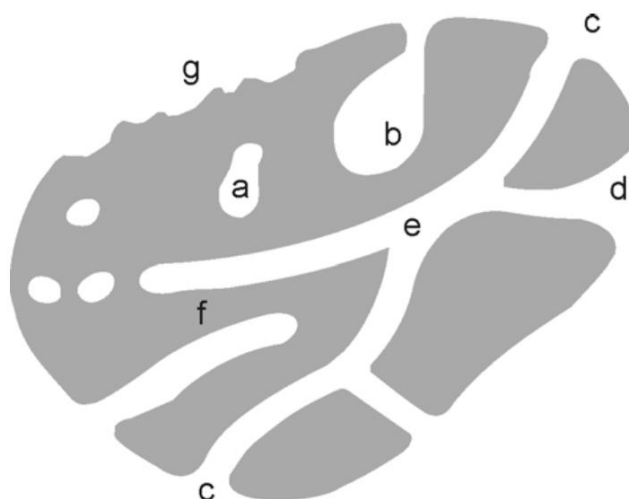
Figure 2.7 - Pore types a) closed pores, b) ink bottle pores, c) open pores, d) funnel pores, e), through (c-e-c) or blind pores (c-e-d) f) slit pores and g) surface pores (Klobes et al., 2006)

The IUPAC classifications of pores sizes according to their width are detailed within Table 2.2.

Table 2.2 - Classification of pores according to their width (Gregg and Sing, 1982)

Pore classification	Pore width
Micropores	< 2 nm
Mesopores	2 – 50 nm
Macropores	> 50 nm

Unlike "specific surface area", "pore size" is not agreeable to a specific definition. Also, pore formations can be superficial, part of an interconnected network or a reticulated pore structure. Therefore, many characterisation techniques depend upon the sequence in which pores are detected by the probe; consequently, quantitative descriptions of pore structure usually are based on model systems. To avoid misinterpretation of the porous morphology of a material often multiple measurement methods are conducted to validate the pore structure.

2.1.3.4 **Types of major adsorbent materials**

2.1.3.4.1 **Granular activated carbon and activated carbon fibres**

Sorbent materials, such as activated carbon (AC), are used in permeable CPC due to their large surface area, adsorptive nature, high thermal conductivity, fire resistance and robustness properties (Kendall et al., 2008).

These amorphous carbonaceous materials have unique micro-structures with high degrees of porosity and extended inter-particulate surface area (Bansal and Goyal, 2005). Common AC adsorbents have a specific surface area of 800-1500 $m^2.g^{-1}$, with a pore volume of 0.2-0.6 $cm^3.g^{-1}$ although, in some instances, the pore volume is as large as 1 $cm^3.g^{-1}$ (Boucher et al., 1970). The surface area contains micropores with effective diameters smaller than 2 nm (Bansal and Goyal, 2005). Hayes (2002) documented activated carbon fibres (ACF) with surface areas as high as 2500 $m^2.g^{-1}$ when measured in N_2 at 77 K using the BET model. Although AC has a high capacity for adsorbing many CWA, there are some associated disadvantages, such as:

- Weight

- The disposal of used or contaminated suits

- The lack of sufficient moisture management properties

- The competitive adsorbency of water

The quantity of adsorbent required to offer complete protection is quite large and can weigh up to 2.5 kg for a full-protective suit with all components attached; however, some suits contain more carbon than others, which can have a significant affect on the mass of the suit. The volumetric density of keratin materials (1320 $kg.m^{-3}$) is about 30% less than that of AC materials (1800-2000 $kg.m^{-3}$) (Bansal and Goyal, 2005), and thus has the potential to reduce the weight of CPC if they both have similar adsorption properties. Another use for porous keratin materials could be within a non-adsorbent textile shell, which is unlikely to provide the same level of protection as AC materials; however the physiological burden would be substantially less.

In terms of disposal, the nerve and mustard agents physically adsorb onto AC without undergoing any chemical change; thus, handling and disposal should be performed with the greatest caution in the event of an exposure (Ramaseshan and Ramakrishna, 2007). Since AC materials have limited absorption properties they have poor moisture management capacities. Also, water has an affinity for itself; therefore, localised moisture situated within the pore structure of the AC reduces the volume of porosity available for specific adsorbate (Bradley et al., 2011).

AC is commercially available in a wide variety of forms including granular, powder, spherical, fibrous and cloth. Generally, granular AC has a large internal surface area and small pore diameters, whereas powder AC has a smaller internal surface area and larger pore size diameters (Bottani and Tascón, 2008). ACFs and activated carbon cloths (ACCs) have higher specific surface areas and specific pore volume to granular and powder forms (Bansal and Goyal, 2005). These higher contact efficiencies and uniform micro-porous structure from the internal surface to the core of the fibre lead to fast adsorption rates (Lordgooei et al., 1996).

It is well documented that activated carbon is an efficient adsorbent due to its high surface area, porosity and sustainability; however, its application is limited by its hydrophilic nature and finite pore volume. According to Fletcher et al. (2007), the hydrophilic nature of activated carbon is caused by concentration of polar sites, mainly covalently bound oxygen functionalities, situated at the edges of the graphene carbon layer-planes and at the in-plane defects (Stoeckli, 1974),

There are many precursors for ACFs; Hayes (2002) investigated the nanostructure of activated carbons and the kinetics of adsorption and desorption using Kynol Novoloid fibres. The Kynol Novoloid fibres are suitable as they have high carbon content, an amorphous structure and can be formed into various textiles structures, including woven, knitted and nonwoven fabrics prior to activation. Novalac resin with 78.3 % carbon content (Figure 2.8) is meltspun and then acid-catalysed cross-linked to form

cured phenol-aldehyde Kynol novoloid fibres (Figure 2.9) with 75.8 % carbon content
and a three dimensional network (*Kynol Europa GmbH Prospectus*, 2014).
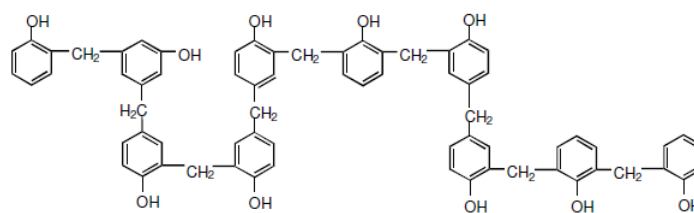
Figure 2.8 - Novalac resin chemical structure, 78.3% carbon (Hayes, 2002)
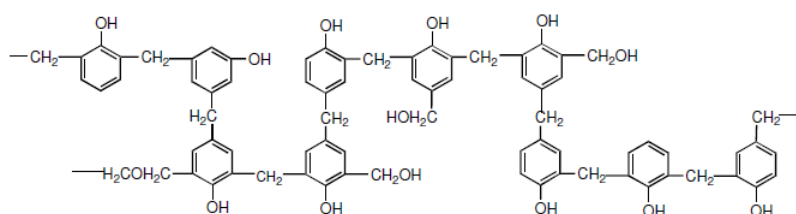
Figure 2.9 - Novoloid fibre chemical structure, 75.8% carbon (Hayes, 2002)

In addition to the high carbon content, the polymer contains only hydrogen and oxygen.
Novoloid fibres are often converted by pyrolysis into carbon or activated carbon fibres
for respective non-porous and porous fibres. During carbonisation in an inert
atmosphere such as nitrogen, the ultimate temperature is the main factor affecting the
chemical composition and structure of the polymer. Secondary factors, such as rate of
heating and dwell time, have minor affects provided the bi-product gases are rapidly
and continuously removed (Hayes, 2002). Figure 2.10 illustrates the changes in
chemical composition and structure of the polymer throughout the carbonization
process; as the temperature reaches 300 °C, hydroxyl (-OH) and methylol (-CH$_2$OH)
groups are removed through gasification.

Novoloid fiber, 75.6% carbon

Pyrolized in N_2 at 300°C, ~76% carbon

400+°C, 85% carbon

500+°C, 90% carbon

700+°C, 95% carbon
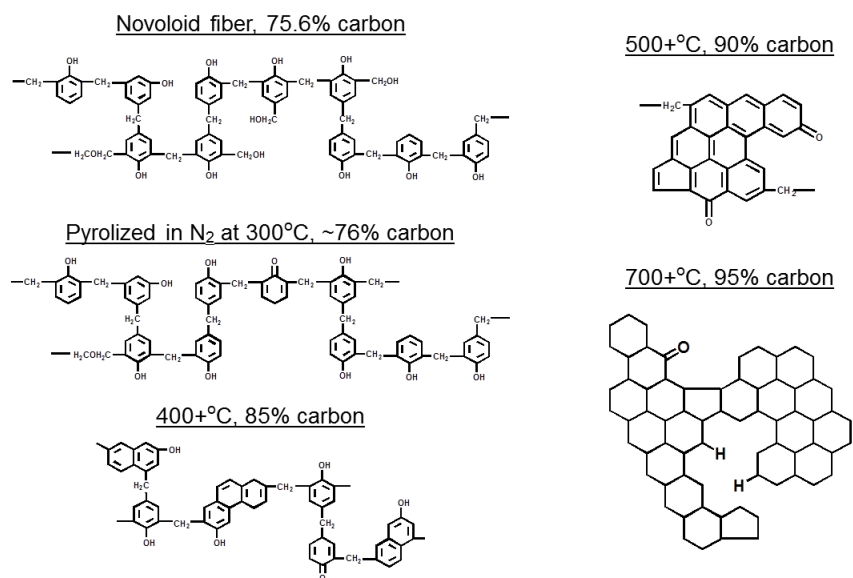
Figure 2.10 - Polycyclic carbonaceous structure formation from Novoloid fibres
(Hayes, 2002)

Further heating leads to the continued loss of non-cyclic elements such as methylene (-CH_2-) bridges, and then hydrogen, causing aromatic compound cohesion. Eventually, the polycyclic carbonaceous structure becomes more apparent and a planar hexagonal carbon structure is achieved (Hayes, 1994); however, these graphene fragments show discontinuous carbon binding and a superficial resemblance to the atomic configuration of graphite.

Contrary to the Novoloid-based carbon fibres process, Novoloid-based activated carbon fibres are exposed to activating gases such as CO_2 and H_2O during pyrolysis or at an additional stage. The specific surface area ($m^2.g^{-1}$) and total pore volume dramatically increases throughout the activation process. Hayes (2002) found that the majority of the pore volume was in the form on micropores (width < 2 nm) with a low amount mesopores (2 to 50 nm) and virtually no macropores (50 nm). Figure 2.7 illustrates the correlation between specific surface area (the notional surface area in square meters per gram) and the total volume of pores of pore radiuses less than 10 nm as determined by gas adsorption porosimetry, as well as the negligible volume of larger pores measured by mercury intrusion porosimetry. This demonstrates that the

pores with radiuses less than 10 nm have greater pore volumes than the pore with radiuses greater than 10 nm. Also, for pores with radiuses less than 10 nm the pore volume is directly proportional to the surface area.
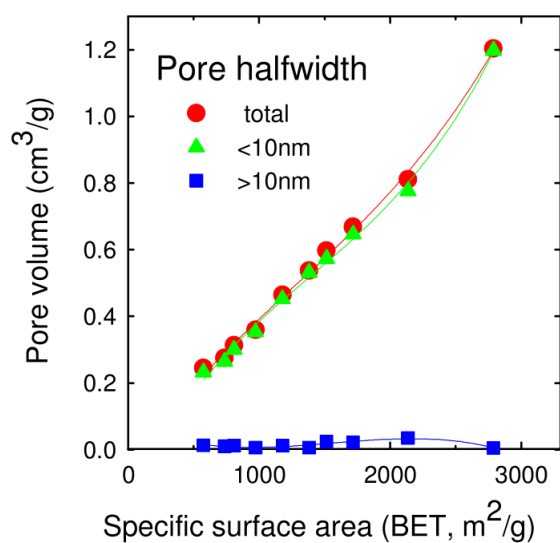
Figure 2.11 - Contributions of small and large pores to total pore volume (Hayes, 2002)

Activated carbons (ACs) are very effective at removing a wide range of toxic chemicals; however, ACs have to be impregnated with reactive functional groups with compounds containing both acidic and basic chemistry in order to provide a broad spectrum of protection. Furthermore, the efficacy of these introduced functionalities will reduce over time as they react with one another due their proximity within the pores of carbons. Therefore, the covalent binding of functional groups to the surface of adsorbent materials is an attractive solution for binding specific toxic chemicals (DeCoste and Peterson, 2014).

Through the crystal design of materials, such as MOFs, these specific functionalities can be applied to the surfaces of substrates within CPC.

2.1.3.4.2 Metal organic frameworks

MOFs have been investigated extensively in the literature for the removal of toxic gases (DeCoste and Peterson, 2014), gas separation (Li, J.R. et al., 2009; Li, J.R. et

al., 2012; Yang, Q. et al., 2013), gas storage (Han et al., 2009; Sumida et al., 2012; Suh et al., 2011; Wu et al., 2012; Duren et al., 2009; Liu et al., 2012), gas catalysis (Yoon et al., 2011; Lee et al., 2009) and molecular sensing (Kreno et al., 2011; Cui et al., 2011; Rocha et al., 2011).

According to the Cambridge Structural Database there are over 54,000 types of metal organic frameworks assuming MOFs are 1D, 2D and 3D frameworks containing transition metals and organic atoms (CSD, 2015). However, 3D frameworks, of which there are over 6,000 (Furukawa et al., 2013; Zhou et al., 2012) have received particular interest, due to the suitability of their properties for gas adsorption. These properties include:

- High surface area;

- High thermal stability and

- Tailorability

The combinations of these properties are rarely available within common adsorption materials, such as ACs and zeolites. Farha, O.K. et al. (2012) reported that many MOFs are highly porous materials with surfaces areas reaching 7140 $m^2.g^{-1}$, with thermal stabilities typically above 573 K and in some cases as high as 773 K (Cavka et al., 2008; Farha, O.K. et al., 2012; Farha, O. K. et al., 2007).

Examples within literature of tailorable MOFs are isoreticular metal-organic frameworks (IRMOFs) (Eddaoudi et al., 2002; Roswell and Yaghi, 2006), where the linker length can be varied, as well as the functional groups present. Whereas, variants of the Material of Institut Lavoiser (MOI) materials, MOF-74 and MOF-101, and MOF-74 allow the interchanging of various metal ions while maintaining identical topologies (Rosi et al., 2005; Férey, Gérard et al., 2004; Férey, G. et al., 2005).

There are various critical reviews of literature conducted on the utilisation of MOFs for air purification, which included an investigation of the removal of toxic chemicals, under the static and dynamic conditions, using chemical warfare agents and simulants including ammonia, carbon monoxide, oxides of nitrogen, hydrogen sulphide, sulfur

dioxide, other sulfur-containing compounds and other toxic compounds (DeCoste and Peterson, 2014; J Rosseinsky et al., 2015). It was reported that the parameters used to evaluate the sorption capacity of various MOFs were very inconsistent across the papers reviewed. The studies related to adsorption of ammonia demonstrated that adsorption occurred by chemisorption at the coordinatively unsaturated sites (-COOM, M = Cu, Ag, Na, or K) (Kim, K.C. et al., 2013), by hydrogen bonding at –OH and –NH$_2$ sites and to coordinatively unsaturated sites through coordinative covalent bonds as found in Cu-BTC and MOF-74 (Glover et al., 2011; Ahmed et al., 2013; Peterson, G.W. et al., 2009; Watanabe et al., 2011). Also, Kim, K.C. et al. (2013) and Yu et al. (2012) conducted density functional theory (DFT) and grand canonical Monte Carlo (GCMC) simulations to study the binding of ammonia on a variety linkers used in MOFs and physisorption of ammonia in a variety of MOFs, respectively.

Table 2.3, demonstrates the lowest binding energies in kJ.mol^{-1} of ammonia and water on specific functional groups. The last column represents the difference between the lowest binding energy of water and ammonia for each case. The top ten cases all demonstrate that the binding of ammonia is greater than water. One short coming for this work is that the research is theoretical and has not been proven practically.

Table 2.3 - Lowest binding energies in kJ.mol^{-1} of ammonia on specific functional groups (Kim, K.C. et al., 2013)

Functional group	NH$_3$	H$_2$O	BE$_{H2O}$ − BE$_{NH3}$
R-COOCu	-161.2	-97.8	63.4
R-COOAg	-84.9	-51.5	33.4
R-HSO$_4$	-65.9	-46.9	19.0
R-COOLi	-81.1	-70.2	10.9
R-OOH	-37.2	-27.7	9.5
R-SO$_3$H	-52.1	42.7	9.4
R-OP(=O)OH$_2$	-54.2	-44.9	9.3
R-P(=O)(OH)$_2$	-50.8	-42.7	8.1
R-OH	-34.3	-26.5	7.8
R-COOH	-41.8	-37.2	4.6
R-Cl	-11.2	-11.9	-0.7
R-NCO	-15.6	-16.8	-1.2
R-NO$_3$	-14.7	-16.7	-2.0
R-F	-12.9	-15.2	-2.3
R-NH$_2$	-18.8	-21.2	-2.4
R (naphthalene)	-8.2	-10.7	-2.5
R-COONa	-62.3	-65.0	-2.7
R-CH$_2$-F	-13.9	-19.5	-5.6
R-C(=O)-H	-16.4	-23.4	-6.9
carbonyl	-16.1	-23.4	-7.3
R-CH$_2$-NH$_2$	-18.3	28.1	-9.8
R-COOK	-48.0	-61.8	-13.8

Functional groups, such as –NH$_2$ and -COOH are present within the amino acid side chains of the polypeptides in keratin (Höcker, 2002). If specific functional groups within the keratin wool fibres are accessible to toxic chemicals that react to these functional groups, then similar to MOFs, it is possible selective physisorption or hydrogen bonding may occur.

Similar to other adsorbent materials, the uptake and stability of MOFs are affected by the presence of moisture; therefore, studies have been conducted to improve these properties by additional surface treatments (Peterson, G. et al., 2012; McPherson et al., 2015; T Wilcox et al., 2015).

2.1.3.4.3 Zeolites

The unique molecular structures of zeolites make them suitable materials for adsorption (Barthomeuf, 1996; Fajula and Plee, 1994), catalyst (Weitkamp, 2000) and ion exchange (Kuhl., 1999; Misaelides et al., 1999) applications. For adsorption applications, Molecular Seize Zeolites are used for both purification and bulk separations (Flanigen, 1980). According to the *Handbook of Molecular Sieves* there are over 500 listed Zeolite frameworks (Szostak, 1992), including over 40 naturally occurring materials (Tschernich, 1992; Abrams and Corbin, 1995).

Zeolites are microporous crystalline frameworks composed of $(SiO_4)^{4-}$ and $(AlO_4)^{5-}$ building blocks, which form intricate channels and cavities (Abrams and Corbin, 1995). Typically, natural zeolites have low silicon (Si)/ aluminium (Al) ratios as the organic agents necessary for forming these complex structures are absent. However, synthetic zeolites can be produced with low, intermediate and high silica compositions depending on the application, although it is difficult to synthesise zeolites with large crystals within a laboratory (Payra and Dutta, 2003).

Zeolites have high accessible surface area, which is typically in the range of 300-700 $m^2.g^{-1}$. These materials have significant accessible internal surface areas, which can equate to 98% of the total surface area (Payra and Dutta, 2003). The high surface area is due to the intracrystalline voids of zeolites, which occurs through rings composed of aluminium (Al) or silicon (Si) and oxygen (O) atoms. Ions and molecules can be trapped within these 1-3 dimensional intracrystalline spaces. Pore sizes can be as small as 0.2 nm with pore volumes can vary between 0.10-0.35 $cm^3.g^{-1}$. The framework projections and pore sizes from some common zeolites are shown in Figure 2.12.
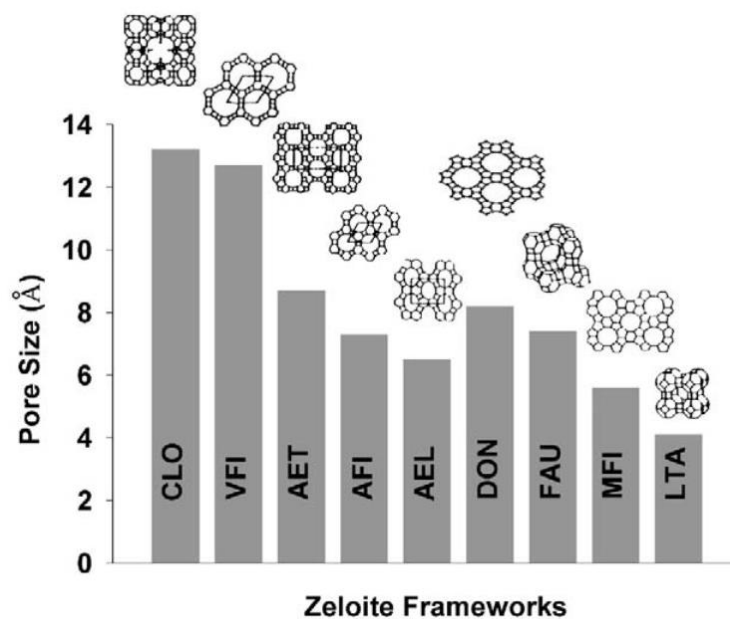
Figure 2.12 - Comparison of pore sizes of different Zeolite frameworks. The acronyms within the graph are specific zeolite names (Payra and Dutta, 2003)

The thermal stability of Zeolites vary between frameworks containing different compositions of silica. Low-silica zeolites is stable at ~700 °C, whereas high-silica zeolites, such as silicate is stable up to 1300 °C (Payra and Dutta, 2003).

Due to the porous nature of zeolites, studies have been conducted to determine their effectiveness at adsorbing CWA. It has been reported that 13X zeolites are capable of adsorbing gaseous HD (Bellamy, 1994) and sorbents impregnated with AgF are able to decompose VX and HD (Spafford, 1996). Wagner and Bartram (1999) demonstrated that VX nerve agent hydrolysed on NaY and AgY zeolites at room temperature, through the cleavage of the P-S bond. Yang, S.-W. et al. (2006) demonstrated that dimethyl methylphosphonate (DMMP) decomposed to methylphosphonate in sodium X zeolite (NaX) by nucleophilic zeolite reactions. However, it was reported that enlarging the pores from microporous to meso-porous enhanced the adsorption capacity. Furthermore, increasing the number of active sites (-Si-O(Na)-Al-) increases with Al content of the zeolite (Sambur et al., 2008). More recently, Meng et al. (2011) adsorbed

trimethyl phosphate (TMP), a organophosphate (OP) representative, on to NaX and a low silica X zeolite.

2.1.3.4.4 Polymers of internal micro-porosity (PIMs)

Polymers of internal micro-porosity (PIMs) are micro-porous materials according to the IUPAC definition (Everett, D. H., 1972), as they have been shown to contain pores with throat diameters less than 2 nm. These materials have been known to behave like molecular sieves due to their unique rigid and contorted molecular structures, which are unable to packed efficiently (Budd, P. M. et al., 2006). Also, some variations of these materials are soluble and can be precipitated from solution as powders or cast into membrane form (Budd, P.M. et al., 2004a; Budd, P.M. et al., 2004b; Budd, P. M. et al., 2005). These materials are attractive from an adsorption perspective due to their ability to be processed and their distinct free volumes within their molecular configurations.

Zhang et al. (2015) reported that there are many types of PIMs being developed for many applications, including gas separation (Budd, P. M. et al., 2005), hydrogen storage (Budd, P.M. et al., 2007; McKeown, N. B. et al., 2006), adsorption (Maffei et al., 2006), heterogeneous catalysts (McKeown, N.B. et al., 2005) and nanofabrication (Tsarkov et al., 2012). PIM-1 is a specific type of polymer that has had considerable commercial and industrial interest, which has led to a significant amount of studies of the synthesis of this material. This polymer can be synthesised by condensation polymerisation of 5,5,6,6-tetrahydroxy–3,3,3,3-tetramethyl–1,1′-spirobisindane (TTSBI) and 2,3,5,6-tetrafluoroterephthalonitrile (TFTPN), as shown in Figure 2.13.
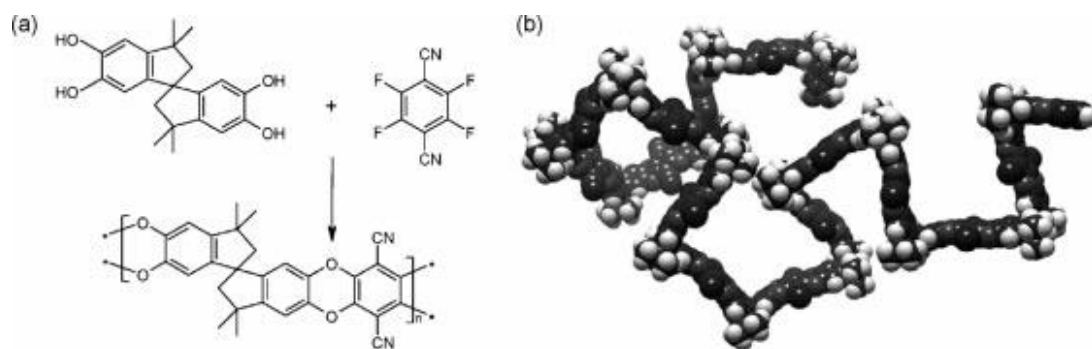
Figure 2.13 - (a) Preparation of polymer PIM-1. Reagents and conditions: K₂CO3, DMF, 65 8C. (b) Molecular model of a fragment of PIM-1 demonstrating the irregular and kinked shape of the molecule (Budd, P.M. et al., 2004b)

PIM-1 has a BET surface area of 620-850 $m^2.g^{-1}$ (Zhang et al., 2015), which makes it an attractive material for the application of adsorbing VOCs. Furthermore, this polymer is soluble in organic solvents, such as tetrahydrofuran (THF) and chloroform (CHCl₃).

2.1.3.4.5 Silica and silicone aerogel

Silicon and silicone aerogels are currently used for applications, such as, super thermal application, acoustic insulation, Cerenkov radiation detectors, low dielectric constant aerogel films in ultra large scale integrated circuits, superhydrophobic aerogels for oil-spill clean-up, in catalysis, and intertial confinement fusion targets in thermonuclear fusion re-actions (Rao et al., 2006).

Du (2014), investigated the thermal insulation properties of a flexible MTMS based silicone aerogel and its application in aerogel-spacer fabrics. Aerogels are made by a sol-gel method detailed in Figure 2.14 (Hüsing and Schubert, 2000). The precursor solution is firstly dissolved in an organic solvent that is miscible in water, and then the acid and base catalysts are added separately to speed up the hydrolysis and condensation reactions to obtain the wet gel, which is then aged and strengthened in a solvent. Finally, the strengthened wet gel is dried to form porous aerogels (Du, 2014). When the wet gel was dried using supercritical CO₂ (SCCO₂) drying process, the material had BET surface area >450 $m^2.g^{-1}$; therefore, similar to PIMs, MTMS based silicone aerogels are an attractive material for the application of adsorbing VOCs.
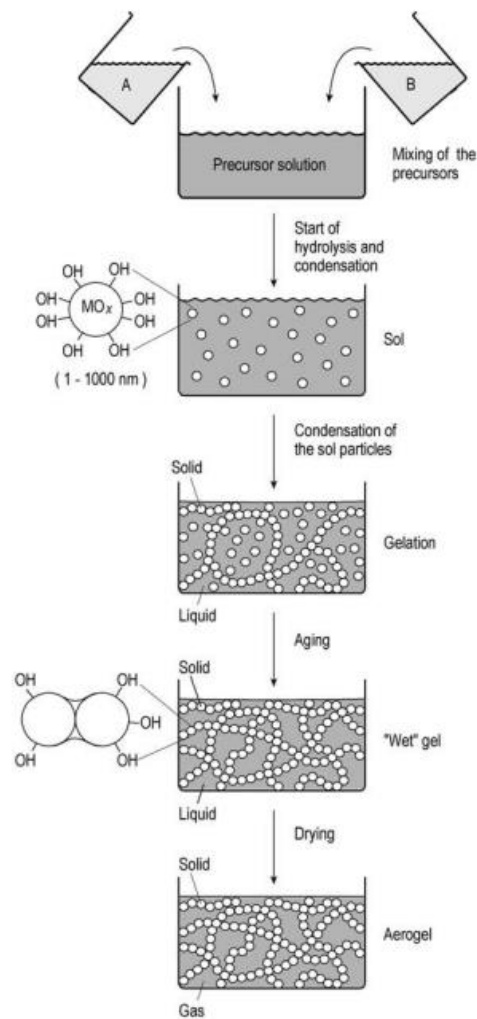
Figure 2.14 - Schematic diagram of sol-gel synthesis method for the preparation of aerogels (Hüsing and Schubert, 2000)

These aerogels were formed using a two-step acid-base catalysed sol-gel process, which produces an aerogel with high porosity, small pore sizes and a narrow pores size distribution. Bauer (2012) and Fricke and Fojan (2014), have both applied for patents for forming aerogel composite materials. Bauer (2012) has filed an application relating to a composite containing a fibrous material, binder and aerogel particulates. Fricke and Fojan (2014) have filed an application relating to a composite containing a polymer shell, which comprises a core of aerogel particles.

2.1.3.5 **Competitive adsorbency with water**

A major constraint for adsorbent materials is the competitive adsorbency of water, which reduces the volume of porosity available for specific adsorbate. Consequently, the efficient adsorption of toxic organic species for chemical protective clothing and respiratory equipment is affected by the continuous exposure to humid airstreams. Water has an affinity for itself; therefore, localised moisture situated within the pore structure causes the acceleration of additional sites (Adams et al., 1988), which reduces the volume of porosity and impedes the access of other pores (Bradley et al., 2011).

Fletcher et al. (2007) investigated the effects of oxygen surface functional groups in activated carbons on the adsorption characteristics of water vapour and determined that, at low relative pressure, the water vapour adsorption was dramatically enhanced by the presence of functional groups, in particular, carboxylic groups.

Bradley et al. (2011) investigated the effectiveness of novel hydrophobic active carbons developed for respirators. Polar oxygen groups were removed from the granular active carbons by a thermal treatment and a hydrophobic, fluorine-containing surface nano-layer was then applied using plasma enhanced chemical vapour deposition (PECVD) treatment. At low relative pressures, the competitive adsorption occurs at specific (polar) adsorption sites, which are situated at the edges of the graphene carbon layer-planes and at the in-plane defects, as opposed to within the micropores (Stoeckli, 1974), which is described as the result of enhanced dispersion forces (Everett, Douglas H. and Powl, 1976). At higher relative pressures, competitive adsorption also occurs within micropores and mesopores. Overall, the concentration of polar sites, mainly covalently bound oxygen functionalities (Fletcher et al., 2007), determines the hydrophilicity of the structure. Decreasing the polar free energy of the surface reduces the amount of water adsorbed and retards the water diffusion mechanism of water molecules into the micropores (Bradley et al., 2011).

CPC is used in a variety of external environments containing moisture; therefore, it is likely that water will decrease the adsorbent capacity of the material if there is a high concentration of polar sites. Consequently, it is important to remove moisture residues while characterising the chemically modified materials to get a fair assessment of the porous structure.

2.1.3.6 Methods for the characterisation of porous structure of keratin adsorbent materials

The chemical and physical structures of the porous materials can be very different and often materials are selected for an application based on their specific pore features. Therefore, to select, enhance, synthesise or differentiate between porous materials complex characterisation techniques have been developed to understand the parameters associated with porosity. Examples of techniques used to characterise porous materials and their associated pore size measurement capabilities are demonstrated in Figure 2.15.
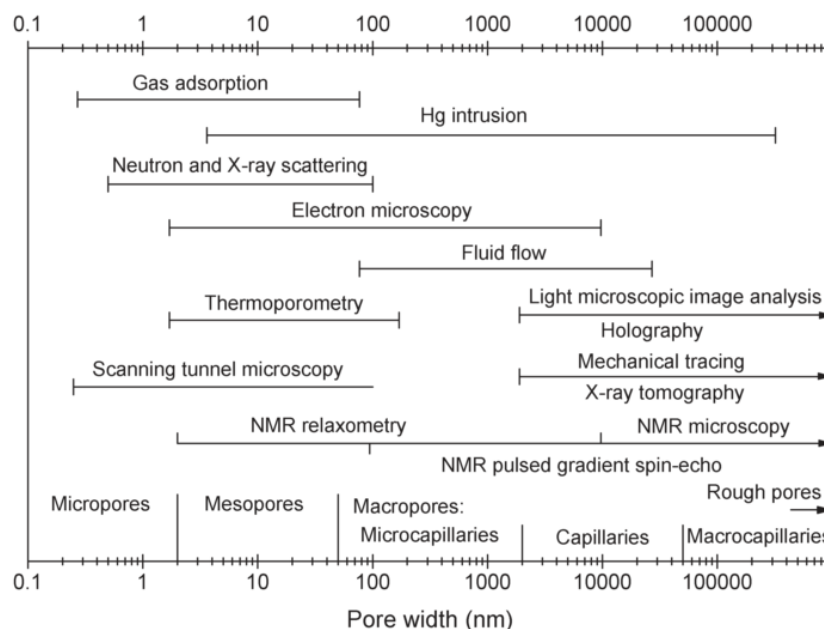
Figure 2.15 - Pore analysis instruments and their ranges (Meyer et al., 1997)

In some studies it is necessary to study the pore shape and interconnectivity and to determine the internal and external specific surface area of the materials, but generally the characterisation of porous materials usually involves the study of pore size distributions and the total pore volumes (BS ISO BSISO15901-1, 2005). Also, BS ISO BSISO15901-1 (2005) describes porosity as the ratio of the volume of the accessible pores and voids to the total volume occupied by a given amount of the solid. However, a solid may contain inaccessible pores, as well as accessible pores. These isolated cavities are difficult to characterise as applied gases and liquids used to measure parameters associated with porosity are unable to penetrate the material. Characterisation techniques for measuring porosity are not always in agreement because the complexity of most materials means that these techniques cannot be relied upon in isolation. Therefore, characterisation techniques are selected based on the materials chemical and physical form, the range of pores sizes and application. Pore sizes are classified as micro-, meso- and macropores, the pores sizes associated with these categories are detailed in Table 2.2 (Gregg and Sing, 1982).

These pores can be channels, cavities or apertures within a solid form or as interstices or voids between the solid features. Techniques for measuring porosity are most commonly used for measuring solid particles in bed, compact or aggregate; however, it is possible these techniques could be adapted for measuring fibrous materials.

Within this study, analytical techniques for characterising the porous features of wool fibres include SEM, BET surface area helium pycnometry and mercury porosimetry.

2.1.3.6.1 Scanning electron microscopy

Scanning electron microscopy (SEM) is a well adapted technique often used to generate high resolution microscopic 2-dimensional images of objects. The use of this technique to characterise the morphology of wool fibres is well documented in literature. The system uses high energy electrons to generate signals from electron-sample interactions. The accelerated electrons decelerate when impacted with the

solid sample, which generates secondary electrons, back scattered electrons, diffracted back scattered electrons, photons, visible light and heat. The signals generated from the secondary and backscattered electrons are used to produce images demonstrating the sample morphology (Reimer, 1998; Goldstein, 2003; Egerton, 2005).

2.1.3.6.2 Brunauer–Emmett–Teller (BET) surface area

BET surface area is a gas adsorption analysis technique for the measurement of the specific surface area of material. This theory is an extension of Langmuir theory (monolayer molecular adsorption), which assumes that gas molecules physically adsorb on a solid in layers, there is no interaction between each adsorbent layer and that the Langmuir theory can be applied to each layer.

The British standard for the determination of the specific surface area of solids by gas adsorption, states the BET method is "applicable only to adsorption isotherms of type II (disperse, nonporous or macro-porous solids) and type IV (meso-porous solids, pore diameter between 2 nm and 50 nm)" (*BS ISO 9277*, 2010). Also, inaccessible pores are not detected, so internally cavities are not measured.

Criticisms of BET surface area (Gregg and Sing, 1982) include:

1. The model assumes all the adsorption sites on the surface to be energetically identical; however, homogeneous surfaces of this kind are the exception.

2. The model restricts attention to the forces between the adsorbent and the adsorbate molecules (neglects the forces in between an adsorbate molecule and its neighbours in the same layer)

2.1.3.6.3 Helium pycnometry

Helium Pycnometry systems, such as AccuPyc 1330 Pycnometer determines density and volume by measuring the pressure change of helium in a calibrated volume, allowing computation of the sample solid phase volume (*AccuPyc 1330 Pycnometer*

2001). This non-destructive method enables the calculation of true, absolute, and apparent volume and density for a wide variety of powders, solids, and slurries. The British Standard Institute definition of density:

- True density – the mass of a particle divided by its volume, excluding open and closed pores.

- Absolute density – The mass of particle per unit of absolute particle volume.

- Apparent density – the mass of material divided by its apparent volume.

The system uses inert gases (helium or nitrogen) as the displacement medium and the displacement calculations are claimed to be more accurate and reproducible than the traditional Archimedes water displacement method (*AccuPyc 1330 Pycnometer* 2001). This method is not restricted to poor size range like other common characterisation techniques, such as gas adsorption, high pressure carbon dioxide and mercury porosimetry (see Figure 2.12), which makes it an attractive technique for studying the pore formations of chemically and physically modified wool fibres.
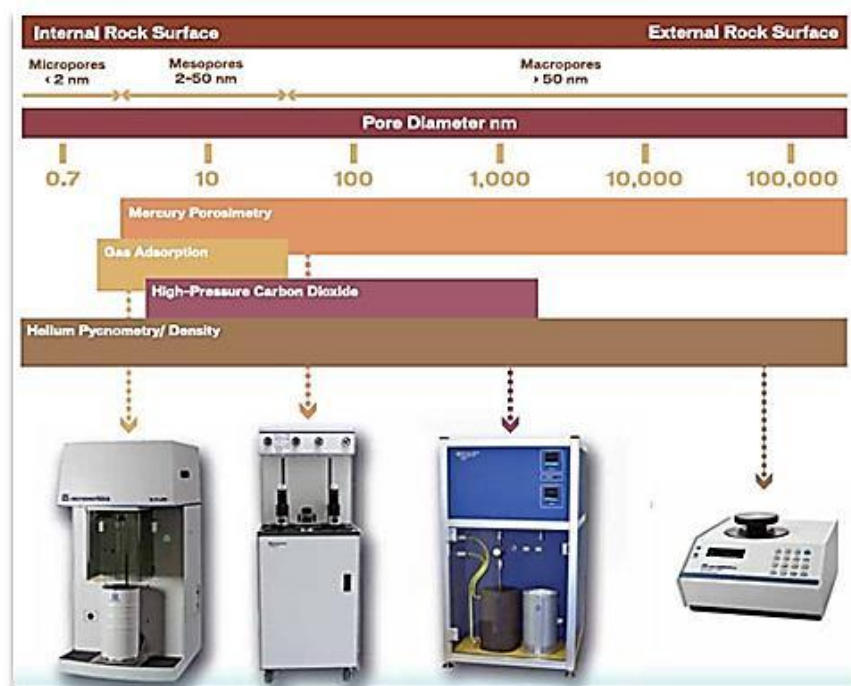
Figure 2.16 - Methods for measuring the porosity of materials and their capabilities (Klobes et al., 2006)

2.1.3.6.4 Mercury porosimetry

The physical properties of a material can be considerably influenced by its porosity. Techniques for measuring porosity can give an understanding of the material form and structure, and its potential for various applications. Mercury porosimetry is used to quantify the porous morphology of a material. Non-wetting substances such as Mercury have high surface tensions and are unable to spontaneously intrude pores by capillary action. Therefore, external pressure is required to enable the mercury to penetrate these pores. The external pressure applied is inversely proportional to the size of the pores. The system is capable of measuring the complex progressive pressure increments versus intrusion data and generates volume and size distributions using Washburn's Equation (4). This equation gives the relationship between pressure and pore diameter assuming the pores have a cylindrical shape. The system uses Equation (4) to convert pressure readings into pore diameter and plots the data as pore volume distributions (Micromeritics, 2014b).

$$D = \frac{-4\gamma cos\theta}{P} \quad (4)$$

D = pore diameter

γ = surface tension of mercury

θ = contact angle of mercury

P = pressure

Differential pore volumes are calculated from the Incremental Hg intruded volumes divided by the total volume of Hg (mL.g^{-1}) and the Total pore volume can be calculated from the Total incremental Hg intruded volumes divided by the total volume of Hg (mL.g^{-1}).

Although a well adopted measurement technique, mercury porosimetry has its limitations and may not be suitable for characterising all porous materials (Giesche, 2006). One key issue for testing fibres is that the process measures both particle and

inter-particle porosity, but is not capable of differentiating between the two where they co-exist (BSISO15901-1, 2005). This could be problematic for measurements for both wool fibres and fabrics as spaces between fibres could be misinterpreted as pores. Also, the system only measures superficial pore throat data as illustrated in Figure 2.17. Therefore, this measurement procedure does not provide a full representation of the porosity of a material. For instance, a pore may have a large cavity, but a small superficial pore throat; however, the system will only calculate the external pore throat data. The data associated with that feature will not be a true representation of the fibre porosity; consequently, additional measurement techniques, such as BET surface area, SEM and helium pycnometry should be applied to gain a greater understanding of material fibre morphology.
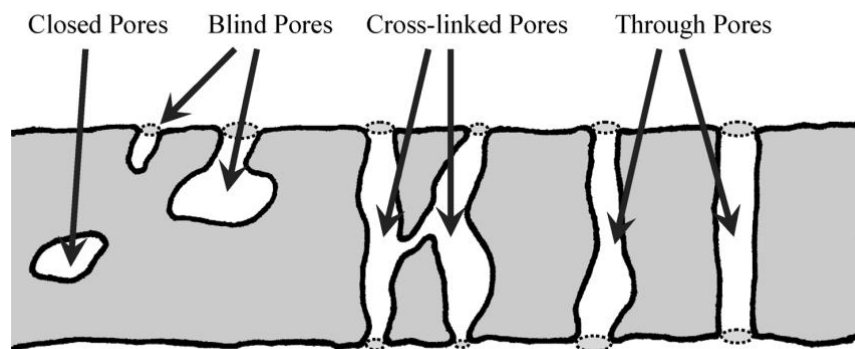
Figure 2.17 - Schematic representation of pores measured using mercury porosimetry (Giesche, 2006)

The Micrometrics system exports the data as a cumulative pore area measurement with relation to the pore throat diameter. However, for adsorption materials, such as activated carbon, the material porosity is often characterised using pore volumes. This research has developed a method for expressing the mercury porosimetry pressure versus intrusion data as total pore volumes and pore volume distributions with relation to the incremental pore throat diameters. The total mercury volume entering the system (V_T) and the intrusion fraction (I_F) with relation to throat diameters are calculated by the system. Therefore, the product of these two values gives the intrusion volume (V_I) of

the mercury, which can be interpreted as the total pore volume for specific pore sizes. This data can be expressed incrementally based on the pore throat diameter; consequently, the pore volume data of accessible pores can be expressed as total pore volume for the sample and pore volume distributions. This methodology also enables the calculation of total pore volumes and pore volume distributions for specific pore sizes/ ranges. This is a unique method for characterising the porous features of fibrous materials.

2.1.4 Keratin wool fibres

Wool fibres are abundant, renewable and natural resource. It is inherently environmentally friendly and it is well known for its natural flame resistance and moisture management properties (Mather and Wardman, 2011). Wool has a complex physical and chemical structure that supports an attractive combination of properties and performance attributes. They also contain reactive groups, such as carboxylate and amine, which are proved binding sites for metal ions and VOCs (Renes, 1985). Wool fibres have been proven to be effective at sorption of chemical hazards and VOCs (Mehta, 1980). Also, wool has underlying structures that suggest it can be made into an adsorbent material by introducing pore structures.

2.1.4.1 Types of wool fibres

Wool has been developed through mammalian evolution, commonly associated with the hair of domesticated sheep, but the generic name given to all animal hair (Höcker, 2002). The hairs present on mammals are all part of the same category of proteins called α-keratins. These fibres are formed in follicles in the skin have a similar chemical structure to all types of epithelial cell such as finger nails, horn, hooves, skin and feathers (Postle et al., 1988). Wool is the protein fibres grown on sheep.

It is difficult to determine how many breeds of sheep there are worldwide, as only developed countries maintain breed registries. However, the wool fibres vary significantly depending on the breed. The wool fleeces are graded by fibre fineness

and length. The quality of the wool fibres are heavily influenced by the breed and health of the sheep and the climate. Whole fleeces are separated as different areas contain varying qualities of wool. Generally, the sides and shoulders of the animal contain the best Australia, New Zealand, South Africa, China and the United States are the leading produces of apparel quality wool; whereas, Russia, Argentina and Turkey are renowned for producing coarser products such as carpet grade wool. Merino wool has the most crimp, drape, strength, resilience, elasticity, hand and scales on the surface. Therefore, Merino wool is considered the best type of wool in terms of quality (Cohen et al., 2012).

Wool is also the terminology used to describe the keratin fibres from alpaca, camel, cashmere goats, llamas, and Angora goats and rabbits. These specialty fibres are described in Table 2.4**.**

Table 2.4 - Types of specialty wool fibres (Cohen et al., 2012; IYNF, 2009)

Wool type	Animal	Location	Fibre diameter	Application	Qualities
Alpaca wool	Alpaca	South America	20 – 70 µm	Sweaters and ponchos	Durable, silky and very lustrous
Camel hair	Two hump camel	Mongolia, Tibet and other Asian countries	~20 µm	Overcoats	Weak fibre with a texture similar to wool
Cashmere wool (inner coat hair)	Asian Cashmere goat	China	14-19 µm	Luxury sweaters, suits and coats.	Fine and very soft
Llama wool	Llama	South America	20-40 µm	Sweaters and blankets	Weaker than camel hair and alpaca wool
Mohair	Angora goat	Turkey, South Africa and United States (Southwestern states)	23 – 38 µm	Luxury clothing and furnishing	Very strong/ abrasion resistant and high lustre
Angora wool	Angora rabbit	China, France, Argentina, Chile, Czech Republic and Hungary	14-16 µm	Luxury clothing	N/A

There are more than 60 different breeds of sheep in Britain with different structural characteristics, depending on where they live, on hills or lower land. The breeds can be divided into groups (BWMB, 2014):

- Mountain (Swaledale, Blackface, Welsh Mountain).

- Hill (Cheviot, Beulah, Hill Radnor).

- Cross (Mule).

- Medium (Romney, Lleyn, Texel).

- Fine (Suffolk, Clun Forest).

- Lustre (Bluefaced Leicester, Wensleydale, Devon & Cornwall, Longwool).

- Naturally Coloured (Jacob).

However, a comparison of the specific structural characteristics of each British wool type has never been reported.

British wool samples are generally courser than fine wools, such as Merino wool. Coarse and semi-coarse wool have different distributions and proportions of para-cortex and ortho-cortex cells inside the wool fibre structure in comparison to fine wool. Such difference might lead to a difference in its adsorption and absorption properties after chemical modifications (Ward and Mao, 2014).

2.1.4.2 **The use of keratin wool fibres within clothing**

Wool was been used by primitive humans for cloth before 10,000 BC. There are archives suggesting wool was spun and woven in Mesopotamia and northern Europe tribes, despite their tools for spinning and weaving being relatively basic (IWTO, 2017a). More recently, wool fibres are used for a wide range of products including warm outer garments, base layer wear, fashion apparel, luxury interiors and products requiring fire retardant properties (Henry et al., 2015; IWTO, 2013; Haly, 1974). According to IWTC, two thirds of the world's wool harvest is used for apparel and about one third is used for interior products, such as carpets, upholstery and rugs. The remaining harvest (approximately 5%) is mainly used for industrial uses such as insulation (IWTO, 2017b).

These natural fibres have unique properties, which make them suitable materials for clothing. They are hygroscopic in nature, which makes them natural insulators and multi-climatic as the wearers are able to maintain thermophysical comfort in both cold and warm weather. The fibres absorb and release water as the humidity of the surrounding environment rises or falls, respectively. During the absorption phase heat is generated and retained. Crimped wool fibres that are closely packed together are able to absorb and release moisture without compromising the thermal efficiency due to air pockets within the fibre structure. Also, it has a large capacity for absorbing water

(approximately a third of its own mass), which makes it very breathable (CFW, 2017).

In addition to their performance related properties, wool fibres are often selected for particular applications because they are renewable and abundant, easy to care for and biodegradable (CFW, 2017).

Wool fibres have become a popular alternative to synthetic fibres for sports clothing due to their performance properties. Also, recent market trends have led to global companies considering the ethical and sustainability of their products (ISPO, 2016). More recently, Armardillo Merino® a merino wool performance clothing manufacturer have claimed to have supplied garments to UK and US military, fire services, police services and space programs. They claim on their website that "Armadillo Merino® garments enhance user safety and performance with super soft merino wool providing exceptional next-to-skin comfort. The fabric does not melt or drip and provides a natural barrier of flame resistance up to 600°C (Armadillo, 2017).

2.1.4.3 Chemical composition of keratin wool fibres

Wool is an α-keratinous nano-composite fibrous material (Wortmann, 2009) that protects animals during exposure to environmental conditions (Klobes et al., 2006). It is part of a larger group of biological functional, high relative molecular mass long chain polymers called keratins (Wortmann, 2009). These natural proteins are made up of α-amino acids residues (Höcker, 2002) joined into long polypeptide chains with a planar structure. The amino acids are distinguished by their side chains and are characterised by the empirical monomer shown in Figure 2.18.
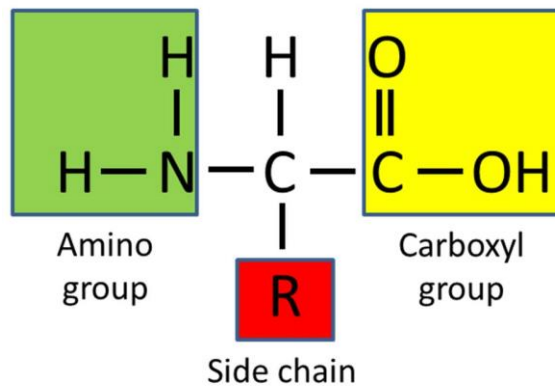
Figure 2.18 - Structure of an amino acid

Amino acids are the building blocks of proteins and contain a central carbon atom bonded to a hydrogen atom, an amino group ($-NH_2$), a carboxyl group - (COOH) and a functional side chain (R), with varying atoms. Höcker (2002) describes wool as a protein fibre containing the elements detailed in Table 2.5.

Table 2.5 - Keratin wool fibre elements (Höcker, 2002)

Element	Weight (%)
Carbon	50-52
Hydrogen	6.5-7.5
Oxygen	22-25
Nitrogen	16-17
Sulphur	3-4
Ash	0.5

The different amino acids and their element compositions present within wool fibres are detailed Table 2.6.

Table 2.6 - Amino acid composition of keratin wool fibres (Kozlowski, 2012)

Amino acid	Structure	Mol %[a]	Nature of side-chain
Glycine	$CH_2(NH_2)COOH$	8.4	Non-polar
Alanine	$CH_3CH(NH_2)COOH$	5.4	Non-polar
Phenylalanine	⟨C6H5⟩—$CH_2CH(NH_2)COOH$	2.9	Non-polar
Valine	$CH_3CHCH(NH_2)COOH$ / CH_3	5.6	Non-polar
Leucine	$CH_3CHCH_2CH(NH_2)COOH$ / CH_3	7.7	Non-polar
Isoleucine	$CH_3CH_2CHCH(NH_2)COOH$ / CH_3	3.1	Non-polar
Serine	$HOCH_2CH(NH_2)COOH$	10.4	Polar
Threonine	$CH_3CHCH(NH_2)COOH$ / OH	6.4	Polar
Tyrosine	HO—⟨C6H4⟩—$CH_2CH(NH_2)COOH$	3.9	Polar
Aspartic acid	$HOOCCH_2CH(NH_2)COOH$	6.5	Acidic
Glutamic acid	$HOOCCH_2CH_2CH(NH_2)COOH$	11.9	Acidic
Histidine	(imidazole)—$CH_2CH(NH_2)COOH$	0.9	Basic
Arginine	$H_2NCNH(CH_2)_3CH(NH_2)COOH$ / NH	6.9	Basic
Lysine	$NH_2(CH_2)_4CH(NH_2)COOH$	3.0	Basic
Methionine	$CH_3S(CH_2)_2CH(NH_2)COOH$	0.5	Sulfur containing
Cystine	$HOOCCH(NH_2)CH_2SSCH_2CH(NH_2)COOH$	10.3	Sulfur containing
Tryptophan	(indole)—$CH_2CH(NH_2)COOH$	0.5[b]	Heterocyclic
Proline	(pyrrolidine)—$COOH$	6.6	Heterocyclic

[a] Mol % values are the mean values from References 9 and 10.
[b] Determined by enzyme digestion.

An example of the amino acid configurations, polypeptide chains and chemical structures of important cross-linking components are detailed within Figure 2.19.
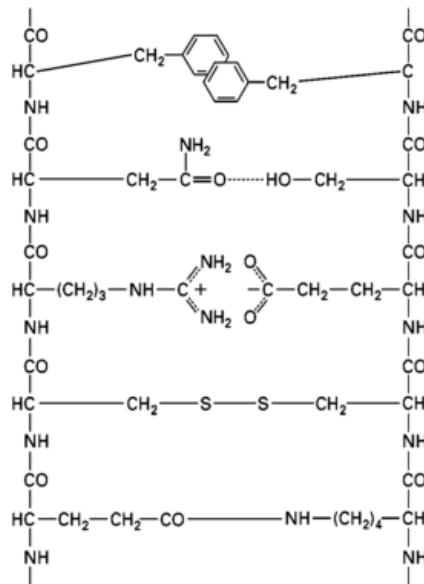
Figure 2.19 - Structural formula of peptide chain to illustrate important interactions between amino acid side chains in keratin (Rippon, 2013)

The structural complexity of wool influences the physical and mechanical properties of the fibres (Hearle, J W S, 2002) and the chemical composition contains combinations of various polypeptides creating a heterogeneous composite material (Li, J.Y., 2001).

2.1.4.4 The microstructure of keratin wool fibres

Figure 2.20 is a schematic of the hierarchical morphology of a wool fibre. Although the fibre consists of many components, the fibre morphology is generally categorised by three components: the Cuticle, Cortex and Cell membrane complex (CMC). Unlike synthetic polymer fibres, keratin fibres are heterogeneous along their fibre lengths and the three cell divisions originate at the bulbous area of the fibre follicle (Klobes et al., 2006).

Epicuticle
Exocuticle
Endocuticle

Low-S High-S
proteins proteins
high-tyr
proteins

Nuclear
remnant

a

Cuticle

Right-
handed
α-helix

Left-
handed
coiled-coil
rope

Matrix

Microfibril

Macrofibril

Cell
membrane
complex

Para cell Ortho cell

Cortex

1   2   7   200   2 000   20 000 nm
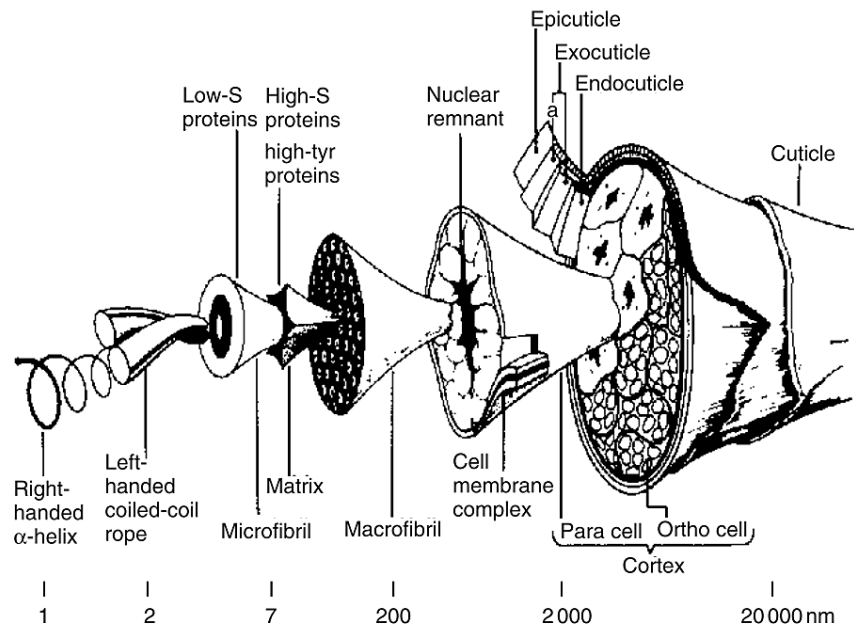
Figure 2.20 - Keratin wool fibre structure [Drawn by Robert C Marshall, CSIRO]
(Hearle, J W S, 2002)

Table 2.7, describes the morphological components of wool and their percentage masses in relation to the whole wool fibre. The table also shows the high composition of keratin proteins with all wool fibre components.

Table 2.7 - Morphological components in fine wool % o.w.f. (Bradbury, 1973)

Component	Sub-component	Keratinous proteins	Non-keratinous proteins	Non-protein matter	Total
Cuticle	Exocuticle	6.4	-	-	10.0
	Endocuticle		3.6	-	
Cortex	Microfibrils	35.6	-	-	86.7
	Matrix	38.5	-	-	
	Nuclear remnants and intermacrofibrillar material	-	12.6	-	
Cell membrane complex	Soluble proteins	-	1.0	-	3.3
	Resistant membranes	1.5	-	-	
	Lipids			0.8	
Total	-	**82.0**	**17.2**	**0.8**	

2.1.4.4.1 The Cuticle

The cuticle cells form the external layer of the wool fibre and constitute 10% w/w of the fibre mass (Bradbury, 1973). These scales have rectangular geometry (Caven, 2010) and comprise three subcomponents; the epicuticle, exocuticle and endocuticle. The cuticle cells conceal the Cortex and are aligned in a single direction with the fringes overlapping in an inter-digitating manner (Höcker, 2002).

- The epicuticle is made from keratin chains and a small amount of lipids. It forms the external layer of the wool fibres, which conceals the cuticular and cortical cells (Mather and Wardman, 2011).

- The exocuticle layer is rich in cysteine and composed of two layers. The A-layer has greater cysteine content than the B-layer (Li, J.Y., 2001) and lies adjacent to the epicuticle.

- The endocuticle is a non-keratinous protein and lies below the exocuticle. Mechanically, the endocuticle is a weak component of the wool fibre, despite comprising *ca.* 40 % of the cuticle.

2.1.4.4.2 The Cortex

The cortex is a major contributor to the mechanical behaviour and makes up approximately 90% of the wool fibre. The ortho-cortical and para-cortical cells are two distinct areas within the cortical cell and are differentiated by the morphology of the non-keratinous material distributed throughout the macro-fibrils (Rippon, 2013). The para-cortical has a more extensive network of cross-linking between the intermediate filaments in each cell. Consequently, the ortho-cortical cell is more accessible to reagents and is more chemically reactive (Bradbury, 1973).

Natural crimp of fine wool fibres is caused by the bilateral segmentation of the two types of cortical cell. Similar to the way bimetallic strips bend in response to temperature, fibres with a bilateral cortical structure change their crimp shape with the

change in moisture content (Denby, 1983). Micro-fibrils within the para-cortical cells range in shape from perfect hexagonal cross-sections to completely irregular constructions, whereas, microfibrils within the ortho-cortical cells are arranged in whorls (Li, J.Y., 2001). Figure 2.21, demonstrates the relationship between these segments, with the ortho-cortical cell oriented towards the outside of the curl of the crimp (Mather and Wardman, 2011).
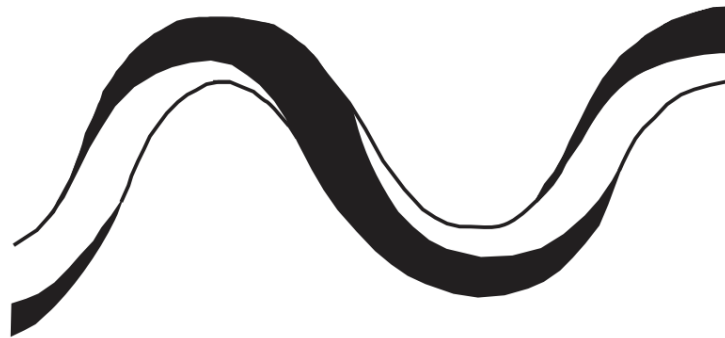
Figure 2.21 - Relationship between fibre crimp and ortho- and para-cortical segmentation (Mather and Wardman, 2011)

The cortical cells are cemented together by an intercellular membrane complex, typically 25 nm thick. The membrane can be easily swollen and is often responsible for the breakdown of the wool fibres, caused by fatigue and abrasion (Postle et al., 1988). This fibril-reinforced matrix consists of polypeptides interconnected physically and chemically. The fibrils are regarded as α-keratins and are often described as Keratin intermediate filaments (KIF) embedded into a structurally irregular protein matrix called Keratin associated proteins (KAP) (Höcker, 2002).

Filamentous materials, called macro-fibrils, are aligned longitudinally and span the length of the cortical cells. The macro-fibrils are composed of smaller structural units called micro-fibrils that are regarded as the main mechanical unit within the wool fibres and are formed from keratin chains comprising four sections of a-helix separated by three non-helical segments (Mather and Wardman, 2011).

2.1.4.4.3 Cell membrane complex

The main components of the cell membrane complex (CMC) of wool fibres are cholesterol esters, free fatty acids, sterols, ceramides, glycosyl-ceramides and cholesterol sulphate. These components are situated within the β-layers (Alzaga et al., 1999). It accounts for 3–3.5 % of the fibre and provides adhesion between the cells. The CMC is relatively weak and is often the site where fracture occurs between the spaces between adjacent cortical cells. This is due to the lipid component that, despite its low concentration, has a significant effect on the mechanical properties of the fibre (Mather and Wardman, 2011).

2.1.5 Chemical modification of wool fibres

The chemical modification of keratin fibres is well documented for various functions and applications. Degradation techniques such as hydrolysis, reduction, oxidisation, acylation, arylation, alkaylation, reaction with reactive dyes, electrophilic reagents, condensation with carbonyl agents and crosslinking agents have been studied extensively (Ashquith, 1977).

These degradation techniques are commonly used to remove the cuticles, F-layer or epicuticle, modify the exocuticle or CMC, and cleave the peptide chains and amino acid side chains. These techniques are capable of causing cuticle removal Fan et al. (2007), fibre fibrillation (Li, J.Y., 2001) and protein solubilisation (Arai et al., 1990; Schrooven et al., 1998; Yamauchi et al., 1996). Furthermore, the structural and morphological alterations caused by these degradation techniques are used to improve the following wool fibre properties:

- Handle and lustre (Mcphee and Shaw, 1984)

- Frictional properties, felting and shrink resistance (Moncrieff, 1953)

- Wettability, prickle and pilling (Ashquith, 1977)

- Dyeability (Barritt and Elsworth, 1948)

Despite the potential improvements to some fibre properties these degradation techniques can also have detrimental effects, including reduction in strength, yellowing, poorer dyefastness and low abrasion resistance (Li, J.Y., 2001).

Keratinous materials such as wool fibres contain high levels of intra- and intermolecular disulfide crosslinking. The chemical deconstruction of these materials can be achieved by breaking intermolecular disulfide bonds, while maintaining the covalent bond of the polypeptide chains. However, Ghosh and Collie (2014) reported that it is difficult to extract keratins using chemical treatments and retain the desired properties of the natural fibres. Reduction, oxidation, sulfitolysis or oxidative sulfitolysis are processes that are capable of breaking the disulfide bonds within the keratinous materials (Poole et al., 2009). Irreversible reactions and their associated chemical mechanisms are detailed within (a) and (b). Reaction (a) demonstrates the reaction when strong oxidants convert cysteine residues in to cysteic acid. Typically oxidants include hydrogen peroxide and performic acid.

$$KSSK + O_2{}^{2-} \xrightarrow{[O]} KSO_3{}^- \quad \text{(a)}$$
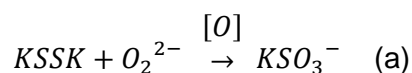
Reaction (b) illustrates an oxidative sulfitolysis reaction which converts the disulfide into two S-sulfonate anions.

$$KSSK + 2SO_3{}^{2-} + H_2O \xrightarrow{[O]} 2KS - SO_3 + 2OH^- \quad \text{(b)}$$
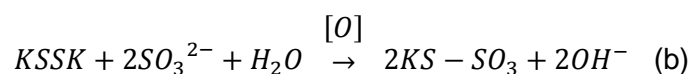
Reversible reactions are detailed within (c) and (d). The mechanism detailed within (c) is a nucleophilic displacement reaction, caused by the reduction of cysteine bonds by thiols, such as mercaptoethanol and thioglycolic.

$$KSSK + RS^- \leftrightarrow KSSR + KS^- \quad \text{(c)}$$
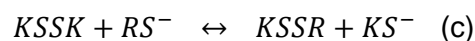
Similarly, mechanism (d) is an irreversible reaction called sulfitolysis, which cleaves disulfide bonds. The sulfite ion produces an S-sulfonate anion.

$$KSSK + 2SO_3{}^{2-} \quad \leftrightarrow \quad KS - SO_3{}^- + KS^- \quad \text{(d)}$$

As well as the cleavage of disulfide bonds, there are non-covalent attractive forces that need to be considered during the solubilisation or partial solubilisation of keratin materials. Ghosh and Collie (2014) identified the following forces;

- The ionic interactions or salt brides between charged acidic and basic amino acid residues;

- Hydrogen bonding between polar amino acid side chains and,

- Hydrophobic interactions or van der Waals forces between non-polar regions of the protein.

Therefore, in order to dissolve the bulk these soluble proteins, aqueous solutions of urea or guanadium hydrochloride can be used (Arai et al., 1990; Schrooven et al., 1998; Yamauchi et al., 1996). Furthermore, the use of ionic liquids for the solubilisation of proteins has been reported (Ghosh et al., 2013; Li, R. and Wang, 2013; Idris et al., 2013; Xie et al., 2005; Sun et al., 2009).

2.1.5.1 Oxidation treatments of wool fibres

The reaction between wool keratin and oxidizing agents has long been recognised (Stoves, 1949). The selective degradation of disulphide bonds is extremely complex, often other groups are oxidised and considerable degradation is found. Identifying the reacted functional groups can be a difficult process, due to the chemical complexity of the wool fibres.

2.1.5.1.1 Formic acid treatment

Fan et al. (2007) developed a procedure for rapidly removing the cuticle layer from Merino wool fibres. Initially the wool samples were boiled in highly concentrated formic acid (98%) for various durations; however, it was concluded that long treatment durations caused serious fibrillation and uneven removal of the cuticle. Consequently, the formic acid concentration was reduced to 88% and the treatment duration was reduced to 10 minutes, enabling the liberation of cuticles, before being subjected to consecutive ultrasonic treatments in fresh formic acid (88%) at 400 W and 200 W for respective 10 and 20 min time intervals. It was shown as an effective and rapid method to remove cuticle layer from Merino wool fibres. Additionally, an ultrasonic treatment could be employed after the formic acid treatment to cleave the excess cuticles from the wool fibres. This may enable a reduction in formic acid treatment time, which would prevent extreme cortex degradation and longitudinal crack formation (Fan et al., 2007). Researchers from the University of Leeds determined that various types of wool fibres require the following formic acid treatment times (see Table 2.8) to remove the cuticle layer within British wool fibres.

Table 2.8 - Wool sample formic acid treatment times

Wool Sample Code	British medium fine wool (Lowland) (MFL)	British medium fine wool (Hill) (MFH)	British cross wool (C)	British lustre wool (L)	British hill wool (H)	British black colour wool (B)	British mountain wool (M)
Treatment Time (min)	120	60	60	60	120	180	60

2.1.5.1.2 Urea hydrogen peroxide treatment

Mao (2013) found that a significant amount of macropores could be created within the wool microstructure after being treated in urea hydrogen peroxide (UHP) solutions. A British medium fine hill wool (MFH) was treated with 4% UHP for 5, 10 and 15 min time intervals at 20 °C. The resultant wool fibre cross-sections were investigated using

SEM. Furthermore, the amount of pore volumes had a positive correlation with the UHP solution treatment times. From previous research at The University of Leeds, urea was known to be a swelling assistant agent for the wool cortex layer and CMC. Its derivative, urea hydrogen peroxides (UHP) (i.e., carbamide peroxide, and urea peroxide), an adduct of hydrogen peroxide and urea, was used as an improved diffusion and swelling agents in medicine areas. While hydrogen peroxide is used to bleach cotton, wool, flax and wood fibre, the effect of the urea hydrogen peroxide (UHP) on the treatment of wool fibre was not reported. In addition to UHP solutions, Mao (2013) investigated urea solutions and UHP solutions with alkaline additives (Na_2CO_3 and Na_2SiO_4), since bleach treatments using hydrogen peroxide and alkaline additives have been proven to release oxygen oxidised gaseous more quickly within textile materials. However, it was found that both treatments did not increase the macro porosity of the wool fibres and there was evidence of damage to the cortex layer.

2.1.5.1.3 Ozone treatment

Ozone treatments are a growing research field due to the large range of emerging applications, changes to environmental legislation and increasing market demands (Perincek, S. et al., 2011). Thorsen (1965), described ozone on wool as an oxidative treatment that had been explored since the early decades of the 20th century. It was understood in early research that wool under ordinary atmospheric conditions reacted very slowly with ozone (Brown, 1928); however, moistened fabric reacted at a much higher rate. Subsequently, the use of ozone in wet textile processes is well documented within more recent published research journals (Benli and Bahtiyari, 2015). The main applications are fibre bleaching (Prabaharan and Rao, 2001; Perincek, S.D. et al., 2007) and improving the dyeability of fibres (Atav and Yurdakul, 2011; Perincek, S. et al., 2008). Ozone reacts with organic compounds directly in acidic/ neutral conditions or indirectly by decomposition at a highly alkaline pH (Gültekin and Ince, 2006). It can easily breakdown ingredients that cannot be

decomposed by conventional oxidisers (Perincek, S. et al., 2011). Wan and Yu (2011) demonstrated that the surface physical and chemical properties within the surface of hydrogen peroxide pre-treated wool fabrics was affected after ozone treatment in water. SEM demonstrated that crimp was generated and some scales were removed as a result of the treatment. Fourier transform infrared spectra (FTIR) results suggested that the absorbency and the oxidation of disulfide bonds increased after the treatment. Finally, the crystallinity of the treated wool fibres slightly increased based on the X-ray results. However, the effect of the treatment on the pore formation within wool fibres was not considered.

2.1.5.2 **Reduction treatment of wool fibres by sodium hydroxide**

Previous research at the University of Leeds (Mao, 2013) determined that British wool fibres (MFH) experienced a shrinking phenomenon. In this research, untreated and FA treated British hill wool fibres (H) were subjected to different concentration of NaOH solutions for different time durations to determine NaOH treatment parameters that affect the pore formation within wool fibres.

It was found that, after subjected to the treatment in sodium hydroxide (NaOH) solutions of relatively greater concentrations, the cuticle layer of the wool fibres become deformed rather than being removed (Figure 2.22 and Figure 2.23). The fibres was found experienced a significant reduction in fibre weight (~15-20%), and the sodium hydroxide solution becomes yellowish and a sulphurous odour was present during and after the treatment. This implied that certain components of the wool fibres were dissolved into the solutions while these dissolved components were not identified in this research.
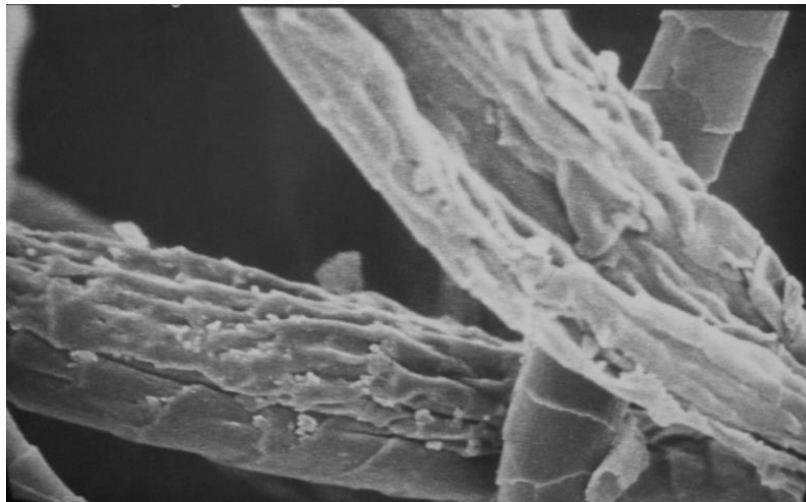
Figure 2.22 - British hill wool fibres (H) subjected to NaOH solution (5% w: v) for 10 min
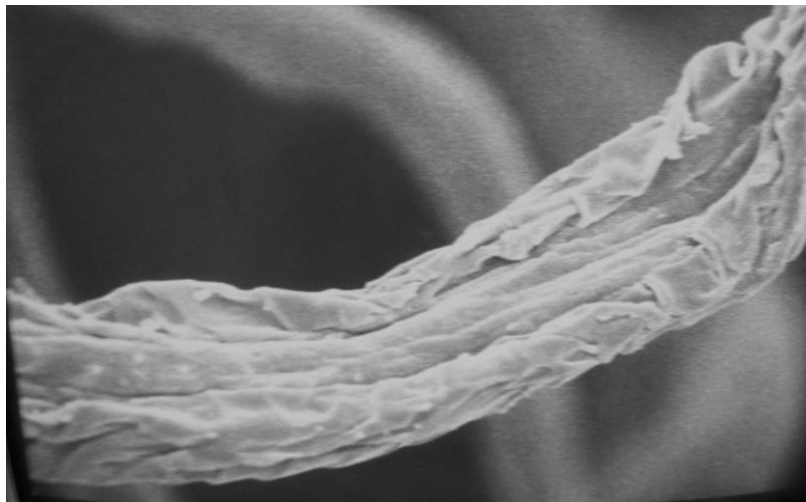
Figure 2.23 - British hill wool fibres subjected to NaOH solution (5% w: v) for 10 min

The wool fibres exhibited a marked reduction in apparent density after the sodium hydroxide treatments, suggesting the volume of accessible pores within the wool fibres increased. It is possible the sodium hydroxide solubilises part of the cortex of the wool fibre leading to the formation of channels and pores within the internal wool structure.

2.1.6 Methods for exposing the internal pore formations within the chemically modified fibres

Advances within the fabrication of nanoscale structures have been predominately driven by the electronics industry to develop optical and micromechanical devices (Kazuo, 2008). These fabrication techniques are either categorised as either 'bottom-up' or 'top-down' approaches. The 'bottom-up' approach is based on the deposition of nanoparticles to create intricate surface morphologies. However, this approach is restricted by the fact that it relies upon the self-organisation of the particles during the growth process. The 'top-down' approach removes superficial material to form complex surface features, using either physical or chemical treatments (Biswas et al., 2012). By investigating the mechanisms associated with these approaches the wool fibres could be modified further to expose the internal pore features created by the chemical pre-treatments (Ward and Mao, 2015).

2.1.6.1 Material modification using high energy electron impact

The stability of proteins when exposed to ionizing radiation has been explored previously for various applications. Early studies for the purpose of crystallographic examination determined that the contraction of wool fibres increased in steam when the fibres were exposed to X-ray radiation (Astbury and Woods, 1933). Also, O'Connell and Waldne (1957) and Zahn et al. (1959) both reported that the strength and extensibility of wool decreases after exposure to ionizing radiations. Alexander et al. (1960) determined that the secondary structure of solid serum albumin, as well as some other globular proteins could be altered by irradiation, presumably by the rupture of hydrogen bonds. Various possibilities for the breakage of hydrogen bonds using single ionization has been discussed by Platzman and Franck (1958), however, the mechanism associated with this phenomenon is not known.

Allen and Alexander (1961) used analytical techniques to investigate the supercontraction behaviour and to detect the disorientation in the hydrogen bonds

within the wool fibres when subjected to irradiation in concentrated aqueous solutions of lithium bromide and in solutions of sodium bisulfite. Supercontraction occurs spontaneously when wool is treated with a solution capable of breaking hydrogen bonds or if treated with a reagent that disrupts disulfide bonds (Alexander and Hudson, 1954). One conclusion drawn from the research conducted by Allen and Alexander (1961) was that wool contracts by breaking the disulfide bonds in the matrix in which micelles are held when exposed to either lithium bromide or sodium bisulfite. Also, this effect is increased significantly by irradiation, particularly when treated with lithium bromide. Therefore, there is evidence to suggest that different chemically modified wool fibres will supercontract or degrade differently when exposed to irradiation.

Di Modica and Marzona (1968) investigated the variations of content of some amino acids within wool fibres as a result of exposure to ionizing radiation. The wool fibres were exposed to 50 Mrad under oxygen or nitrogen and the amino acid compositions were compared to untreated wool fibres. A reduction in the content of amino acids was evident when the wool fibres were irradiated in the presence of both nitrogen and oxygen. Also, there were discrepancies between the reduction content of amino acids when nitrogen and oxygen were present. The research suggested that the presence of oxygen changed the cysteine and cysteine content, which suggested a breakdown of disulfide bonds. The research also determined that the disruption to the wool fibres was only at low-energy level linkages and on the secondary tertiary structure of the wool fibres. It is worth noting that this was early work and the analytical techniques used for quantifying the amino acid compositions were limited; therefore, any experimental design concepts proposed from conclusions drawn from this research will be evaluated accordingly.

Electron beam irradiation processes are often used for sterilisation or material modification. Bombarded electrons can penetrate materials while reacting with molecules to form free radicals or cross-linked materials, causing enhanced mechanical, thermal and chemical properties. In this study the effect of irradiation after

58

individual and consecutive chemical treatments and treatment durations will be investigated. Furthermore, the effect of irradiation in the presence of similar effect oxygen (relate to oxygen plasma treatment) will be investigated to determine whether the treatment is capable of causing pore formation within the wool fibres.

2.1.6.2 Low pressure plasma treatment of wool fibres

Plasma processes have become popular within the textile industry due to the unique physical and chemical characteristics of the plasma environment. Plasma is an ionised gas, comprising a dynamic mix of ions, electrons, neutrons, photons, free radicals, meta-stable excited species and molecular and polymeric fragments (Shishoo, 2007). The plasma medium is produced by coupling electromagnetic power into a process gas volume. The species move under magnetic fields and diffusion gradients, and interact with the textile substrates, causing various surface modifications (Graham, 2007). These modifications include:

- Surface activation caused by the breakage of bonds causing reactive sites.

- Grafting of chemical moieties and functional groups.

- Material volatilisation and etching.

- Removal of surface contaminants (scouring/ cleaning).

There are various forms of plasma reactors with power ranges between 10-5000 W, depending on the size of the reactor and the desired treatments. The reactors are capable of producing low-pressure and atmospheric pressure plasmas. Low pressure plasmas are a mature technology and are advantageous due to their controlled and reproducible environments. Typically, the pressure within the chamber/ vessel is reduced to a range between 10^{-2} to 10^{-3} mbar and the gas which is introduced into the chamber is ionised with the help of a high frequency generator (Shishoo, 2007).

Examples of atmospheric pressure plasmas include corona treatment, dielectric barrier discharge and glow discharge. Corona and dielectric barrier discharge treatments produce less controllable plasmas than low-pressure plasma treatments; consequently,

these processes produce less uniform surface characteristics. Conversely, glow discharge treatment is capable of producing uniform, homogeneous and stable discharge similar to low-pressure treatments. This cold-plasma method has many of the benefits of vacuum treatments and could be advantageous from an upscale perspective (Shishoo, 2007). However, the low pressure plasma technique was selected due to the processing environment similarities with the SEM technique.

The plasma state can be reached if the gas is under sufficiently low-pressure and when electromagnetic energy is provided to the gas volume. If these conditions are reached then the process gas will be partially decomposed into radicals and atoms and will be partially ionised. In order to attain an equilibrium state where a high density of charged particles is reached, the pressure range within the system will need to adjust depending on the frequency of the electromagnetic energy. For the radiofrequency range (40 kHz or 13.56 MHz) and microwave range (300 GHz to 300 MHz), the working gas pressure is typically kept in the lower 0.1 mbar and 0.05-0.1 mbar ranges, respectively. Lippens (2007) describes that in order to effect the plasma treatment in pure gas conditions, a base pressure in the lower 0.01 mbar needs to be reached. Furthermore, Lippens (2007) describes different plasma modes as either 'soft' or 'hard' plasmas. The type of mode depends on whether only radicals and/or atoms are used or whether charged particles are also allowed to impede on the substrate (Lippens, 2007).

One major effect of the plasma treatments is etching. Low-pressure plasma systems are commonly used for surface material removal as significant etching effects require longer treatment times and almost all etching gases can be used in low-pressure plasma. Three basic etching methods are used to modify materials surfaces, including, ion etching, chemical plasma etching and reactive ion etching. Ion etching effect is based on the ejection of atoms and molecules from the material through the kinetic energy of the accelerated electrons in the electromagnetic field. Chemical plasma etching converts atoms and molecules within the substrate into gaseous products when

reacted with radicals within the plasma. Reactive ion etching combines the effects of ion etching and plasma etching, which has the potential to increase the etching rate.

2.2 Objectives of the research

It is known that wool fibres are capable of absorbing a certain level of VOCs during to their chemical compositions of keratin protein. However, their current adsorption capacities are limited and their physical adsorption capacities have hardly been explored yet. Therefore, this research attempts to modify the complex hierarchical structure of wool fibre to form reticulated internal porous structures within the fibre in order to ultimately enhance its adsorption capacities while maintain its moisture management properties.

The objectives of this research are as follows:

1) To form macropores, mesopores and micropores if possible, by using various chemical modification processes such as

        (a) Formic acid treatment

        (b) Ozone treatment in water and UHP solution;

        (c) Sodium hydroxide.

        (d) Consecutive treatments

        the feasibility of creating porous wool fibres using alternative methods including microwave and Rapid expansion of supercritical solutions (RESS) might also be explored.

2) To form porous wool fibres having accessible pores by using various methods, e.g., selective degradation of keratin polymers including plasma treatment.

3) To achieve adsorption capacities of wool fibres through incorporating nanoporous materials into resultant porous wool fibres;

4) To identify suitable methods to differentiate and quantify the characteristics of the resultant porous wool fibres containing closed and open pores.

Chapter 3 Research Methodology and Experimental Plan

In this chapter, the methodology and background theories employed in this research are elaborated, and corresponding experimental plan, techniques, materials and equipment used are explained.

3.1 Research methodology

3.1.1 Strategy for forming porous wool fibres

To achieve the objectives of the research shown in the section 2.2, the research methodology we intend to implement is formulated into three steps below.

1. To form macropores (> 50 µm), and potentially meso-/micro- pores (< 50 nm) in wool fibres, the effect of individual and consecutive chemicals treatments on the changes of fibre microstructures is investigated (see Chapter 4).
   At the same time, the methodologies and their possible combinations to characterise different types of pores and pore distributions will be identified.

2. As pores formed in wool fibres during chemical treatment could be both accessible pores and non-accessible pores, the effect of selective degradation process such as plasma and high energy electron beam/ X-ray radiation on the pore structures in the resultant wool keratin polymers are studied (see Chapter 5).

3. After accessible pores created in step 2, the technologies of incorporating nanoporous materials which is known to have excellent adsorption properties into porous wool fibres will be studied to achieve porous wool fibres having adsorbent properties (see Chapter 6).

The experimental strategy was explored using the experimental strategy illustrated within Figure 3.1, which incorporates individual and consecutive chemical treatments, impact of high energy particles and incorporation of micro-porous materials.
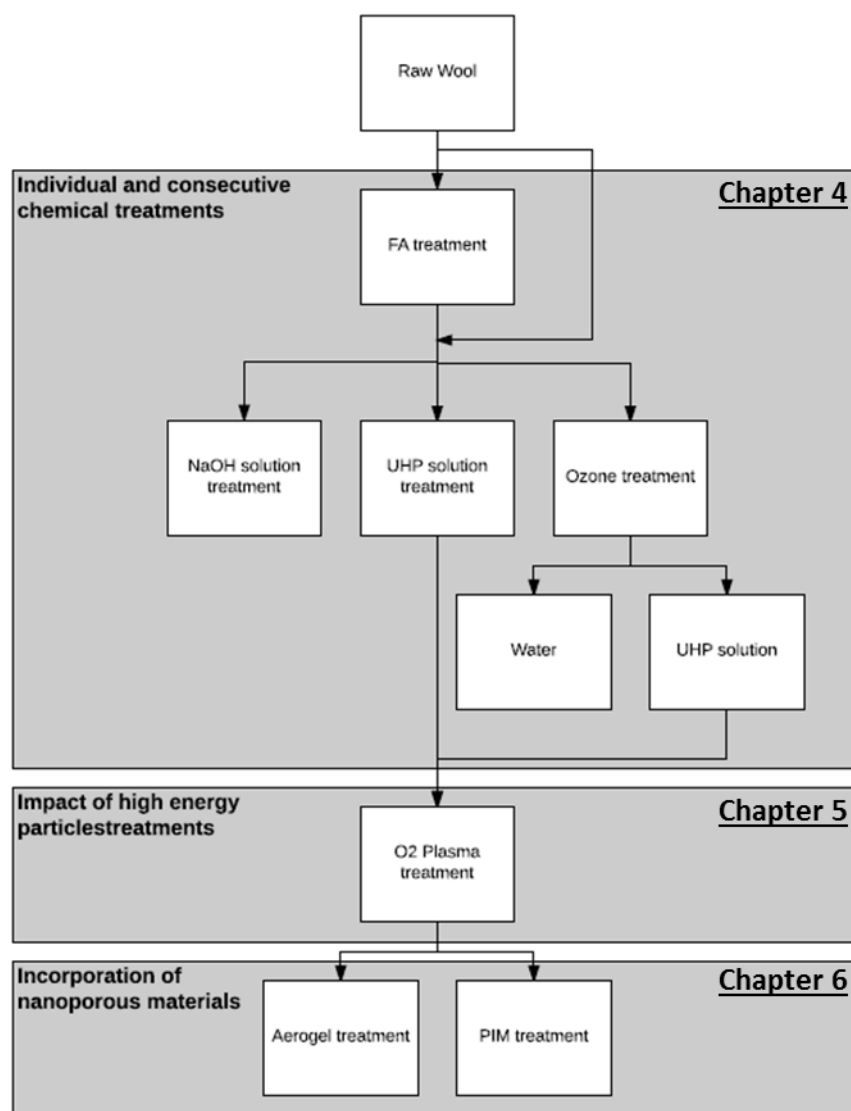
Figure 3.1 - Flow chart of experimental plan

The envisaged changes of wool fibre microstructures are illustrated within Figure 3.2. Firstly, macro-/ meso-/ micropores and fibrillation of wool fibres are resultant from chemical and physical treatment (Figure 3.2 (b)), and the inaccessible/ closed pores are further opened and filled with nanoporous particles (Figure 3.2 (c)) to enhance the adsorption capacity of the keratin wool fibres.

(a) Raw wool fibre　　(b) Porous wool fibre　　(c) Porous wool fibre containing nanoporous materials
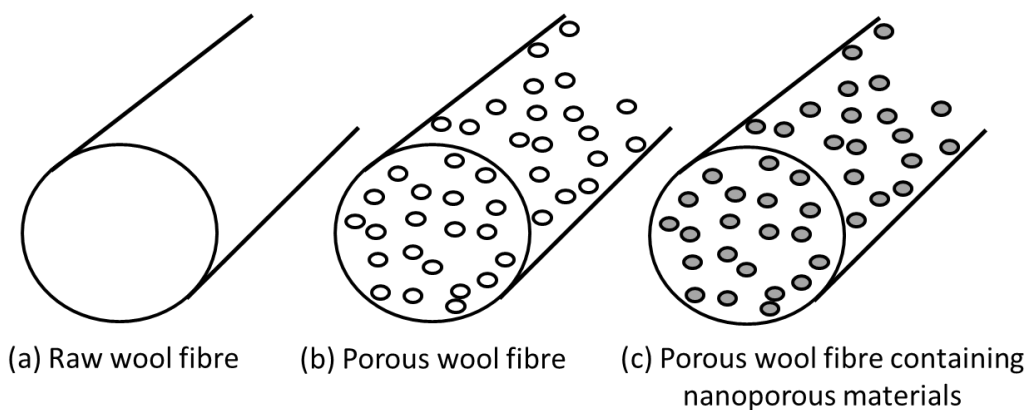
Figure 3.2 - Experimental strategy (wool fibres and cross-sections)

To create porous wool fibres, illustrated by Figure 3.2 (b), individual and consecutive chemical treatments will be employed (see Chapter 4) to modify the morphology of the wool fibres causing macro-/ micro-pore formation and fibrillation (see Figure 3.3 (1)). Selective degradation techniques will then be employed to expose inaccessible or closed pores (see Chapter 5). The resultant porous fibres will then be filled with nanoporous materials (see Figure 3.3 (2)) to create affective adsorption materials (see Chapter 6).

2. Create additional micro-pores within wool fibre macro-pores

1. Macro-pores, micro-pores and fibrillation
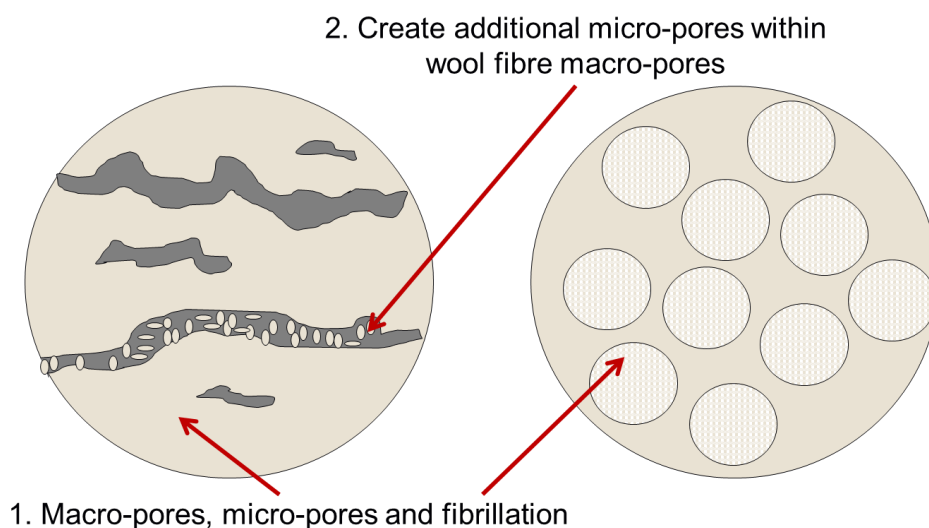
Figure 3.3 - Experimental strategy (wool fibre cross-sections)

The explanation of individual chemical treatment processes are explained in section 3.2. The techniques used for selective degradation and incorporating nanoporous materials are detailed within sections 3.3 and 1.1, respectively.

3.1.2 Strategy for the characterisation of resultant porous wool fibre structure

To differentiate and quantify the pores created using subsequent chemical treatments, the surface and internal morphology of the resultant wool fibres were characterised using scanning electron microscopy (SEM), mercury porosimetry (MP) and Brunauer–Emmett–Teller theory porosimetry (BET). Features and purposes of employing each of these characterisation techniques in this project are described in Table 3.1.

Table 3.1 - Methods for characterisation of porous structures

Analysis method	Features of pores measured	Range of pore size
SEM	Both accessible and inaccessible pores shown	Macropores (>50 nm)
Helium pycnometry	Only inaccessible pores $\uparrow$ AD $\rightarrow$ More inaccessible pores become accessible $\downarrow$ AD $\rightarrow$ More inaccessible pores created	Unable to determine pore size No restrictions
Mercury porosimetry	Only accessible pores (pore volume, pore size distribution)	3 nm – 400 μm
BET	Surface area of accessible pores	2 nm – 100 nm

To ensure the characterisation techniques represented the whole sample, wool fibres and fabrics were cut into staple fibres and strips, respectively. Then a proportion of the staple fibres and slivers were selected for testing. However, the limited sample output from the chemical modification trials restricted the number of repetitions tested for helium pycnometry, mercury porosimetry and gas adsorption using BET surface area characterisation techniques. Also, the testing duration and costs for mercury porosimetry and gas adsorption by BET restricted the number of samples that could be tested.

3.1.2.1 Fibre surface and internal morphology by Scanning Electron Microscope

To characterise the resultant wool fibres after chemical and physical modification, SEM was used to analyse the macro-structure of both the fibres surfaces and cross-sections. This technique is an effective method of determining whether pore formation is evident after treatments; however, differentiating between accessible an inaccessible pores is difficult to determine.

SEM systems used within this study:

- Carl Zeiss EVO MA15 - *Leeds Electron Microscopy and Spectroscopy Centre (LEMAS), School of Chemical and Process Engineering, Faculty of Engineering, University of Leeds, Leeds. LS2 9JT, United Kingdom. The materials were coated in platinum (Pt) using a Cressington 208 HR Sputter Coater.*

- JEOL JSM 6610LV - *School of Chemistry, University of Leeds, Leeds. LS2 9JT, United Kingdom. The materials were coated in gold (Au) using a Quorum Q15OR S Sputter Coater.*

- FEI Quanta 200 SEM - *Faculty of Biological Sciences, University of Leeds, Leeds. LS2 9JT, United Kingdom.*

3.1.2.2 Apparent density by Helium pycnometry

Helium pycnometry was used to measure the apparent density (AD) of the keratin wool fibres after the samples were conditioned in an oven for a minimum of 18 h at 100°C to remove any water residue. True density (TD), is also known as the skeletal density of solids obtained by helium pycnometry and varies with the volume of the pores accessible by helium molecules. However, inaccessible pores in the porous wool structure are accounted for as solid materials rather than pores due to the mechanism of this analytical technique. As the helium molecules are unable to access the internal pores (inaccessible pores), the density values obtained in this research are referred to

as AD. Mao (2013), identified that the AD measurement is an effective method for determining the porous structural changes in wool fibres. According to equation detailed in Figure 3.4 the AD of the material should increase if the internal cavities within the fibres become accessible to helium gas molecules used in the Micrometrics Accupyc 1330 Pycnometer; while AD decreases if any new inaccessible pores are created, or the volume of inaccessible pores created is more than the volume of accessible pores created. However, it is noted that no changes in AD does not mean that no new pores created, it might also means that the volume of accessible pores created equals the volume of inaccessible pores (see Figure 3.4).

Helium

Wool fibre cross - sections

ρ $\rho \downarrow$ $\rho \uparrow$ $\rho \uparrow or \downarrow$

More non-accessible pores   less non-accessible pores   More accessible and more non-accessible pores

$$\rho = \frac{m}{v}$$

Apparent density (ρ), mass (m) & volume (v).
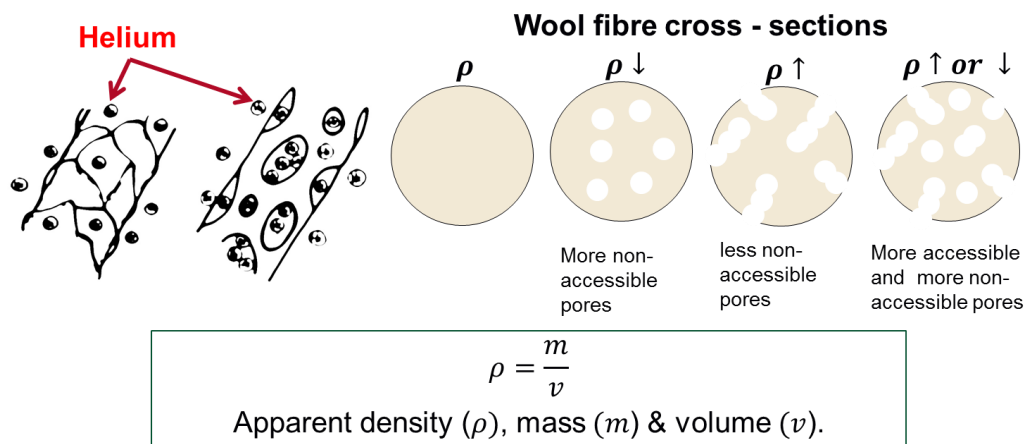
Figure 3.4 - Helium pycnometry analysis of wool fibres

Helium pycnometry system used within this study:

- Micromeritics' AccuPyc 1340 Pycnometer, Gas Displacement Pycnometry System - *ParticlesCIC, Faculty of Engineering, University of Leeds, Leeds. LS2 9JT, United Kingdom.*

3.1.2.1 **Specific surface area by gas adsorption, BET surface area (BET)**

BET is the capable of measuring pores >2 nm and has an upper pore size limit of 100 nm. Within the preliminary experiments, the wool fibres were conditioned in an oven at 50 °C to remove any excess water residue that could block the pores within the wool fibres. However, it is possible that this temperature was too low to evaporate the water

residue and could be the reason why BET surface area results were not attainable for all wool fibres types. Therefore, the wool fibres for all experiments were conditioned at 100 °C for a minimum of 18 h. To measure the BET surface area, wool samples measuring 0.2 g ± 0.001 fibres were inserted into a Micrometrics TriStar 3000. Both the sample tube and the sample tube containing the wool sample were measured gravimetrically before and after conditioning, using the same balance (capable of measuring to four decimal places). The conditioning process enabled water residue and any contaminants to be removed. These measurements were then used to calculate the true mass of the sample. The wool samples were cooled under vacuum at cryogenic temperature (77 K,-195 °C), using liquid nitrogen. A nitrogen adsorbate was then applied in 40 controlled increments. After each increment, the pressure was equilibrated and the quantity of adsorptive is calculated. The quantity of gas required to form a monolayer over the external surface of the solid is determined by an adsorptive isotherm, which is defined as the quantity adsorbed at each pressure increment.

A Micrometrics Tristar II system was used within the preliminary study; however, for the main study a Micrometric Gemini VII system was used as this system was more consistent at measuring the surface area of wool fibres. If the BET surface area results were unattainable the process was repeated until a measurement was recorded, with a maximum of three attempts. To ensure an accurate measurement and to obtain a result representative of the whole sample, the fibres and fabrics were cut into staple fibres and slivers respectively and mixed before loading into the sample tubes.

BET systems used within this study:

- Micrometrics Gemini VII – *School of Earth and Environment, Maths/Earth and Environment Building, University of Leeds, Leeds. LS2 9JT, United Kingdom.*

- Micrometrics Tristar II – *ParticlesCIC, Faculty of Engineering, University of Leeds, Leeds. LS2 9JT, United Kingdom.*

3.1.2.1 **Total pore volume and pore volume distribution by Mercury porosimetry**

Mercury porosimetry was used to measure the pore volumes of accessible pores of the keratin wool fibres and fabric. It has the capacity of measuring pores ranging from 3 nm to 400 µm; therefore, mercury porosimetry was used to measure both mesopores and macropores. The wool fibres were cut into 3-5 mm staple fibres (for the purpose of accessing pores created inner wool fibres); whereas, the worsted woven merino wool fabrics were cut into strips with 50 mm by 5 mm dimensions (for the purpose of filling the Mercury Penetrometer sealed sample cup). The samples were then conditioned in an oven for a minimum of 18 h at 100°C to remove any water residue. Figure 3.5 details four possible effects the chemical treatments will have on the wool fibres and how these effects will influence the total fibre pore volume (V_{pores}).
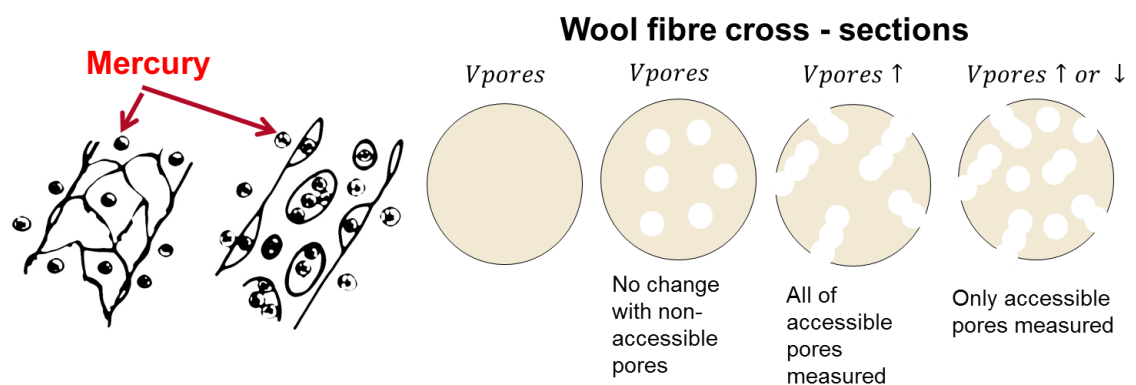
Figure 3.5 - Mercury porosimetry analysis of wool fibres

One shortcoming from this characterisation technique is that a single repetition was measured for each sample as the time duration to record a single sample was significant and costly. Therefore, to ensure a more accurate measurement and to obtain a result representative of the whole sample, the fibres and fabrics were cut into staple fibres and strips respectively and mixed before loading into the sample tubes.

Mercury porosimetry system used within this research:

- Micromeritics' AutoPore IV 9500 Series - *School of Earth and Environment, Maths/Earth and Environment Building, University of Leeds, Leeds. LS2 9JT, United Kingdom.*

3.1.2.2 Pore orientation angle and pore area distributions

Pore formations created using oxygen plasma treatments were characterised using image analysis software, FIJI. This software enables the features within the samples to be measured by calibrating the amount of pixels with the scale bar generated by the SEM software.

FIJI Image analysis software was used to quantify and differentiate between pores formed within the chemically pre-treated wool fibres after O_2 plasma treatment. Pore size distributions in terms of pore area and frequency were plotted, as well as, calculation of total pore area and total number of pores per 78.12 μm^2.

SEM images of chemically modified wool fibres were analysed using FIJI software in order to characterise the pore formation after consecutive chemical and subsequent plasma treatment. Two Areas of Interest (AOI) of 500 $pixel^2$ were selected for each fibre type from two SEM images with x8000 magnifications. The Image Type was set to 8-bit and the Threshold was set to 75 to create a monochrome image (see Figure 3.6). The pixel to scale ratio was calibrated using the scale bar in each SEM image.
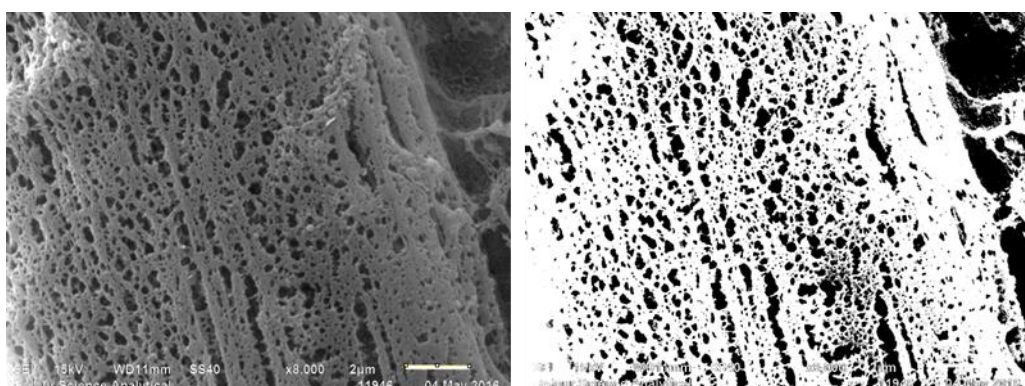
Figure 3.6 - Converting SEM image of wool fibres (Left) into monochrome format (Right)

To determine the pore area distributions the pores were converted into ellipses. The software is capable of measuring the length, width and angle of the fitted ellipses. The length and width are the primary and secondary axis of the best fitting ellipse. The 'Angle' is the angle between the primary axis and a line parallel to the X-axis of the image. The pore area distribution measured using image analysis in this paper is in a surface area of 78.12 μm^2 in wool fibre surfaces. For the pore area distributions the pore widths were plotted against the pore areas, which were obtained by differentiating between the clusters of white and black pixels (see Figure 3.7).
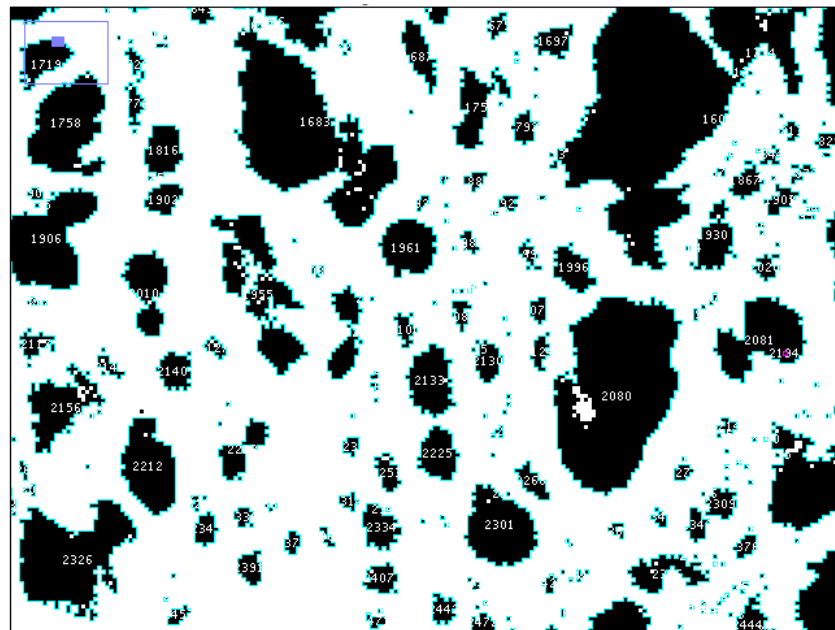
Figure 3.7 - The Image analysis software is capable of calculating the pore area of asymmetric pores detailed within monochrome SEM image by differentiating between the clusters of white and black pixels

The pore orientation angles for pores evident after treating chemically pre-treated wool fabrics with O_2 plasma were investigated using SEM and FIJI software. The software is capable of estimating individual pore areas, as well as, calculating the length (primary axis) and width (secondary axis) of the pores by modelling the pores as best fitting ellipses. The pore orientation angle is the angle between the primary axis and a line parallel to the X-axis of the image, as demonstrated within Figure 3.8.
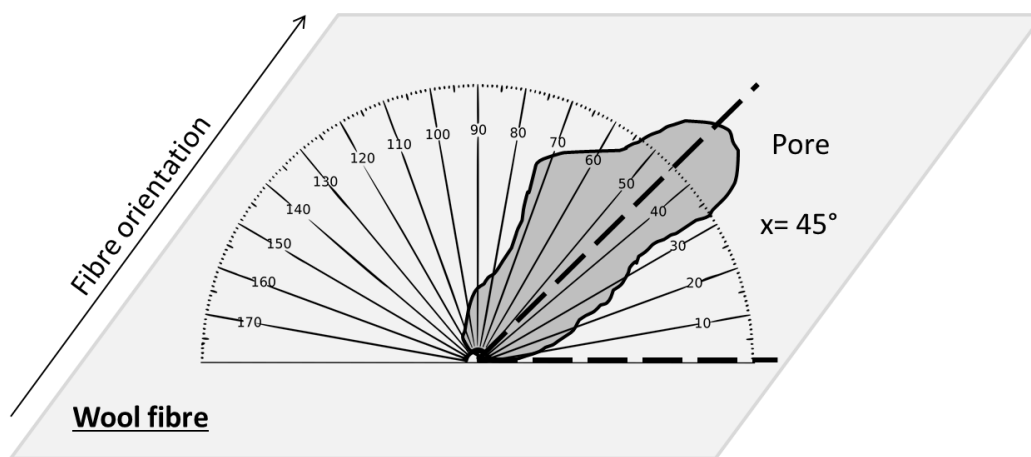
Figure 3.8 - Schematic demonstrating the method for calculating the pore angle of orientation. The angle between the pore length axis and the horizontal axis is called the pore orientation angle

3.1.2.3 **Dynamic Vapour Sorption (DVS)**

To investigate whether the developed wool-aerogel composite material is capable of adsorbing CWA, resultant wool fibres and fabrics were tested using a Dynamic Vapour Sorption (DVS) instrument (Surface Measurement Systems Ltd, Alperton, UK) at the DSTL. The DSTL performed cyclohexane adsorption capacity testing using this equipment. Cyclohexane is often used as a simulants for VOCs due to its molecular size and extensive use in industrial applications (Wang et al., 2015).

Dynamic Vapour Sorption system used within this study:

- *Cyclohexane adsorption in Dynamic Vapour Sorption (DVS) was done at the Defence Science and Technology Laboratory (DSTL), Porton Down, Idmiston, Salisbury SP4 0JG.*

3.1.2.4 **Characterisation of wool fibres**

It was found in the porosimetry and BET measurements that drying of wool samples significantly affects the pore size distribution obtained. If wool sample is not properly dried, neither an appropriate mercury amount against external pressure applied in porosimetry measurement nor a correct adsorption curve against applied N_2 gas

72

pressure for the sample could be obtained. Any water residue within the wool fibres could block the pores and prevent the intrusion of mercury/N_2 gases, which is fundamental to this analysis as the data is calculated as function of the pressure required for the mercury to enter the pores. Therefore, further investigation is required to determine the effect of water residue on the wool fibre adsorption properties and its influence on the measurement of pore structure of wool keratin fibres using the apparent density, mercury porosimetry and BET methods.

There is evidence in SEM that macro-pore volumes of the wool fibres increased after consecutive treatments. Also, partial cleaving of the cuticles causes an increase in surface area. Therefore, by partially exposing the cortex, the wool fibres can experience solvent saturation enabling swelling of the pores without compromising the benefits gained from leaving components of the cuticle still intact.

In a summary, each of the above techniques in isolation have their limitations in characterisation of wool fibre microstructures and their pore characteristics. In this research, multiple analytical techniques are thus employed to understand the effect of the individual and consecutive treatments on the internal microstructures of wool fibres created. For characterising the accessible pore formation within wool fibres, it was determined that using both SEM (external and internal features) and mercury porosimetry (total pore volumes and pore size distributions) in combination was the most effective way of quantifying and differentiating between pores formed. Apparent density obtained from a helium pycnometry test machine is used to characterise inaccessible pores/voids within wool fibres. Finally, DVS was used to measure the adsorption capacity of the resultant wool fibres and fabrics.

3.2 Techniques for chemical modification of keratin wool fibres

Before any chemical treatment of wool fibres, raw wool contains high levels of impurities (25–40 %), including wool grease, suint, dirt and vegetable matter, such as

seed and burrs. Wool grease is composed of a mixture of esters and fatty acids. Suint is mainly composed of the potassium salts of fatty acids plus sulfate, phosphate and nitrogenous compounds and arises from perspiration (Kozlowski, 2012). Therefore, scouring processes are required to remove such impurities.

For the scouring process, 20 grams of wool samples (fibres or fabric) were scoured in a non-ionic surfactant detergent (Hostapal NIN (Sigma Aldrich)) water solution of 600 ml with a concentration of 2g/L and pH value of 6.5-7.0, the scouring process was carried out at 60 °C in a Grant OLS200 water bath (School of Design, University of Leeds) for 30 minutes. The scoured wool samples were then rinsed using 2 litres of hot and then cold distilled water, followed by 500ml of distilled water before being dried at ambient conditions (~25 °C) for a minimum of 24 h.

3.2.1 Wool fibres and wool fabrics

In this research, there are two wool materials being modified, loose wool fibres and worsted wool fabrics. The loose fibres are used for the purpose of determining the effect of individual and consecutive chemical treatments on the morphological changes of wool fibres; whereas, the worsted wool fabric is used for the easier determination of the degradation effects on wool fibre surfaces during plasma treatments. The specifications and symbols of the wool materials used are shown in Table 3.2 below.

Table 3.2 - Specifications and symbols of the wool materials used in this research

Sample code	Description
MFL	British medium fine lowland wool fibres
MFH	British medium fine hill wool fibres
C	British cross wool fibres
L	British lustre wool fibres
H	British hill wool fibres
B	British black colour wool fibres
M	British mountain wool fibres
MWov	Australian worsted woven merino wool fabrics

Seven British crossbred wool fibres were supplied by the British Wool Marketing Board, Wool House/Sidings Cl, Bradford, BD2 1AZ. These fibres were selected for this study

as they are generally courser than fine wools, such as Merino wool. Also, British wool fibres are abundant materials that are relatively less expensive than finer wools.

Worsted woven Merino wool fibres were supplied by Whaleys (Bradford) LTD. Harris Court, Great Horton, Bradford, West Yorkshire, BD7 4EQ England. These fibres were selected for investigating the effect of exposing wool fibres to air and O_2 plasma after various chemical treatments. Initially, raw and chemically modified wool fibres were treated; however, the consistency of the high energy particle impacts was variable as the fibres were freely movable within the treatment chamber. Therefore, woven wool fibres were selected as they remain more stationary within the plasma chamber.

3.2.2 Formic acid treatment

British wool fibres were placed within round bottom flasks, containing a magnetic stirrer and Formic acid (≥98%, Sigma Aldrich) at 110 °C. The wool to FA liquor ratio was 1:50. The flask was attached to a condenser and suspended in an oil bath on a Fischer Scientific FB15001 heated magnetic stirrer (School of Design, University of Leeds). The temperature can be maintained in various time intervals depending on the requirements of treatments (Fan et al. (2007). However, the process was not followed by an ultrasonic treatment, the treatment times were considerably longer and a higher concentration of formic acid was used. The samples were then rinsed using 2 litres of hot and cold water, followed by 500 mL of distilled water before being dried at in an oven at 80 °C for 24 h.

3.2.3 Urea hydrogen peroxide treatment

Similar to Mao (2013), FA treated wool fibres and fabrics were treated with urea hydrogen peroxide (UHP) solution (4% hydrogen peroxide, 97%, Alfa Aesar), with liquid-to-wool ratio 80:1 v/w at RT. The samples were then rinsed using 2 litres of hot and cold water, followed by 500 mL of distilled water before being dried at in an oven at 80 °C for 24 h.

3.2.4 Ozone treatment

Raw and FA pre-treated British wool fibres were treated with ozone using an in-house Ozone treatment system (School of Design, University of Leeds), developed at the University of Leeds by using Ozone generator TCB-913GC (Trump Electronics, China). In this treatment, the wool fibres were saturated in either distilled water or a urea hydrogen peroxide (UHP) solution (4% hydrogen peroxide, 97%, Alfa Aesar) , with liquid-to-wool ratio 80:1 v/w, in a 500 mL measuring cylinder, within which the ozone outlet tube was positioned. The measuring cylinder was used in this experiment due to its narrow internal volume which enabled the wool fibres thoroughly treated by ozone gases by regulating the ozone gas flow bubbling through most of the wool fibre assemblies than an alternative wider vessel, such as a beaker. To prevent the wool fibres from floating onto the surface of the solution or becoming trapped between the side of the container and the ozone inlet tube the fibres were formed into small clusters and submerged into the solvent, which enabled the fibre clusters to move freely with ozone gas flows within the measuring cylinder, which maximised the chances of the ozone bubbles coming into contact with the wool fibres. The samples were then rinsed using 2 litres of hot and cold water, followed by 500 mL of distilled water before being dried at in an oven at 80 °C for 24 h.

For investigations detailed within Chapters 5 and 6, wool fabrics were treated instead of loose wool fibres for practical purposes as the woven fabric was easily positioned within the plasma chamber. Consequently, the ozone treatment apparatus configuration was modified and is illustrated within Figure 3.9.
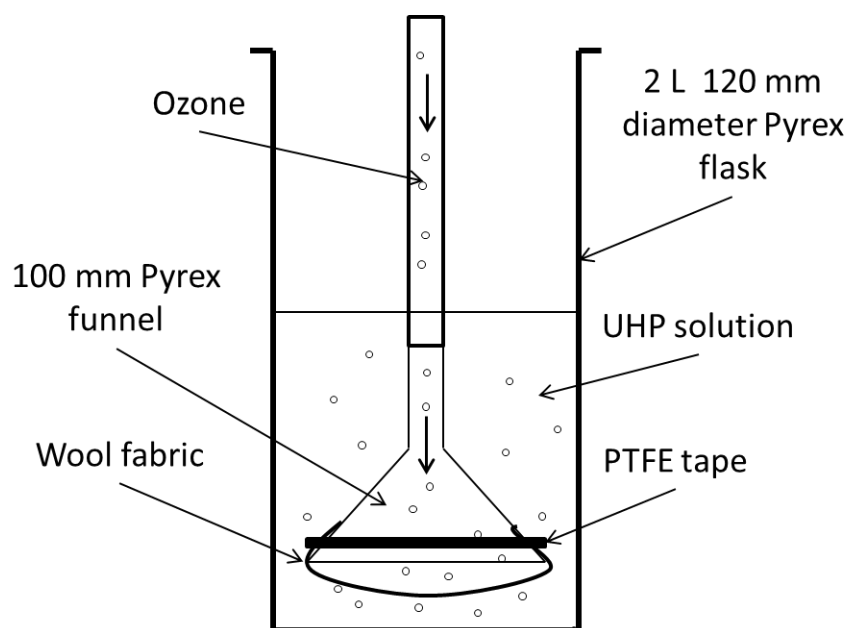
Figure 3.9 - Apparatus configuration for the ozone-UHP treatment

FA pre-treated MWov fabrics (10 g) were saturated in 800 mL of urea hydrogen peroxide (UHP) solution (4% hydrogen peroxide, 97%, Alfa Aesar), with liquid-to-wool ratio 80:1 v/w. The ozone generator outlet tube was attached to a 100m diameter Pyrex funnel and the FA pre-treated MWov fabrics were fixed to the funnel using PTFE tape. The FA pre-treated MWov fabrics were exposed to both UHP solution and ozone for 96 h at room temperature. The samples were then rinsed using 2 litres of hot and cold water, followed by 500 mL of distilled water before being dried at in an oven at 80 °C for 24 h.

3.2.5 Sodium hydroxide treatment

Sodium hydroxide (NaOH) (ACS reagent, ≥97.0%, pellets (Sigma Aldrich)) were dissolved into water for a minimum of 1 h with agitation to ensure a homogeneous solution. British hill wool (H) (2 g) was immersed in 100 mL of sodium hydroxide (NaOH) aqueous solution in a 500 mL beaker container. The wool samples were subjected to different concentrations of NaOH solutions (1% and 5%, w/v) for various time durations (2, 5 and 10 min). After sodium hydroxide treatment, the samples were

then neutralised using 100 mL of 1M sulphuric acid, 99.999% (Sigma Aldrich) aqueous solution. The samples were then rinsed using 2 litres of hot and cold water, followed by 500 mL of distilled water before being dried at in an oven at 80 °C for 24 h.

3.2.6 Consecutive treatments of wool fibres

In this project, the effect of the combination of several chemical treatments on the microstructure of wool fibres to maximise the amount of micropores and mesopores formed were also studied. These techniques include cuticle removal process by using formic acid treatment, swelling/oxidising treatment by using both urea hydrogen peroxide and ozone treatments, and a reduction treatment using sodium hydroxide.

3.3 Techniques for selective degradation of keratin polymers to form accessible macropores

A selective degradation technique was identified in this research while examining chemically modified wool fibres, using SEM. The mechanisms associated with this technique were investigated to determine whether alternative physical treatments will have the same or a similar effect to the microwave treatment of wool fibres.

3.3.1 Impact of high energy particles in SEM

Initially, raw and chemical modified wool fibres were examined using a Carl Zeiss EVO MA15 SEM machine (Leeds Electron Microscopy and Spectroscopy Centre (LEMAS), School of Chemical and Process Engineering, Faculty of Engineering, University of Leeds). The materials were coated in platinum (Pt) using a Cressington 208 HR Sputter Coater.

Subsequently, the effect of electron beam impact on British medium fine hill wool (MFH) with different chemical pre-treatments was investigated. FA pre-treated fibres and FA-ozone treated fibres in UHP solution for 24 and 96 h were subjected to electron impacts in a JEOL JSM 6610LV SEM system (School of Chemistry, University of

Leeds). The wool fibres were coated in gold (Au) using a Quorum Q15OR S sputter coater.

Energy-dispersive X-ray spectroscopy (EDX) was conducted in sequence with the SEM analysis. Initially, SEM pictures of wool fibre specimens were captured using an acceleration voltage of 20 kV. Then EDX analysis was conducted at 20 kV for 10 frames to determine the element compositions before exposing the specimen to a higher energy impact at acceleration voltage of 30 kV for 5 min. The EDX analysis was then repeated before capturing the final SEM image of the modified specimen, both systems use 20 kV of accelerated voltage for recording the effect of the high energy impact for both SEM and EDX in order to limit the effect of the high energy impact during the analysis processes. (Ideally, the acceleration voltage would have been set below 20 kV; however, the EDX system requires this acceleration voltage as a minimum value in order to detect the element composition of the specimen.

3.3.2 Plasma treatment of wool fibres

Chemically modified wool fibres and wool fabrics were exposed to air or oxygen plasmas using a Diener Pico Plasma system (School of Design, University of Leeds). The chamber temperature was regulated between 60-65 °C and the system was set to full power output (300 W). The wool samples were treated for a variety of time durations varying from 5-30 mins. Plasma treated fabrics were also treated on both sides. Compressed gas cylinders with a more consistent digital regulation of the gas flow were attached to the inlet, the gas flow rates were set between 0 - 45 $cm^3.min^{-1}$ depending on the experimental procedure. Plasma type, treatment time duration and gas flow rate were the main variables investigated about their effects on pore formations within chemically modified wool fibres and fabrics.

3.4 Techniques for incorporating nanoporous adsorbent materials into wool fibres

Both polymers of intrinsic micro-porosity (PIM) and silicon aerogels have excellent adsorption properties. They were synthesised to investigate whether they could be were incorporated into porous wool fibres to enhance their adsorption capacity. Synthesis of polymers of intrinsic micro-porosity (PIM) (Budd, P.M. et al., 2004b) and silicon aerogel (Du et al, 2014) can be found in various literature and due to their wet synthesis methods, it is possible the nanoporous materials can be absorbed into the resultant wool fibres filling both accessible and inaccessible pores.

3.4.1 Incorporation of PIM materials into porous wools

Two methods for incorporating the PIM material into FA pre-treated merino wool fibres in worsted woven fabrics were investigated. The main difference between the methods is the sequence of wool fabric saturation. Two different methods were investigated to identify a suitable method of incorporating the PIM materials into the porous wools. Firstly (method 1), the wool fibres were saturated with a solvent mixture and then saturated in water to initiate the PIM reaction within the porous wool fibres. Secondly, (method 2), the PIM reaction was initiated and then the wool fibres were saturated with the reaction mixture.

For method 1 (see Figure 3.10), a stoichiometric amount (0.374 g) of anhydrous potassium carbonate (K_2CO_3) ($\geq$ 99%, Sigma-Aldrich) was added to a mixture consisting of equimolar amounts of 5,5′,6,6′-Tetrahydroxy-3,3,3′,3′-tetramethyl-1,1′-spirobisindane (TTSBI) (97%, Alfa Aesar) (10.25 g, 30.1 mmol) and 2,3,5,6-tetrafluoroterephthalonitrile (TFTPN) (99%, Sigma-Aldrich) (6.02 g, 30.1 mmol). The mixture was then dissolved in anhydrous N,N-Dimethylformamide (DMF) (200 mL) and stirred at 60 °C for 75 h. The FA pre-treated (2 h) MWov wool fibres were then saturated within the mixture. While cooling, water (300 mL) was then added to the

mixture and the wool fibres and crude product were collected using vacuum filtration (Buchner funnel and filtration paper). Both the wool fibres and the crude product were then precipitated three times using 100 mL of methanol (MeOH) (≥ 99.9%, Merck). The experimental procedure for method 1 is illustrated within Figure 3.10 and the resultant PIM was shown in Figure 3.11.
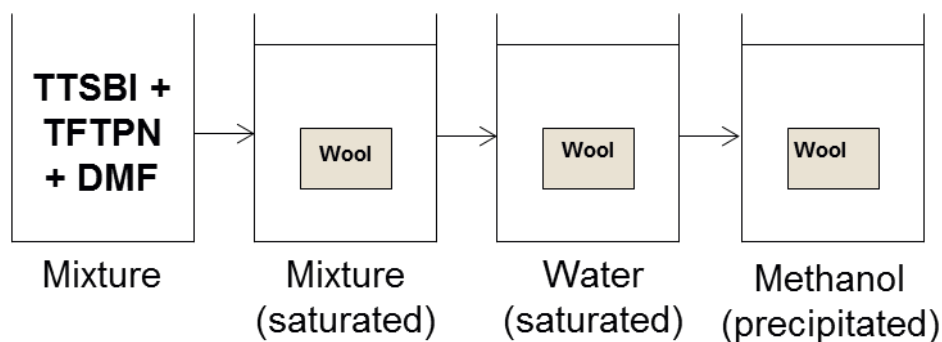
Figure 3.10 - Method 1: Incorporation of PIM into macropores

Figure 3.11 - (a) PIM during precipitation process; (b) PIM crude product

To form PIM films, the precipitated crude product (0.5 g) was dissolved in two different organic solvents, 25 mL of tetrahydrofuran (THF) (99.9 %, Fisher Chemical) and 25 mL of chloroform ($CHCl_3$) (Sigma Aldrich). The polymer solutions were poured into flat-bottomed glass petri dishes were allowed to precipitate at ambient conditions.

For method 2, the mixture preparation was the same as method 1; however, the FA pre-treated MWov fabrics were then saturated for 1 h while cooling and then removed from the mixture. The saturated MWov fabrics were then transferred to a beaker

81

containing 30 mL of water for 30 min. The wool fibres saturated with the crude product were then transferred to another beaker and precipitated three times using 300 mL of methanol (MeOH) (≥ 99.9%, Merck). The experimental procedure for method 2 is illustrated within Figure 3.12.
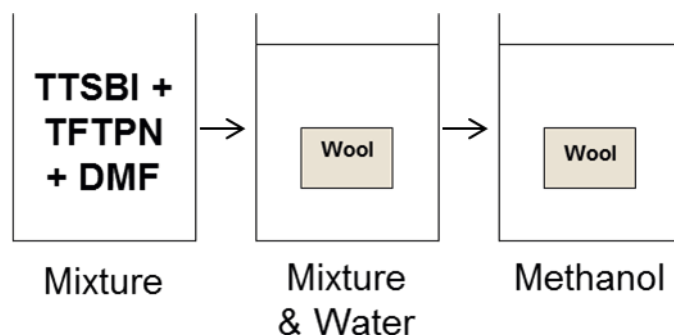
Figure 3.12 - Method 2: Incorporation of PIM into macropores

3.4.2 Incorporation of aerogels into porous wools

Methyltrimethoxysilane (MTMS) based silicone aerogel can be prepared using a two-step acid-base catalysed sol-gel process. Firstly, the MTMS, 97% (Alfa Aesar) precursor was mixed with methanol (anhydrous 99.8%, Sigma Aldrich) (MeOH), at 10:1 MeOH: MTMS molar ratios, then hydrolysed using a 0.01M aqueous solution of oxalic acid (Sigma Aldrich), under stirring at room temperature for 20 h to form a prepared sol. Secondly, 10 M ammonia solution (Sigma Aldrich) was gradually added into the resultant sol at a fixed feed rate of 5 ml.min^{-1} whilst stirring to initiate the condensation reaction. The water added during the sol synthesis stage comes from both the acid solution and the base solution. Therefore, the water from the oxalic acid and ammonia solution was kept constant at 2:1 molar ratio. The prepared sol was stored in an air-tight container at room temperature to allow gelation to occur. The elapsed time from the point of addition of the base solution to the moment of gel formation in the sol is referred to as the gelation time. After gelation, additional solvent (methanol) was added into the gel container and the silicone gel was then aged at room temperature for a

fixed period of 88 h. Finally, the resultant silicone gel was dried using supercritical carbon dioxide (45°C, 200bar) for 10h and then depressurised at a rate of 0.5 bar·min^{-1}. Silicone aerogel was incorporated into wool fibres by immersing wool fabrics into the sol above during condensation process. The above silicone sol was prepared by hydrolysing MeOH and MTMS with an aqueous solution of oxalic acid and stirred for 20 h. The sol was then poured into 20 mL screw-top jars. The ammonia solution was then added to the individual jars containing sol to initiate the condensation reaction. After agitation for 1 h to produce a homogenous solution, the various porous MWov wool fabrics were added to the sol for 10 min (A), 12 h (B) or 24 h (C) during the gelation stage (see Figure 3.13).
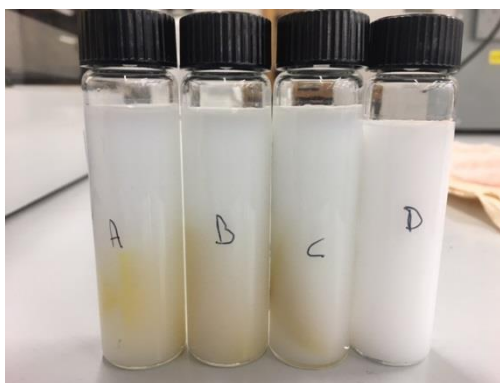
Figure 3.13 - 20 mL screw-top jars containing sol-gel and porous wools during the gelation stage of the aerogel formation process. Gelation stage exposure duration: (A) 10 min, (B) 12 h, (C) 24 h and (D) control

After the specific sol exposure durations the sol or sol-gel saturated wool fabrics were transferred to new jars containing 20 mL of methanol and aged at room temperature for a fixed period of 88 h. Finally, excess wet-gel was removed from the fabrics using a laboratory spatula. Then the resultant wool fabrics saturated with wet gel were dried using supercritical carbon dioxide (45°C, 200 bar) for 10 h and then depressurised at a rate of 0.5 bar·min^{-1}. The process for synthesising the wool-aerogel composite fabric is illustrated in Figure 3.14.

```
┌──────────────────┐
│                  │  Mixing of
│ Precursor solution│  precursors
└──────────────────┘
         │    Start of hydrolysis
         │    and condensation
         ▼
┌──────────────────┐
│                  │
│ Sol + porous wool│  Sol
└──────────────────┘
         │    Condensation of
         │    sol particles
         ▼
┌──────────────────┐
│                  │
│  Sol-gel + wool  │  Sol-gel
└──────────────────┘
         │    Gelation (10 min/
         │    12 h/ 24 h)
         ▼
Separate excess Sol-gel and
Sol-gel saturated wool
         │
         ▼
┌──────────────────┐
│                  │
│Sol-gel saturated wool│
│      + MeOH      │  Sol-gel
└──────────────────┘
         │    Ageing (88h)
         ▼
┌──────────────────┐
│                  │
│ "Wet" gel saturated│
│      wool        │  "Wet" gel
└──────────────────┘
         │    Supercritical CO₂
         │    drying process
         ▼
┌──────────────────┐
│                  │
│  Wool-aerogel    │
│ composite fabric │  Aerogel
└──────────────────┘
```

Figure 3.14 - Process for synthesising wool-aerogel composite fabric

3.5 Exploring other potential methods for producing porous wool fibres

In addition to the chemical treatments of wool fibres described in Chapter 1, two additional potential treatments (e.g., microwave and rapid extraction of supercritical solutions (RESS) treatment) were explored to determine whether a reticulated pore structure can be formed within wool fibres.

Raw wool fibres, sized fibres and partially gelated fibres were subjected to a microwave treatment to investigate the effect of microwave irradiation on the physical property, chemical structure, and surface morphological structure of wool fibres. This treatment was also applied to determine whether the "popping popcorn" mechanism could be applied to form pores within the wool fibres. However, no apparent cracking of cuticle layer has been observed and the porosimetry analytical techniques are unable to detect porous structure of the fibres containing sizing agents.

A RESS method was investigated as a means of replicating the "popcorn popping" mechanism described within the microwave treatment methodology. Similar to the microwave treatment, no apparent cracking within fibres was observed.

3.5.1 Microwave treatment of wool fibres

Raw and chemically modified wool fibres were sized using the following agents:

- Polyvinyl alcohol (PVA):
  - MOWIOL 40-88 (Sigma Aldrich).
- Carboxymethyl cellulose (CC):
  - Tylose MH 300 (Sigma Aldrich).
  - Tylose MH 1000 (Sigma Aldrich).
- Carboxy Methyl Starch (CMS):
  - Potato starch, soluble ACS reagent (Sigma Aldrich).
- Polyacrylate (PA):
  - Sodium polyacrylate, cross-linked (Sigma Aldrich).

The PVA, CMC and CMS solutions were prepared by adding 10% w/v of solid granules to a flask containing 90 mL of cold water. The flask was positioned in a water bath and agitated, and heated at a rate of $1°C.min^{-1}$ to the specified gelation temperature (Table 3.3) for 30 min. The PA size was readily dispersible in water; therefore, the material was mixed with water to obtain the desired concentration and heated to the specific application temperature.

Table 3.3 - Sizing temperature for specific materials (Slauson et al., 1984)

Size material	Sizing temperature (°C)
PVA	75
CMC	90
CMS	95
PA	55

Scoured British cross wool (C) fibres (2g) were saturated in water (100mL) for 10 minutes. The wool fibres were fed into the flask containing the size solutions and then the excess size was removed. The fibres were then dried in an oven for 5 min at 100°C and conditioned at RT for 48 h. After sizing, the wool fibres were positioned within a microwave popcorn maker (HQ Products) and subjected to microwave irradiation at 800W between 10-30 min.

Raw wool fibres, sized fibres and partially gelated fibres were subjected to a microwave treatment to investigate the effect of microwave irradiation on the physical property, chemical structure, and surface morphological structure of wool fibres. This treatment was also applied to determine whether the "popping popcorn" mechanism could be applied to form pores within the wool fibres. Moisture within kernel is superheated, which provides internal pressure. This causes the pericarp to rupture and the pressure forces the internal features of the kernel to expand, forming a reticulated porous structure. Currently, no apparent cracking of cuticle layer has been observed and the porosimetry analytical techniques are unable to detect porous structure of the fibres containing sizing agents. Therefore, investigations using these methodologies were discontinued; however, this concept could be investigated as further work.

3.5.2 RESS treatment of wool fibres

Scoured British cross (C) wool fibres (5 g) were cut into 3-4 mm staple fibres and treated with different concentrations of aqueous solutions containing urea and sodium bisulfite.

Scoured wool fibres (C) were prepared in two forms; raw wool fibres and pre-gelated staple fibres. The pre-gelated staple fibres were synthesised by cutting wool fibres into 3-4 mm snippets and then treated with a solution containing urea (8 M) and $Na_2S_2O_5$ (0.5 M) under shaking for different time durations at 65 °C. Table 3.4 details the samples and the treatment parameters. The wool fibres were washed with 1 L of water using vacuum filtration and left to dry at RT.

Table 3.4 - Time durations and solution concentrations of treated keratin fibres

Sample	Time duration (h)	Concentration of urea (M)	Concentration of sodium bisulfite (M)
1	1	8	0.5
2	2	8	0.5
3	4	8	0.5
4	8	8	0.5
5	24	8	0.5

The raw wool and pre-gelated fibres were subjected to RESS treatment using predetermined processing parameters. The fibres were extracted with an extraction vessel temperature of 100 °C to determine the effect of exposing the wool fibres to rapid depressurization, using a 100 bar extraction vessel chamber pressure. The precipitation vessel temperature and pressure was set to 25 °C and 1 bar, respectively. Ward and Mao (2014) completed a study of internal wool lipid extraction to achieve internal porous structure was investigated using $SCCO_2$ extraction (Chemical solvent in supercritical carbon dioxide extraction). Macro-pore formation was evident after this process. However, the rapid extraction of supercritical solutions (RESS) method was investigated as a means of replicating the "popcorn popping" mechanism described within the microwave treatment methodology. Similar to the microwave treatment, no apparent cracking within fibres has been observed. Both microwave treatment and RESS methods thus did not go ahead.

The techniques detailed within this chapter will be conducted with the aim of modifying wool fibres to achieve reticulated internal porous structures. Also, the resultant fibres

will be incorporated with nanoporous materials. These strategies will be employed in order to ultimately enhance the adsorption capacity of wool and/or its composite fibres.

Chapter 4 Chemical Modification of Wool Fibres to Achieve Porous Wool Structures

In this chapter, the effects of various individual and consecutive chemical treatments on the pore formation within wool fibres are investigated. Treatments of loose fibre assemblies to form macropores and micropores within wool fibres include formic acid treatment, ozone treatment in water and UHP solution, sodium hydroxide treatment and their combinations. Also, the methodologies to characterise different types of pores and pore distributions will be identified.

Wool is in an inhomogeneous composite structure, this is shown in fibre cross-sections due to the magnitude of cross-linking within the para-cortex and ortho-cortex regions (Bradbury, 1973). Also, in the areas where cuticle cells are still intact, chemical modifications to wool fibres might be inhomogeneous and restricted to localised areas. Therefore, multiple fibre cross-sections were examined in this research to get a true indication of the fibre morphology changes after chemical modification.

4.1 Microstructure of untreated wool fibres

Examination of the physical structure of the untreated wool fibres would help determine any changes made to the fibre microstructure and morphologies and help understand the effect of the chemical treatments on the structure of these keratin wool fibres.

SEM images (x750 magnification) of the 7 British wool fibres are shown in Figure 4.1. Interestingly, all samples display considerable differences in terms of fibre cross-section shape and size. Wool fibres MFL, H and M show irregular shaped cross-sections; all the other wool fibres have round or oval shaped cross sections. Also, wool fibres with and without medulla (Alexander and Hudson, 1963) were found among wool

fibres M. At x750 magnification, there are no severe discontinuities evident in the cell matrix or cortex.
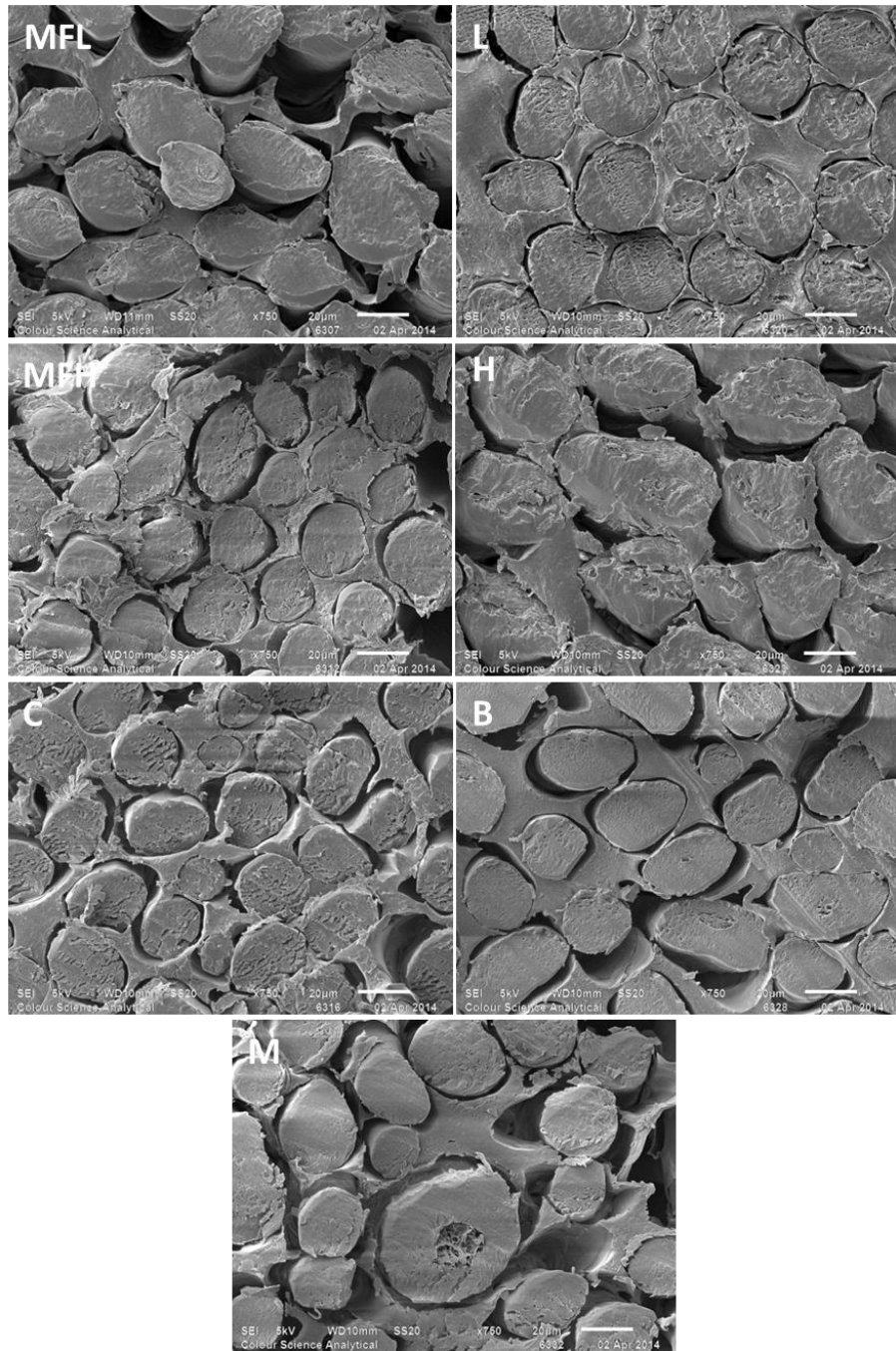
Figure 4.1 - British wool fibre cross-sections post scouring process (Mag. x750)

The apparent density measurement of the scoured wool fibres are detailed within Figure 4.2. The wool fibres have similar AD measurements (1.3070 – 1.3812 g.m^{-3}) with the exception of sample M, which has a greater AD of 1.5816 g.m^{-3}. As previously

identified in Figure 4.1, sample M has wool fibres with and without medulla in the wool samples, and the open pores existing in the medulla fibres could be the reason for the greater AD value of this sample.
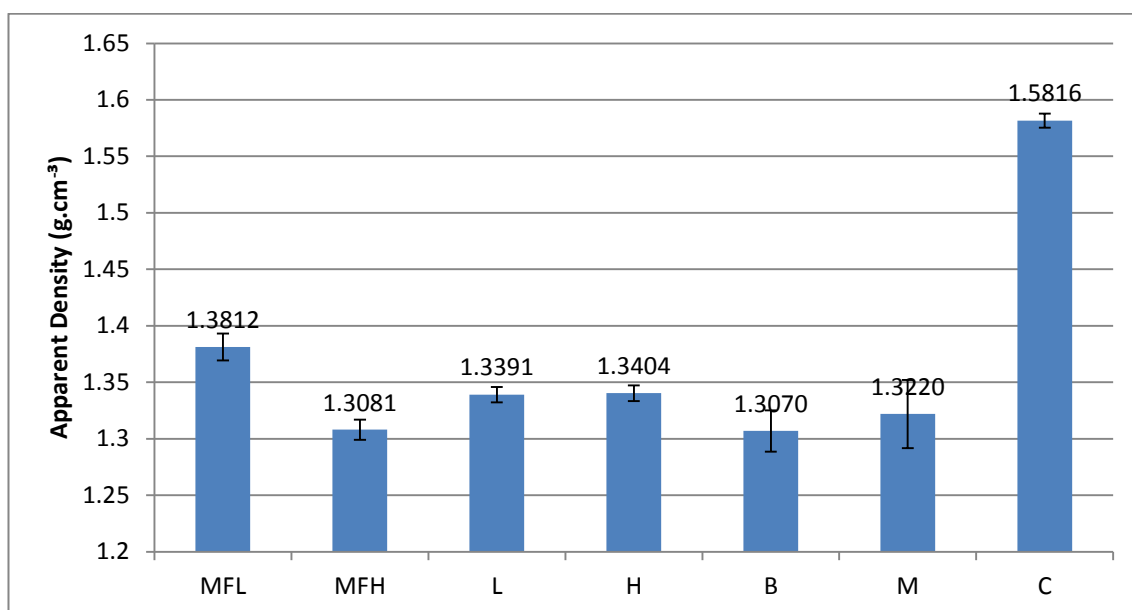
Figure 4.2 - Apparent density of scoured wool fibres

The BET surface areas of some scoured wool fibres are shown in Table 4.1, it is noted that the BET surface area of wool fibres L, H and M could not be measured at the time. This could be due to the limited amount of pores present, moisture blocking the pores or the pore range limitation (2-100 nm) of the characterisation technique (see 3.1.2.1).

Table 4.1 - BET surface area of various scoured wool fibres*

Wool	MFL	MFH	C	L	H	B	M
BET Surface area ($m^2.g^{-1}$)	1.03	1.30	1.15	N/A	N/A	1.94	N/A

BET surface area values for wool fibres L, H and M were unattainable

The British black wool fibres (B) had the greatest surface area (1.94 m^2/g) out of all the fibres tested while this surface area is still significantly lower than that of activated carbon adsorbents (800-1500 $m^2 \cdot g^{-1}$ (Bansal and Goyal, 2005)).

Water residues and contaminants contained in wool fibres may block pores inside the fibres, which would result in an overall lower BET surface area measured. Despite the

wool fibres being placed in a vacuum oven to remove any water residue or contaminants before being examined in BET machine (Micrometrics TriStar 3000); there is no evidence to suggest that the water content was completely removed from the wool fibres.

As a summary, it was found that, similar to Mao (2013), the scoured wool before any chemical treatment had no voids except medulla found in the fibre cross-sections. Also, the wool fibres demonstrated similar apparent densities, despite the variations in fibre diameters and cross-section geometries. The only exception was wool fibre M, which had a higher apparent density and contains medulla fibres.

4.2 The effects of various chemical treatments on the characteristics of pores formed in wool fibres

In this section, the effect of various chemical treatment and their combinations on the pore formation within wool fibres are investigated, and the characteristics of the pores formed are characterised.

4.2.1 Formic acid treatment

British wool fibres are considerably coarser than Merino wools, the method described by Fan et al. (2007) thus needs to be modified for the British wool fibres. Previous research at the University of Leeds (Mao, 2013) focused on the treatment conditions required to remove the cuticle layer of the British wool fibres (see Table 4.2). However, the effect of the formic acid (FA) conditions on the keratin wool fibre internal morphology was not investigated. Since Fan et al. (2007) determined that serious fibrillation was caused by long FA treatment durations, this research will attempt to determine whether pore formation is caused by the formic acid treatment.

(Mao, 2013) determined that the British wool fibres require the following formic acid treatment times to remove the cuticle layer (see Table 4.2).

Table 4.2 - Time durations of FA treatment (98%) for various wool fibres used in the research by (Mao, 2013)

Sample code	Wool type	FA treatment duration (h)
MFL_F2	British medium fine wool (Lowland)	2
MFH_F1	British medium fine wool (Hill)	1
C_F1	British cross wool	1
L_F1	British lustre wool	1
H_F2	British hill wool	2
B_F1.5	British black colour wool	1.5
M_F1	British mountain wool	1

However, the minimum time durations of the FA treatment needed for the removal of cuticles from various British wool fibres were not investigated. Since Fan et al. (2007) determined that serious fibrillation was caused by long FA treatment durations, this research will attempt to determine whether pore formation is caused by the formic acid treatment. The minimum time durations of FA treatment required to remove the cuticles and form internal pores for various British wool fibres are discussed in this section.

4.2.1.1 Changes of wool fibre morphologies in different FA treatment conditions

The formic acid treatment having considerably longer time duration and a higher concentration of formic acid without using ultrasonic treatment, derived from Fan *et al.* (2007) and Mao (2013) was used to remove the cuticle layer from the wool keratin fibres.

Initially, the pore fibres were treated by the same methodology described by (Mao, 2013) and detailed within Table 4.2. It is evident from the SEM images (see Figure 4.3) that the cortex of scoured wool of all the seven types of wool fibres were exposed after the proposed FA treatment.
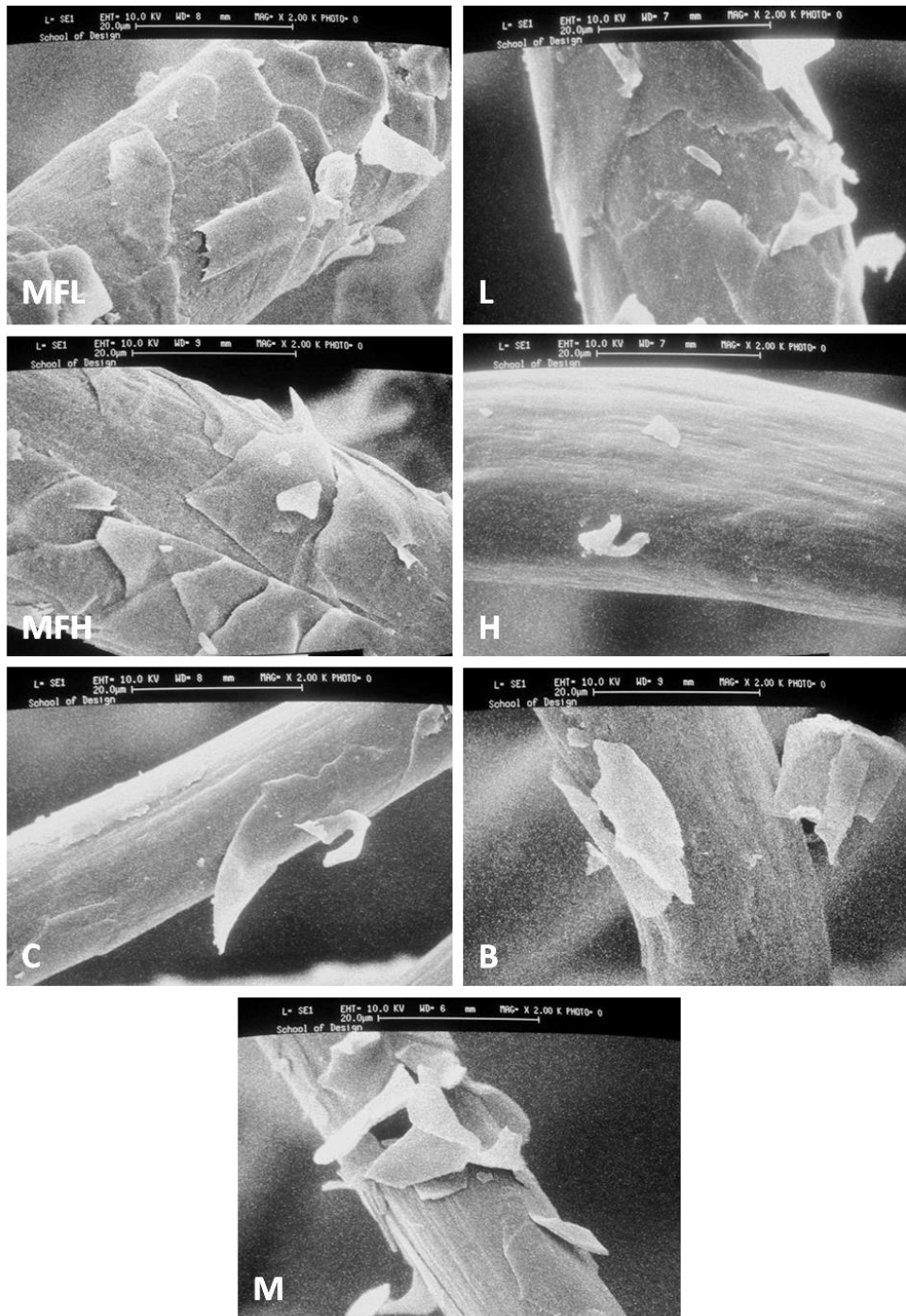
Figure 4.3 - Wool fibres post scouring process and FA Treatment (Mag. x2000)

However, not all cuticle layers have been cleaved; particularly fibres MFL, MFH and M, which were treated with FA for 2, 1.5 and 1 h durations, respectively (see Figure 4.3). This may prevent consistent cortex exposure to subsequent chemical treatments; however, increases of time duration of the FA treatment times eventually lead to severe

cortex degradation. Wool fibres MFL, H and B displayed some cortex degradation (see Figure 4.4). This phenomenon can be explained by findings observed by Fan et al. (2007) when investigating the swelling and disintegration of wool fibre in formic acid. Formic acid is a polar organic acid of small molecular weight, which can form a hydrogen bond with the carbonyl group of the protein. Fan et al. (2007) found that wool fibres exhibit a good affinity with formic acid and swelled intercellular and intermacrofibrillar components degrade before the crystalline features of the wool fires. These regions contain large compositions of lipids (<45%) (Hearle, J.W.S. , 2000), which are dissolved by formic acid, leading to the degradation of the CMC and intermacrofibrillar material coil structure (see section 2.1.4.4).
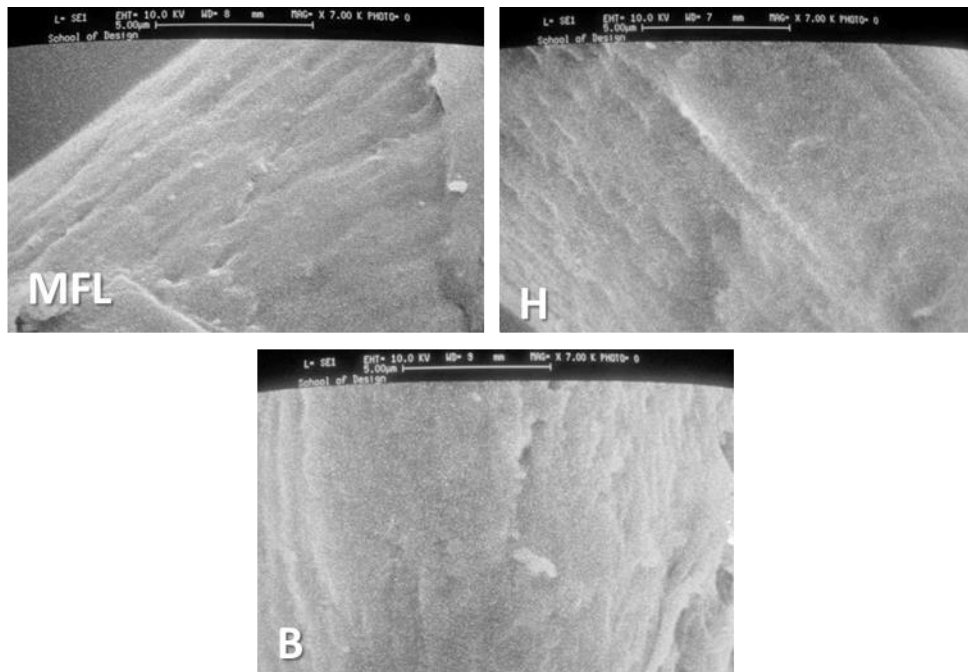
Figure 4.4 - Wool fibres post FA treatment showing cortex degradation

As a summary, wool fibres with limited cortex degradation with most of the cuticles removed could be achieved by adjusting FA treatment time durations and formic acid concentrations to enable further porous wool structure modifications.

4.2.1.2 **The effect of FA treatment on the internal porous structure of wool fibres**

The effect of the formic acid conditions on the keratin wool fibre internal morphology has not been investigated previously; therefore, an investigation to determine whether voids/visible pores could be formed during the formic acid treatment were conducted in this study using British medium fine hill (MFH) wool fibres. MFH wool fibres were treated in FA solutions with different FA exposure time durations (0.5-3 h) and the characteristics of their potential internal porous microstructure were examined. The experimental plan for this investigation is detailed within Table 4.3. Within the preliminary experiments, the wool fibres were treated with FA of 98% in concentration at 100 °C; to ensure the FA consistently remained at boiling temperature the temperature of the oil bath of the FA container immersed in was maintained at 110 °C.

Table 4.3 - The FA treatment for the pore formation within British wool fibres (British medium fine hill wool) (*Temperature: 100 °C; Formic acid (≥98%, Sigma Aldrich)*)

Sample code	FA treatment duration (h)
MFH (Control)	0
MFH_F0.5	0.5
MFH_F1	1
MFH_F2	2
MFH_F3	3

The wool fibre cross-sections for treatment times ranging from 0.5 - 3 h is shown in Figure 4.5, and macropores formed are evident within the cross sections of the MFH wool fibres treated in FA solutions for 1 h at 100 °C; however, the cuticle layer is still intact despite some signs of cuticle removal. After 2 h of FA exposure, the cuticle layers of the MFH wool fibres are apparently damaged and almost completely removed after 3 hours of FA treatment. The wool fibres were found to be brittle beyond 2 h of FA exposure.

Figure 4.5 demonstrates that subjecting wool fibres to FA at 100 °C causes some cracking and voids in fibre cross-sections, this is corresponding to the conclusions in

literature (Bradbury and Peters (1972)) that FA treatments could cause modification of the cell membrane complex and a slight change to the macrofibril-matrix structure of the cortex. This is likely to be caused by the hydrolysis of peptide bonds. Extending the treatment time duration appears to increase the level of modification of both the cell membrane complex and the macrofibril matrix structure of the cortex. However, the number of internal pores formed and their size do not appear to increase beyond 1 h of FA exposure, despite the increase of cuticle removals on the fibre surface and fibre degradation on external cortex. Consequently, a 1 h FA pre-treatment was selected for investigation of the effect of further ozone treatment in H_2O & UHP solutions on the pore formations in cortex exposed wool fibres (i.e., FA treated wool fibres).
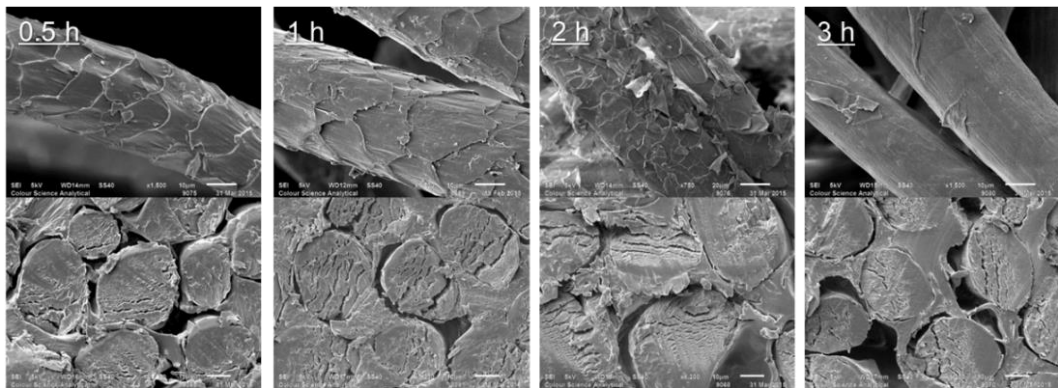
Figure 4.5 - British medium fine (hill) wool after formic acid treatment in different time durations. Columns left-to-right: 0.5, 1, 2, 3 h FA exposure. Fibre (Mag x1500) and fibre cross-section (Mag x2000)

Volumes of pores formed during FA treatment are characterised by using Mercury porosimetry to determine the effect of FA treatment on the wool fibres. The raw wool fibres contain pores with a total pore volume around 1.202 mL.g^{-1}, which is greater than that of the FA treated fibres (0.172 mL.g^{-1}). This is likely to be due to the damage or removal of cuticles on the wool fibres caused by FA treatments and the significant decrease in pore volumes of the pores formed by the cuticles on the wool fibre surfaces. Both phenomena are evident in the SEM images above (see Figure 4.5).

The pore size distribution shown in Figure 4.6 demonstrates that raw wool has pores between 1.2-1.4 µm, which are not detectable when treated with FA. Also, both fibres do not contain any micro- or mesopores.
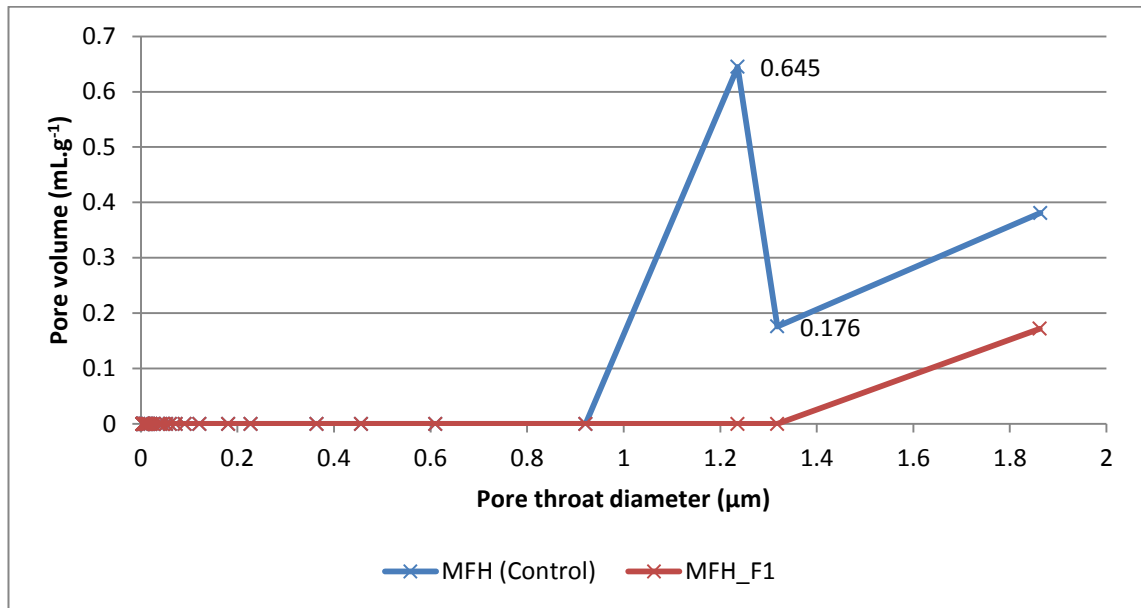
Figure 4.6 - Pore size (<2 µm) distribution of wool fibres with and without FA pre-treatment

The reduction in total pore volume and greater minimum pore size caused by the partial removal of the cuticles after FA treatment are illustrated in Figure 4.7. Additionally, the reduction in total pore volume could also be caused by shrinkage of the wool fibres after oxidation by FA treatment, followed by the drying process (80 °C for 24 h). As discussed earlier, the wool fibres initially swell and then degrade when exposed to the FA treatment. However, extensive exposure can lead to the degradation of both intercellular and intermacrofibrillar components, as well as, the crystalline features within the wool fibres. Fan et al. (2007) reported that the former components degraded first. Therefore, it is possible that subjecting the wool fibres to particular exposure duration will degrade the intercellular and intermacrofibrillar components, while the more crystalline features, such as cuticles, remain un-degraded or the degradation is limited. This affect may reduce the mass and volume of the cortex

leading to a shrinking phenomenon when dried. However, this is only a theory at this stage and further investigations are required to conclude this hypothesis.
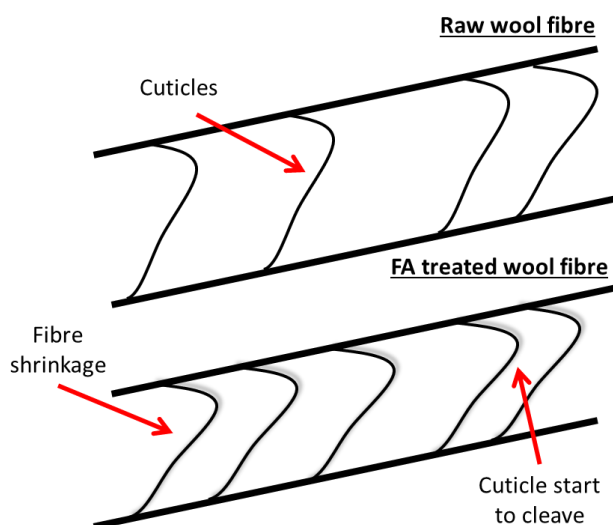
Figure 4.7 - Potential shrinkage of wool fibres and cuticle removal and damage

In summary, FA treatment of wool fibres is capable of introducing macropores within the MFH wool fibres; however, the pores appear to be encased by the cuticle or cortex exterior. Therefore, further treatments are required to further develop and expose these internal pores formed. Extending the treatment duration increases the removal of cuticles from the wool fibres and the cortex becomes exposed after two hours of FA treatment, while further extending the treatment duration beyond 2 hours for MFH wool fibres causes significant fibre brittleness and cortex degradation, and potential shrinkage.

In order to determine whether macro-pore formation within fibres after FA treatment is a common feature for other British wool fibres, the FA treatment was also conducted on British hill (H) wool fibres. Similar to the FA treated MFH wools, the SEM analysis of the fibre cross-sections of H wool fibres demonstrates that the cuticles have been removed and formation of macropores and cortex exposure are evident after FA treatment (Figure 4.8).
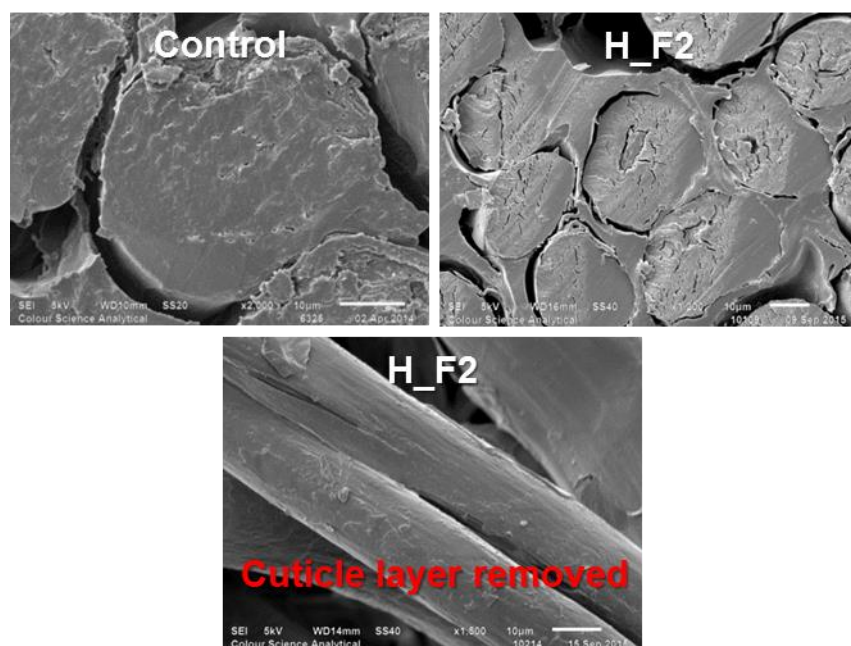
Figure 4.8 - Macropores formed in British hill wool fibres (H) after FA treatment for two hours

The apparent density of the wool fibres H before and after FA treatment, are measured by using helium pycnometry. It is shown that the apparent density values increase from 1.307 g.cm^{-3} for raw fibres to 1.334 g.cm^{-3} for FA treated fibres; this indicates that accessible pores formed within wool fibres during the FA treatment process are likely. Also, based on the results from mercury porosimetry, the total pore volumes of the accessible pores within the fibres increases from 0.052 mL.g^{-1} before FA treatment to 0.751 mL.g^{-1} after FA treatment (Figure 4.9). From this pore size distribution results (Figure 4.9), both the wool fibres before and after the FA treatment contain both macropores and mesopores, with many pores being mesopores.
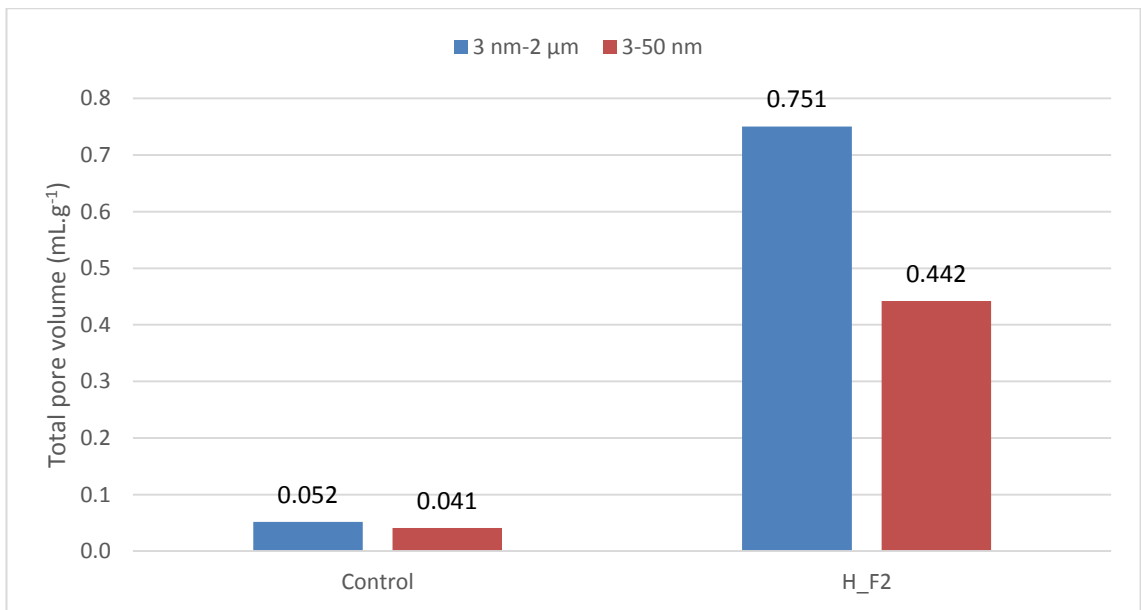
Figure 4.9 - Mercury porosimetry analysis (Total pore volume) of British hill wool fibres before and after FA pre-treatment, maximum pore throat diameter 2 µm

The mercury porosimetry pore size distribution (Figure 4.10) shows that there are a broad range of pore throat diameters of accessible pores after the FA treatment.
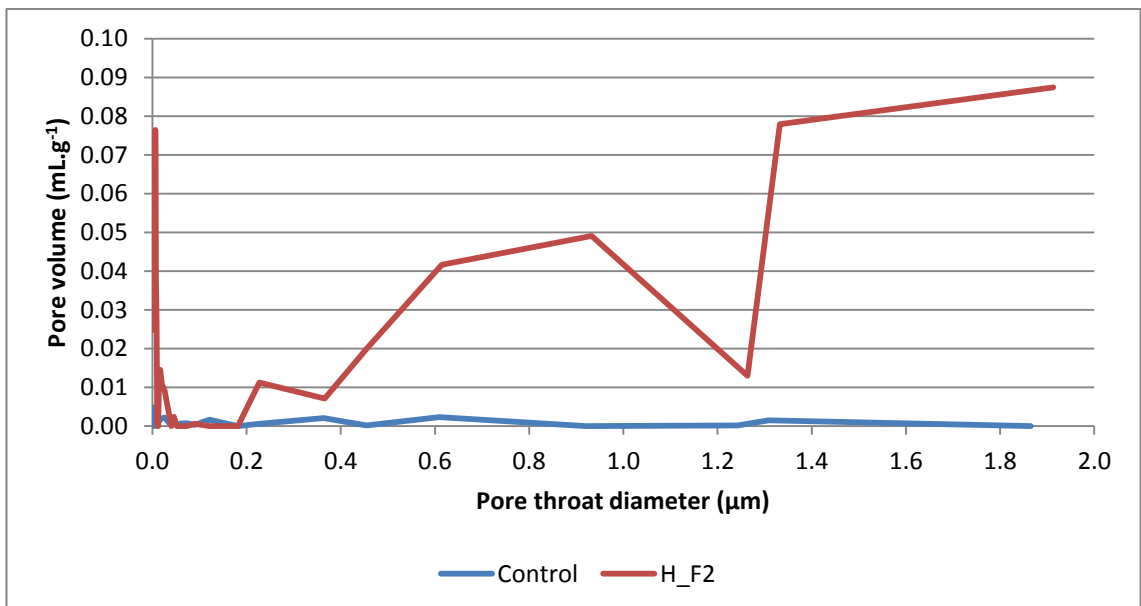
Figure 4.10 - Pore size distribution of British hill wool (H) fibres before and after FA pre-treatment, maximum pore throat diameter 2 µm

Moreover, the pore size distribution detailed in Figure 4.11 shows that meso-pore formation was evident after the FA treatment. Also, because most of the cuticles of FA treated H wool fibres are removed (see the SEM images in Figure 4.8), it is possible that a large proportion of these macro- and mesopores were formed within the cortex of the H wool fibres after two hours of FA treatment.
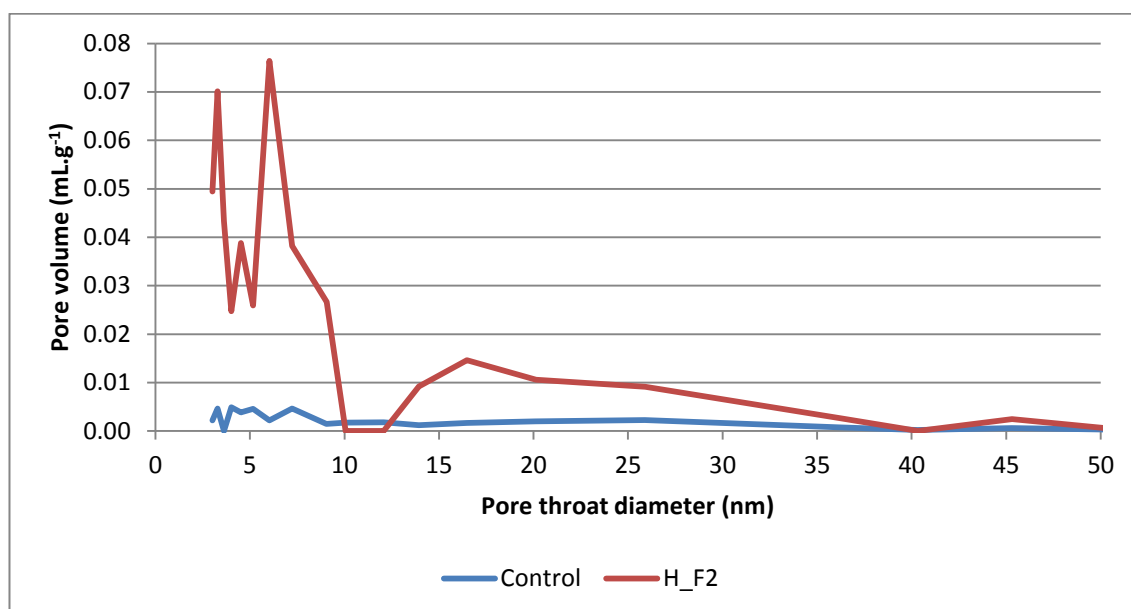
Figure 4.11 - Pore size distribution of British hill wool fibres (H) with and without FA pre-treatment, maximum pore throat diameter 50 nm

In a summary, extensive cortex exposure and internal macro-pore formation within the British hill wool (H) fibres after the 2 h FA treatment were evident in both SEM examination and mercury porosimetry analysis; the volumes of accessible macro- and mesopores formed within H wool fibres were increased after FA treatments.

4.2.1.3 Discussions

The cortical layer and cell-membrane-complex of British wool fibres were exposed after the cuticle layers were removed during formic acid treatment (Mao, 2013), it is thus possible to form pores via formic acid treatments. Different wool fibres contain different chemical compositions of the para-cortex and ortho-cortex within the wool fibres (Bradbury, 1973); therefore, it is possible different wool fibres respond differently to the

FA treatments. Both British medium fine hill (MFH) and British hill wool (H) demonstrated some internal interstices within the raw wool fibre cross-sections and cortex exposure has evidenced after FA treatment.

It was shown in the SEM cross-section images of MFH and H wool fibres that the superficial pore throat diameters of the pores formed hardly exceeded 2 μm, and most of the volumes of the pores greater than 2 μm were formed inter-fibres and between cuticles intra-fibres, therefore the volumes of those pores greater than 2 μm were not included within the discussions.

For MFH wool fibres treated with FA for a shorter time duration, the pores appear to be interior and are encased by the cuticle or cortex exterior. The cortex layer becomes exposed after 2 hours of FA treatment; however, extending the treatment beyond 2 hours cause significant brittleness and degradation, and potential fibre shrinkage (see Figure 4.12) once dried.
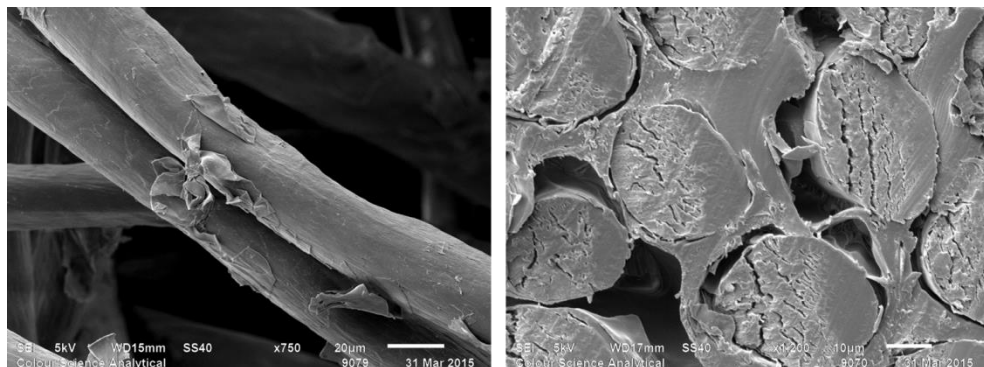
Figure 4.12 - British medium fine (hill) wool after 3 h formic acid treatment. Fibre (Mag x750) and fibre cross-section (Mag x1200)

The total pore volume and extent of the cortex exposure for H wool fibres appears to increase after the 2 h FA treatment, while the total pore volume of the MFH wool fibres decreases after FA treatment for 1 h which might be due to the removal of the cuticles. Therefore, time duration of formic acid pre-treatments is crucial for the pore formations within wool cortex in British wool fibres.

4.2.2 Urea hydrogen peroxide treatment

UHP, once used as an oxidation and swelling agent for bleaching wool (Cockett et al., 1969; Cockett et al., 1971; Arifoglu et al., 1989), was employed in this study to partially oxidise the cysteine residues to form an intermediate material for further reaction (Mao, 2013). UHP aqueous solution has been found to significantly increase the amount of macropores within the wool microstructure (Mao, 2013). It is believed that this swelling agent-oxidant solution could help breakdown the disulphide bonds in the cortical layer of the FA treated wool fibres. The experimental plan for investigating the effect of UHP treatment on the pore formations in 7 British wool fibres is shown in Table 4.4.

Table 4.4 - UHP treatment on the pore formations in 7 British wool fibres

Sample code	Description	FA treatment duration (h)	UHP treatment duration (h)
MFL_F1_UHP0.5	British medium fine wool (Lowland)	1	0.5
MFH_F1_UHP0.5	British medium fine wool (Hill)	1	0.5
L_F1_UHP0.5	British luster wool	1	0.5
H_F1_UHP0.5	British hill wool	1	0.5
B_F1_UHP0.5	British black colour wool	1	0.5
M_F1_UHP0.5	British mountain wool	1	0.5
C_F1_UHP0.5	British cross wool	1	0.5
C_F1_UHP1	British cross wool	1	1

F1: Wool fibres were treated in FA (≥98%, Sigma Aldrich) at 110 °C for 1 h;
UHP0.5 & UHP1: The above FA treated wool fibres were treated in UHP (97%, Alfa Aesar) for 30 minutes or 1 h, respectively.

All the wool fibres are FA treated for 1 hour, with subsequent UHP treatment for either 0.5 or 1 h duration. The effect of the UHP treatment on the pore formations in 7 British wool fibres are shown in the SEM images illustrated within Figure 4.13.
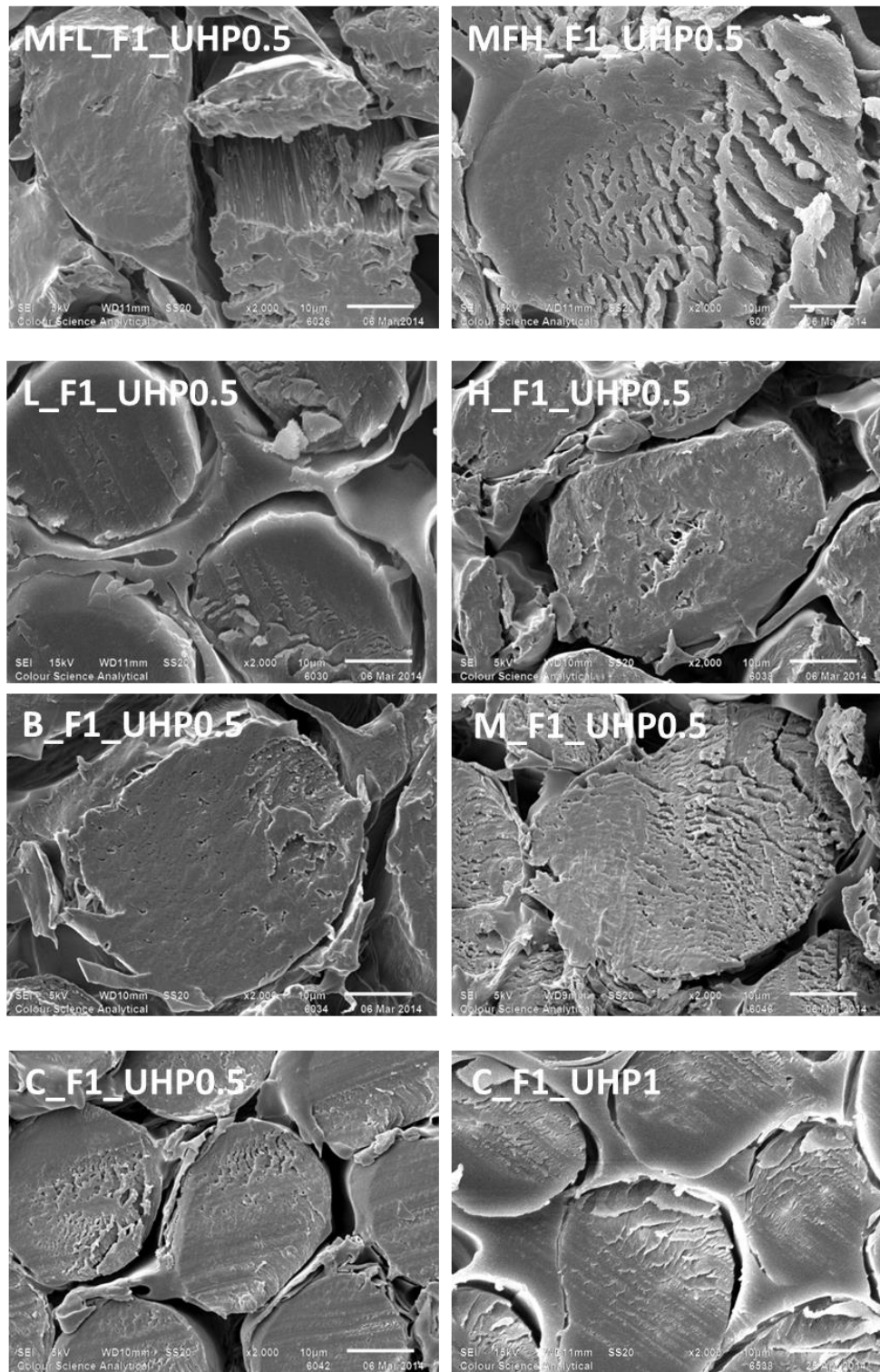
Figure 4.13 - Wool fibres post FA Treatment and UHP treatment (Mag. x2000)

It was shown in Figure 4.13 that after UHP treatments for 0.5 h exposure duration, wool fibres MFL, MFH, C and M appeared to have shown an increased number of interstices and inter-fibre segregation in comparison with original wool fibres. Wool fibres

MFL_F1_UHP0.5 and M_F1_UHP0.5 also displayed some evidence of fibre rupture; however, it is unclear whether these changes are due to the FA pre-treatment or a combination of the FA-UHP treatment.

The effect of the time duration of UHP treatment was investigated for wool fibre C, as shown in Figure 4.13. While wool fibre C_F1_UHP0.5, as well as wool fibres B_F1.5_UHP0.5 and L_F1_UHP0.5, showed limited differences to their raw fibres when the UHP treatment duration was 0.5 hours; wool fibre C_F1_UHP1 showed evidence of increased interstice formations within the fibre cross-section when the time duration of UHP treatment was longer (i.e. 1 hour). Therefore, increasing the time duration of UHP treatment could lead to an increase in interstice formation within wool fibre cross-sections, and this might be a result of the breakdown of the disulphide bonds within the cortical layers.

Table 4.5 - Apparent density of wool fibres post FA Treatment and UHP treatment

Sample	Untreated	Post FA Treatment	Post UHP Treatment (30 mins)	Percentage increase (%)*	Post UHP Treatment (1 h)	Percentage increase (%)*
MFL	1.3812	1.458	1.3634	-6.5%	N/A	N/A
MFH	1.3081	1.4156	1.3649	-3.6%	N/A	N/A
L	1.3391	1.4984	1.4581	-2.7%	N/A	N/A
H	1.3404	1.424	1.4338	0.7%	N/A	N/A
B	1.307	1.4025	1.4074	0.3%	N/A	N/A
M	1.322	1.4606	1.3606	-6.8%	N/A	N/A
C	1.5816	1.3838	1.5352	10.9%	1.3175	-4.8%

Percentage increase values are Post UHP Treatment durations in respect to Post FA Treatment.

It was also found in Table 4.5 that by increasing of the UHP treatment time duration from 0.5 hour (C_F1_UHP0.5) to 1 hour (C_F1_UHP1), the apparent density of wool fibres decreased from 1.5352 to 1.3175 g.cm^{-3} (14.2%), this suggested that there was a decrease in the amount of accessible pores within the wool fibres. Theoretically, the apparent density of the material should increase if the internal cavities within the fibres become accessible to helium gas molecules used in the Micrometrics Accupyc 1330 Pycnometer. Therefore, the reduction in apparent density could indicate the changes of

internal microstructures of the wool fibres and there might be some inaccessible pores (closed pores) created within the wool fibres, as swelling and oxidation processes induced by UHP would breakdown the crosslinks between polypeptide chains within wool fibres.

The apparent density of the seven wool fibres after FA and UHP treatments were shown in Figure 4.14. It was demonstrated that consecutive FA-UHP chemical treatments have certain effects on the apparent density of the wool fibres and the changes of apparent density (AD) with the two chemical treatments were shown in three different patterns:

Group A (MFL, MFH, L & M) – the AD increases after the FA treatment and then reduces after the UHP treatment. However, the AD of the fire MFL after the UHP treatment is smaller than the original fibres, and AD of fibres MFH, L & M are greater than that of the original fibres.

Group B (H & B) – the AD increases after FA treatment, and further increases after UHP treatment.

Group C (C) – the AD reduces after the FA treatment and then increases after the UP treatment, however, the value still remains smaller than that of the original fibre.
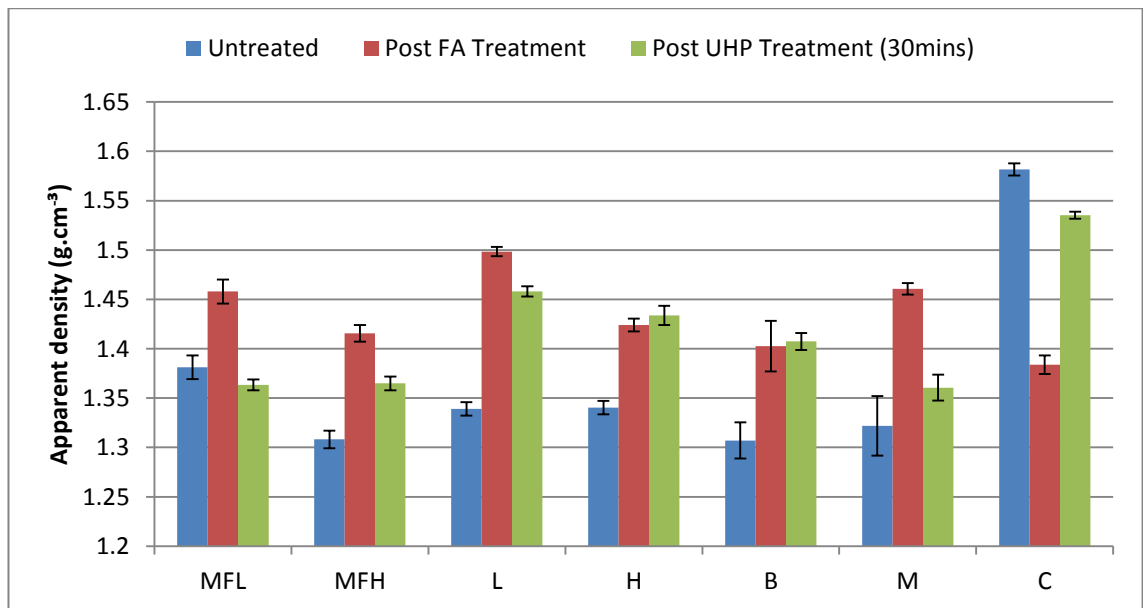
Figure 4.14 - Wool sample apparent density after consecutive chemical treatments (Please note sample C contains data from 30 minutes UHP Treatment)

This indicates that different wool fibres have different reactions to consecutive FA and UHP treatments of identical time durations. With the exception of wool fibre C, the apparent density of other six wool fibres (MFL, MFH, L, H, B and M) increased after the FA treatment in comparison with their original AD. Therefore, the FA treatment is an effective way of removing the cuticle layer and might also increase the accessibility of the internal pores in cortex layers. Also, the AD of five FA-UHP treated wool fibres (MFH, L, H, B and M) are still greater than their original fibres, this indicates that these wool fibres might have either more accessible pores or less inaccessible pores than original fibres after FA-UHP treatments. Four wool fibres (MFH, MFL, L and M) after UHP treatments have smaller AD than that of their corresponding FA treated fibres, suggesting that the internal pores have become less accessible due to swelling of these fibres as a result of the UHP treatment. As indicated in comparison of C_F1_UHP0.5 and C_F1_UHP1 fibres, increases of the time duration of UHP treatment might lead to the creation of more inaccessible pores within wool cortex layers.

This treatment demonstrated the initial stages of increased fibre porosity, particularly for wool sample MFH based on the SEM and porosimetry results. Also, complete BET results were obtained for wool fibres MFH and B (see Figure 4.15). These fibres were selected as they demonstrated different AD trends after UHP solution exposure.
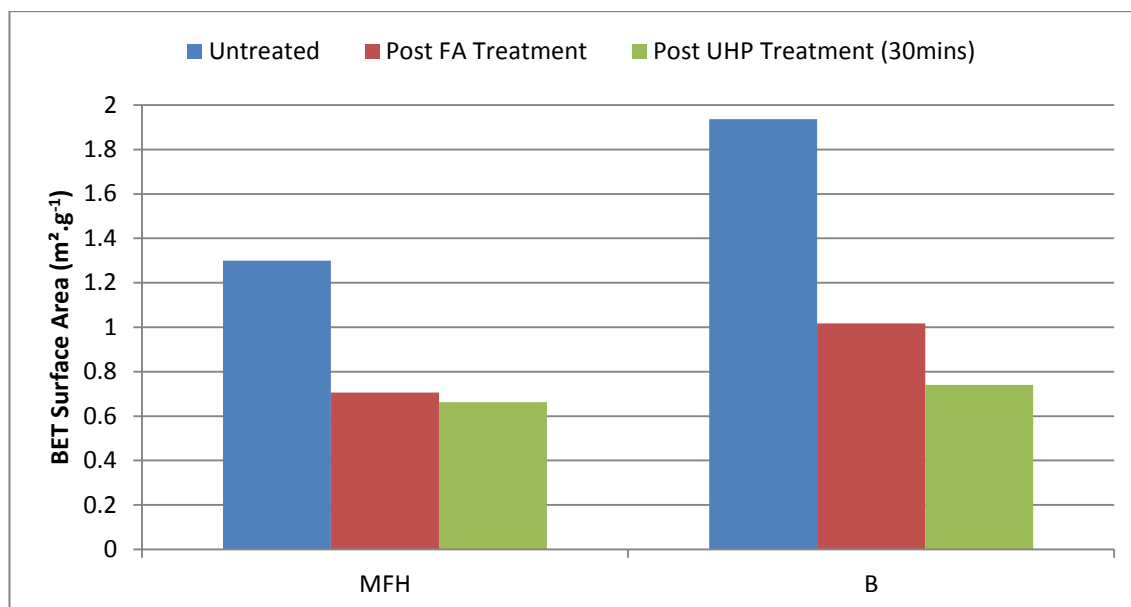
Figure 4.15 - Wool sample specific surface area after consecutive chemical treatments (Please note sample C contains data from 30 minutes UHP Treatment)

Interestingly, these fibres demonstrated similar BET surface area trends. The BET results demonstrated a gradual reduction in surface area after each consecutive chemical treatment (i.e. FA and UHP treatment). One shortcoming of this BET surface area experiment was that only one repetition was recorded for each sample due to the extensive time duration and cost of the procedure. To ensure an accurate measurement and to obtain a result representative of the whole sample, the fibres were cut into staple fibres and mixed before loading into the sample tubes.

There are mixed opinions as to whether UHP penetrates the wool fibre during reaction (Cockett et al., 1969; Cockett et al., 1971; Arifoglu et al., 1989). Arifoglu et al. (1989) suggested that the treatment only swells the surface of the wool fibres and the occurrence of hydrogen bonding between the urea and the wool fibre could make the

fibres less permeable to water. Therefore, it is possible the urea hydrogen peroxide treatment swelled the surface area of the wool fibres, reducing the accessibility of surface and internal pore formations. This phenomenon is aligned with what was observed for both AD and BET analysis.

In a summary, consecutive FA-UHP treatments have an effect on the wool fibre internal microstructure, apparent density and specific surface area.

4.2.3 Ozone treatment

An ozone treatment derived from the experiments showed by Wan and Yu (2011) were conducted to investigate the effect of ozone treatment on the pore formation within raw and chemically pre-treated British wool fibres. The consecutive treatments including FA-UHP treatment was proved to be an effective method to create pore formation within the wool fibre cross-sections of British wool fibres (Mao, 2013). However, the combination of ozone with such treatments has not been studied previously. The effects of ozone treatments on untreated and FA treated British wool fibres are studied in this research to determine ozone treatment parameters that affect the pore formation within wool fibres.

The choice of solvents for ozone treatment is also important. Water and UHP solution have been selected for this research. UHP solution is a known swelling and oxidation agent (Mao, 2013) and combing this treatment with additional oxidation via ozone exposure may affect the pore formation within wool fibres. Water was selected as a comparison to UHP solution as it has the ability to penetrate and saturate wool fibres and will give an indication of the affect of ozone on the formation of pores within wool fibres.

MFH British wool fibres were saturated in an aqueous solution (either water or UHP) and subjected to ozone treatment for 24 to 96 h to investigate the effect of pre-treatment (FA), different solvents, time durations of ozone treatments on the pore formation within raw and chemically treated wool fibres. These treatment durations

were selected as preliminary experiments demonstrated that the proportion of meso- and macropore formation varied between these ozone treatment durations. The research methodology and experimental plan is detailed within Section 3.2.4 (Chapter 3).

4.2.3.1 **Effect of Ozone treatment on British wool fibres without any pre-treatment**

The cuticles of wool fibre MFH without any pre-treatment were still intact; the changes of their pore volumes, the surface morphology and internal porous features of the wool fibres after being subjected to ozone treatments in different exposure time durations and solvents were investigated. The experimental plans for investigating the effect of treatment time duration and solvent are detailed within Table 4.6 and Table 4.7, respectively. The resultant fibres were examined using SEM and mercury porosimetry.

Table 4.6 - Ozone treatment time duration on British wool fibres without any pre-treatment

Sample code	Ozone exposure duration (h)	Reaction solvent
MFH_OZ24_H2O	24	H_2O
MFH_OZ96_H2O	96	H_2O
MFH_OZ24_UHP	24	UHP
MFH_OZ96_UHP	96	UHP

UHP: The above wool fibres were treated in UHP (97%, Alfa Aesar).

Table 4.7 - Ozone treatment solvent on British wool fibres without any pre-treatment

Sample code	Ozone exposure duration (h)	Reaction solvent
MFH_OZ24_H2O	24	H_2O
MFH_ OZ24_UHP	24	UHP
MFH_ OZ96_H2O	96	H_2O
MFH_ OZ96_UHP	96	UHP

UHP: The above wool fibres were treated in UHP (97%, Alfa Aesar).

The effect of time duration and treatment solvent of ozone treatment on British medium fine (hill) wool using SEM are shown in Figure 4.16. The wool surface morphology and fibre cross sections are shown.
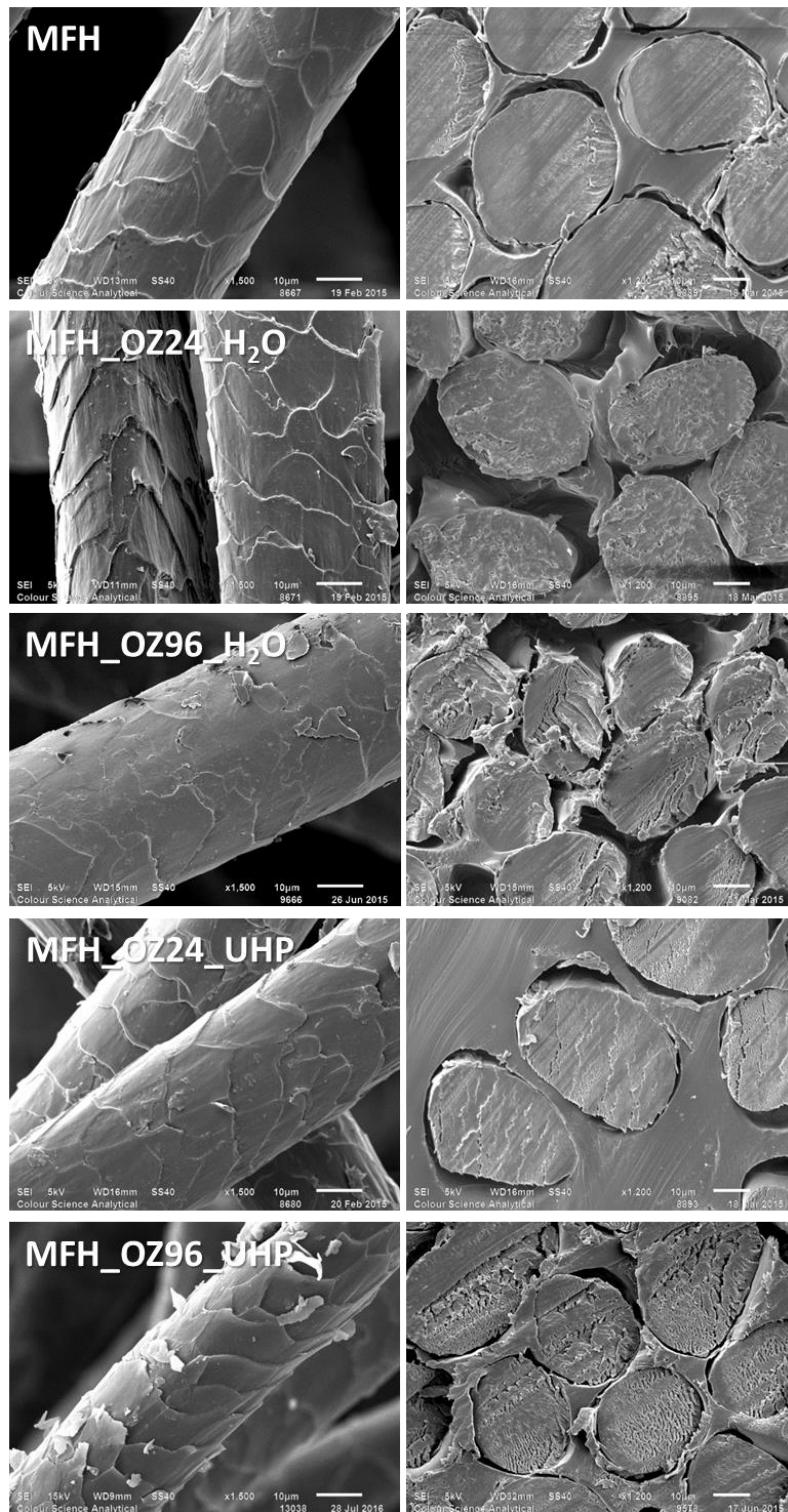
Figure 4.16 - Cuticle degradation and pore formation in British medium fine hill (MFH) wool fibres after ozone treatment in water or UHP solution for 24 and 96 h. Fibre morphology (Mag x 1500) and cross-section (Mag x 1200)

The total pore volumes of pores between 3nm - 2µm, measured using mercury porosimetry, in MFH fibres ozone treated in water and UHP are detailed within Figure 4.17.
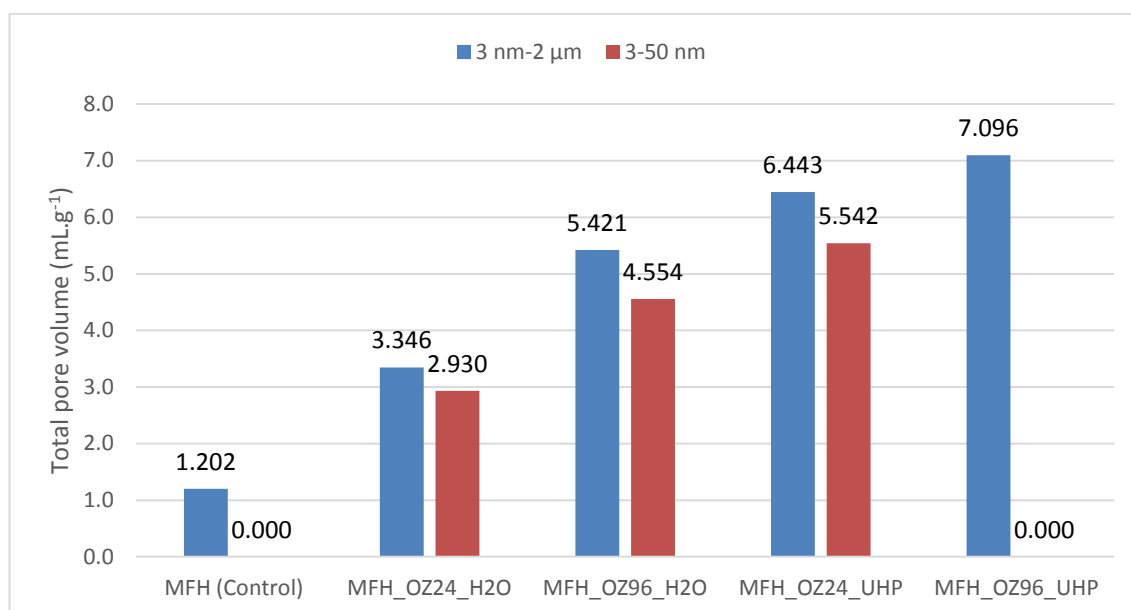
Figure 4.17 - Pore volume of total pores (3nm - 2µm) and mesopores (3 - 50nm) in pore throat diameter) in MFH fibres ozone treatment in water or UHP solution for 24 and 96 h

Table 4.8 details the percentage increase in total pore volume for pores between 3nm - 2 µm and proportion of mesopores (3nm - 50 nm) within MFH fibres ozone treated in water and UHP solution for different time durations.

Table 4.8 - Percentage increase in total pore volume for pores between 3nm - 2 µm and proportion of mesopores (3nm-50 nm) within MFH fibres ozone treated in water and UHP solution for different time durations

Sample code	Total pore volume of pores between 3nm - 2 µm (ml.g^{-1})	Total pore volume of pores between 3nm -50 nm (ml.g^{-1})	Percentage increase in total pore volume for pores between 3nm - 2 µm (%)	Proportion of Mesopores, 3nm - 50 nm (%)
MFH	1.202	-	-	-
MFH_OZ24_H2O	3.346	2.930	64	88
MFH_OZ96_H2O	5.421	4.554	78	84
MFH_OZ24_UHP	6.443	5.542	81	86
MFH_OZ96_UHP	7.096	-	83	-

Pore size distribution of mesopores (3 - 50nm in pore throat diameter) and meso- and macropores (3nm - 2 µm in pore throat diameter) in MFH fibres after different ozone treatments are detailed within Figure 4.18 and Figure 4.19, respectively.
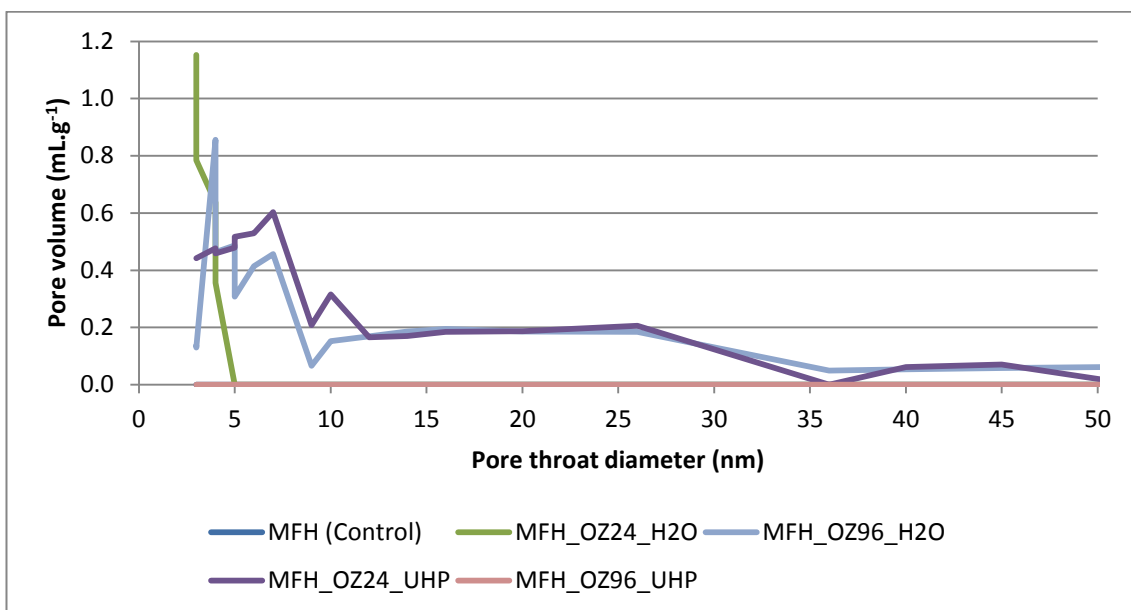
Figure 4.18 - Pore size distribution of mesopores (2 - 50nm in pore throat diameter) in MFH fibres after different ozone treatments
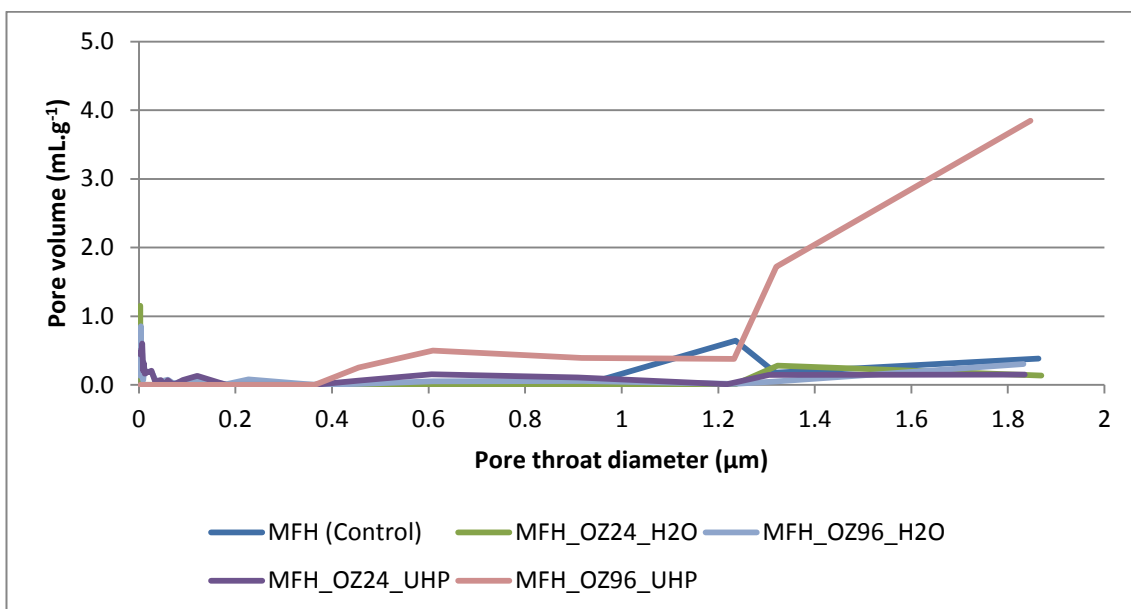
Figure 4.19 - Pore size distribution of pores (3nm - 2 µm in pore throat diameter) in MFH fibres after different ozone treatments

It is evident from Figure 4.16 that the fibres treated with ozone in water have a tightly bonded cuticle layer and the fibre cross-section contains a limited amount of macropores. Whereas, macropore formation is evident after ozone treatment in UHP solution despite the cuticles remaining intact. Cuticle degradation is evident in all fibres after ozone treatments although the majority of the cuticles appear to be intact. Despite poor cortex exposure, it is evident from the fibre cross-section SEM images that internal pores were formed in cortex layers after the ozone treatments (see Figure 4.16). This suggests that ozone penetrates into the cuticle layer and is capable of oxidizing and swelling the wool cortex swollen in the solvents (water or UHP). However, it is still unclear from the SEM images whether the pores formed are accessible or completely encapsulated by the cuticle layer.

4.2.3.1.1 Effect of treatment time duration

Greater cortex exposure and the pore formation are evident after extending the treatment time duration for both ozone-water and ozone-UHP treatments (See Figure 4.16). However, pore formation is only evident after extended exposure duration (96 h) for the ozone-water treated wool fibres. The pore formation evident after the ozone-UHP treatments for 24 h and 96 h are quite apparent in comparison with the cross-section structure of corresponding raw wool fibres, particularly after 96 h. Interestingly, by observing the wool fibres cross-section, the wool fibres treated for 24 h appears to have hardly any pores greater than 1 μm, whereas the wool fibres treated for 96 h appear to have a lot of pores greater than 1 μm.

Extending the treatment duration increases the total pore volume of pores from 3nm - 2μm for both ozone-water and ozone-UHP treatments (see Figure 4.17). Also, the total pore volume of mesopores increases by extending the treatment duration for ozone-water treated wool fibres. Whereas, the total pore volume of mesopores increases for ozone-UHP treated wool fibres after 24 h; however, no mesopores are detected after extending the treatment duration to 96 h. In addition, the changes of the pore size

115

distributions after different ozone treatments might also indicate the internal microstructure changes after different ozone treatment processes. As shown in Figure 4.17, meso-pore formation is evident after ozone-water solution treatment for both 24 h and 96 h (2.930 ml.g^{-1} and 4.554 ml.g^{-1}), and ozone-UHP solution treatment for 24 h (5.542 ml.g^{-1}), but not after 96 h. This suggests that the mesopores created within the fibres after ozone-UHP for 24 h might swell to form into macropores after 96 hours of exposure in UHP.

These characteristics are also demonstrated within the pore size distribution of mesopores in wool fibres shown in Figure 4.18. Wool fibres evident with meso-pore formations demonstrate similar trends with respect to the pore size distribution, a significant proportion of mesopores formed ranges from 3 to10 nm after ozone-water and ozone-UHP treatments for 24 hours, and after ozone-water treatment for 96 h. It is possible that mesopores formed during 24 h ozone-UHP solution treatment are enlarged by the UHP swelling agent, leading to greater pore volumes of the pores whose throat diameters are between 0.4 and 2 μm, particularly for pores greater than 1.2 μm (see Figure 4.19).

4.2.3.1.2 Effect of treatment solvent

The effect of ozone treatment reaction solvent on wool fibres exposed for 24 and 96 h, using SEM, are shown in Figure 4.16. The total pore volumes of pores between 3nm - 2μm, measured using mercury porosimetry, in MFH fibres ozone treated for 24 and 96 h are detailed within Figure 4.17.

Cuticle degradation is evident after both ozone-water and ozone-UHP treatments for 24 and 96 h exposure durations (see Figure 4.16). Interestingly, the cuticle degradation appears to be more severe for the ozone-water treated wool fibres exposed for 96 h, as a significant proportion of the cuticles are removed. Pore formations are evident after the wool fibres are treated with ozone-UHP, but not with ozone-water for 24 h. The pores formed appear to be less than 1 μm in diameter. Also, pore formation is evident

after treating the wool fibres with ozone-water and ozone-UHP treatments for 96 h. The fibres treated with ozone-UHP appear to have a greater amount of pores (> 1μm) than the ozone-water treated wool fibres.

Furthermore, the fibres ozone-treated in UHP solutions are found to have greater total pore volume of accessible pores (3nm - 2 μm) in comparison with wool fibres modified with the ozone-water treatment for both treatment time durations (see Figure 4.17). This is also demonstrated by the percentage increase in total pore volume for pores between 3nm - 2 μm as indicated by Table 4.8. The total pore volume for pores between 3nm - 2 μm increases by 64 and 81 % for wool fibres treated for 24 h with ozone-water and ozone-UHP, respectively. A similar trend was observed for wool fibres treated for 96 h, as the total pore volume for pores between 3nm - 2 μm increases by 78 and 83 % for ozone-water and ozone-UHP treatments, respectively.

Meso-pore formation is evident after both treatments; however, for wool fibres treated for 24 h, the total pore volume of mesopores (3-50 nm) is greater within the ozone-UHP (5.542 ml.g^{-1}) than the ozone-water (2.930 ml.g^{-1}) treated fibres. Despite this discrepancy between total pore volumes, the proportion of mesopores (see Table 4.8) formed for both treatments are similar and were measured as 88 and 86 % for the ozone-water and ozone-UHP treatments, respectively.

Similar to the 24 h treatments, the total pore volume for pores between 3nm – 2 μm, for the fibres treated for 96 h, are increased after both the ozone-water (5.421 ml.g^{-1}, 84 % mesopores) and ozone-UHP (7.096 ml.g^{-1}) treatments. However, unlike the ozone-water treated fibres, no mesopores were detected after the wool fibres were treated with ozone-UHP for 96 h (see Figure 4.17), suggesting that the mesopores formed within the ozone-UHP treated wool fibres swell and form macropores after an extended treatment duration. This phenomenon is evident within the pore distribution detailed within Figure 4.19.

Macropores appear evident within untreated wool fibres for macropores between 0.9 – 1.9 μm, however, from observing the SEM image of the surface morphology (see

Figure 4.16), there are no evidence of macropores present within the fibres. Therefore, these pores measured are likely to be the spaces between the wool fibres. These pores or spaces between the wool fibres are not detectable when the wool fibres are treated with ozone-water for 96 h. However, a significant proportion of macropores are detected with pore throat diameter up to 2 µm for the wool fibres treated with ozone-UHP for 96 h. It is unclear whether the enhanced total pore volume is caused by the exposure of inaccessible pores or cavities created between the partially cleaved cuticles as all wool fibres demonstrate lifted cuticles after extending the treatment time duration for both ozone-water and ozone-UHP treatments (See Figure 4.16).

In summary, accessible macro- and meso-pore formations are evident when the wool fibres are treated with ozone for both solvents, however, for the longer treatment duration mesopores are only evident after the ozone-water treatment. This suggests that the mesopores formed within the ozone-UHP treated wool fibres swell and form macropores after extended treatment duration. Since there is uncertainty as to whether the pores formed within the cortex of the wool fibres are obstructed by the cuticle layer, formic acid pre-treatment of wool fibres, of which the cuticle layer was at least partially or completely removed to expose the cortex layer, might be necessary prior to the ozone treatment process for the purpose of forming accessible pores in cortex after ozone treatments.

4.2.3.2 **Effect of ozone treatment on wool fibres having formic acid pre-treatments**

The effect of ozone treatment on wool fibres, with the cortex exposed, are investigated within this study. Similar to the previous section, the wool fibres were subjected to ozone treatments in H_2O and UHP solutions for 24 h and 96 h treatment durations. The cortex of the wool fibres were exposed by applying a FA pre-treated on British medium fine hill wool fibres (MFH). The surface morphology and internal porous features of the FA pre-treated wool fibres after ozone treatments in different exposure time durations

and solvents were investigated. The experimental plans for investigating the effect of treatment time duration and solvent are detailed within Table 4.9 and Table 4.10, respectively. The resultant fibres were examined using SEM and mercury porosimetry.

Table 4.9 - Ozone treatment time duration on British wool fibres with FA pre-treatment

Sample code	FA treatment duration (h)	Ozone exposure duration (h)	Reaction solvent
MFH_F1_OZ24_H2O	1	24	H_2O
MFH_F1_OZ96_H2O	1	96	H_2O
MFH_F1_OZ24_UHP	1	24	UHP
MFH_F1_OZ96_UHP	1	96	UHP

F2: Wool fibres were treated in FA (≥98%, Sigma Aldrich) at 110 °C for 1h;
UHP: The above FA treated wool fibres were treated in UHP (97%, Alfa Aesar).

Table 4.10 - Ozone treatment solvent on British wool fibres with FA pre-treatment

Sample code	FA treatment duration (h)	Ozone exposure duration (h)	Reaction solvent
MFH_F1_OZ24_H2O	1	24	H_2O
MFH_ F1_OZ24_UHP	1	96	UHP
MFH_ F1_OZ96_H2O	1	24	H_2O
MFH_ F1_OZ96_UHP	1	96	UHP

F2: Wool fibres were treated in FA (≥98%, Sigma Aldrich) at 110 °C for 1 h;
UHP: The above FA treated wool fibres were treated in UHP (97%, Alfa Aesar).

The effect of time duration and treatment solvent of ozone treatment on FA pre-treated British medium fine (hill) wool using SEM are shown in Figure 4.20. The wool surface morphology and fibre cross sections are shown.
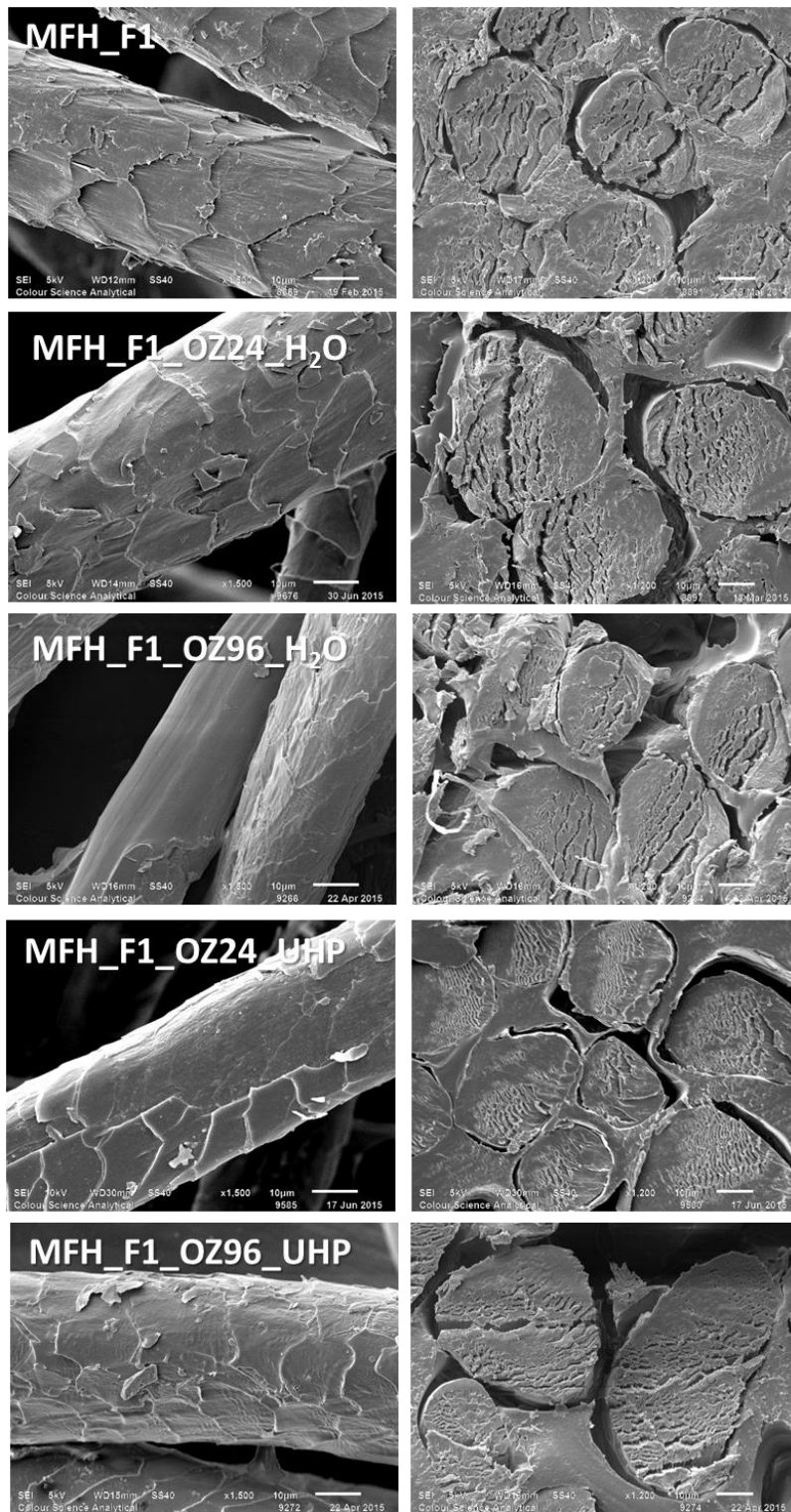
Figure 4.20 - Cuticle degradation and pore formation in FA pre-treated British medium fine hill (MFH) wool fibres after ozone treatment in water or UHP solution for 24 and 96 h. Fibre morphology (Mag x 1500) and cross-section (Mag x 1200)

120

The total pore volumes of pores between 3nm - 2µm, measured using mercury porosimetry, in FA pre-treated MFH fibres ozone treated in water and UHP are detailed within Figure 4.21.
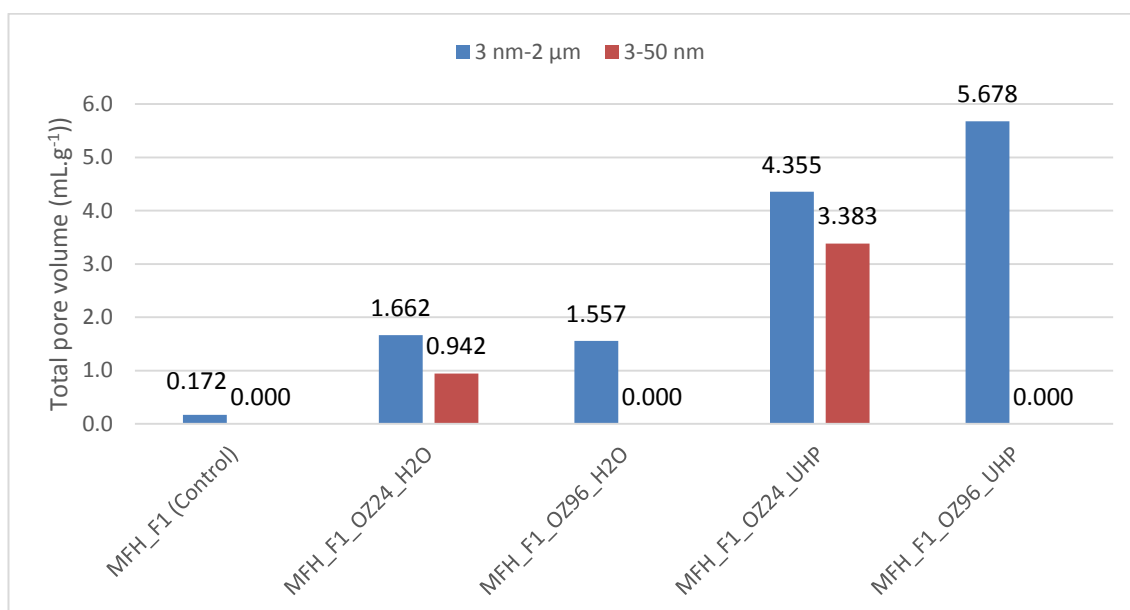
Figure 4.21 - Pore volume of total pores (3nm - 2µm) and mesopores (3 - 50nm) in pore throat diameter in FA pre-treated MFH fibres ozone treated in water or UHP solution for 24 and 96 h

Table 4.11 details the percentage increase in total pore volume for pores between 3nm - 2 µm and proportion of mesopores (3nm-50 nm) within FA pre-treated MFH fibres ozone treated in water and UHP solution for different time durations.

Table 4.11 - Percentage increase in total pore volume for pores between 3nm - 2 µm and proportion of mesopores (3nm - 50 nm) within FA pre-treated MFH fibres ozone treated in water and UHP solution for different time durations

Sample code	Total pore volume of pores between 3nm - 2 µm (ml.g^{-1})	Total pore volume of pores between 3nm - 50 nm (ml.g^{-1})	Percentage increase in total pore volume for pores between 3nm - 2 µm (%)	Proportion of Mesopores, 3nm - 50 nm (%)
MFH_F1 (Control)	0.172	-	-	-
MFH_F1_OZ24_H2O	1.662	0.942	90	57
MFH_F1_OZ96_H2O	1.557	-	89	-
MFH_F1_OZ24_UHP	4.355	3.383	96	78
MFH_F1_OZ96_UHP	5.678	-	97	-

Pore size distribution of mesopores (3 - 50nm in pore throat diameter) and meso- and macropores (3nm - 2 μm in pore throat diameter) in FA pre-treated MFH fibres after different ozone treatments are detailed within Figure 4.22 and Figure 4.23, respectively.
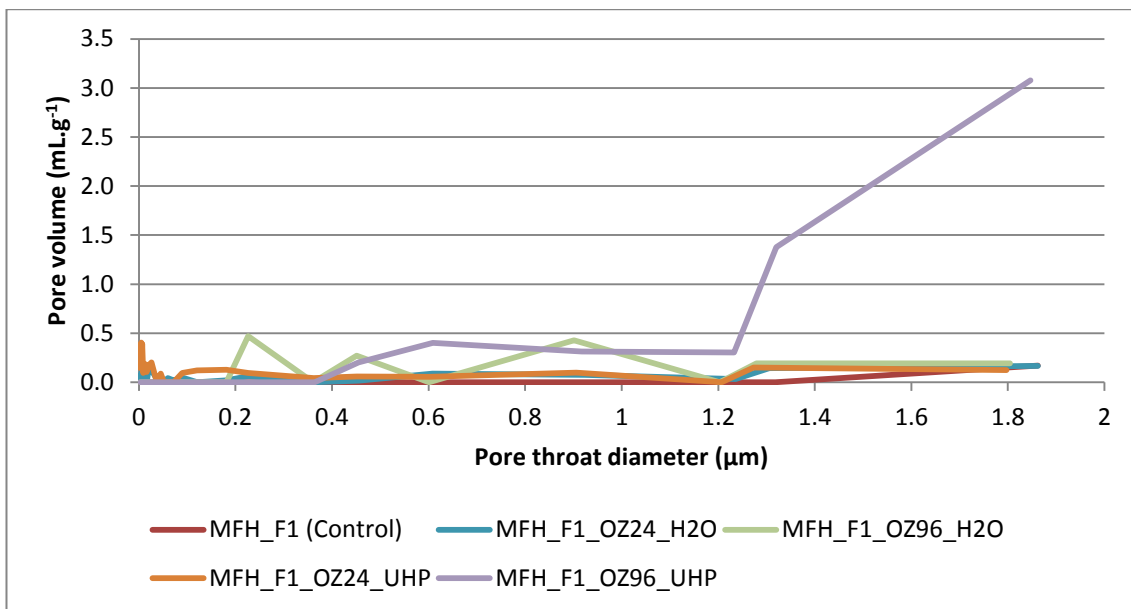
Figure 4.22 - Pore size distribution of ozone-solution modified formic acid pre-treated British medium fine hill wool fibres, maximum pore throat diameter 2 μm
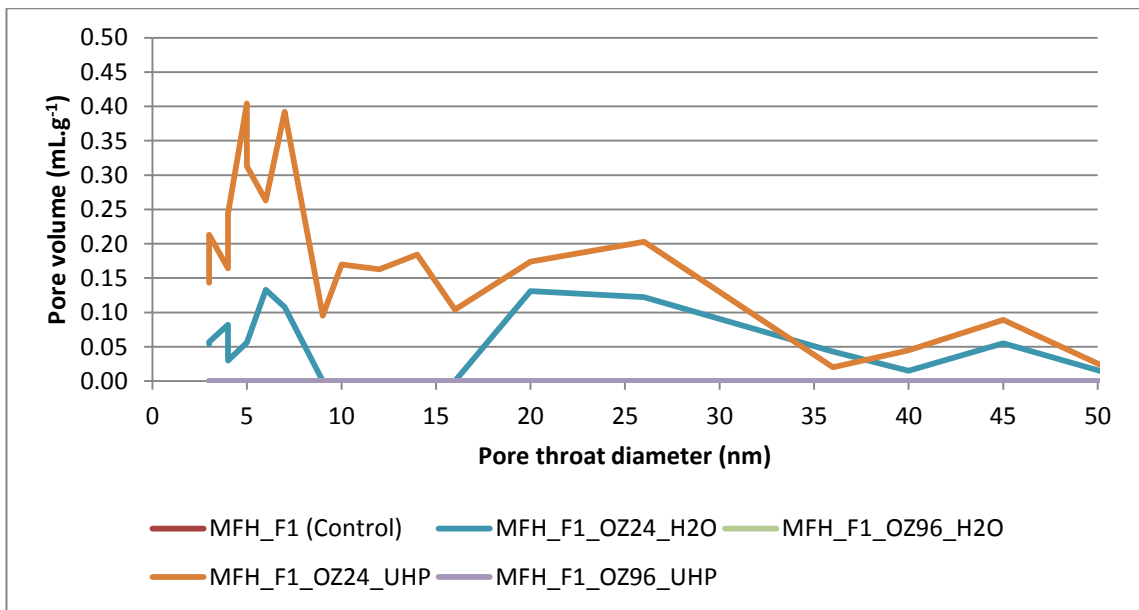
Figure 4.23 - Pore size distribution of ozone-solution modified FA pre-treated British medium fine hill wool fibres, maximum pore throat diameter of 50 nm (MFH_F1, MFH_F1_OZ96_H2O and MFH_F1_OZ96_UHP are in the same line as x-axis)

4.2.3.2.1 Effect of treatment time duration

The effect of time duration of ozone treatment on FA pre-treated wool fibres saturated in water and UHP solution using SEM are shown in Figure 4.20. To understand the effect of the consecutive FA and ozone treatments, the surface morphology and fibre cross sections of the raw British medium fine (hill) wool were analysed using SEM. SEM analysis determined that macro-pore formation was evident within all treated fibres (Figure 4.20). However, because macropores were evident after FA treatments, it is inconclusive from the SEM analysis whether pores were formed or exposed after the ozone-solution treatments for both time durations using SEM analysis alone.

Consequently, mercury porosimetry was employed to determine whether pores were formed or exposed within the wool fibres. The volumes of accessible pores increased after all ozone-solution treatments for both time durations (see Figure 4.21). Also, wool fibres treated with ozone-UHP solution had a greater total pore volume than the wool fibres treated with ozone-H_2O solution for both time durations, particularly for the 96 h. The wool fibres treated in both ozone-solutions for 24 hours demonstrated the

formation of mesopores; whereas, the fibres treated in both ozone-solutions for 96 hours demonstrated the formation of macropores only.

This suggests that, as a result of extending the ozone treatment duration to 96 h, the mesopores formed after 24 h of ozone treatment are either the pores between the partially cleaved cuticles or the exposed pores within the cortex swell and become macropores. This is particularly evident for the wool fibres treated with ozone-UHP solution for 96 h as significant volumes of the macropores between 1.2 and 2 μm are evident within the pore size distribution (see Figure 4.22) and SEM (see Figure 4.20).

It is possible the inaccessible pores created after the 24 h treatments become accessible by extending the treatment time duration to 96 h. This could explain the increase of the pore volume of pores with approximately 1.2 – 1.8 μm in pore throat diameters.

The FA treated wool fibres that formed mesopores (see Figure 4.23) demonstrated similar trends to the fibres without FA pre-treatment (see Figure 4.18), although these wool fibres exposed to the ozone-UHP treatment generally demonstrated greater pore volumes between pore throat ranges of 3 - 50 nm, which again could be caused by swelling induced by the ozone-UHP effect.

4.2.3.2.2 Effect of treatment solvent

Cortex exposure, cuticle degradation and macro-pore formation within all treated wool fibres, including the control sample (MFH_F1) are evident (see Figure 4.20). Therefore, it is not possible to conclude whether the ozone treatment solvent has an effect on the pore formation within FA pre-treated fibres, using SEM alone.

Consequently, mercury porosimetry was used to determine the volume of total pores formed for pores between 3nm – 2 μm (see Figure 4.21). It is evident within these graphs that the total pore volume increases after both ozone treatments. Also, a high proportion of the pores formed for the 24 h treatment are mesopores; whereas, there are no mesopore formations for the 96 h treatment using either solvents. This suggests

124

that extending the treatment duration swells the mesopores formed using both ozone treatment solvents. As indicated within Table 4.11, the proportion of mesopores formed for ozone-water and ozone-UHP wool fibres are 57 and 78 %, respectively. Furthermore, it is evident that applying ozone treatment using water or UHP solution increases the total pore volume for pores between 3nm - 2 µm by 89 - 96 %, which demonstrates these treatments are capable of either forming capable of forming pores or exposing pores created by pre-treatments.

4.2.3.3 Discussions

In this study, the effect of swelling/oxidising treatment by using ozone treatment on the porous structure of British medium fine hill wool (MFH) fibres in both urea hydrogen peroxide and water were investigated.

Pore distributions of the pore throat diameters in the ranges of 3nm - 2 µm and 3 nm - 50 nm for the wool fibres resultant from ozone treatments are shown in Figure 4.24 and Figure 4.25, respectively. Figure 4.24 gives an indication of the pore throat diameters for both macro- and mesopores, while Figure 4.25 demonstrates solely the pore throat diameters for mesopores.

One shortcoming of the mercury porosimetry experiment was that only one repetition was recorded for each sample due to the extensive time duration and cost of the procedure. To ensure an accurate measurement and to obtain a result representative of the whole sample, the fibres and fabrics were cut into small and short pieces and segments respectively and mixed before loading into the sample tubes.
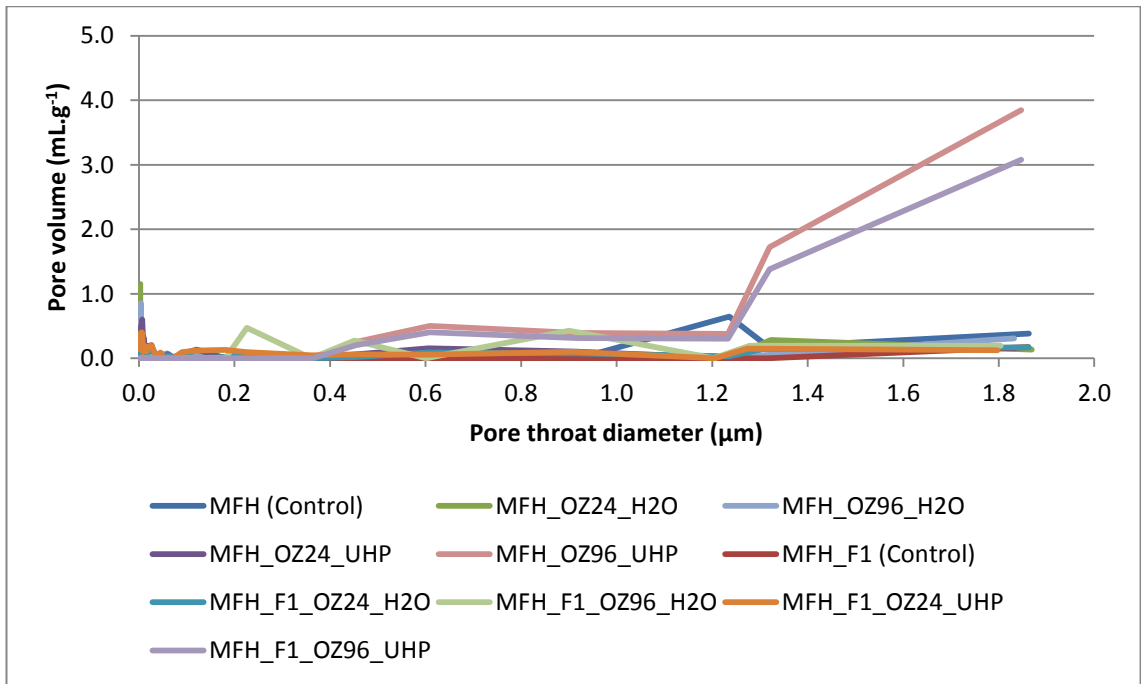
Figure 4.24 - Pore size distribution (3nm - 2.0 µm) of MFH wool fibres after their exposure in UHP solutions
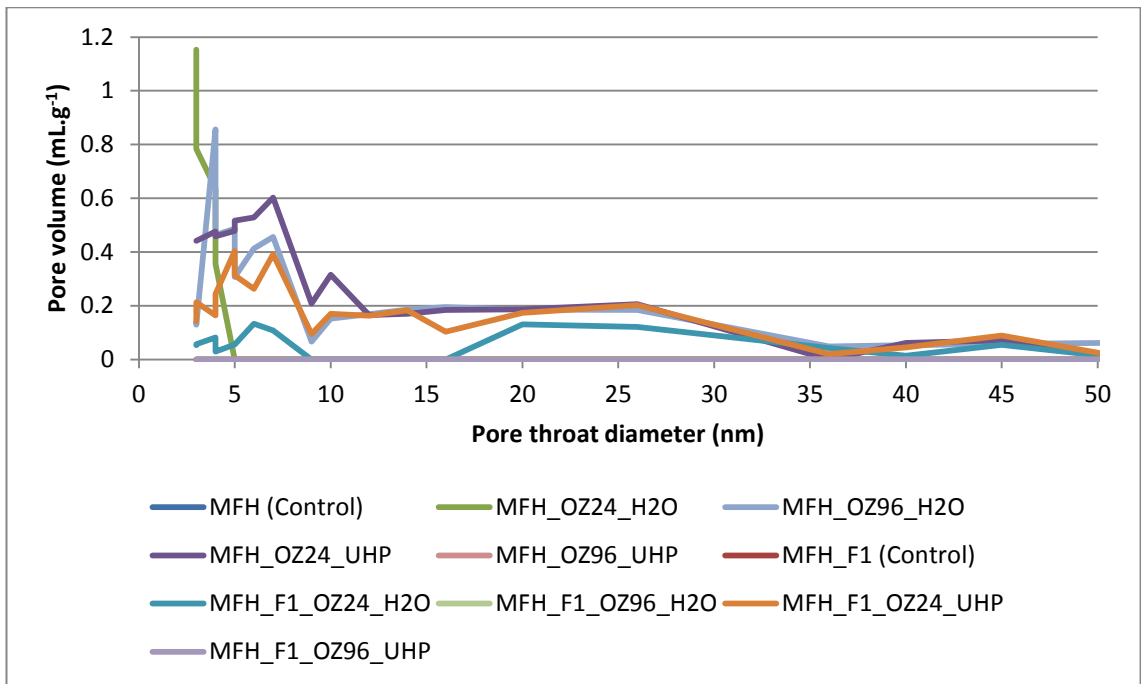
Figure 4.25 - Pore size distribution (2 - 50nm) of MFH wool fibres with and without Ozone treatments

It is interestingly noticed that, among all of the ozone treatments of wool fibres, both wool fibres with and without FA pre-treatment after ozone-UHP treatment for 96 hours demonstrate significant increases in pore volume of the macropores (1.3 and 2 μm). This suggests that wool fibres swells significantly after the extended durations (i.e. 96 hours) of wool exposure in ozone-UHP solution, this might be due to the expansion of the smaller pores formed initially.

Furthermore, increased amount of mesopores (2 - 50nm) formed in wool fibres without FA pre-treatment were evident after they were treated with ozone in water for 24 hours and 96 hours, as well as in UHP for 24 hours as demonstrated in Figure 4.25.

The total pore volumes and volumes of mesopores of wool fibres with and without FA pre-treatment after various treatments are compared in Figure 4.26. It is apparent that, regardless of wool fibres treated with FA pre-treatment, greater total pore volumes are evident in all of wool fibres after ozone-water/UHP solution treatments in comparison with the raw MFH fibres. Also, the total pore volumes increase with the increases of time duration of the ozone-water/UHP solution treatment for all treatments (see Figure 4.26).
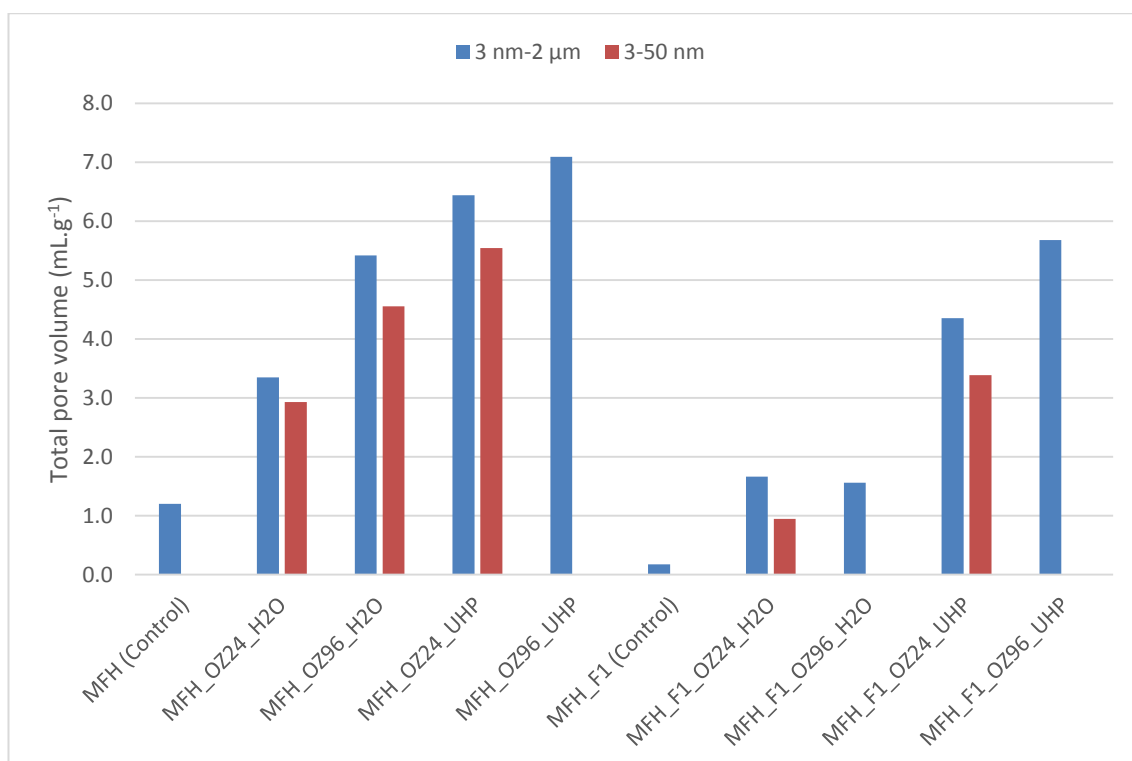
Figure 4.26 - Total fibre pore volume of ozone-solution modified British medium fine hill wool fibres (Pore sizes: 3nm - 2µm & 3 - 50nm)

Wool fibres treated without FA pre-treatment have all the cuticles intact prior to the ozone-solution treatments. Consequently, the increased total pore volumes could be partially caused by both the raising inclining angles of the cuticles and pore formations within the cuticle and cortex layers. As the wool fibres with FA pre-treatment have fewer cuticles intact (see Figure 4.5) in comparison with the fibres without FA pre-treatment, this trend corresponds to the observation in Figure 4.26 that smaller total pore volumes of wool fibres with FA pre-treatment than that of the fibres without FA pre-treatment, this might be because the wool fibres with FA pre-treatment have much smaller pore volumes formed between cuticles. However, both wool fibres with and without FA pre-treatments have increased pore volumes with the increase of time duration of ozone treatments.

A significant proportion of the total pore volume for wool fibres (without FA pre-treatment) treated with ozone-water for 24 and 96 h, as well as ozone-UHP treatment

for 24 h, consists of mesopores (3-50 nm). Similarly, a significant proportion of the total pore volume for FA pre-treated wool fibres treated with ozone- water/UHP solutions for 24 h consists of pores of throat diameters between 3nm – 50 nm. However, by extending the treatment duration from 24 hours to 96 hours for wool fibres after ozone treatments in water and UHP solutions, the mesopores seem to completely disappear and the total pore volume consists of pores within the range 50 nm – 2 µm in throat diameter.

Therefore, longer time duration of ozone treatment appears to have three effects on the wool (see Figure 4.27):

(1) the raise of cuticle inclining angles due to ozone treatment might increase the pore volumes of the pores between cuticles, and the relationship between the inclining angle of cuticles and the total pore volume is illustrated in Figure 4.28;

(2) the increasing partially degradation of cuticles might reduce the volumes of the pores between the cuticles;

(3) the new pores formed in cortex layers underneath cuticles are exposed. When cuticles are partially or completely removed as a result of oxidation from the ozone treatments, it is possible for the macropores to be observed in the fibre cross-sections, no matter whether they are accessible.

Raw wool fibre

Cuticles

Volume between cuticles

Treated wool fibre

Cuticles raised as a result of chemical treatment

Extended treatment of wool fibre

Cuticles become damaged as a result of chemical treatment

Cleaving of cuticles

Exposure of pores

Exposure of pores formed during chemical treatments
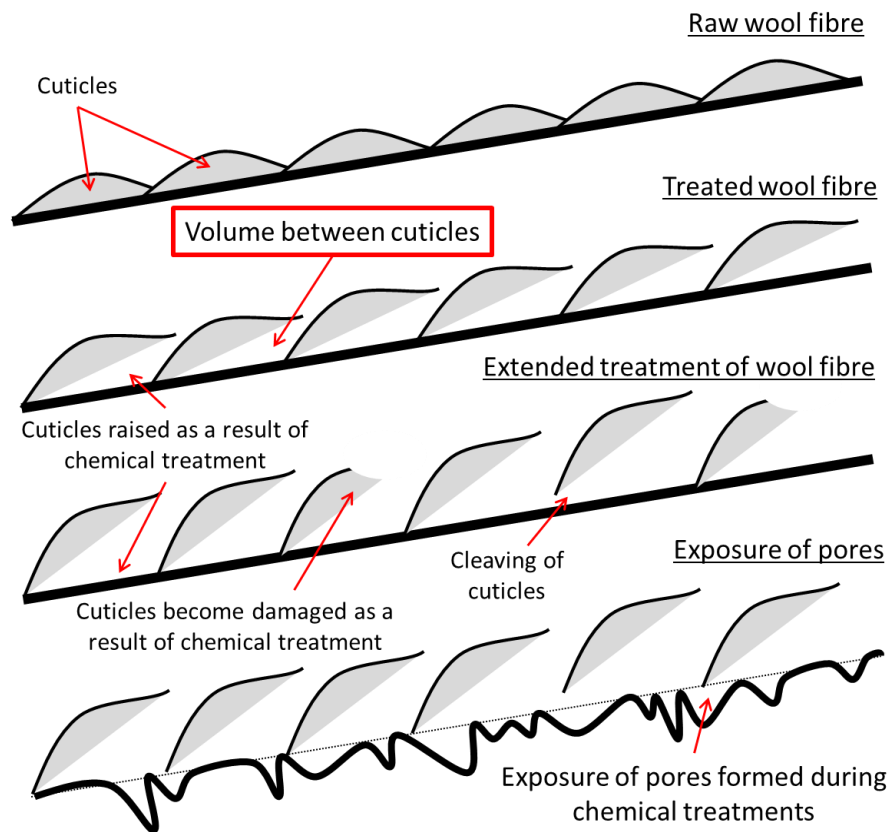
Figure 4.27 - Schematic demonstrating pore formation within wool fibres. Chemical treatment may cause partial cleavage of cuticles introducing pore volumes between the cuticles and cortex, which could increase further with treatment duration. Eventually, full cleavage of cuticles might reduce the volumes of the pores between the cuticles, although new pores formed in the cortex layers underneath cuticles may become exposed
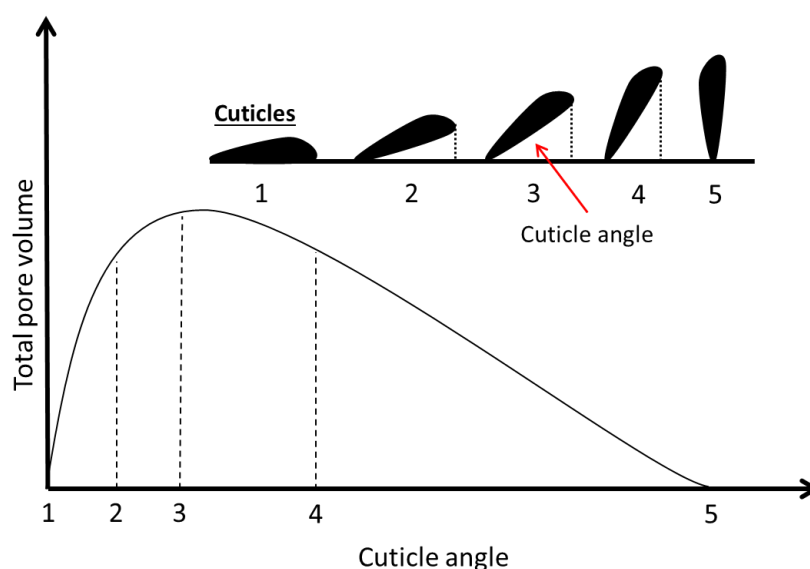
Figure 4.28 - Schematic of the increasing volume of the pores between cuticles with the increases of time duration of the ozone treatment (phases 4 and 5 were hardly observed in this experiment)

4.2.4 Sodium hydroxide treatment

Previous research at the University of Leeds (Mao, 2013) determined that British wool fibres (MFH) experienced a shrinking phenomenon. The wool fibres exhibited a marked reduction in apparent density after the sodium hydroxide treatments, suggesting the volume of accessible pores within the wool fibres increased. It is possible the sodium hydroxide solubilises part of the cortex of the wool fibre leading to the formation of channels and pores within the internal wool structure.

Therefore, untreated and FA treated British hill wool fibres (H) were subjected to different concentration of NaOH solutions for different time durations to determine NaOH treatment parameters that affect the pore formation within wool fibres. To determine whether the size of the channels and pores within the wool fibre structure can be controlled, the effect of both the sodium hydroxide solution concentration and exposure time durations are investigated.

4.2.4.1 The effect of sodium hydroxide treatment on wool fibres without any pre-treatment

The pore formations within raw British hill wool fibres (H) treated in NaOH aqueous solutions of lower (1%) and higher (5%) in concentrations as well as different time durations of 2, 5 and 10 min were investigated and are shown in Table 4.12. Preliminary investigations determined that the wool fibres significantly degraded beyond 10 min exposure. Thus, 10 min was the maximum exposure duration used during this study.

Table 4.12 - Sodium hydroxide treatment on wool fibres without any pre-treatment

Sample code	NaOH solution concentration (%)	Treatment duration (min)
H_1%NaOH_2min	1	2
H_1%NaOH_5min	1	5
H_1%NaOH_10min	1	10
H_5%NaOH_2min	5	2
H_5%NaOH_5min	5	5
H_5%NaOH_10min	5	10

4.2.4.1.1 Effect of time duration in sodium hydroxide solutions of lower concentration (1%)

The pore formation within untreated H wool fibres after exposure to lower concentrated NaOH solutions for 2, 5 and 10 min are shown in Figure 4.29. It was evident in Figure 4.29 that macropores formed within the wool fibres treated in sodium hydroxide solutions for a longer time durations (5 and 10 min); This suggests that longer treatment time durations are required to form macropores within the wool fibres without FA pre-treatment when the fibres are treated in NaOH of lower concentrations.
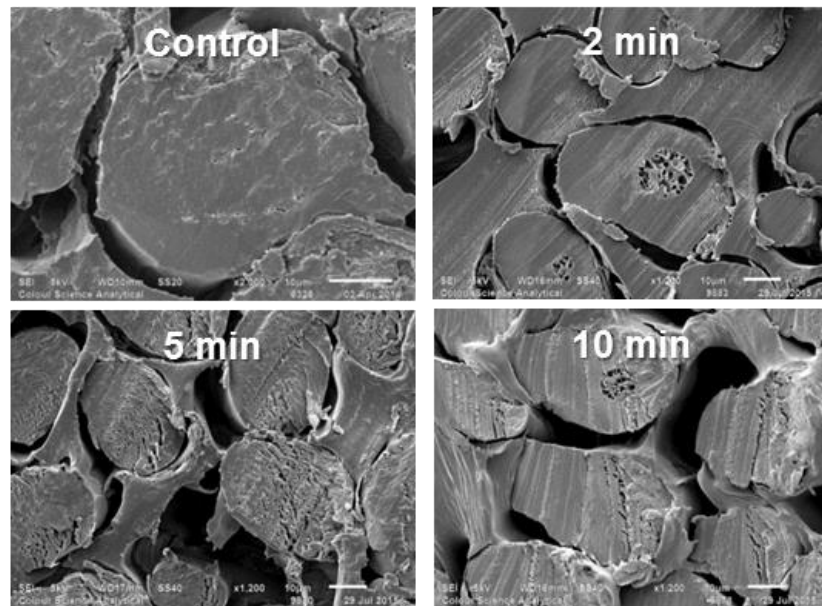
Figure 4.29 - Accessible and inaccessible pores for wool fibres treated with a lower (1%) concentration of NaOH. Control fibre: Mag. x2000) and NaOH treated fibres (Mag. x1200)

The pore size distribution of wool fibres obtained from the mercury porosimetry testing was shown in Figure 4.30. Figure 4.30 indicates that the total pore volumes of the fibres increase with the increases of the exposure time duration (2 to 10 min) of the treatment in NaOH solutions of lower concentrations. Also, the majority of pore volumes (83 % and 88 %, respectively) formed for both treatment durations are mesopores.
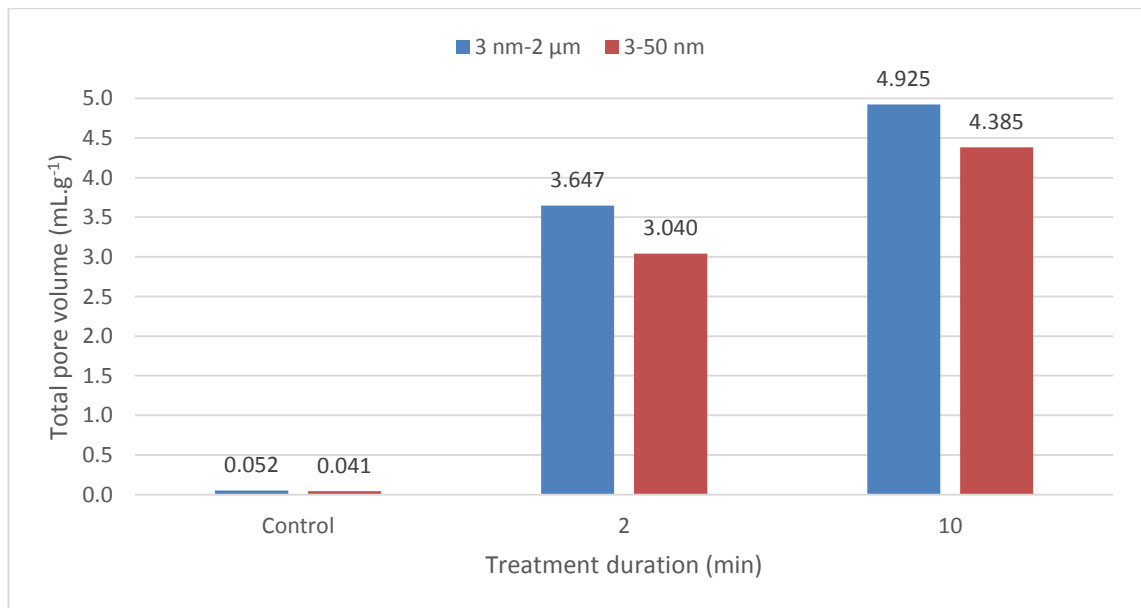
Figure 4.30 - Total fibre pore volume and mesopore volumes of wool fibres H treated in NaOH solution of lower concentration

A pore size distribution of lower concentrated NaOH solution modified wool fibres is demonstrated within Figure 4.31. It is clear from observing this graph that the control fibres demonstrate limited pore volumes of macro- and mesopores; however, pore volumes for both macro and mesopores are present after wool fibres are treated with lower concentrated NaOH solution for 2 and 10 min exposure durations. Therefore, it is possible that this treatment is capable of forming both macro- and mesopores within H wool fibres.
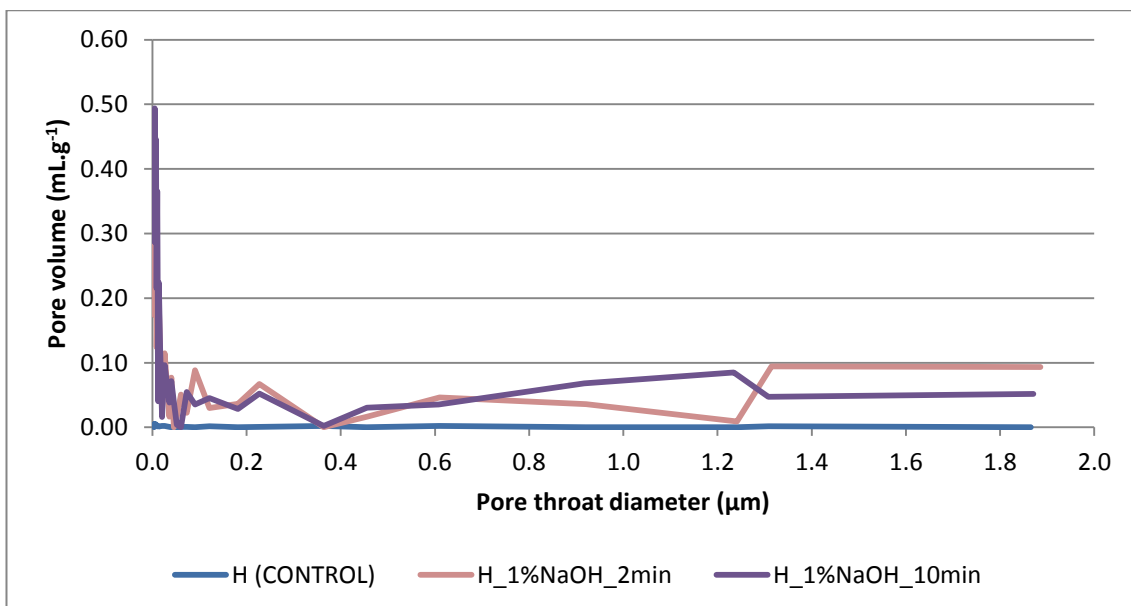
Figure 4.31 - Pore size distribution of lower concentrated NaOH solution modified wool fibres (Pore sizes: 3nm - 2µm)

This pore size distribution of the mesopores formed is detailed in Figure 4.32. It is evident that the total pore volumes of mesopores formed increased after both of the treatments. The wool fibres treated for 10 min demonstrate greater pore volumes for pores having pore throat diameters between 3 – 12 nm, while there is hardly any meso-pores detected within the control wool fibres.
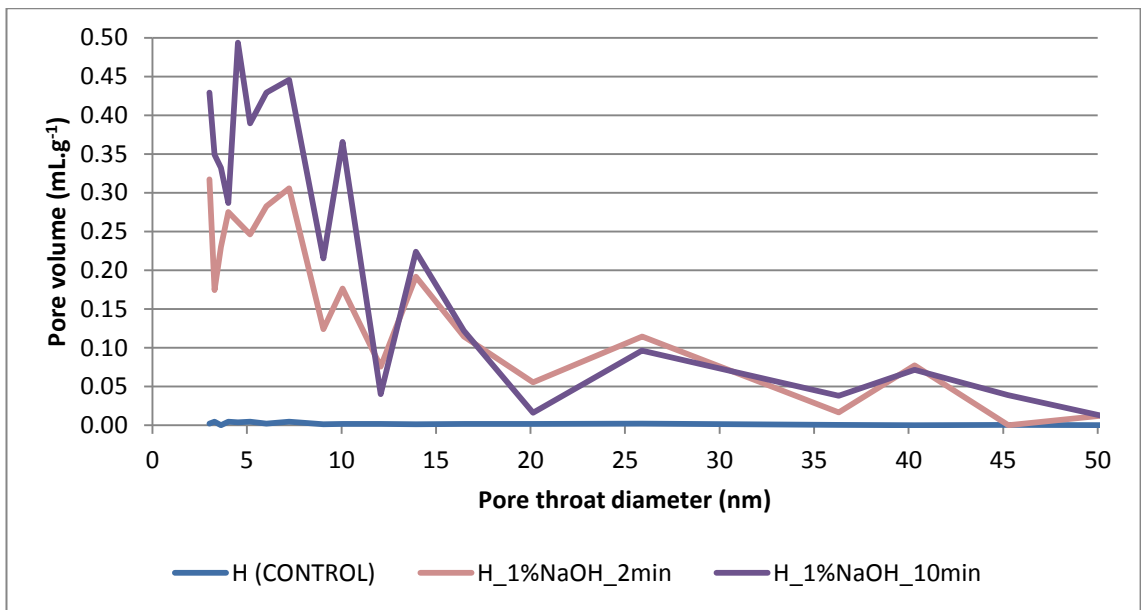
Figure 4.32 - Pore size distribution of mesopores (3 - 50nm) formed in the treatment in NaOH solution of lower concentrations

Macropores formed in NaOH treatment in both of the treatment durations are also evident in Figure 4.33, as the pore volumes for the macropores of pore throat diameters between 50 nm and 2.0 μm for the control fibres do not exceed 0.002 mL.g^{-1}). Also, similar to the graph demonstrating the total pore volumes (see Figure 4.35); it is clear within the pore distribution (see Figure 4.31) that the majority of pores formed are mesopores (83 - 88 %).
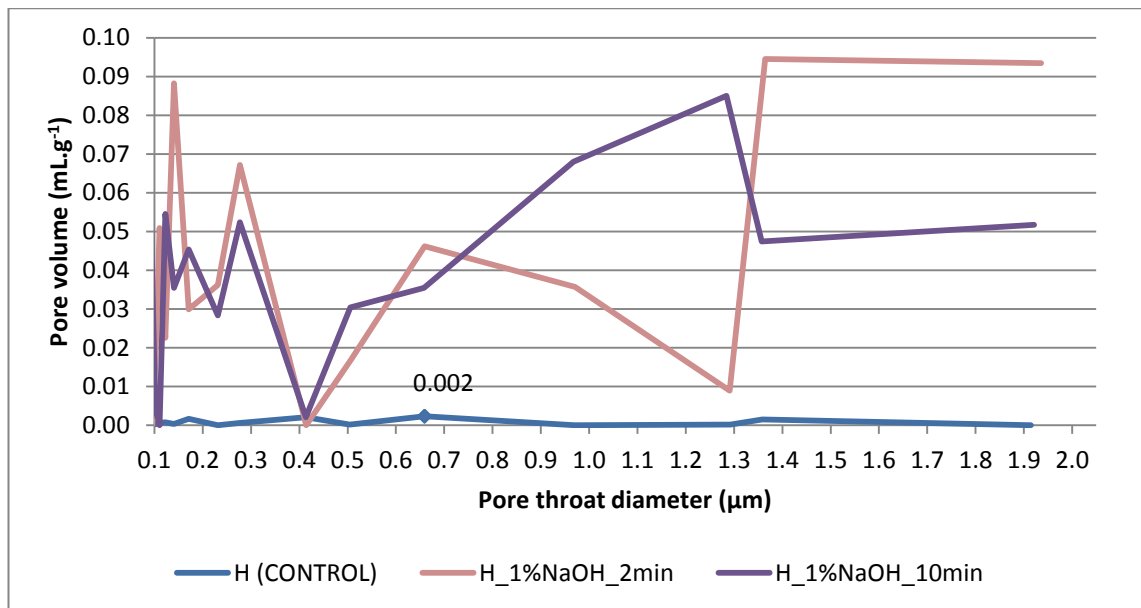
Figure 4.33 - Pore size distribution of mesopores (50nm -2 μm) formed in the treatment in NaOH solution of lower concentrations

While exposing the wool fibres in a NaOH solution of lower concentrations appears to create pores (SEM) successfully and the creases of treatment time duration increases both accessible meso- and macropores (mercury porosimetry), then it would be of great interests to investigate if wool fibres treated in NaOH solutions of higher concentrations could lead to a greater amount of pores created within the wool fibres. This will be discussed in the next section.

4.2.4.1.2 Effect of time duration in sodium hydroxide solutions of higher concentration (5%)

The effect of time duration on H wool fibres in sodium hydroxide solutions of higher concentration (5%) were shown in Figure 4.34 - Figure 4.36.

It is evident from Figure 4.34 that the wool fibres treated in NaOH solutions of higher concentration (5%) for different time durations (2 and 5 mins) demonstrated significant amount of pores formed within wool fibres. Contrary to the fibres treated with lower NaOH concentration (1%) after 2 min, macropores formation in the wool fibres treated in NaOH of higher solution (5%) after 2 and 5 mins was evident.
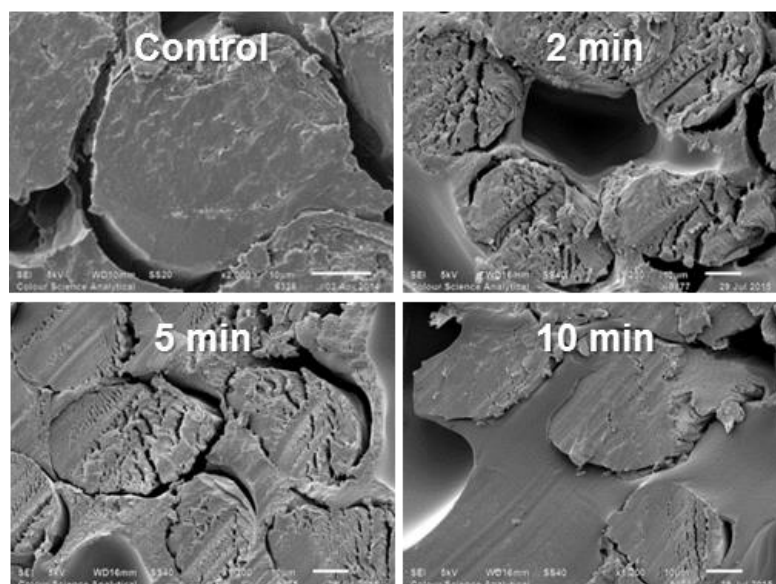
Figure 4.34 - Pores formed in wool fibres treated with a NaOH solution of higher (5%) concentration. Control fibre: Mag. x2000) and NaOH treated fibres (Mag. x1200)

The total pore volumes for the fibres treated in NaOH solutions of higher concentration (5%) were obtained from mercury porosimetry and are indicated in Figure 4.35. It is noted that the amount of the pore volumes of the pores formed is much smaller than what was observed in the NaOH treatments in lower concentration (1%). The total pore volume for fibres treated in a longer treatment time duration (5 and 10 mins) is much smaller than that of fibres obtained in a treatment of shorter time duration (2 mins). Also, pores with 3 - 50 nm widths disappear for all treated wool fibres. This could be caused by extensive degradation and dissolving of wool fibres when treated for a longer time duration.
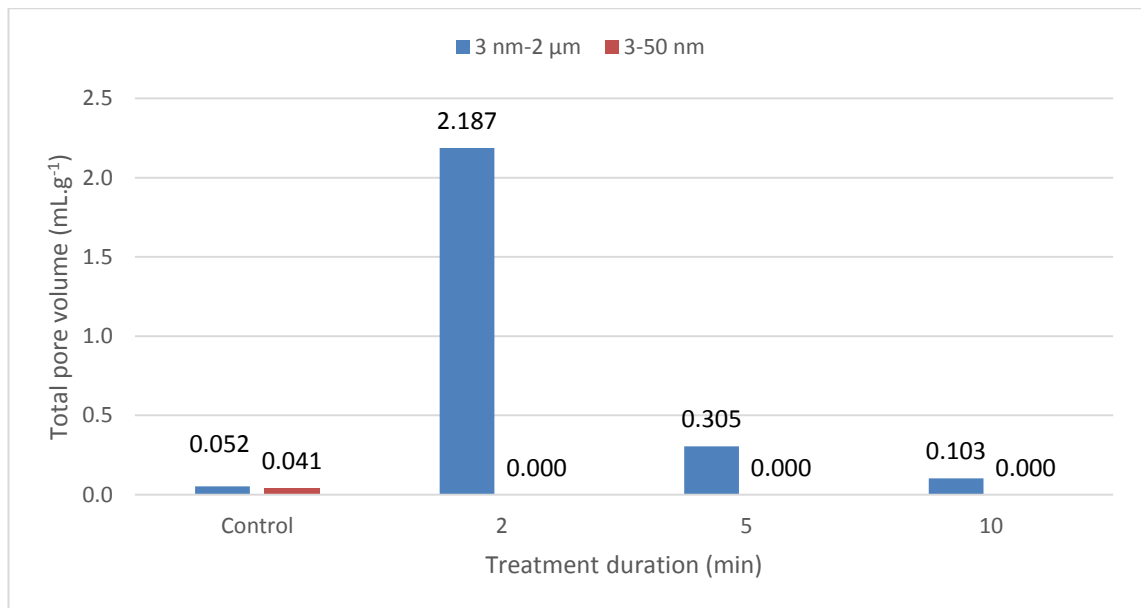
Figure 4.35 - Total fibre pore volume of higher NaOH solution modified wool fibres (Pore sizes: 3nm-2μm & 3-50nm)

Pore size distribution of the pores created (see Figure 4.36) tells more details of the pores created in the treatment. It was found in Figure 4.36 that a significant amount of pore volume of macropores were created after the 2 min treatment, particularly for pore throat diameter ranges 100 - 400 nm and 1.2 - 1.8 μm. Similar to the total pore volumes shown in Figure 4.35, these pores volumes appear to decrease with the increases of the treatment durations.
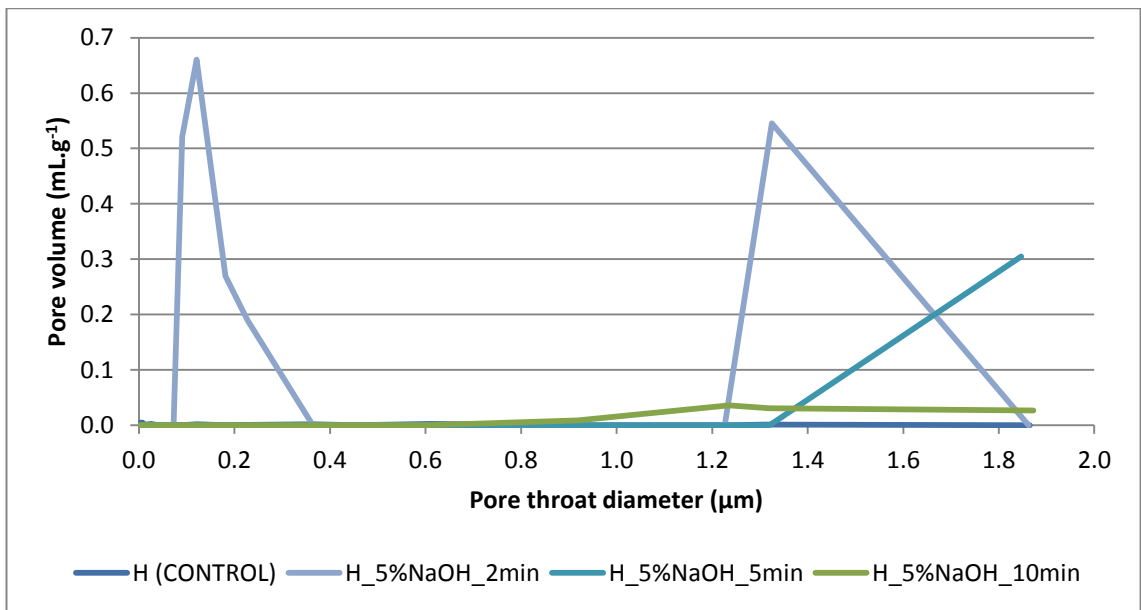
Figure 4.36 - Pore size distribution of wool fibres modified in NaOH solution of higher concentration (5%)

SEM images demonstrated that macro-pore formation within the wool fibre cross-sections was evident after 5 min and 2 min for the lower and higher concentrated NaOH solution treatments, respectively. The fibres treated with lower concentrated solution experienced an increase in total pore volume as a result of increasing the exposure duration; whereas, the fibres treated with a higher concentrated NaOH solutions demonstrated a significant increase in total pore volume after 2 min exposure, but then decreased incrementally by extending the treatments to 5 and 10 min. Therefore, to create accessible macro-/meso-pore formation within wool sample H without pre-treatment, longer treatment durations are required for fibres treated with a lower concentration of NaOH solution. For the fibres treated with higher concentrated solutions, macro-pore formation is possible after lower exposure times; however, significant fibre degradation and reduced pore volumes are evident by extending the fibre exposure beyond 2 min.

4.2.4.2 The effect of sodium hydroxide treatment on wool fibres with formic acid pre-treatment

In the previous sections, the effect of sodium hydroxide treatment on the pore formation in wool fibres without pre-treatment was investigated. In section 3.2.1, the research demonstrated that the majority of the cuticle layer could be completely removed by subjecting the British hill wool (H) to a FA pre-treatment. Therefore, this investigation will attempt to understand the effect of treating cortex exposed wool fibres with NaOH solutions.

The pore formations within FA pre-treated British hill wool fibres (H) treated in NaOH aqueous solutions of lower (1%) and higher (5%) in concentrations as well as different time durations of 2, 5 and 10 min are investigated and are shown in Table 4.13.

Table 4.13 - Sodium hydroxide treatment on wool fibres with formic acid pre-treatment

Sample code	NaOH solution concentration (%)	Treatment duration (min)
H_F2_1%NaOH_2min	1	2
H_F2_1%NaOH_5min	1	5
H_F2_1%NaOH_10min	1	10
H_F2_5%NaOH_0.5min	5	0.5
H_F2_5%NaOH_1min	5	1
H_F2_5%NaOH_2min	5	2
H_F2_5%NaOH_3min	5	3
H_F2_5%NaOH_4min	5	4
H_F2_5%NaOH_5min	5	5

4.2.4.2.1 The effect of lower concentration sodium hydroxide treatment on the pore formation in FA pre-treated wool fibres

The morphological effect of FA pre-treated H wool fibres after exposure to lower concentrated NaOH solutions for 2, 5 and 10 min were shown in Figure 4.37. Also, mercury porosimetry was used to prepare the total pore volume graph (see Figure 4.38) and pore distributions (see Figure 4.39 and Figure 4.40) used to investigate the pore formations within the wool fibres.

The SEM images demonstrated in Figure 4.37 indicate that fibre fibrillation is evident after FA pre-treated wool fibres are subjected to lower concentrated NaOH solutions for 2-10 min.
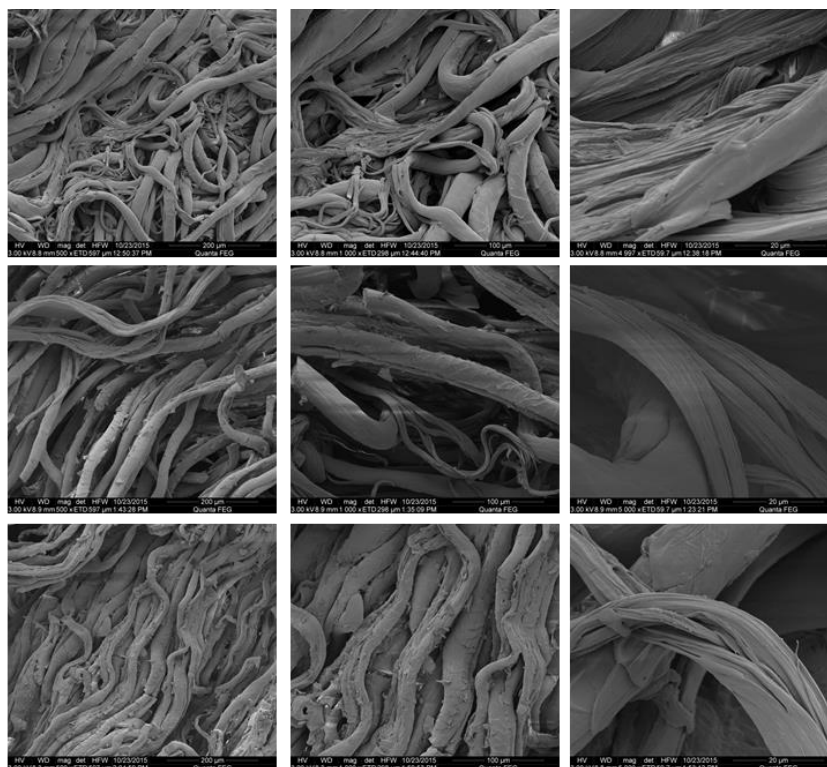
Figure 4.37 - SEM of pore formation and fibre fibrillation for FA pre-treated wool fibres treated with a lower (1%) concentration of NaOH solution. Top row: H_F2_1NaOH_2min, middle row: H_F2_1NaOH_5min and bottom row: H_F2_1NaOH_10min. Magnification (Left to right): x500, x1,000 and x5,000

According to the total pore volume data obtained by mercury porosimetry (Figure 4.38); all FA pre-treated wool fibres experienced an increase in total pore volume after the NaOH treatment. The meso-pore formation evident after the FA pre-treatment appears to disappear after the 2 min NaOH exposure; however, meso-pore formation is then evident after 5 and 10 min treatment durations. This suggests that the mesopores present after the FA treatment began to fibrillate, which increased the pores to macropores. After further treatment, mesopores appeared as a result of further fibrillation. Thus, increasing the lower concentrated NaOH treatment duration to 10 min enhances the fibrillation and meso-pore formation within FA pre-treated wool fibres.
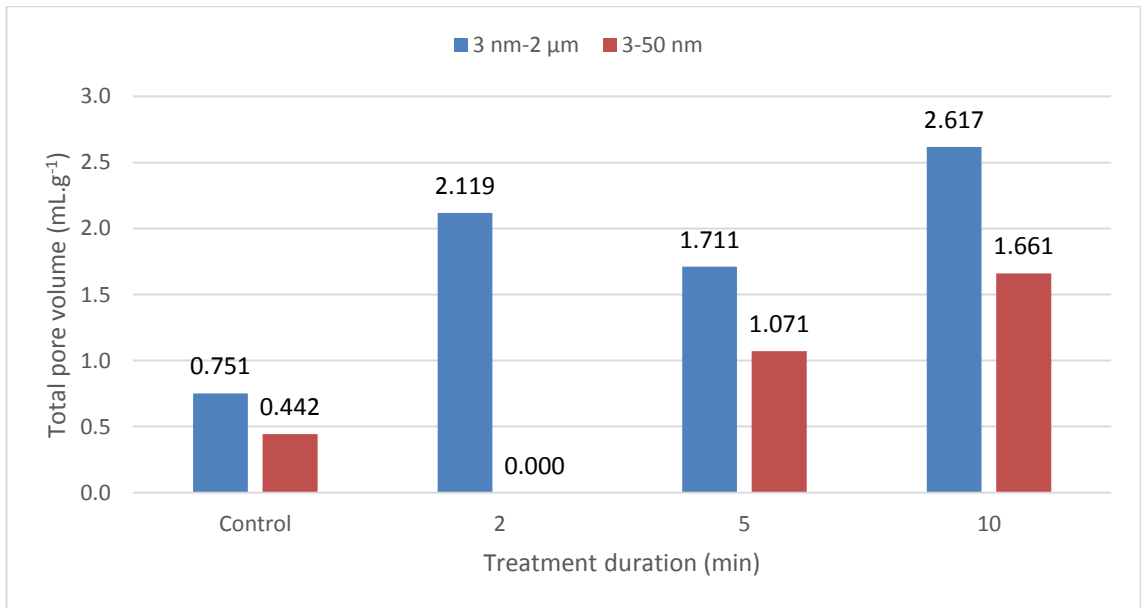
Figure 4.38 - Total fibre pore volume of lower NaOH solution modified wool fibres with FA pre-treatment (Pore sizes: 3nm-2µm & 3-50nm)

The meso-pore and macro-pore formation after the 2 min treatment duration is evident within the pore size distribution illustrated in Figure 4.39 and Figure 4.40, respectively.
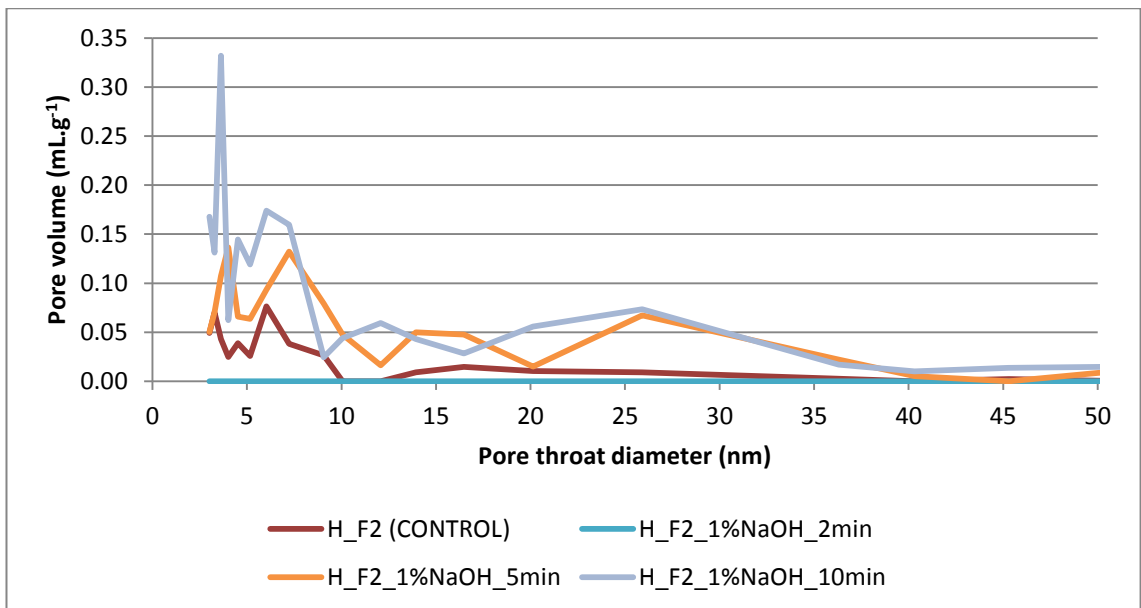
Figure 4.39 - Pore size distribution of lower NaOH solution modified wool fibres with FA pre-treatment (Pore sizes: 3 - 50nm)

There is a significant increase in pore volumes for pores between 0.05 - 0.6 μm, suggesting the mesopores from the FA treatment increased in size as a result of the 2 min NaOH solution exposure.
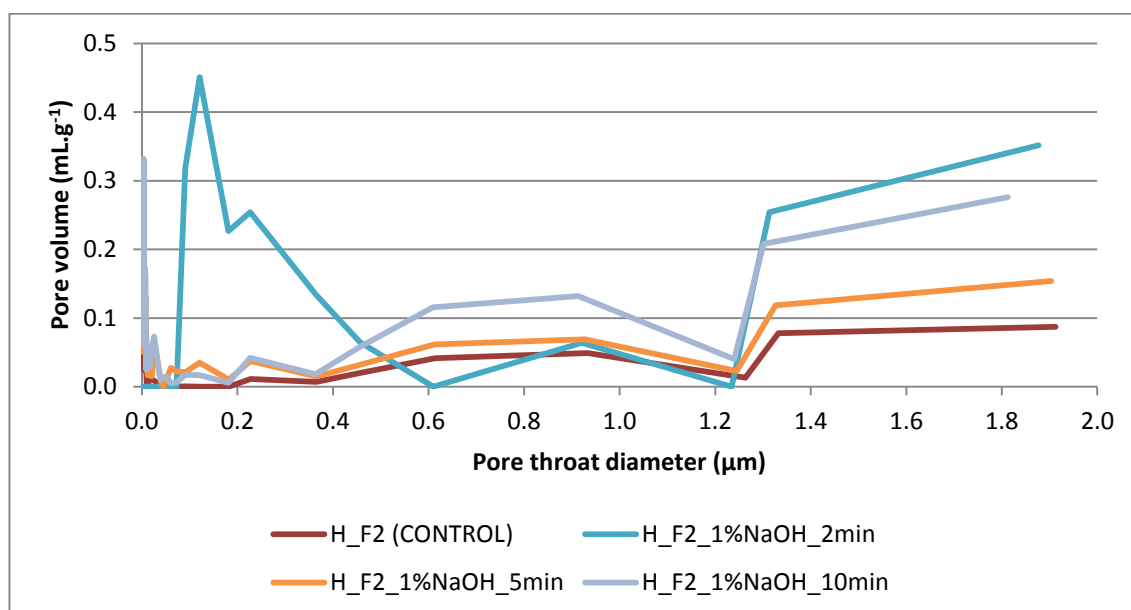
Figure 4.40 - Pore size distribution of lower NaOH solution modified wool fibres with FA pre-treatment (Pore sizes: 3nm - 2μm)

Similar to the wool fibres without FA pre-treatment the lower concentrated NaOH treatment appeared to be an effective way of introducing macro- and mesopores within the British hill wool (H) fibres. The main difference between the treatment effects is that the FA pre-treated fibres, with the cortex exposed, demonstrated fibrillation as a result of the NaOH solution exposure. It was suggested that the initial fibrillation evident after 2 min exposure caused the mesopores to expand into mesopores; whereas, extending the treatment to 5 and 10 min introduced mesopores as the exposed fibrils began to separate further.

4.2.4.2.2 The effect of higher concentration sodium hydroxide treatment on the pore formation in FA pre-treated wool fibres

To understand the effect of treating the FA pre-treated H wool fibres with higher concentrated (5%) sodium hydroxide aqueous solutions, the FA pre-treated fibres were initially treated for up to 5 min; however, this caused the fibres to almost completely dissolve.

The SEM images detailed in Figure 4.41 demonstrate the extent of the degradation caused to the FA pre-treated wool fibres by the higher concentrated NaOH solutions for 2-4 min time durations.
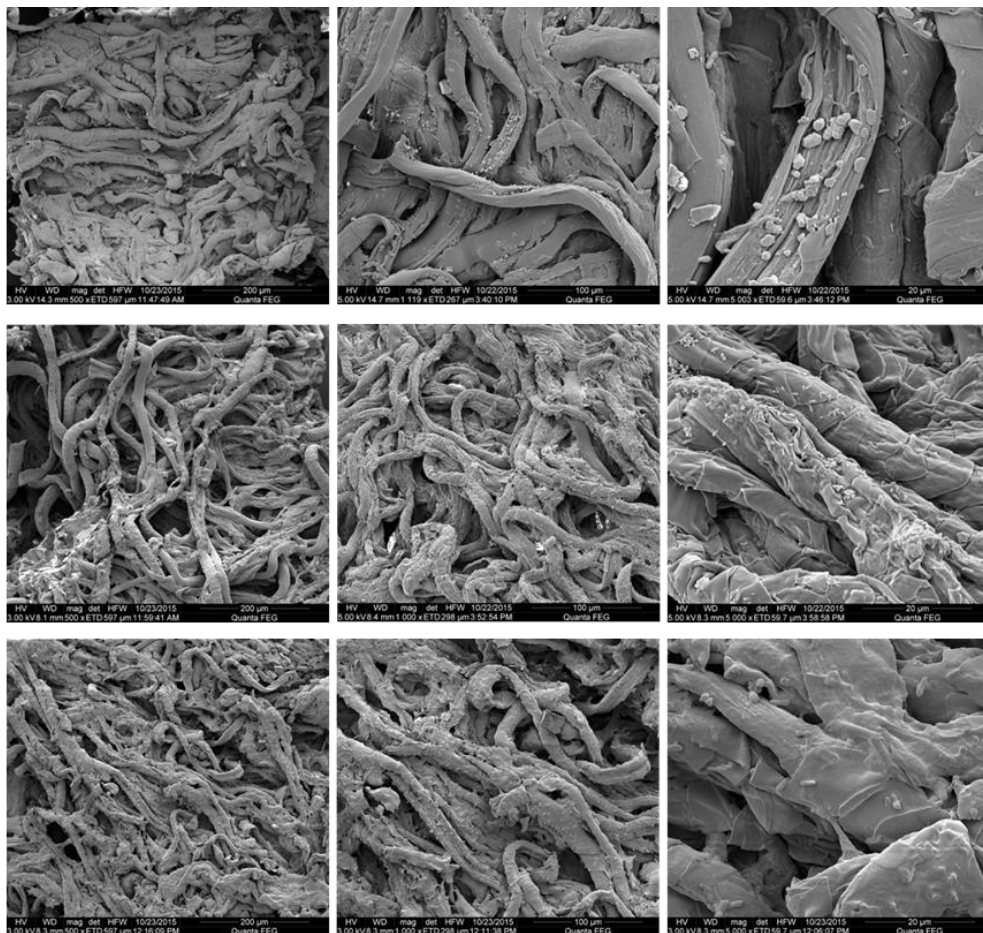
Figure 4.41 - SEM of wool fibres (H) pre-treated with FA and higher (5%) concentrated NaOH solution for extended time durations. Top row: H_F2_5NaOH_2min, middle row: H_F2_5NaOH_3min and bottom row: H_F2_5NaOH_4min. Magnification (Left to right): x500, x1,000 and x5,000

Consequently, the treatment time durations were reduced to 0.5 and 1 min. The effect of the treatment duration was analysed using SEM (see Figure 4.42) and mercury porosimetry to analyse the total pore volume and pore volume distributions of pores width pore widths between 3nm-2µm.

When comparing the fibre cross-sections of FA treated fibres (Figure 4.8) using SEM and FA pre-treated and sodium hydroxide treated fibres (see Figure 4.42), it is clear that both NaOH treatment durations cause further macro-pore formation within the fibre cross-sections.
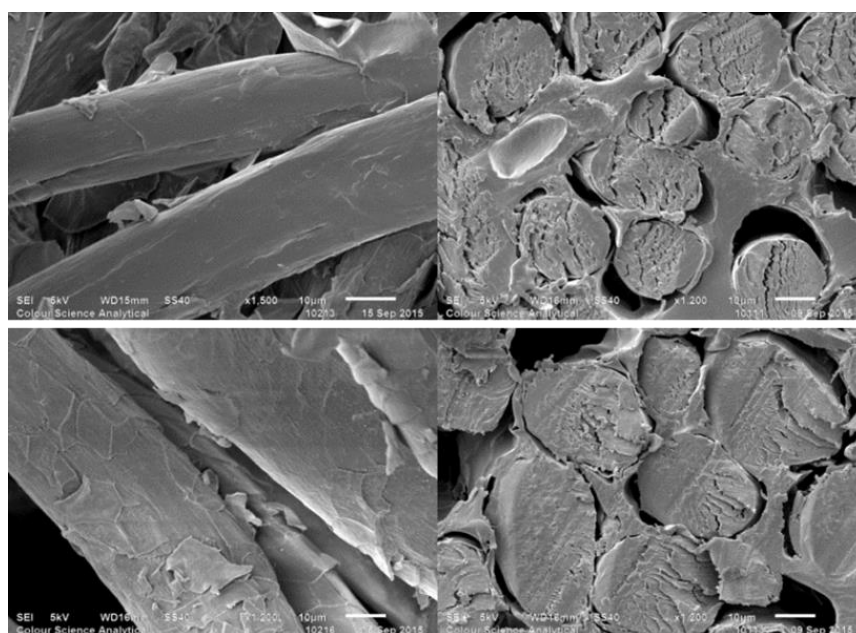
Figure 4.42 - SEM of accessible and inaccessible pores for wool fibres (H) pre-treated with FA and higher (5%) concentrated NaOH solution. Top: 0.5 min and bottom: 1 min exposure duration

To determine whether these pores are accessible mercury porosimetry was employed. The total pore volume data described in Figure 4.43 shows that the both treatment durations increase the macro- and meso-pore formations with the wool fibres. Despite the overall total pore volumes (3 nm - 2 µm) remaining fairly similar, it is evident that the meso-pore total pore volume decreases by extending the treatment duration to 1 min. The proportion of mesopores formed decreases from 75 to 45 % by increasing the exposure duration.
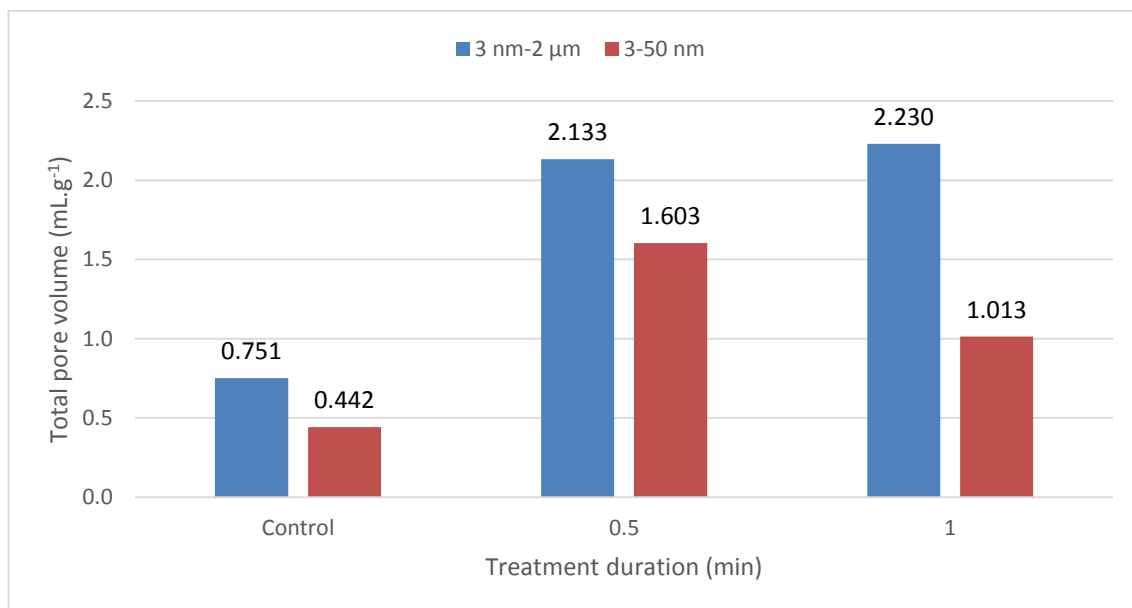
Figure 4.43 - Total fibre pore volume of higher NaOH solution modified wool fibres with FA pre-treatment (Pore sizes: 3nm - 2µm & 3 - 50nm)

This case is also represented within the pore size distributions detailed in Figure 4.44 and Figure 4.45 . The fibres treated with NaOH show greater pore volumes for pore throat diameters above 50 nm. This suggests the mesopores are either increasing as a result of enhanced fibrillation or more internal pores are becoming accessible or both.
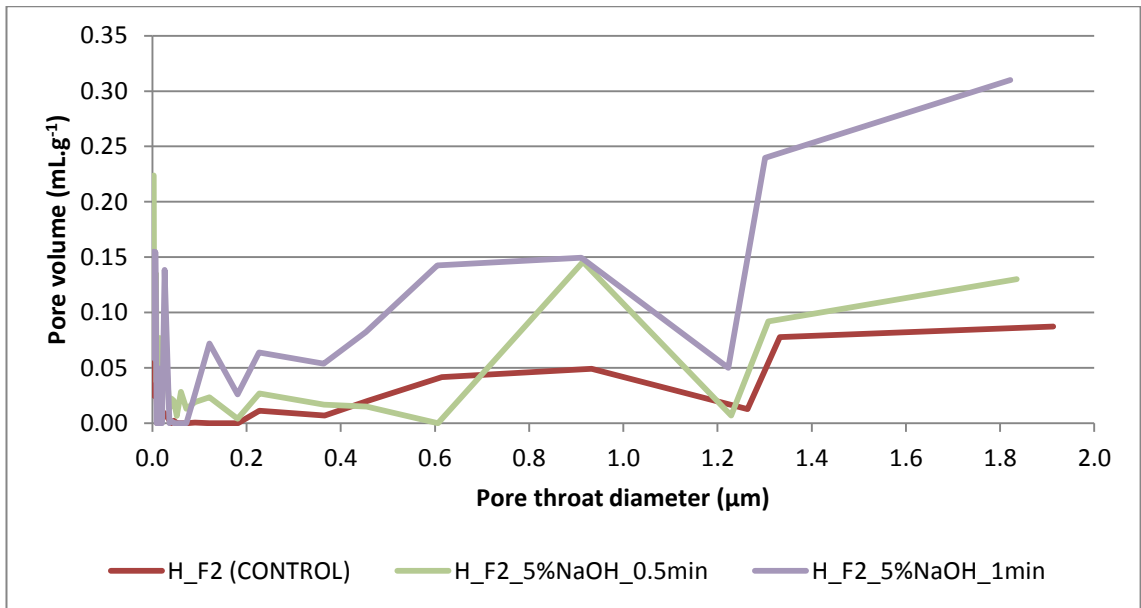
Figure 4.44 - Mercury porosimetry analysis (Pore size distribution) of higher NaOH solution modified wool fibres with FA pre-treatment (Pore sizes: 3nm - 2µm)

This phenomena is also evident within the meso-pore pore size distribution (Figure 4.45), as there is an increase in pore volumes for pores with pore throat diameters of approximately 27 nm (0.138 ml.g^{-1}).
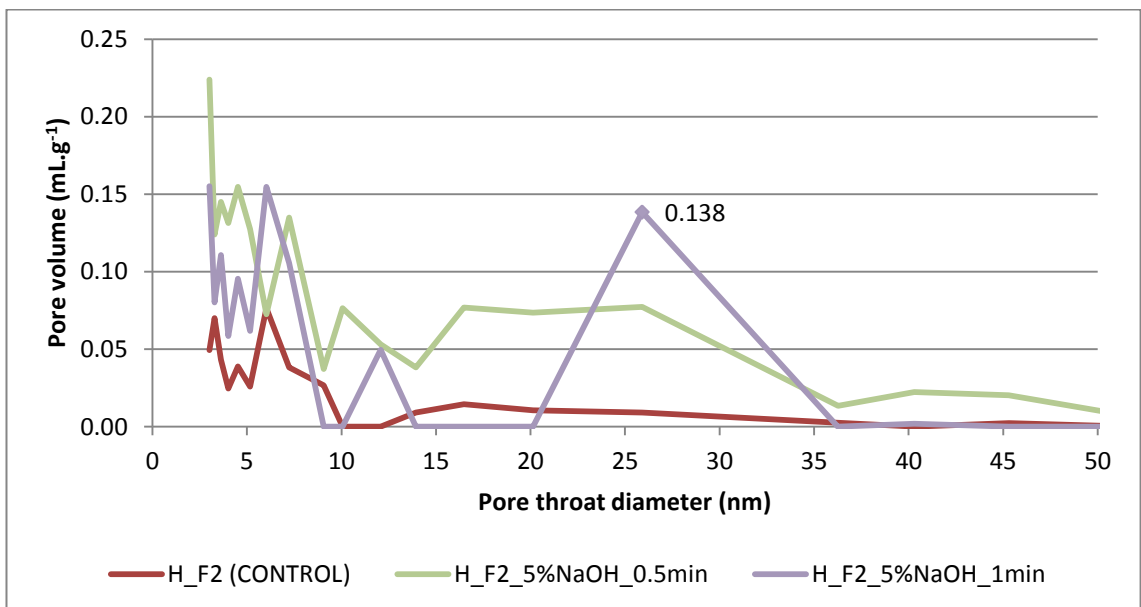
Figure 4.45 - Mercury porosimetry analysis (Pore size distribution) of higher NaOH solution modified wool fibres with FA pre-treatment (Pore sizes: 3 - 50nm)

The FA pre-treated wool fibres experienced significant degradation as a result of exposure to higher concentrated NaOH solutions, particularly beyond 1 min treatment durations. However, macro- and meso-pore formation was evident between 0.5 - 1 min treatment exposure durations. Similar to the lower concentrated treated fibres it is propose these pore formation are the result of partial fibre fibrillation. The meso-pore formation appeared to reduce as a result of extending the treatment duration to 1 min; however, further testing using increased exposure time increments are required to fully understand this theory.

4.3 Summary

The effects of several novel chemical treatments and their combinations on the microstructure of wool fibres have been studied in order to improve the adsorption properties of the wool fibres. The techniques studied include oxidation (Formic acid treatment), oxidation/swelling (Ozone treatment in urea hydrogen peroxide solution) and reduction treatments (Sodium hydroxide treatments) and their combinations.

Meso- and macro-pore formation was evident after wool fibres and fabrics were treated with individual and consecutive chemical treatments. However, additional physical selective degradation techniques are required to expand accessible pores or expose inaccessible pores formed after chemical treatment.

One shortcoming of this experiment was that only one repetition was recorded for each sample when using mercury porosimetry due to the extensive time duration and cost of the procedure. To ensure an accurate measurement and to obtain a result representative of the whole sample, the fibres were cut into staple fibres and mixed before loading into the sample tubes.

Chapter 5 Formation of Porous Wool Fibres using Physical Selective Degradation Processes

It was concluded in Chapter 4 that the pores formed in wool fibres during various chemical treatments could be either accessible or non-accessible. It is thus desirable to identify various methods to both open and expose these inaccessible internal pores produced in the chemical treatments. In this chapter, the effects of two selective degradation processes, high energy electron beam irradiations and plasma treatment, on the formation of porous fibre structures in the wool keratin polymers are studied.

British medium fine hill wool fibres (MFH) were selected for investigating effects of selective degradation processes due to evidence of meso- and macropore formation after individual and subsequent FA-ozone chemical treatments (see Chapter 4, section 4.2.3). These wool fibres were used for both the electron beam irradiation and air plasma studies to determine whether a subsequent treatment was capable of exposing inaccessible pores formed during chemical treatment. The proportion of meso- and macropore formation was different for FA-ozone(UHP) treated MFH fibres when the ozone treatment duration was varied from 24 to 96 h. Therefore, both FA pre-treated MFH fibres treated with ozone for 24 and 96 h were selected for this study.

Australian worsted woven merino wool fabric (MWov) was selected for part of the air plasma study and the oxygen plasma study to determine whether it was possible to selectively degrade the surface fibres of wool fabrics rather than randomly organised loose wool fibres. From a practical perspective, the plasma treatment on fabrics could be more effective as the fibres were regularly aligned in the fabric plane within the plasma machine and also could be more beneficial from commercial manufacturing perspective. Mercury porosimetry demonstrated meso- and macropore formation within MWov fabrics after exposure to the individual and consecutive chemical treatments, which were explored in Chapter 4 for MFH wool fibres (see Appendix).

5.1 Degradations of wool fibres under the irradiation of high energy electron beams

Selectively degradation of the outer surface of wool fibres was identified when wool fibres was exposed to the bombardment of high energy electron beam in SEM analyse (Ward and Mao, 2016). When wool fibres were placed under the irradiations of high energy electron beams and high magnifications in SEM systems, the surface layers of the wool fibres appeared to be selectively degraded in reticulated patterns.

In this section, the wool fibres are exposed to the irradiations of electron beams of different energy levels in scanning electron microscopies, the effect of different electron beam radiation conditions on the selective degradation of wool fibres after different chemical modifications was investigated.

Higher and lower electron beam current SEM systems were used within this study. For the higher electron beam current experiments, the wool fibres were coated in platinum (Pt) using a Cressington 208 HR Sputter Coater, and exposed to the electron beam in a Carl Zeiss EVO MA15 SEM system. Whereas, for the lower electron beam current experiments, the wool fibres were coated in gold (Au) using a Quorum Q15OR S Sputter Coater and a JEOL JSM 6610LV SEM system.

5.1.1 The effect of different electron beam irradiation conditions on the selective degradations of wool fibres

The energy level of electron beam bombardments on targeted wool fibres in SEM system varies with various parameters such as applied voltage, working distance and magnifications (Reimer, 1998; Goldstein, 2003; Egerton, 2005). Higher applied voltage, smaller working distance, higher magnifications and greater exposure time duration will lead to higher electron beam energy transferred to the wool fibres. The effect of different electron beam irradiation conditions on the selective degradations of wool fibres are investigated in this section.

The experiments for the exposure of these wool fibres to different electron beam radiation conditions are detailed in

Table 5.1. SEM images demonstrating the effect of electron beam radiation on untreated wool fibres and three types of chemically treated wool fibres (wool fibres after FA treatment, FA and Ozone-UHP treatment for 24 hours, and FA and Ozone-UHP treatment for 96 hours) were shown in Figure 5.1 - Figure 5.6, respectively.

The aim of this preliminary experiment was to identify and understand treatment conditions required to form reticulated pore structures on raw and chemically modified wool fibres. Chemically modified wool fibres were exposed to various electron beam currents, applied voltages, working distances and exposure time durations as these standard operating variables are capable of varying the electron beam intensity in the SEM system. The selective degradation of the wool fibres was evident visually when exposed to electron bombardment. So, instead of investigating the effect of specific variables the conditions were varied until noticeable degradation appeared and the parameters were recorded. This is the reason for the variation, variables and unconventional experimental plan detailed in

Table 5.1.

Table 5.1 - Experiments of exposing chemically modified British medium fine hill (MFH) wool fibres in electron beam radiations in SEM system

Sample coding	Chemical treatment	Electron beam current	Applied voltage (kV)*	Working distance (mm)	Exposure time duration (min)
A	MFH_F2	Higher	10	13.5	1
B	MFH_F2	Higher	20	10.0	5
C	MFH_F2	Higher	20	13.0	5
D	MFH_F2	Lower	30	14.0	5
E	MFH_F2_OZ24 _UHP	Higher	20	13	1
F	MFH_F2_OZ24 _UHP	Lower	30	17	5
G	MFH_F2_OZ96 _UHP	Higher	20	13	1
H	MFH_F2_OZ96 _UHP	Lower	30	16	5

Magnification x10,000

It is expected that the selective degradation of wool fibres might be further developed if the wool fibres exposed to electron beams of higher energy in extended time duration, this could possibly lead to the creation of pores on the fibre surfaces. Therefore, the selective degradation in FA treated wool fibres in an electron beam of higher applied voltage of 20 kV, a shorter working distance of 10 mm and extended exposure duration of 5 mins in the above SEM system (Carl Zeiss EVO MA15 system) is investigated.
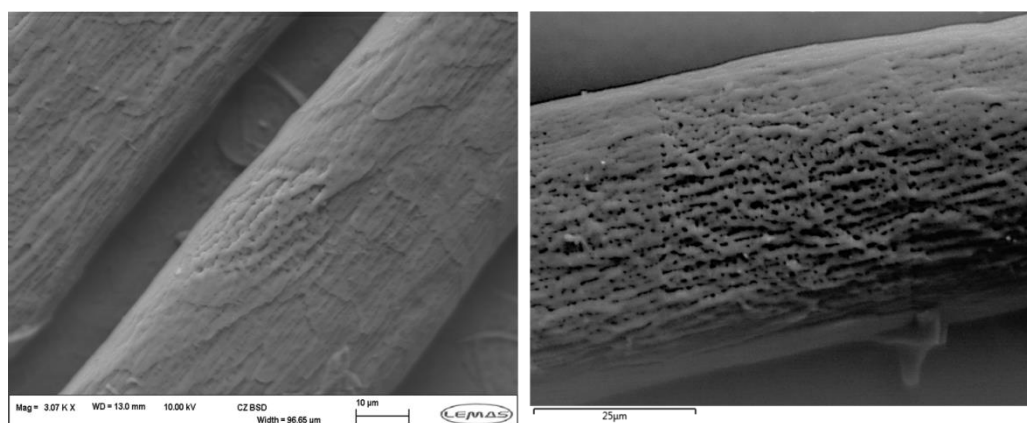
Figure 5.1 - Selective degradation of MFH wool fibres after FA treatment under high energy electron impacts. Left: (Sample A) Higher frequency SEM system, Applied voltage: 10 kV, Working distance: 13 mm and Exposure time duration: 1 min. Right: (Sample B) Higher frequency SEM system, Applied voltage: 20 kV, Working distance: 10 mm and Exposure time duration: 5 min

As shown in Figure 5.1, partial fibrillation and reticulated macropores were formed on the fibre surface with the size of majority of the pores created are less than 1 µm. However, it is unclear whether the structure of the reticulated pores extends in to the core of the wool fibre.

The selective degradation of FA treated MFH fibres before and after high energy electron are shown in Figure 5.2. The surface degradation did not appear when the fibres were under smaller magnifications. However, selective degradation on the fibre surface was evident, as illustrated by the rectangular section shown in the image, when the magnification of the image increased up to x10,000. This is because the FA treated

153

wool fibres were exposed to a more intense electron beam bombardment with the increase of the SEM magnification.
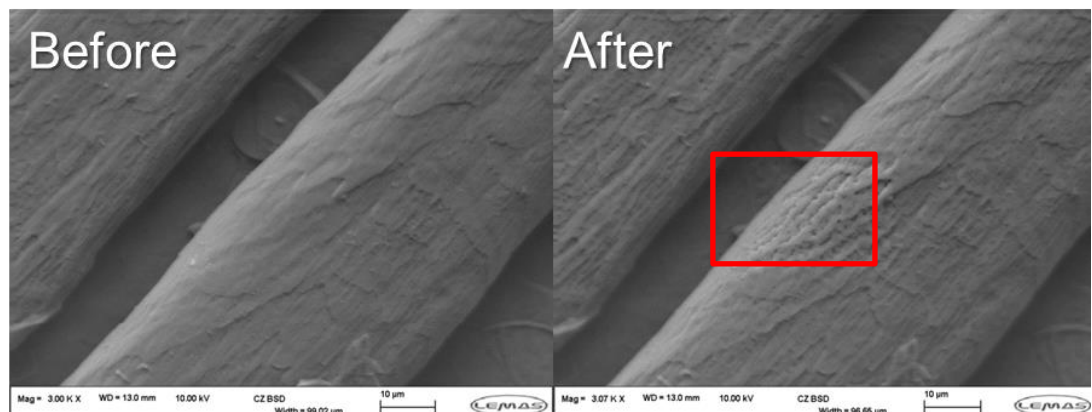
Figure 5.2 - Selective degradation of MFH wool fibres after FA treatment under high energy electron impacts

It is thus clear that only the part of the fibre surface exposed to the electron beam in a higher SEM magnification was degraded while the working distance between the fibre surface and the electron gun was maintained at 13 mm; it appears that the electron beam intensity is responsible for the selective degradation of the wool fibres. However, it is noticed that there is no apparent pores formed on the fibre surface.

The intensity of energy a sample is exposed to depends upon many factors, including system configurations and capabilities. However, the key factors include the energy of electron beam emitted and the dose of electrons that interact with the sample or defined sample area (Reimer, 1998; Egerton, 2005). The energy of electron beam emitted or the probe current is determined by the current of the filament and the accelerating voltage applied. A high current and acceleration voltage will increase the dose of electrons within the beam, However, the dose of electrons that interacts with the sample or defined sample area can be manipulated by varying the system configuration, including the magnification, aperture, depth of field and stage working distance.

Reducing the electron beam diameter on a specific area will increase the amount of electrons interacting with a particular sample area. Increasing the magnification reduces the area exposed to the electron beam, which increases the intensity of electrons interacting per unit area of the sample. Also, the electron beam diameter exposed to the wool fibres is affected by the condenser and objective lens configuration, aperture, depth of focus of the SEM system and the working distance of the sample. The aperture is positioned between the lenses. The adjustment of the condenser lens enables you to control the electron beam/ probe diameter and the probe current. The excitation of the condenser lens determines the amount of electrons able to pass through the aperture. If the excitation is increased, the electron beam greatly broadens on the aperture and therefore the number of electrons / amount of probe current reaching the objective lens reduces. Conversely, if the excitation of the condenser lens decreases then the electron beam diameter reduces and most of the electrons are able to pass through the aperture (JEOL, 2009).
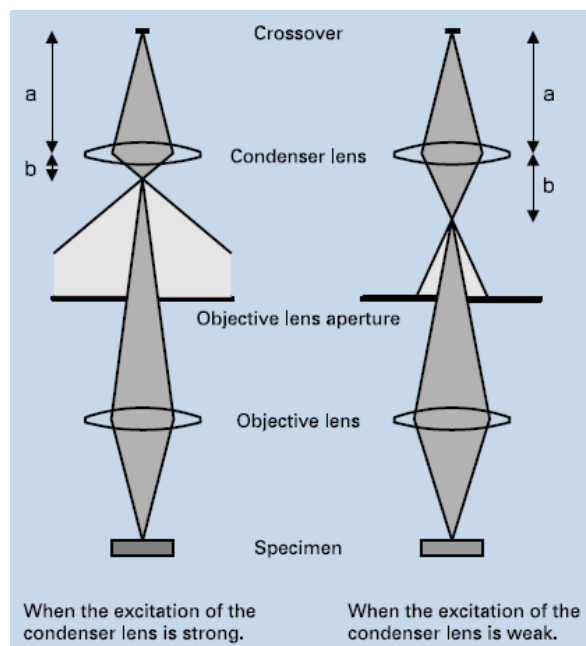
Figure 5.3 - Formation of the electron probe by the condenser and objective lenses. High condenser lens excitation can reduce the electron probe current and increase the probe diameter (JEOL, 2009)

It is expected that increasing the electron dose within the beam, while focusing the beam on a defined sample area will increase the energy subjected to the sample, which will increase the selective degradation of the wool fibres. Also, t is expected that an SEM system with a higher electron probe current capability would show greater selective degradation with the creation of pores on the surface. To compare the effect of a using such a system, selective degradation of wool fibres after FA treatment under high energy electron impacts for exposure duration of 5 mins in the above SEM system (Carl Zeiss EVO MA15 system) was investigated. The resultant wool fibres for both higher and lower frequency electron exposure are detailed within Figure 5.4.
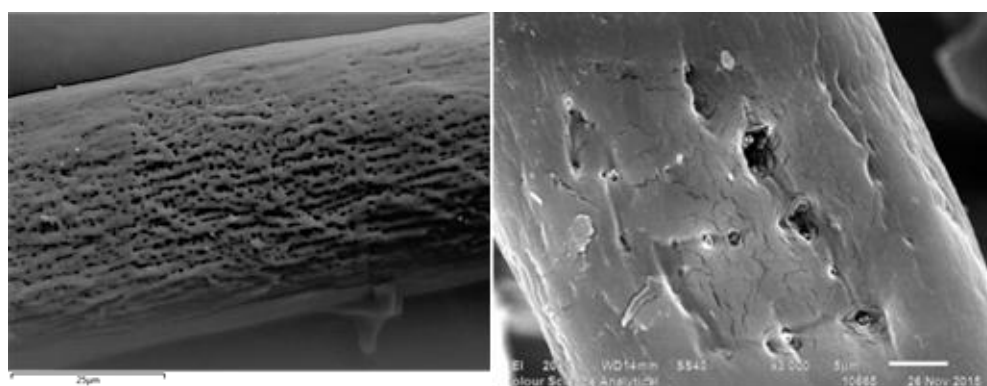
Figure 5.4 - Selective degradation of wool fibres after FA treatment under high energy electron impacts. Left: (Sample C) Higher frequency SEM system, Applied voltage: 20 kV, Working distance: 13 mm and Exposure time duration: 5 min. Right: (Sample D) Lower frequency SEM system, Applied voltage: 30 kV, Working distance: 14 mm and Exposure time duration: 5 min

Despite using a higher applied voltage the resultant wool fibres after subjection to lower frequency SEM system demonstrated fewer pores and crack formation. Again, it appears that the electron beam intensity is responsible for the selective degradation of the wool fibres and pore formation is evident after exposing the chemically modified wool fibres to higher electron beam intensity.

To investigate the effect of a using higher frequency SEM systems further, FA and ozone-UHP treated for 24 hours (see Figure 5.5) and FA and ozone-UHP treated for 96 hours (see Figure 5.6) were exposed to selective degradation under high energy electron impacts for an exposure duration of 5 mins.
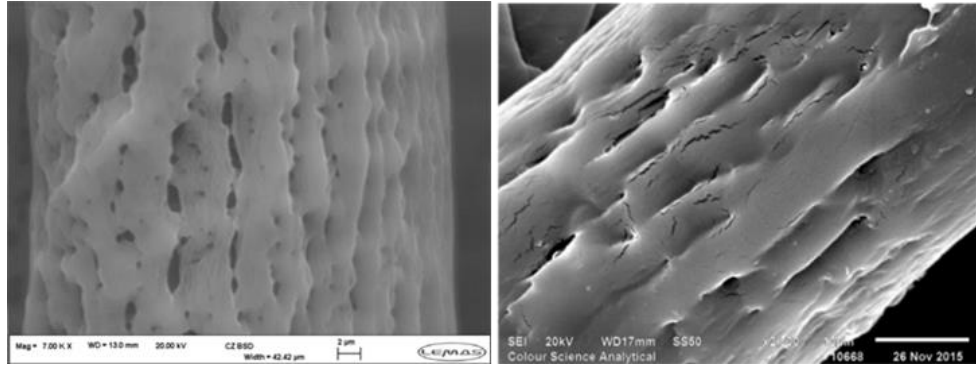
Figure 5.5 - Selective degradation of wool fibres after FA and Ozone-UHP treatment for 24 hours under high energy electron impacts. Left: (Sample E) Higher frequency SEM system, Applied voltage: 20 kV, Working distance: 13 mm and Exposure time duration: 1 min. Right: (Sample F) Lower frequency SEM system, Applied voltage: 30 kV, Working distance: 17 mm and Exposure time duration: 5 min
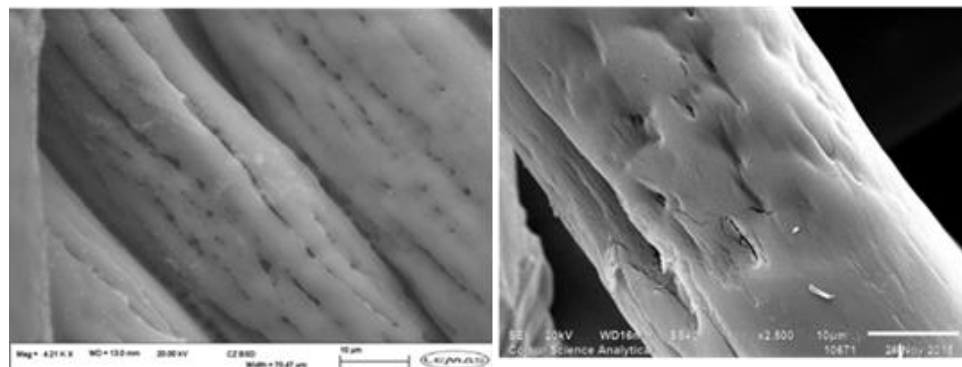
Figure 5.6 - Selective degradation of wool fibres after FA and Ozone-UHP treatment for 96 hours under high energy electron impacts. Left: (Sample G) Higher frequency SEM system, Applied voltage: 20 kV, Working distance: 13 mm and Exposure time duration: 1 min. Right: (Sample H) Lower frequency SEM system, Applied voltage: 30 kV, Working distance: 16 mm and Exposure time duration: 5 min

Similar to the selective degradation of MWov after FA treatment, pore formation and fibrillation was evident after selective degradation of FA and Ozone-UHP treated fibres using the SEM system capable of producing a higher probe current.

In summary, degradation and pore formation is evident after exposing the wool fibres to selective degradation under high energy electron impacts; however, sufficient electron beam intensity and exposure durations are required to form pores on the chemically

modified wool fibres. Therefore, the main parameters associated with selective degradation and pore formation are exposure time duration and electron beam intensity, which can be altered by varying the applied voltage, magnification, working distance, and the SEM system.

5.1.2 The effect of different chemical modifications on the selective degradations of wool fibres under higher energy electron beam irradiations

In this research, this method of degrading various chemically modified wool fibres was further explored to determine whether it is capable of forming pores on the surface of any particular fibres. Macro-pore formation by selective degradation was evident for wool fibres pre-treated with FA and ozone in UHP solution for 24 h and 96 h, suggesting the fibres partially fibrillate after the chemical treatments. It is possible the additional selective degradation using high electron impact on fibre surfaces could improve the adsorption capability of the wool fibres.

The aim of this study is to investigate the mechanism of selective degradation by analysing the change in chemical composition of various chemically modified wool fibres after electron beam exposure. The experimental plan for the study is detailed within Table 5.2. The various electron beam exposed wool fibres were analysed by SEM and EDX.

Table 5.2 - The effect of different chemical modifications of wool fibres on their selective degradations under electron beam irradiations

Sample coding	Applied voltage (kV)	Exposure duration (min)
MFH (Control)	10	1
MFH_F2	10	1
MFH_F2_OZ24 _UHP	20	1
MFH_F2_OZ96 _UHP	20	1
MFH_F2	30	5
MFH_F2_OZ24 _UHP		
MFH_F2_OZ96 _UHP		

Working distance: 13 mm, magnification: x10,000

The effect of the electron beam on untreated and FA treatment MFH wool fibres are shown in the SEM image detailed in Figure 5.7.
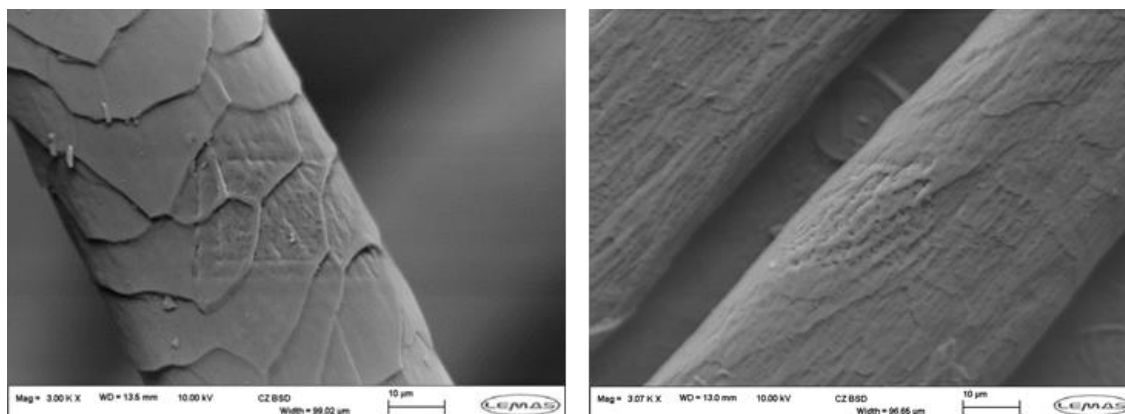
Figure 5.7 - Selective degradation of untreated MFH (Left) and FA pre-treated MFH wool fibres (Right) under high energy electron impacts

It is found that the surface degrades for both wool fibres, but the internal structures of the fibres appear unaffected. Also, the selective degradation is evident on both the cuticle (untreated MFH fibre) and exposed cortex (FA treated MFH fibre).

The extent of degradation of wool fibres with different chemical modifications under the high energy beam irradiations might be different. The selective degradations of FA treated wool fibres are compared with that of the wool fibres with FA and additional ozone-UHP chemical modifications under the same high electron beam irradiation conditions. The surface degradation of FA and ozone-UHP treated wool fibres after electron beam irradiations are shown in Figure 5.8.
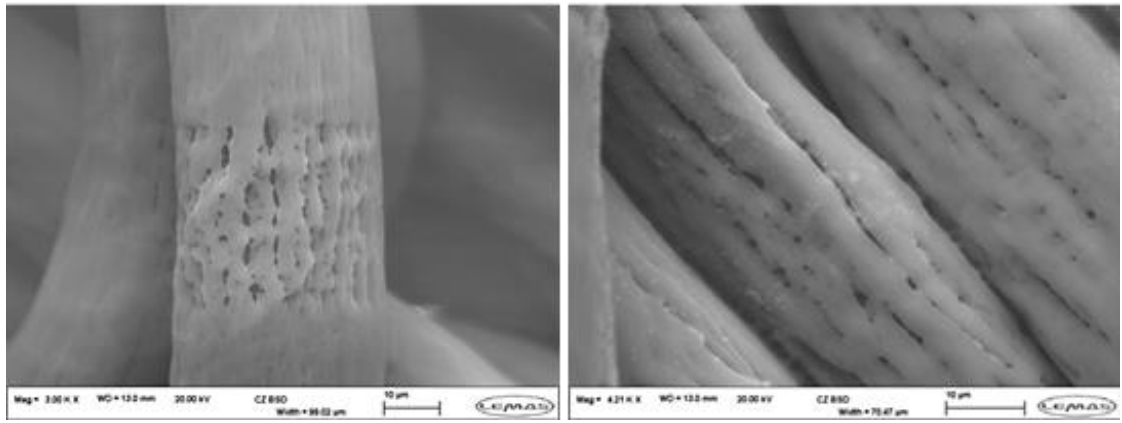
Figure 5.8 - Selective degradation of MFH wool fibres after FA and Ozone-UHP treatment for 24 (Left) and 96 (Right) hours under high energy electron impacts

It is interesting to note that macro-pore formation is evident on the fibre surface of both FA and ozone-UHP treated wool fibres after its exposure to high intensity electron beam for 5 mins. For the fibres treated in ozone for 24 hours, the pores appear to be <1 μm; however, it is uncertain whether the treatment forms internal pores or a reticulated structure. Also, after the wool fibres exposure to the electron beam, the macropores appeared to be along the longitude of cortical cells as the ribs created on the fibre surface are around the size of 2 μm which is the width of cortical cells, suggesting the high energy electron impacts degraded the CMC between cortical cells. Similar pore formation was observed on the fibre surface of wool fibres with FA and ozone-UHP treatment for 96 h after electron beam irradiations; the macropore formations appeared in multiple wool fibres and much more pores were created, these could be possibly caused by the extended duration of chemical oxidisation of the cortex layers by using ozone treatment in UHP solution.

It is thus suggests that additional selective degradation with irradiations of using high energy electron beam is required to degrade wool fibres and consecutive chemical modifications of these wool fibres are a pre-requirement for forming macropores on the fibre surfaces and to expose the internal microstructure of wool fibres.

The images illustrated within Figure 5.9 demonstrate the effect of high energy impact by SEM on MFH wool fibres with different chemical pre-treatments. All fibres experience crack and show pore formation, and selective degradation happens within the cortex after the impact of 30 kV electron beam for 5 min. Similar to the research conducted previously, macro-pore formation by selective degradation was evident for wool fibres pre-treated with FA and ozone in UHP solution for 24 and 96 h, suggesting the fibres partial degraded after the chemical treatments and an additional treatment of high electron impact would selectively degrade the wool fibres. This suggests that both the pre-chemically treatments and the selective degradation might cause the disruption to the cell membrane complex, and the ozone-UHP treatment for 24 h appears to have enhanced selective degradation of wool fibres during electron beam impact in comparison with the ozone-UHP treatment for 96 h.

Before 30 kV exposure   After 30 kV exposure
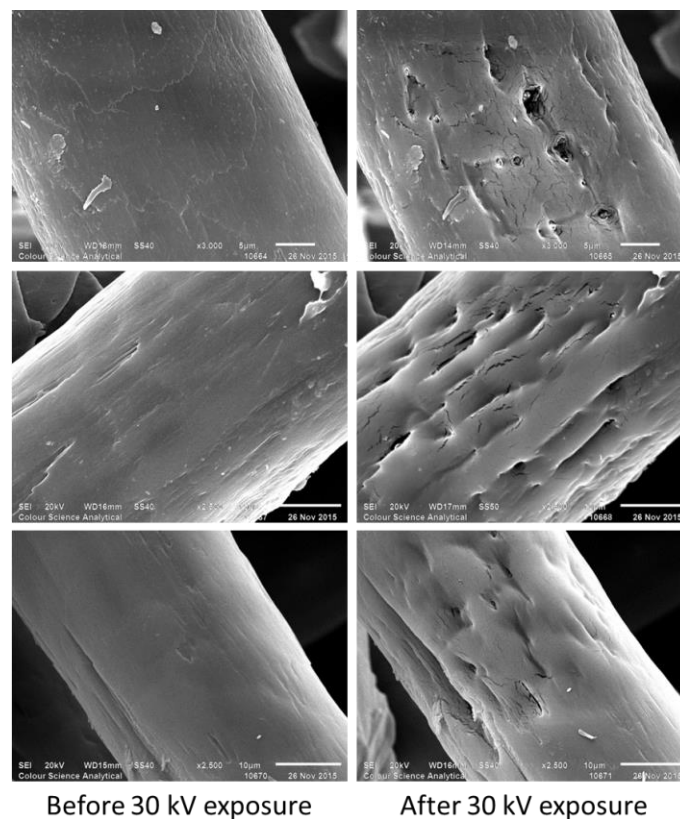
Figure 5.9 - Chemically modified MFH wool fibres (Left) exposed to electron beam radiation (Right). Top row: MFH_F2, middle row: MFH_F2_OZ24_UHP and bottom row: MFH_F2_OZ96_UHP

Enhanced degradation to chemically modified wool fibres was reported by Allen and Alexander (1961), when wool fibres treated with solutions, capable of breaking hydrogen bonds or reagents that disrupt disulfide bonds, were exposed to irradiation. It was concluded that different chemically modified wool fibres will supercontract or degrade differently when exposed to irradiation. Therefore, it is possible that the individual or consecutive chemical treatments disrupt the hydrogen bonds within the polypeptide backbone or amino acid side chains. To investigate this theory further EDX analysis was conducted before and after high energy irradiation exposure to different chemically treated wool fibres. Unfortunately, EDX is unable to measure the presence of hydrogen; therefore, the amount of alternative elements that form hydrogen bonds, such as oxygen, sulphur and carbon could be analysed to determine whether these bonds have been disrupted.

For the FA pre-treated wool fibre treated with O_2 plasma, the EDX analysis of the percentage element composition demonstrates that carbon, oxygen, sulphur and nitrogen are present after the high energy impact exposure; however, the EDX analysis was not able to detect nitrogen prior to the treatment. Therefore, it is possible the treatment exposes molecules containing nitrogen; this might indicate that the selective degradation is related to the exposure of nitrogen groups of keratin molecules. Alternatively, this could be a limitation of the EDX system as nitrogen elements are often difficult to obtain.

The pre- and post-treatment data for wool fibres treated with ozone-UHP treatment for 24 and 96 h is comparable as both pre- and post- treatment data sets demonstrate the same types of element compositions. The element percentage composition graphs are illustrated for ozone-UHP treatment for 24 and 96 h time durations within Figure 5.10 and Figure 5.11, respectively. Similar to the SEM analysis the EDX analysis shows similar trends in terms of pre- and post-treatment element percentage compositions.
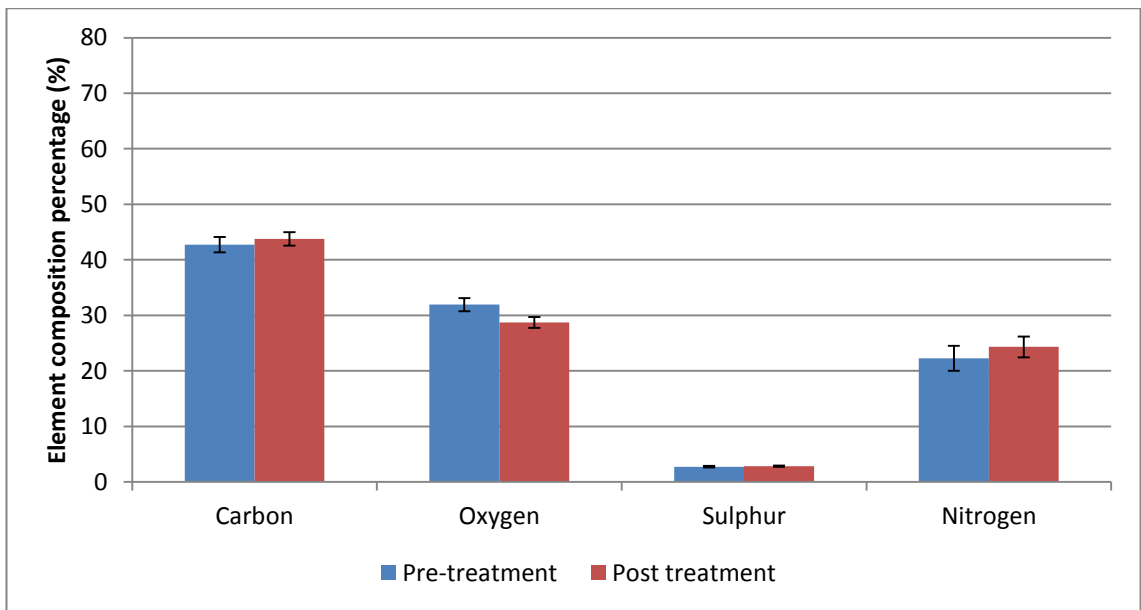
Figure 5.10 - Element composition percentage of FA pre-treated MFH wool fibres with ozone-UHP treatment for 24 h
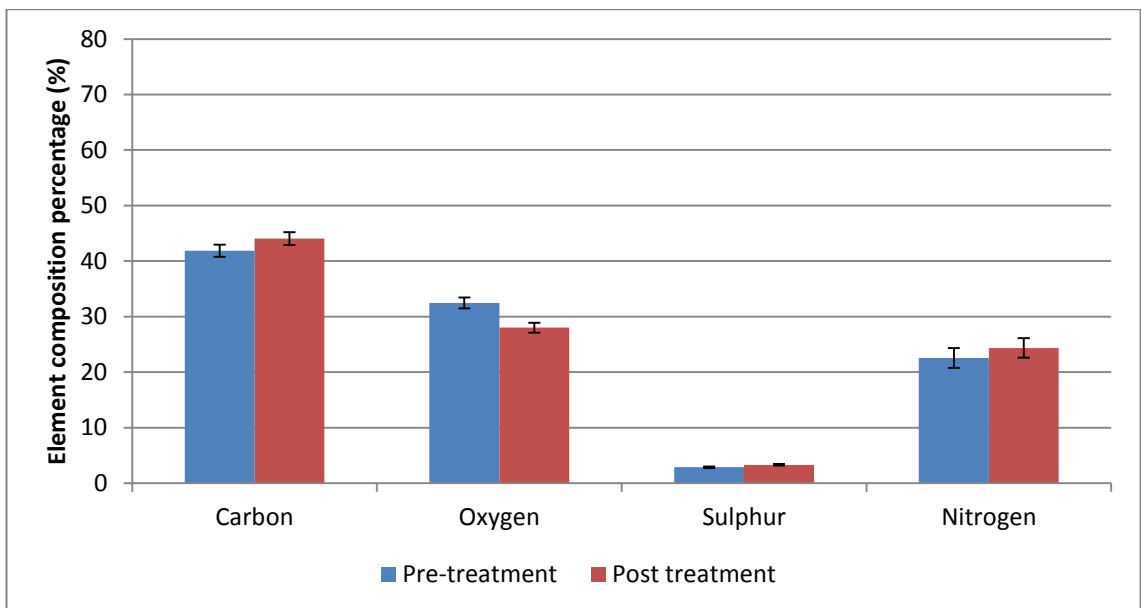
Figure 5.11 - Element composition percentage of FA pre-treated MFH wool fibres with ozone-UHP treatment for 96 h

As the element percentage composition trends are similar for FA pre-treated wool fibres treated with ozone-UHP solutions for 24 and 96 h, Table 5.3 was constructed to demonstrate whether there was a disruption in element composition after high energy

impact exposure. Carbon, sulphur and nitrogen element percentage compositions appear to increase, while the oxygen composition appears to reduce for both fibres.

Table 5.3 - Element composition of chemically modified MFH wool fibres exposed to electron beam radiation *(Cannot compare pre- and post-treatment data for MHF_F2 as data is irrelative)*

Element	Percentage element composition	Sample code		
		MFH_F2	MFH_F2_OZ24_UHP	MFH_F2_OZ96_UHP
Carbon	Pre-treatment (%)	65.39	42.73	41.87
	Post-treatment (%)	51.22	43.75	44.06
	Variance (%)	N/A	1.0	2.2
Oxygen	Pre-treatment (%)	23.37	31.92	32.45
	Post-treatment (%)	21.33	28.7	28.01
	Variance (%)	N/A	-3.2	-5.5
Sulphur	Pre-treatment (%)	11.25	2.74	2.87
	Post-treatment	7.3	2.82	3.32
	Variance (%)	N/A	0.1	0.5
Nitrogen	Pre-treatment (%)	0	22.28	22.53
	Post-treatment(%)	20.15	24.33	24.36
	Variance (%)	N/A	2.0	1.8

It is possible that the increase in carbon, sulphur and nitrogen could be caused by an increase in surface area as internal features of the cortex become exposed due to pore formation. Also, the reduction in oxygen composition could be caused by a reduction reaction caused by the high energy impact. The EDX data for both FA pre-treated MFH fibres treated with ozone-UHP for 24 h and 96 h are comparable but irrelative as they are expressed as percentage compositions, it is possible that the amount of carbon, sulphur and nitrogen does not increase, but appears to as a result of the oxygen

content reducing. If this is the case, then it is possible that the oxygen content decrease is due to a reduction reaction of the backbone or the side chains of the polypeptides within the wool fibres.

The amino acids present within polypeptides found in wools are detailed within Figure 5.12. It is possible that wool is degraded by ionising radiation which causes a reduction reaction between the oxygen containing side chains within the amino acids, which includes Serine, Theronine, Tyrosine, Aspartic acid, Glutamic acid and cysteine (Kozlowski, 2012).

Amino acid	Structure	Mol %[a]	Nature of side-chain
Glycine	$CH_2(NH_2)COOH$	8.4	Non-polar
Alanine	$CH_3CH(NH_2)COOH$	5.4	Non-polar
Phenylalanine	⬡—$CH_2CH(NH_2)COOH$	2.9	Non-polar
Valine	$CH_3CHCH(NH_2)COOH$ $\vert$ CH_3	5.6	Non-polar
Leucine	$CH_3CHCH_2CH(NH_2)COOH$ $\vert$ CH_3	7.7	Non-polar
Isoleucine	$CH_3CH_2CHCH(NH_2)COOH$ $\vert$ CH_3	3.1	Non-polar
Serine	$HOCH_2CH(NH_2)COOH$	10.4	Polar
Threonine	$CH_3CHCH(NH_2)COOH$ $\vert$ OH	6.4	Polar
Tyrosine	HO—⬡—$CH_2CH(NH_2)COOH$	3.9	Polar
Aspartic acid	$HOOCCH_2CH(NH_2)COOH$	6.5	Acidic
Glutamic acid	$HOOCCH_2CH_2CH(NH_2)COOH$	11.9	Acidic
Histidine	(imidazole)—$CH_2CH(NH_2)COOH$	0.9	Basic
Arginine	$H_2NCNH(CH_2)_3CH(NH_2)COOH$ $\Vert$ NH	6.9	Basic
Lysine	$NH_2(CH_2)_4CH(NH_2)COOH$	3.0	Basic
Methionine	$CH_3S(CH_2)_2CH(NH_2)COOH$	0.5	Sulfur containing
Cystine	$HOOCCH(NH_2)CH_2SSCH_2CH(NH_2)COOH$	10.3	Sulfur containing
Tryptophan	(indole)—$CH_2CH(NH_2)COOH$	0.5[b]	Heterocyclic
Proline	(pyrrolidine)—$COOH$	6.6	Heterocyclic

[a] Mol % values are the mean values from References 9 and 10.
[b] Determined by enzyme digestion.

Figure 5.12 - Amino acids present within polypeptides found in wools (Kozlowski, 2012)

Despite the uncertainty with regards to whether the fibre morphology is modified as a result of physical electron impact or chemical reaction, it is evident that exposing the fibres to high energy impact in a low pressure/ vacuum environment causes selective degradation to the wool fibres and macro-pore formation is possible. Furthermore, exposing FA-ozone-UHP pre-treated fibres appears to partially fibrillate the fibres; however, it is possible this fibrillation phenomenon is enhanced after the high energy impact exposure. Also, it is possible that the type and concentration of hydrogen bond

166

disrupting reagent and the time duration of exposure could affect the magnitude of degradation to the wool fibres.

Selective degradation of chemically modified wool fibres under high energy electron impacts has its limitations for creating pores due to the limited area exposed to the electron beam radiation. Therefore, alternative selective degradation techniques capable of creating pores on wool fibres are investigated. The following section investigates plasma degradation techniques as an alternative to electron beam irradiation due to its ability to modify larger areas of both fibres and fabrics.

5.2 Pores formed in wool fibres under exposure of low pressure plasma treatments

Previous research has identified plasma technology as capable of degrading polymers (Weikart and Yasuda, 2000; Tsoi et al., 2010), creating nanospots on wool and other polymer surfaces. Therefore, this study will investigate whether pores can be formed in wool fibres under exposure of low pressure plasma treatments.

The coupling of electromagnetic power into a process gas volume generates the plasma medium comprising a dynamic mix of ions, electrons, neutrons, photons, free radicals, meta-stable excited species and molecular polymeric fragments. Low pressure plasma technology was investigated as an alternative to electron beam radiation as low pressure plasmas are a highly mature technology and is capable of similar conditions to SEM systems, including low pressure environments and high energy particle impacts. The technology is often used for surface etching to produce controlled and reproducible rough surface structures within materials. Therefore, this technology was investigated as an alternative selective degradation technique to electron beam radiation. The effect of both air and oxygen plasmas were studied.

5.2.1 Air plasma treatment of wool fibres and fabrics

5.2.1.1 **Loose fibrous assembly of British medium fine hill (MFH) wool**

fibres

Raw MFH fibres, FA pre-treated MFH fibres and FA pre-treated MFH fibres treated with ozone-UHP treatment for 24 h were exposed to an air-plasma treatment for 10 and 30 min time durations to determine whether there was any evidence of degradation of pore formation similar to the characteristics observed during the impact of high energy particles using SEM (see section 5.1). The experimental plan is detailed in Table 5.4. and SEM was used to analyse the effect of exposing the wool fabrics to air plasma.

Table 5.4 - Air plasma treatment durations for various chemically modified British medium fine hill wool fibres

Sample	Time durations (min)	Chamber pressure (mbar)	Air flow rate ($cm^3.min^{-1}$)
MFH	10	~0.32	5
MFH_F2	10, 30	~0.33	5
MFH_F2_OZ24_UHP	10, 30	~0.33	5

Initially, the raw wool fibres were treated for 10 min and the SEM image (see Figure 5.13) demonstrates that although cuticle degradation is evident after air plasma exposure, no pore formation was observed. The SEM images were captured using a FEI Quanta 200 SEM (Faculty of Biological Sciences, University of Leeds, Leeds. LS2 9JT, United Kingdom). The fibres were coated in platinum (Pt) using a Cressington 208 HR Sputter Coater.

Figure 5.13 - Air plasma treated raw MFH wool fibres

The SEM image demonstrated within Figure 5.14 shows the effect of air plasma treatment to the surface morphology of the wool fibres. For both FA pre-treated MFH fibres and MFH wool fibres after FA pre-treatment with subsequent ozone-UHP treatment for 24 h, there was evidence of pore formations on the fibre surface. A more significant etching effect was evident when the fibres were exposed for longer time durations.

Figure 5.14 - Air plasma treated FA pre-treated MFH fibres

Also, the etching effect was inconsistent throughout the wool fibres. Such inconsistency might be either due to the occurrence of the selective degradation only on some of wool fibres on the outside layer of loose wool fibre assemblies and thus not always picked up in SEM observations. Therefore, to improve the observation of the effect of plasma treatment on wool fibres, worsted merino wool fabrics were used for the rest of the research. Similar to loose wool fibres, meso and macropore formations are evident after the chemical treatment of wool fibres (see Appendix).

5.2.1.2 **Worsted woven fabric made from merino wool fibres**

The same procedure was conducted in raw MWov, FA pre-treated MWov fabrics with FA pre-treated MWov fabric treated with ozone-UHP for 24 h and 96 h, which were exposed to an air plasma treatment, to determine whether it was possible to selectively degrade the surface fibres of wool fabrics rather than randomly organised loose wool fibres. From a practical perspective, the plasma treatment on fabrics could be more effective as the fibres were regularly aligned in the fabric plane within the plasma machine and also could be more beneficial from commercial manufacturing

perspective. Furthermore, it was noticed during the initial study that the temperature of the system gradually increased up to 60 °C throughout the series of treatments. Therefore, for this procedure the temperature of the system was maintained at 60 °C throughout the duration of the treatments. The experimental plan for this study is detailed within Table 5.5 and SEM was used to analyse the effect of exposing the wool fabrics to air plasma.

Table 5.5 - Experimental plan for investigating the effect of air plasma exposure on raw and chemically modified worsted woven fabrics made from merino wool fibres

Sample	Time durations (min)
MWov	30
MWov _F2	30
MWov _F2_OZ24_UHP	30
MWov _F2_OZ96_UHP	30

The gas environments within plasma systems are very complex and the gas, containing atoms and molecules, can be flowing due to temperature and density gradients. Kinetic theory (Graham (2007)) based on following assumptions was established to understand gas behaviour in plasma treatment process,

1. The gas consists of identical molecules;

2. Individual molecules are small compared to the average space between them;

3. The molecules are relatively incompressible;

4. The molecules are in constant random motion.

Graham (2007) expressed the relationship between temperature and kinetic energy, mean speed of molecules and impact pressure of molecules. All parameters have a positive correlation with temperature. Also, the relationship between electron and ion temperature was discussed and it was stated that in low pressure (<100Pa) plasmas, electron temperature (20,000 K) considerably higher than the ion and gas temperature (300 K).

Therefore, it is possible that by increasing and regulating the temperature within the system the surface morphology of the wool fibres could be adapted further.

It is evident from the SEM images demonstrated within Figure 5.15 and Figure 5.16 that surface selective degradation is evident after exposure to the air plasma treatment for 30 min. For the raw wool fibres there is evidence of degradation of cuticle fringes, this could suggest that the plasma treatment is disrupting the CMC that cements the cuticles layers.
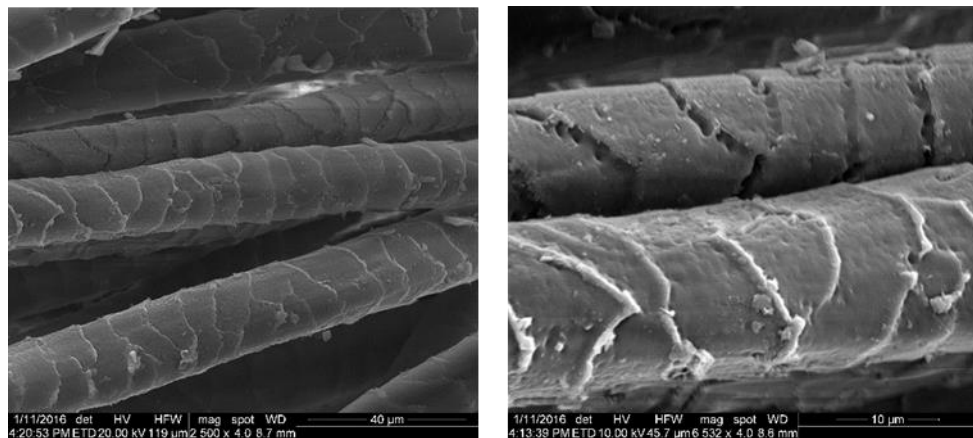
Figure 5.15 - Effect of air plasma treatment on untreated MWov fabrics

For the fibres pre-treated with FA (see Figure 5.16), the etching or surface selective degradation of the fibres are significantly increased as a result of air plasma treatment. Also, similar to Allen and Alexander (1961) the pre-treatment of the wool fibres appears to enhance the degradation of the material after exposure to high energy particle impacts.
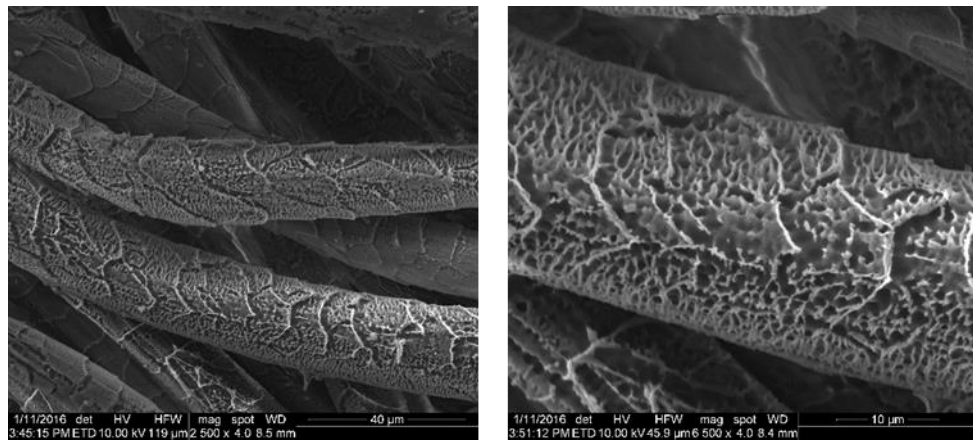
Figure 5.16 - Effect of air plasma treatment on the morphology of FA pre-treated MWov fabrics

The effect of the air plasma treatment on FA pre-treated MWov fabrics subsequently treated with ozone-UHP for 24 h and 96 h are shown in Figure 5.17 and Figure 5.18, respectively. Significant macro-pore formation is evident on the surface of the wool fibres after exposing the fibres to air plasma for 30 min.
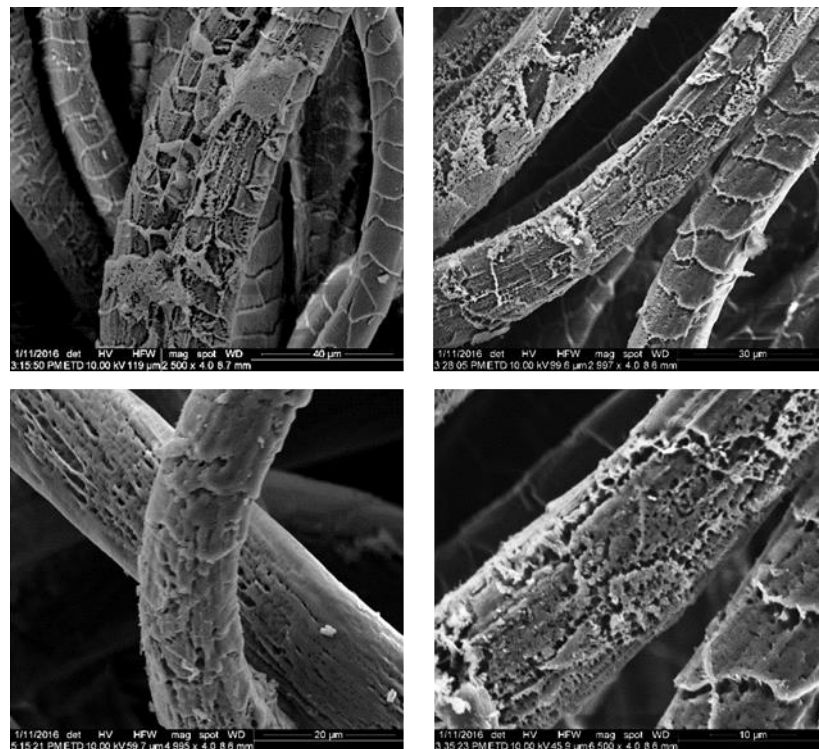
Figure 5.17 - Effect of air plasma treatment on the wool fibres on MWov fabrics (FA pre-treated and subsequently ozone treated in UHP for 24 h)

173
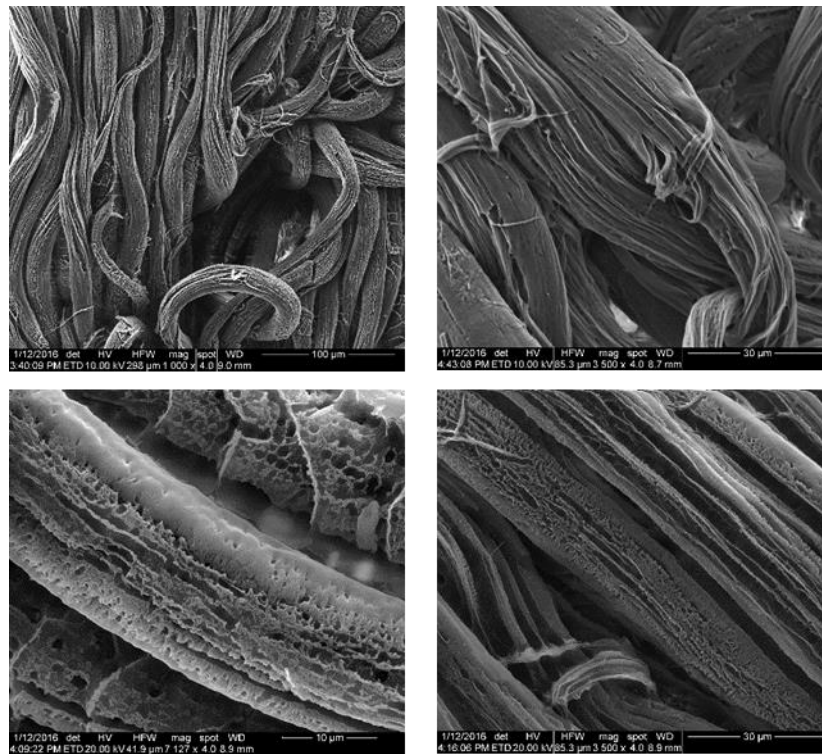
Figure 5.18 - Effect of air plasma treatment on the wool fibres on MWov fabrics (FA pre-treated and subsequently ozone treated in UHP for 96 h)

Both fibres appear to commence fibrillation; however, this phenomenon is more apparent for the sample that has been treated for a longer ozone-solution time duration (see Figure 5.19). Therefore, it is possible that the extent of the macro-pore formation or fibrillation could be controlled by controlling the chemical pre-treatment processes.

Figure 5.19 - Pores created in a great amount of fibres in MWov fabrics (FA pre-treated and subsequently ozone treated in UHP for 96 h)

In conclusion to this study, it is evident that the air plasma treatment causes degradation to both MFH and MWov raw and chemically treated wool fibres. Also, the chemical pre-treatments and treatment duration, as well as the air plasma treatment duration appear to have different effects on the morphology of the resultant wool fibres. Therefore, it was decided that these parameters should be investigated further. Moreover, the inconsistent macro-pore formation could be due to the air plasma containing multiple species of atoms and molecules. Therefore, within the following sections, the effect of plasma with a single type of ionised atoms (oxygen) on treating wool fibres will be investigated.

5.2.2 Oxygen plasma treatment

Oxygen plasma was investigated as an alternative to air plasma to increase the oxidation effect within the reaction chamber. Therefore, similar to the air-plasma treatment (see section 1.1.1), the effect of a low pressure oxygen plasma treatment on chemically modified wool fibres was investigated; oxygen was supplied to the plasma chamber and the chamber temperature was controlled at 60 °C. The fibres were treated for either 15 or 30 min time durations. Again, the system was set to full power output (300 W) and the oxygen gas supply was fixed to inlet 3 to enable the flow rate of the oxygen supply to be digitally controlled. For the oxygen plasma trials, worsted merino wool fabrics were selected for practical purposes as the woven fabric was easily positioned within the plasma chamber. Scoured worsted woven merino wool (MWov) fibres , FA pre-treated MWov fabrics, FA pre-treated MWov fabrics treated with UHP solution for 96 h and FA pre-treated MWov fabrics treated with ozone-UHP treatment for 96 h were exposed to the oxygen plasma treatment.

The main purpose of the oxygen plasma treatment was to investigate the effect of processing parameters of plasma treatment with a single type of ionised atoms (oxygen), including O_2 flow rate, chamber pressure, exposure duration, on various chemical pre-treated MWov fabrics.

5.2.2.1 The effect of oxygen flow rate of plasma treatment on the degradation of the wool fibres

Firstly, an investigation has been conducted to determine the correlation between oxygen gas flow rates and the oxygen pressure within the plasma chamber in the oxygen plasma process.

The graph detailed in Figure 5.20 demonstrates the relationship between oxygen pressure in the chamber and the oxygen flow rates in the range between 0 - 35 $cm^3.min^{-1}$. It is clear from the graph that the oxygen pressure in the chamber is

positively correlated with the oxygen flow rate. Therefore, an increase of the oxygen flow rate increases the pressure within the plasma machine chamber.
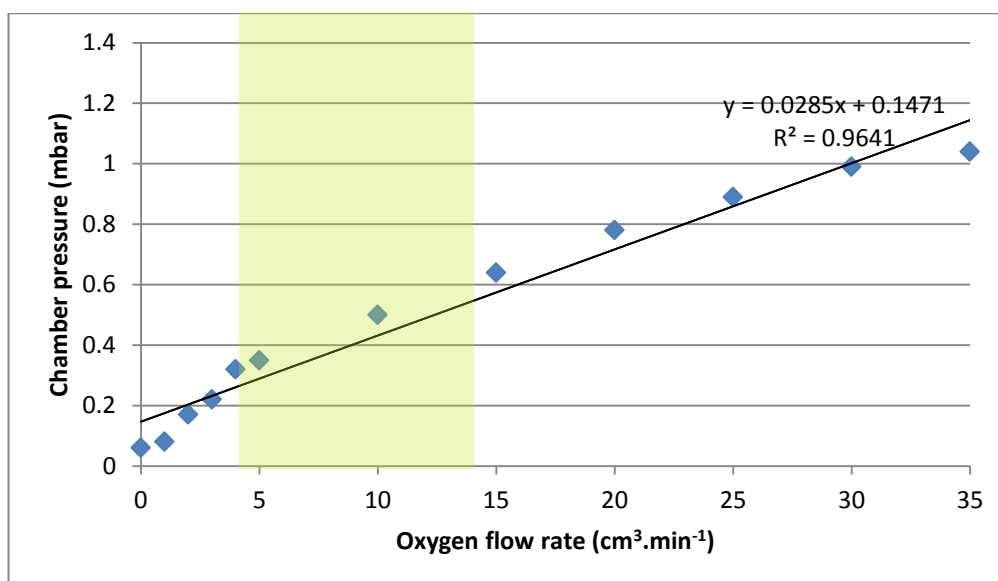
Figure 5.20 - Relationship between oxygen flow rate and chamber pressure for flow rates between 0-35 cm³.min⁻¹

To replicate the environment within the high energy particle impacts caused by electron beam irradiation (see section 5.1), the chamber would be in vacuum state. Therefore, the chamber pressure at the lower range of oxygen flow rates was investigated. It was noticed that increasing the oxygen flow rate from 0 to 35 $cm^3.min^{-1}$ gradually changed the colour of the plasma from purple to white, which suggests that the oxygen density within the system affects the plasma dynamics.

In this study, the effect of oxygen flow rates on the selective degradation of chemically modified wool fibres in an oxygen plasma treatment was investigated. To understand the effect of the applied oxygen flow rate, the FA pre-treated MWov fabrics treated with UHP solution for 96 h were exposed to 5, 15 and 34 $cm^3.min^{-1}$ and the chamber pressure was controlled at 60 °C. Also, the FA pre-treated MWov fabrics treated with ozone in UHP solution for 96 h were exposed to 5 and 15 $cm^3.min^{-1}$. The experimental plan plans for the different chemically modified fibres are detailed within Table 5.6 and Table 5.7. The effect of the O_2 flow was analysed using SEM.

Table 5.6 - The experimental plan for investigating the effect O$_2$ flow rate during a plasma treatment on FA pre-treated MWov fabrics treated with UHP solution for 96 h

Sample	O$_2$ flow rate (cm^3.min^{-1})	Chamber pressure (mbar)	Time duration (min), each side
MWov_F2_UHP96	5	~0.47	15
MWov_F2_UHP96	15	~0.69	15
MWov_F2_UHP96	34	~1.00	15

Table 5.7 - The experimental plan for investigating the effect O$_2$ flow rate during a plasma treatment on FA pre-treated MWov fabrics treated with ozone in UHP solution for 96 h

Sample	O$_2$ flow rate (cm^3.min^{-1})	Chamber pressure (mbar)	Time duration (min), each side
MWov_F2_OZ96_UHP	5	~0.46	15
MWov_F2_OZ96_UHP	15	~0.67	15

It is clear from the SEM images within Figure 5.21 that the wool fibres after different chemical treatments have different surface morphologies after the plasma treatments. The wool fibres treated with 5 cm^3.min^{-1} O$_2$ flow rate appear to have pore formation as a result of selective degradation, while etchings were evident after exposing the wool fibre to 15 cm^3.min^{-1} O$_2$ flow rate. Also, the wool fibre exposed to the highest O$_2$ flow rate showed evidence of pattern/ indentation formation.
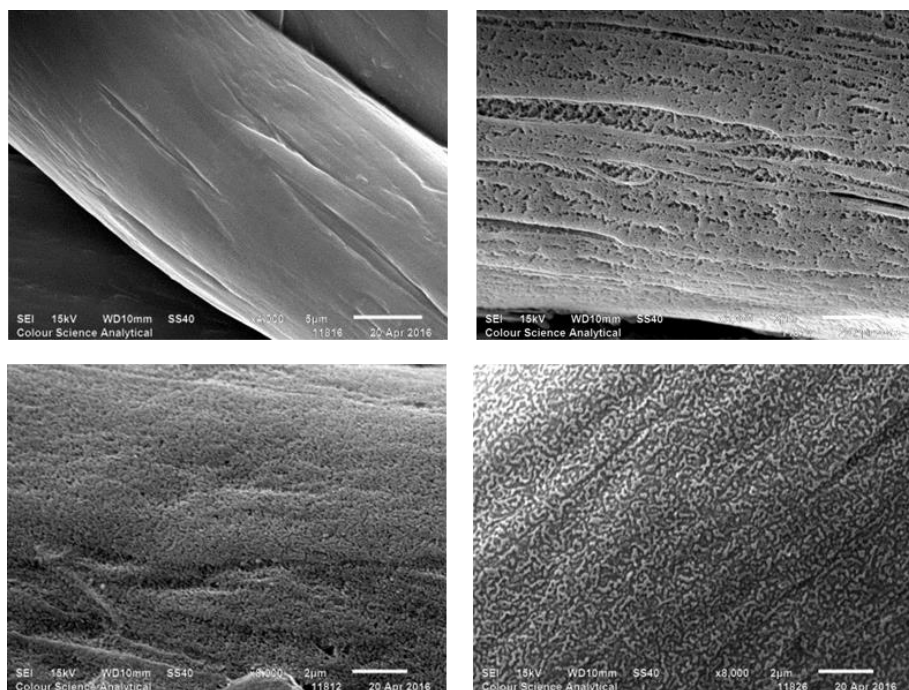
Figure 5.21 - FA pre-treated MWov fabrics and subsequently treated in UHP solution for 96 h were exposed to 5, 15 and 34 cm^3.min^{-1} oxygen flow rates while exposed to oxygen plasma. Top left: Control, Top right: 5 cm^3.min^{-1}, Bottom left: 15 cm^3.min^{-1}, and Bottom right: 34 cm^3.min^{-1}

Similar pore formations were observed for different oxygen flow rates for the FA pre-treated MWov fabrics with subsequently ozone treated in UHP for 96 h. The effect of oxygen flow rates is detailed in Figure 5.22.
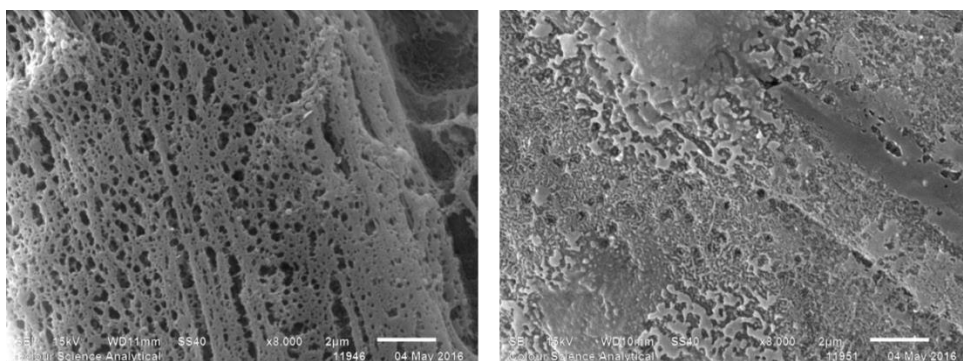
Figure 5.22 - SEM images of oxygen plasma treated FA pre-treated MWov fabrics and subsequently ozone treated with in UHP for 96 h. Left: Oxygen flow rate: 5 cm^3.min^{-1} and Right: 15 cm^3.min^{-1}. 15 minute oxygen plasma exposure

Reducing the oxygen flow rate reduces the pressure within the system; therefore, it is not clear whether the wool fibre surface modifications were caused by varying the oxygen flow rate or the pressure or both. However, it is evident that treating both chemically modified wool fibres at 5 $cm^3.min^{-1}$ for 15 mins exposure duration caused pore formation on the fibre surfaces. Therefore, at these processing parameters it is evident that there is sufficient oxygen within the chamber and the chamber pressure is sufficient in order to cause selective degradation.

5.2.2.2 **The effect of chamber pressure of plasma treatment on the degradation of the wool fibres**

To investigate the effect of these processing parameters further an experiment comparing high and low O_2 flow exposure was conducted. Firstly, the oxygen flow rate was set to 0 $cm^3.min^{-1}$ and the chamber pressure was recorded as 0.12 mbar. Secondly, the oxygen flow rate was pre-set to 34 $cm^3.min^{-1}$ and the chamber pressure was recorded as 1.00 mbar.

Table 5.8 - The effect of increasing the oxygen flow rate within the plasma chamber

Oxygen flow ($cm^3.min^{-1}$)	Chamber pressure (mbar)
0	0.12
34	1.00

The surface morphologies of these fabrics are illustrated in Figure 5.23. It is evident that minimal surface etching was present after the first trial; whereas, the second trial showed evidence of pattern/ indentation formation.
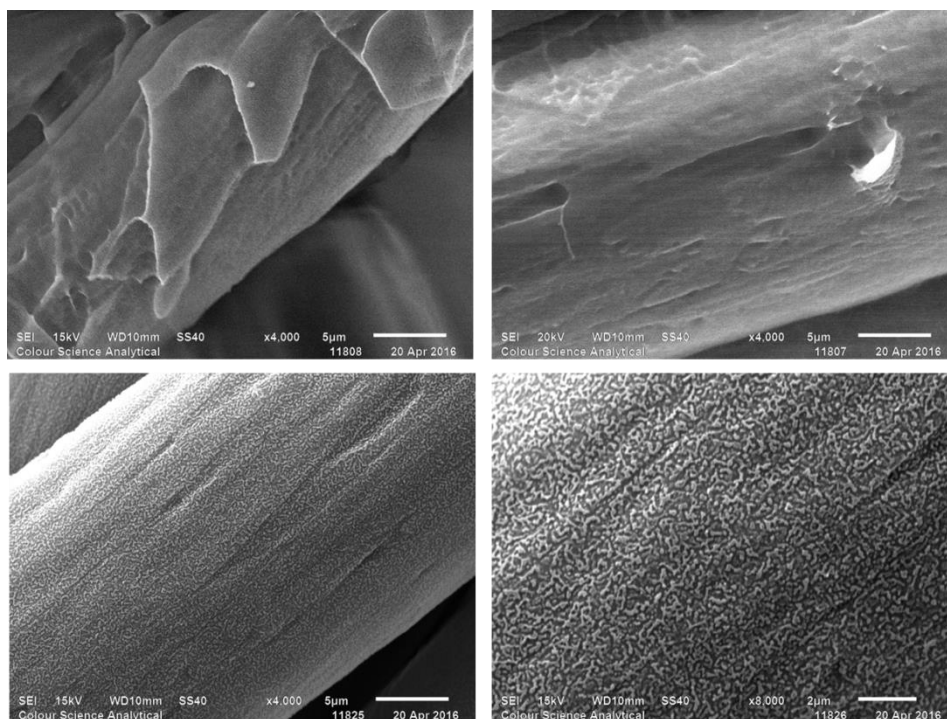
Figure 5.23 - SEM images of plasma treated FA pre-treated MWov fabrics treated with UHP solution for 96 h. Top row: Oxygen flow rate (0 cm^3.min^{-1}) and Bottom row: Chamber pressure (1.00 mbar)

Increasing oxygen flow increased the pressure within the chamber. It seems that a lower oxygen pressure is required to increase etching intensity/ macro-pore formation; however, if the oxygen concentration is too low then the surface modification is minimal. Therefore, there is a trade-off between oxygen concentrations/ oxygen flow rates and reduced pressure for having sufficient etching intensity/ pore formations, which was what was expected as there was minimal oxygen present within the reaction chamber.

5.2.2.3 The effect of time duration of oxygen plasma treatment on the degradation of wool fibres

It would appear that the surfaces changes and pores formed on the wool fibres are a consequence of polymer degradations, which is interesting as the aim of the study was to expose the fibre inner structure created by chemically modification. Therefore, to investigate whether the inner structure could be exposed, and the surface changes and

pores formed could be modified further the modified wool fibres were exposed to an increased exposure time duration.

5.2.2.3.1 Morphological features of degraded wool fibres

To investigate the effect of extending the O_2 plasma exposure duration on the chemically pre-treated wool fabrics, the fabrics pre-treated with FA-UHP were exposed to O_2 plasma for 15 and 30 min exposure durations at 5 $cm^3.min^{-1}$ oxygen flow rate.

It is evident from the SEM images detailed with Figure 5.24 that the morphological features are quite different after exposing the chemically modified fibres to different O_2 plasma exposure durations. The fabric exposed to the shorter exposure duration appears to have a greater proportion of smaller pores, while the fabrics exposed for long duration appear to a greater proportion of macropores. Also, the fabric exposed for the longer duration appears to have formed a reticulated pore structure as matrices of pores are evident within the wool fibres. However, the depth of this reticulated structure is unclear. As mentioned within section 5.2.2.4.1, the fibre exposed for a lower duration appears to partially fibrillate as a result of the O_2 plasma treatment, although the pores appear to increase in size and potentially merge as a result of the increased exposure.
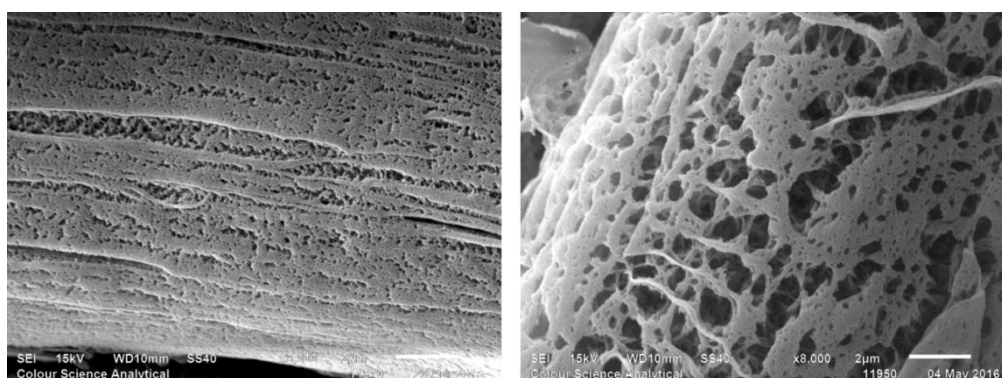
Figure 5.24 - The effect of extending the O_2 plasma treatment on FA-UHP pre-treated MWov fabrics (Mag. 8,000). Oxygen flow rate: 5 $cm^3.min^{-1}$, Chamber pressure: 0.5 bar, O_2 plasma exposure duration: 15 min (Left) and 30 min (Right)

182

5.2.2.3.2 Pore sizes and specific surface area

As the sizes of the pores formed are a significant feature of fibre degradation, Image analysis was employed to quantify and differentiate between the pores formed. SEM images were captured for both O_2 plasma exposure durations for the wool fabric pre-treated with FA-UHP. By analysing the SEM images using Image Pro Plus, it was evident that the pores did not exceed 1 μm; therefore, data beyond this range was expelled from the characterisation investigation. Also, the minimum pore size detectable visually was approximately 20 nm. Consequently, data below this value was also discarded.

It evident from the pore area distribution (see Figure 5.25) that greater pore areas for the larger pore widths are present after extending the O_2 plasma exposure duration, particularly between 0.6 – 1 μm. However, pores with 850nm pore widths are evident after the lower O_2 plasma exposure duration, which is likely to be caused by fibrillation.
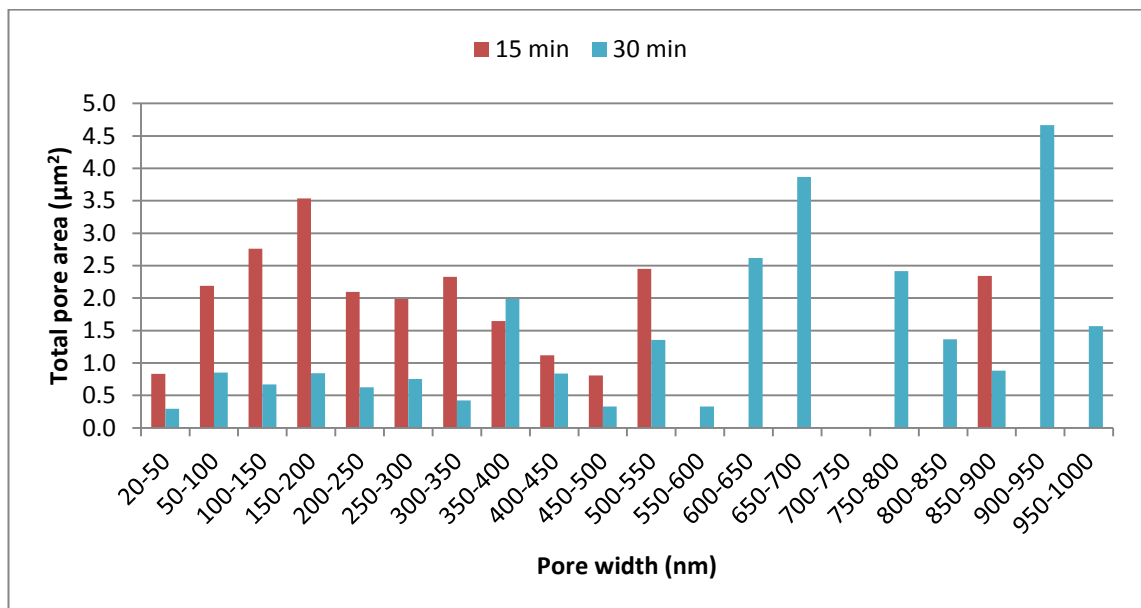
Figure 5.25 - The effect of extending the O_2 plasma exposure duration for FA-UHP pre-treated wool fibres

The pore areas present for smaller pore widths (20 nm – 0.6 μm) significantly reduce when extending the O_2 plasma exposure duration, this suggests that extending the O_2

plasma exposure increases the size of the pores formed. Also, it is possible the pores formed after the 15 min O_2 plasma exposure increase and merge with other pores, which is aligned with the trends observed within the pore frequency distribution (see Figure 5.26). The number of pores decrease as the pore widths increase and the number of pores are significantly lower for the wool fabrics exposed to O_2 plasma for a longer duration.
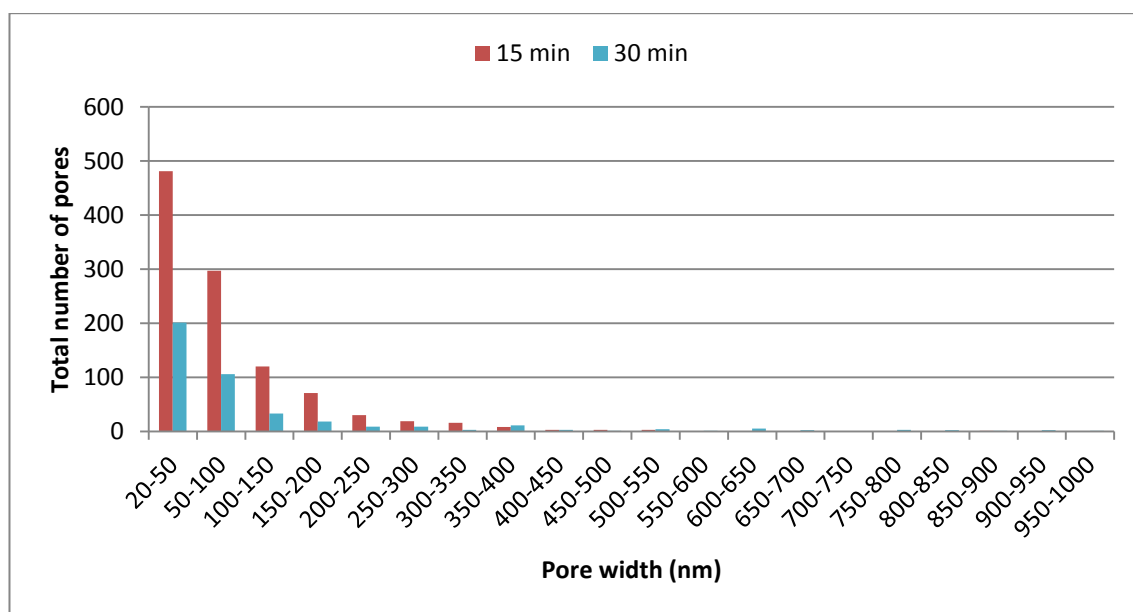
Figure 5.26 - Pore frequency distribution of FA-UHP pre-treated wool fibres treated with O_2 plasma

Furthermore, despite the total number of pores significantly reducing the total pore area increases after the increased O_2 exposure duration (see Table 5.9), which also suggests that the pores increase and merge as a results of extended O_2 plasma exposure.

Table 5.9 - Comparison of total pore area and total number of pores for FA-UHP pre-treated wool fibres treated with different O_2 plasma exposure durations

O_2 plasma exposure duration (min)	Total pore area (μm^2)	Total number of pores
15	24.1	1052
30	20.7	415

184

A matrix of pores is present within the wool fibre illustrated by the SEM image in Figure 5.24, which suggests the early speculation that the pores formed are only superficial can be disregarded. The fibre appears to have a reticulated pore structure and the specific surface area (see Table 5.10) increases from 0.22 to 2.03 $m^2.g^{-1}$ (823 % increase) by exposing the FA-UHP pre-treated wool fabric to O_2 plasma for 30 min. However, this value is still significantly low in comparison to other porous fibres, such as activated carbon fibres, which are reported to have a BET surface area of 2500 $m^2.g^{-1}$ (Hayes, 2002). Furthermore, the specific surface area increases from 0.57 to 2.03 $m^2.g^{-1}$ (256 % increase) by extending the treatment duration from 15 to 30 min. This demonstrates that O_2 plasma exposure duration is a key parameter for the formation of pores within chemically modified wool fibres.

Table 5.10 – Increase in specific surface area by increasing the O_2 plasma exposure duration

O_2 plasma exposure duration (min)	BET surface area ($m^2.g^{-1}$)	Percentage increase from control sample (%)
Control	0.22	-
15	0.57	159
30	2.03	823

In summary, increasing the O_2 plasma exposure increases the size of the pores formed, which is likely to be caused by the merging of smaller pores throughout the treatment. Also, reticulated pore structures can be formed on chemically pre-treated wool fibres; however, the depths of the porous matrices are still uncertain. Further work could be conducted to determine whether extending the O_2 plasma exposure further could create a reticulated pore structure throughout the whole fibre.

5.2.2.4 Effect of chemical modifications on the characteristics of the pores formed on wool fibres

The aim of this study is to characterise the pores formed on chemically modified wool fibres as a result of selective degradation by O_2 plasma. Similar to previous sections,

the resultant fabrics were analysed using SEM to investigate the morphological features, Image analysis for pore area distributions and pore orientation angle, mercury porosimetry for pore volume distributions and gas adsorption porosimetry to measure the specific surface area.

Raw and chemically modified wool fibres were exposed to O_2 plasma at processing parameters found to cause pore formations within chemically treated wool fibres. The processing parameters were kept consistent throughout the study, which included an O_2 flow rate of 5 $cm^3.min^{-1}$, exposure duration of 15 min and a chamber pressure of 0.5 mbar. Degraded wool fibres with various chemical modifications were analysed using SEM to investigate the morphological features evident as a result of O_2 plasma exposure. Fabrics investigated include raw MWov fabrics, as well as, FA, FA-UHP and FA-OZ(UHP) chemically modified wool fabrics.

5.2.2.4.1 Morphological features of degraded wool fibres with various chemical modifications

The aim of this study was to investigate the morphological features evident after O_2 plasma treatment using SEM. The images within Figure 5.27 demonstrate the effect of treating raw wool fibres with O_2 plasma, while the SEM images within Figure 5.28 show the effect of treating FA, FA-UHP and FA-OZ(UHP) pre-treated MWov fabrics with O_2 plasma. All fabrics were exposed to 5 $cm^3.min^{-1}$ oxygen flow rate during the plasma treatment.
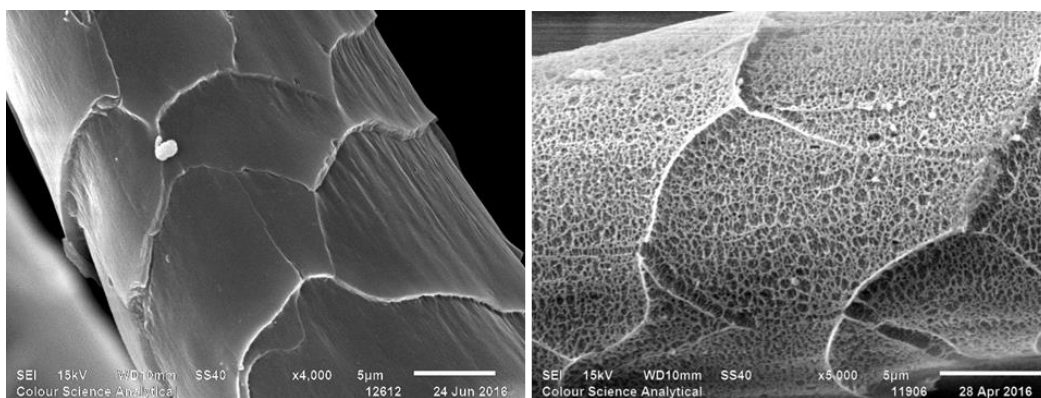
Figure 5.27 - The effect of treating raw wool fibres with O$_2$ plasma. Left: untreated (Mag. x4000) and Right: O$_2$ plasma retreated (Mag. x5000), Flow rate: 5 cm^3.min^{-1} and chamber pressure: 0.5 bar

It is clear that the sample surface morphologies have been affected by the oxygen plasma treatment. Similar to the experiments using high energy particle impacts in SEM and air plasma treatment, the fibre surface morphology appears to vary depending on the pre-chemical treatment. Interestingly, the raw (see Figure 5.27) and FA treated wool fibres (see Figure 5.28) show surface etching and pattern formations, while the FA-UHP and FA-OZ(UHP) wool fibres have significant indentations that pierce the surface of the wool fibres causing cracks and superficial pore formation and potentially a reticulated pore structure.

The FA treatments used an oxidising reaction to cleave the cuticles from the fibre cortex; however, it is possible that FA treatment oxidises the cortex. This phenomenon was evident within previous FA experiments, which reported that the FA treatments were capable of creating internal pore formations within the cortex (Ward and Mao, 2015). The UHP treatments were conducted after the FA treatments; therefore the fibres were already oxidised or partially oxidised. Ozone-UHP treatment has both swelling and oxidising reactions. Therefore, it is possible that a greater proportion of the hydrogen bonds within the wool fibres were disrupted during ozone-UHP treatments. This could be caused by the introduction of an additional oxidising treatment, increasing the oxidising reaction time duration or the urea within the solution

swelling the fibres enabling the internal chemistry to be reacted. In principle, the ozone-UHP treatment will have the most reactive conditions as it will have additional oxidising reactions caused by the ozone, as well as, the UHP on the FA pre-treated wool fibres.
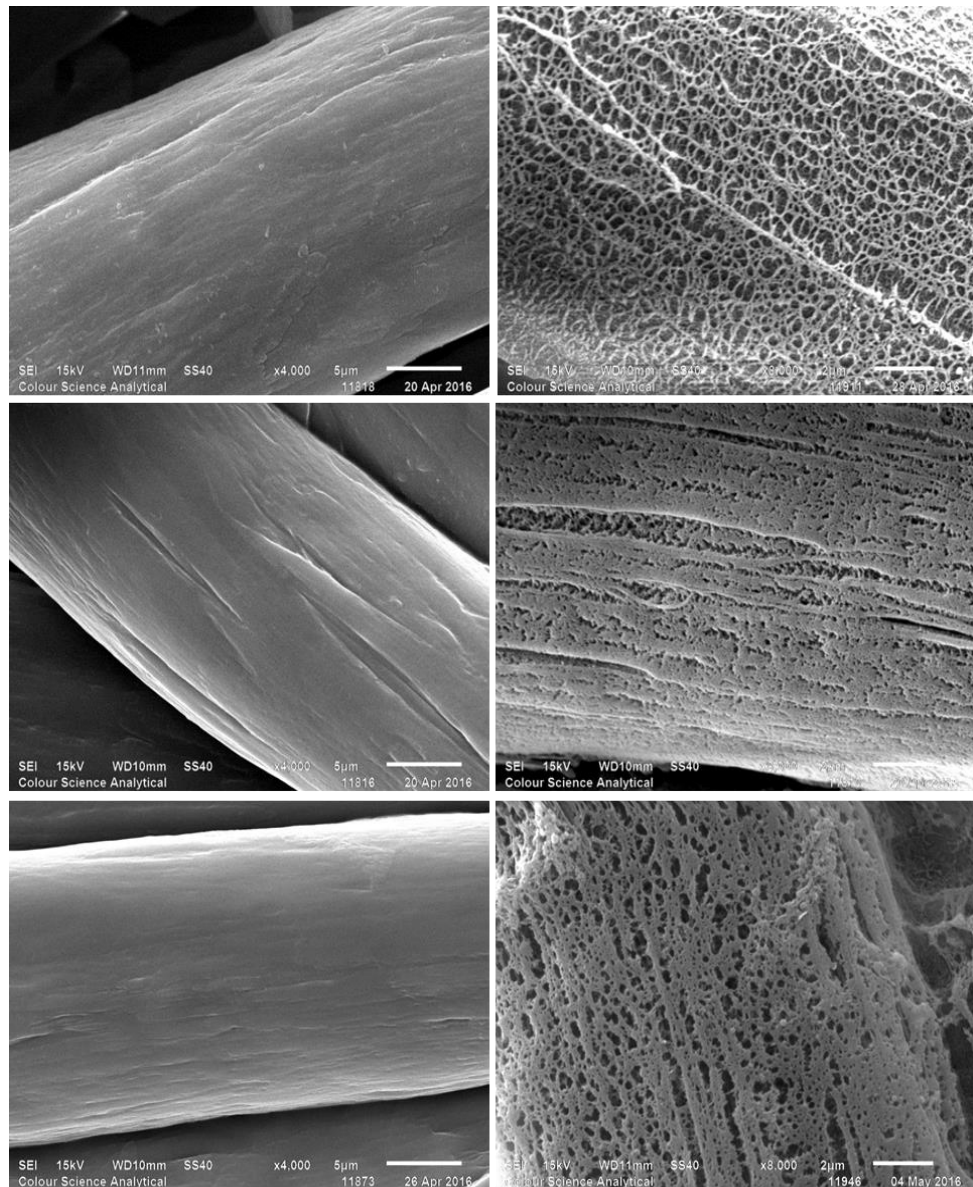
Figure 5.28 - The effect of O$_2$ plasma treatment (O$_2$ flow rate: 5 cm^3.min^{-1}, Chamber pressure: 0.5 bar, Treatment time duration 15 min) on chemically modified worsted woven merino wool fibres. Left: chemically modified fibres (Mag. x4000) and Right: chemically modified fibres treated with O$_2$ plasma (Mag. x5000). Top: FA pre-treated, Middle: FA-UHP pre-treated and Bottom: FA-OZ(UHP) pre-treated

Meso- and macro-pore formation is present on the remaining cuticles as well as the cortex and is illustrated within Figure 5.29. Conversely, to the pore formations evident after high energy particle impact by SEM, the pore formations by plasma are very uniform throughout all the wool fibres, which could be beneficial from a manufacturing perspective. Also, the pore sizes appear to be consistent on both the cortex and the cuticles.
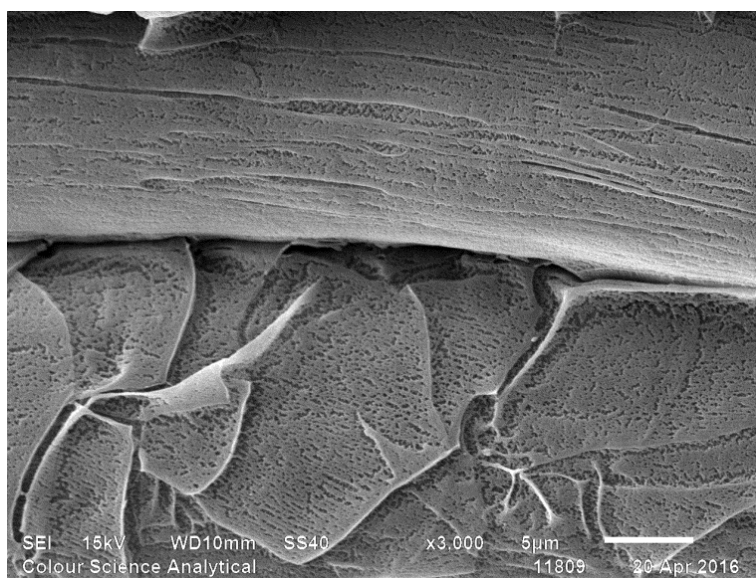
Figure 5.29 - The effect of O$_2$ plasma treatment (Oxygen flow rate: 5 cm^3.min^{-1}, Chamber pressure: 0.5 bar, Treatment time duration 15 min) on FA-UHP pre-treated MWov fabrics (Mag. x3,000)

It is clear from the literature and the SEM electron beam impact and plasma treatments (see Figure 5.28) that the surface morphologies of the wool fibres are different when the fibres have had different chemical pre-treatments. Also, various chemical pre-treatments appear to change the surface morphology of the fibres after selective degradation by high energy particle impact. Crack formation, individual pore formation and reticulated pore structures are evident after the plasma treatment processes. It is possible that various oxidising chemical pre-treatments are disrupting the hydrogen molecules within the peptide back bone, amino acid side chains and/or within the CMC; these disrupted molecules are then degraded/ disrupted further by the high energy particle impacts.

In order to characterise the pore formation Image analysis, mercury porosimetry and gas adsorption porosimetry were used to quantify and differentiate between pores formed.

5.2.2.4.2 Pore orientation angle

The pore orientation angles for pores evident after treating chemically pre-treated wool fabrics with O_2 plasma were investigated using SEM and FIJI software. Wool fibres investigated within this study include FA-UHP and FA-OZ(UHP) pre-treated MWov fabrics. The aim of the study was to determine whether the pore formation observed was related to the fibrillation or partial fibrillation of chemically pre-treated wool fibres. Similar surface morphologies are present when the chemically pre-treated fibres are exposed to O_2 plasma as the impact of high energy particles in SEM. Extensive pore formation and partial fibrillation of wool fibres are evident after both techniques. To investigate whether partial fibrillation was evident after exposing the wool fabrics to plasma, the pore orientation angles were calculated using FIJI image analysis. The software is capable of estimating individual pore areas, as well as, calculating the length (primary axis) and width (secondary axis) of the pores by modelling the pores as best fitting ellipses. The pore orientation angle is the angle between the primary axis and a line parallel to the X-axis of the image, as demonstrated within Figure 3.8.
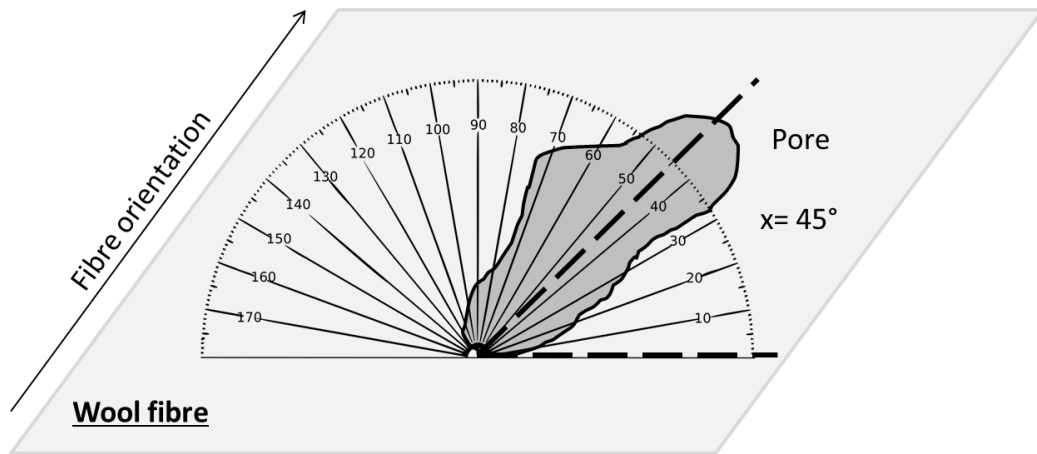
Figure 5.30 - Schematic demonstrating the method for calculating the pore angle of orientation. The angle between the pore length axis and the horizontal axis is called the pore orientation angle

The graphs and SEM images illustrated within Figure 5.31 and Figure 5.32 show the pore orientation for both wool fabrics treated with FA-UHP and FA-OZ(UHP), respectively. As the fibre in Figure 5.31 is aligned horizontally (approximately 170°), we would expect a significant proportion of the pore orientation angle to be represented by 0-20° or 160-180° if the fibres demonstrated partial fibrillation. This is because fibrillation occurs longitudinally to the fibre orientation in wool fibres (Ito et al., 1984).
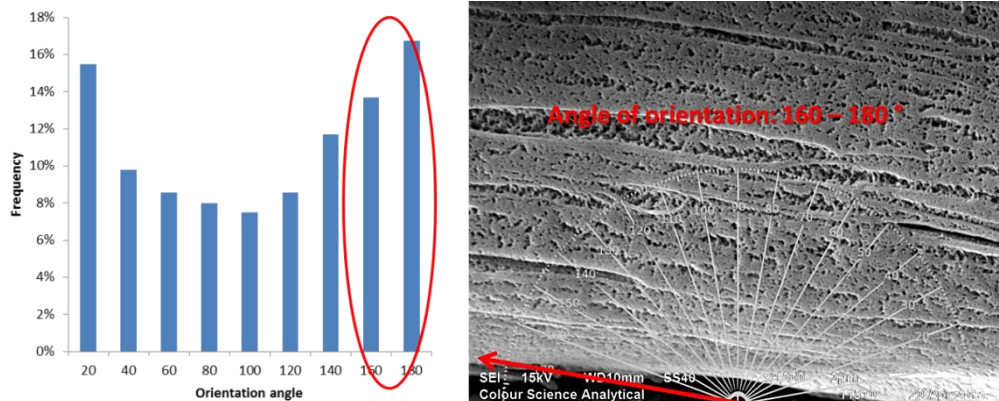
Figure 5.31 - Pore orientation distribution and SEM image for FA-UHP treated with O2 plasma

Conversely, the fibre demonstrated within Figure 5.32 has a more vertical fibre orientation (approximately 110°); therefore, we would expect a significant proportion of

191

the fibre orientation angles to be between 100-120°, which is illustrated within the pore orientation graph (see Figure 3.8).
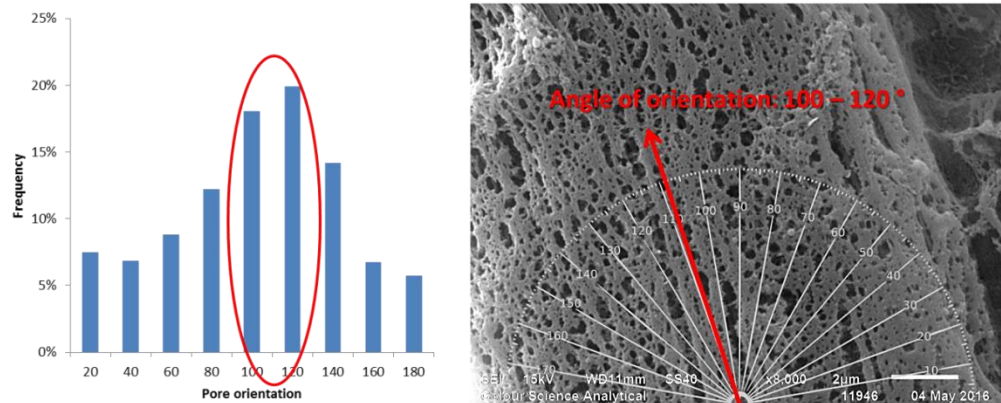
Figure 5.32 - Pore orientation distribution and SEM image for FA-OZ(UHP) treated with O$_2$ plasma

Therefore, it is possible to conclude that the selective degradation technique is capable of causing fibrillation of chemically pre-treated wool fibres. However, the depth of the pores formed and whether the exposure of the inaccessible pores created by chemical pre-treatments or the formation of a reticulated pore structure is uncertain.

5.2.2.4.3 Pore size distributions in terms of pore area

Image analysis using SEM and FIJI software was conducted to characterise and differentiate between the pores created after the O$_2$ plasma treatment. The chemically modified wool fabrics investigated within this study include FA, FA-UHP and FA-OZ(UHP) pre-treated Australian worsted woven merino wool fabrics. Graphs including total pore area and total number of pore, as well as, pore size distributions for the total pore area and total number of pores and were constructed to analyse the pore formation within chemically modified wool fibres.

It is clear from the pore area distribution detailed within Figure 5.33 that the FA pre-treated wool fabrics have greater total pore area in comparison to the FA-UHP and FA-OZ(UHP) pre-treated wool fabrics for pores between 20-600 nm. These increased total pore areas are particularly evident for pores formed between 50-400 nm. However,

from observing the SEM images (see Figure 5.28), it is clear that the features formed are etchings or patterns formed as opposed to pores, which are evident for both FA-UHP and FA-OZ(UHP) pre-treated wool fabrics.
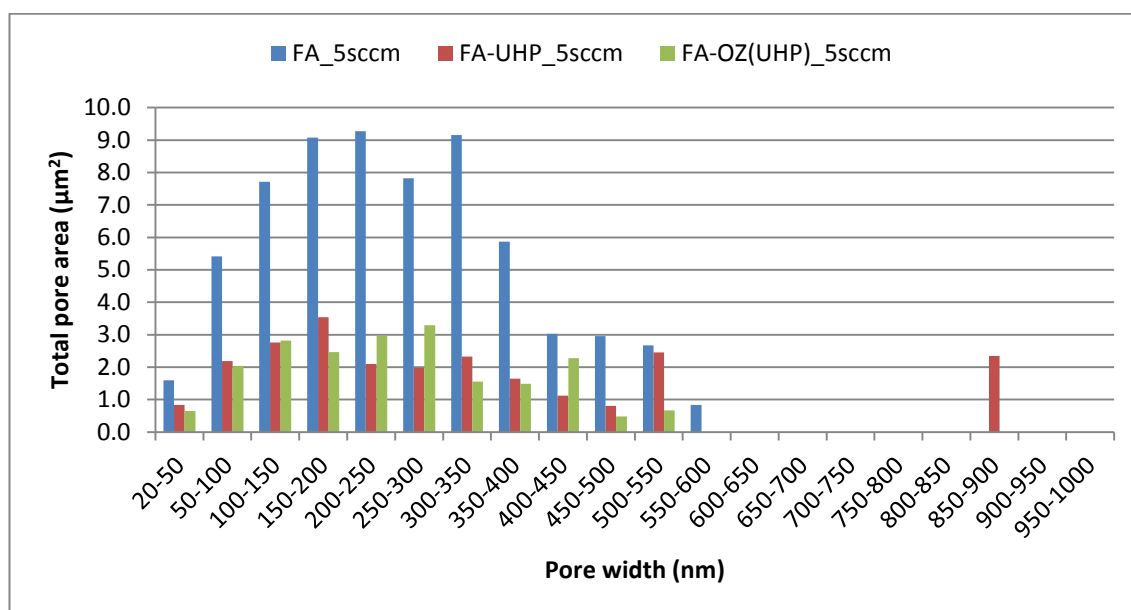
Figure 5.33 - The effect of treating different chemically pre-treated wool fibres (FA, FA-UHP and FA-OZ(UHP)) with O₂ plasma

One shortcoming of this analytical technique is the pore area distributions are not capable of analysing the depth of the pores. Therefore, although the FA pre-treated appears to have significantly higher total pore area for particular pore sizes, the volume of these pores will be restricted by their depth, which may affect their suitability or ability to adsorb VOCs. Consequently, the pore width distribution detailed with Figure 5.34 details the data obtained for the FA-UHP and FA-OZ(UHP) pre-treated wool fibres.

Both chemically pre-treated wool fabrics demonstrate similar trends of pore formations between 20-550 nm, despite demonstrating different pore morphologies (see Figure 5.28). Generally, the FA-UHP pre-treated fabrics haves a higher total pore area for various pores sizes with the exception of pores between 200-300 nm and 440 nm, which could be caused by the condition of the CMC after alternative treatments. Also,

pores with 850nm pore widths are evident after the O_2 plasma treatment of FA-UHP fibres, which is likely to be caused by fibrillation.
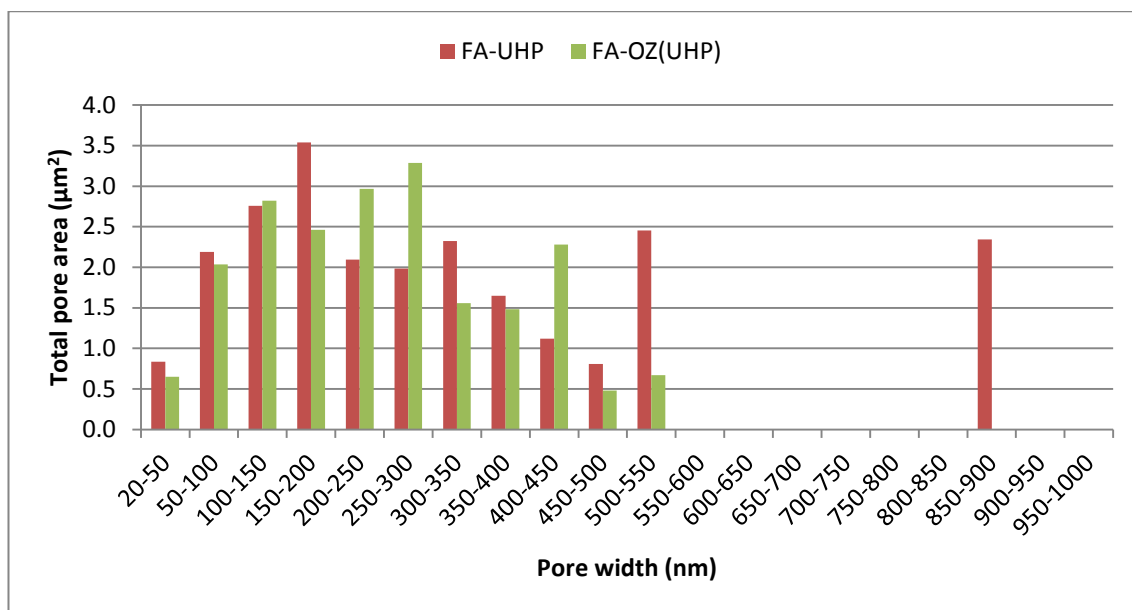
Figure 5.34 - The effect of treating different chemically pre-treated wool fibres (FA-UHP and FA-OZ(UHP)) with O_2 plasma

Interestingly, the pore frequency distribution for each chemical pre-treatment demonstrates the same trend (see Figure 5.35), there are a considerably greater number of smaller pores than larger pores and the total number of pore reduces as the pore size increases. It is possible that the plasma treatment causes a particular pore size and extended exposure increases the size of the pores formed. This would suggest that the pore size could be controlled by varying the plasma exposure duration, which suggests that the parameters of this selective degradation technique could be tailored to produce specific fibre morphology depending on the application or function required.
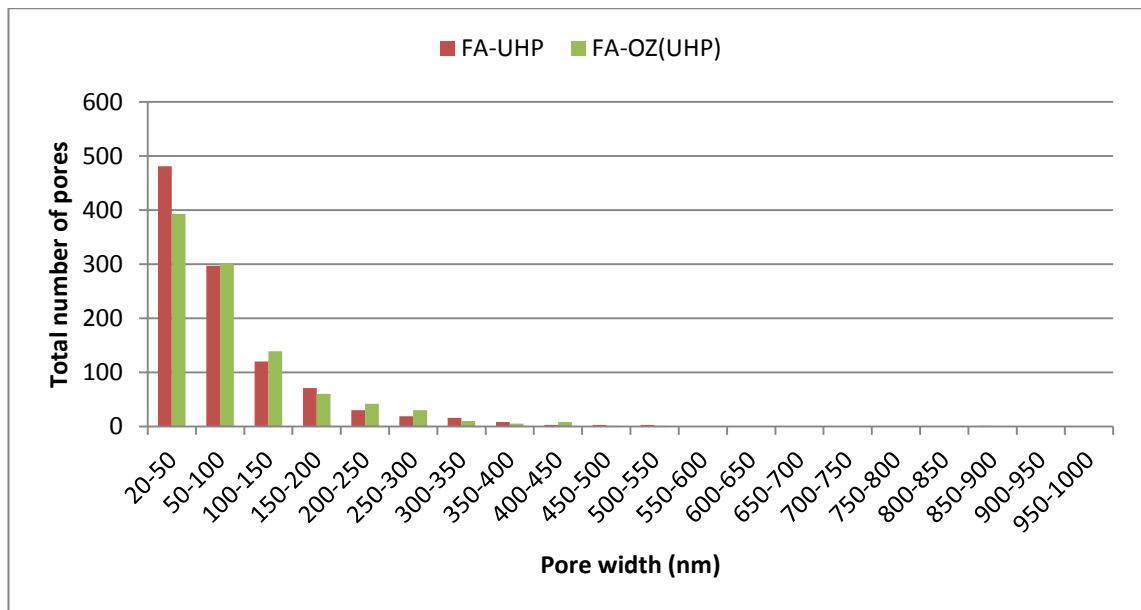
Figure 5.35 - Pore frequency distribution of FA-UHP and FA-OZ(UHP) pre-treated wool fibres treated with O$_2$ plasma

The wool fabric that was FA-UHP pre-treated has a slightly greater total pore volume than the wool fabric pre-treated with FA_OZ(UHP) (see Table 5.11). However, the wool fabric pre-treated with FA-OZ(UHP) has a slightly lower number of pores formed after O$_2$ plasma treatment.

Table 5.11 - Comparison of total pore area and total number of pores for FA-UHP and FA-OZ(UHP) pre-treated wool fibres treated with O$_2$ plasma

Chemical pre-treatment	Total pore area (μm^2)	Total number of pores
FA-UHP	24.1	1052
FA-OZ(UHP)	20.7	991

It is possible the different chemically pre-treatments are responsible for the discrepancy between the total pore areas and total number of pores formed, particularly because the morphology of the pores formed are different despite being exposed to the same O$_2$ plasma treatment.

5.2.2.4.4 Pore size distributions in terms of pore volume

To further investigate the pore formations observed after O$_2$ plasma treatment, mercury porosimetry was conducted to create pore size distributions in terms of pore volumes.

This technique is capable of measuring the depth of the pores which could give further clarification and characterisation of the pores formed. Similar to the previous studies, wool fibres investigated include FA-UHP and FA-OZ(UHP) pre-treated MWov fabrics treated with O_2 plasma.

The pore volume distributions for wool fabrics pre-treated with FA-UHP (see Figure 5.36 and Figure 5.37) and FA-OZ(UHP) (Figure 5.38 and Figure 5.39) are detailed below. An increase in pore volume is evident for both chemically pre-treated fabrics after O_2 plasma treatment. This demonstrates that pores are present after O_2 plasma treatment. One shortcoming of mercury porosimetry experiment was that only one repetition was recorded for each sample due to the extensive time duration and cost of the procedure. To ensure an accurate measurement and to obtain a result representative of the whole sample, the fabrics were cut into slivers and mixed before loading into the sample tubes.
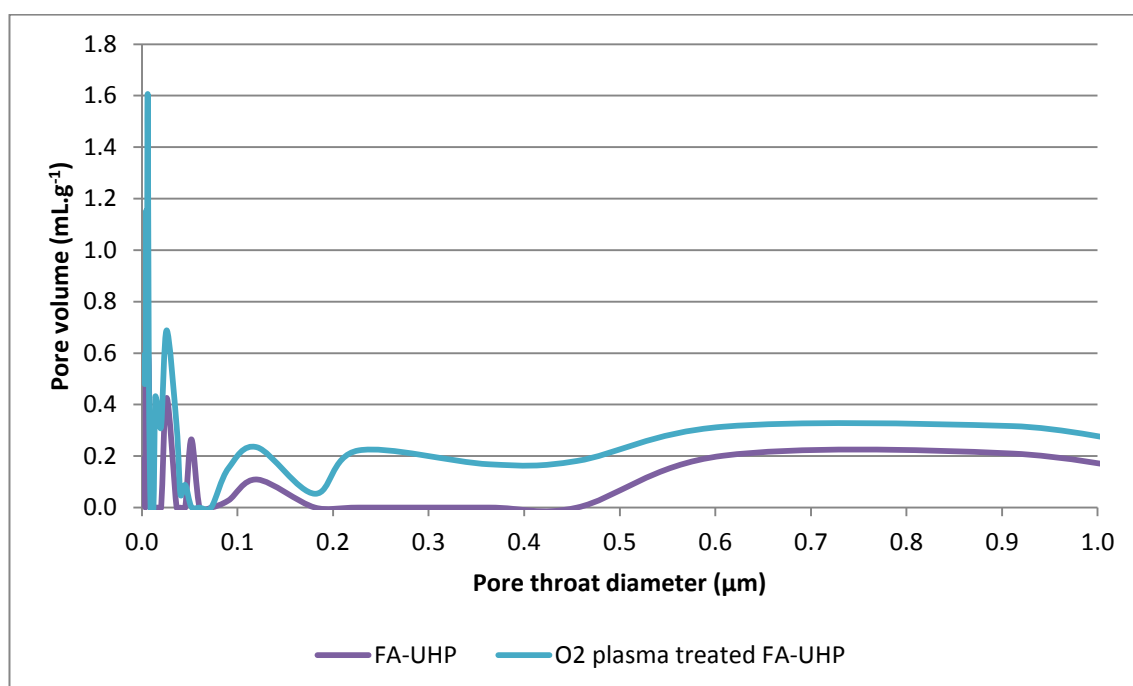
Figure 5.36 - Pore volume distribution (3 nm – 1 µm) of FA-UHP pre-treated wool fibres treated with O_2 plasma
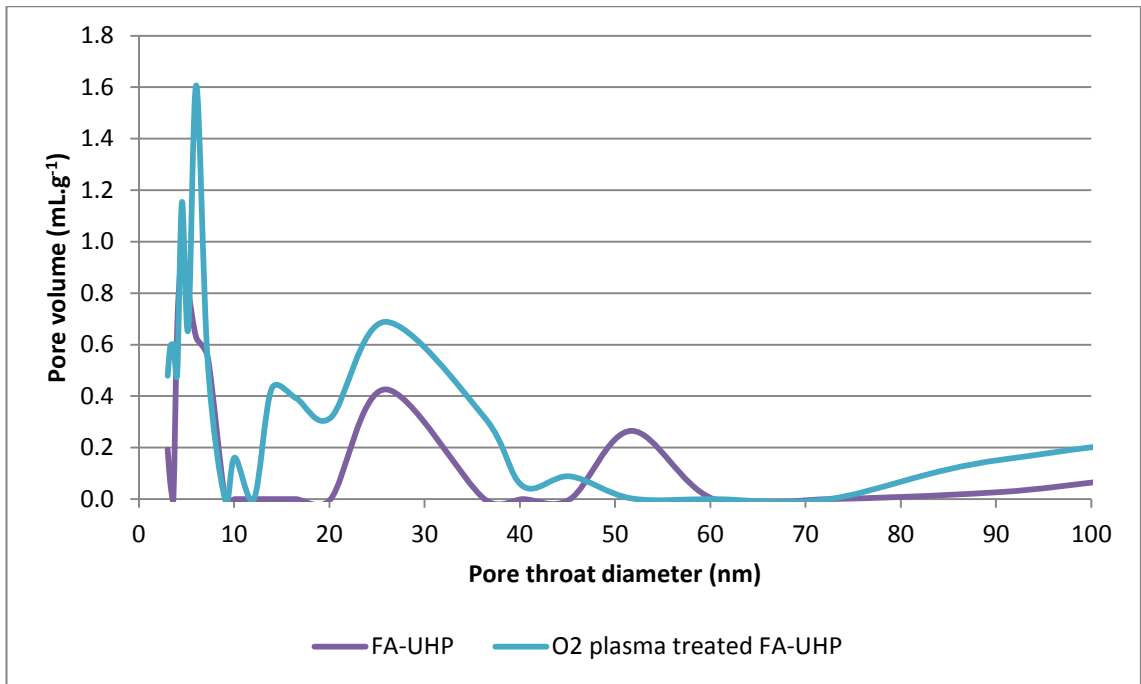
Figure 5.37 - Pore volume distribution (3 - 100 nm) of FA-UHP pre-treated wool fibres treated with O_2 plasma
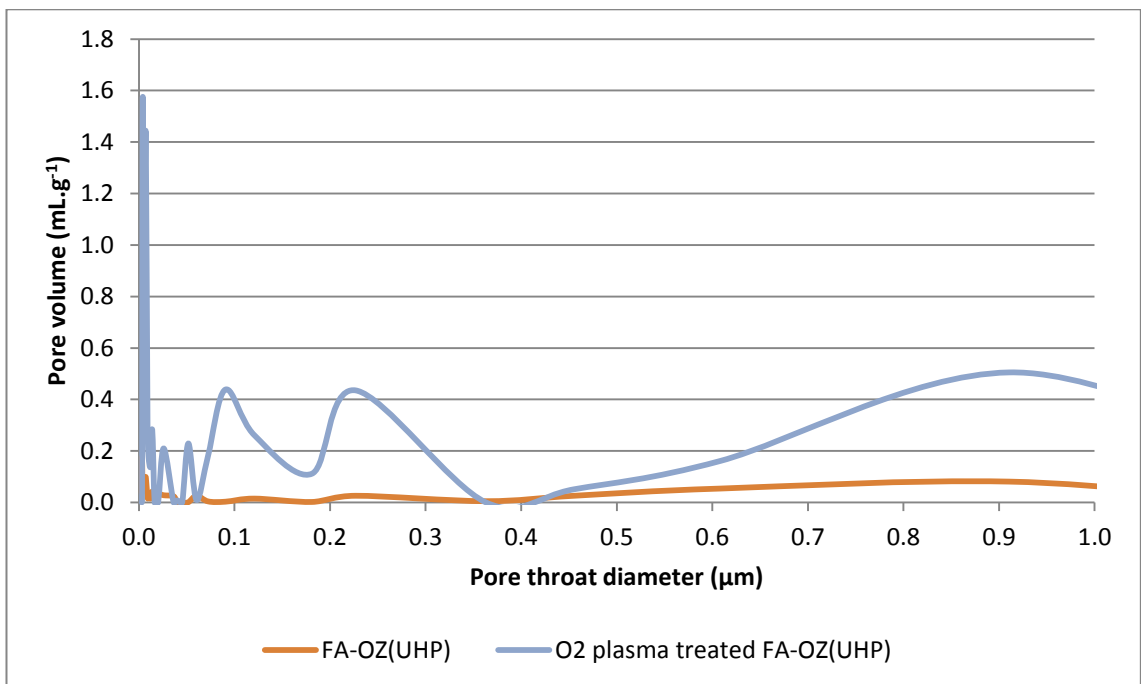
Figure 5.38 - Pore volume distribution (3 nm – 1 μm) of FA-OZ(UHP) pre-treated wool fibres treated with O_2 plasma
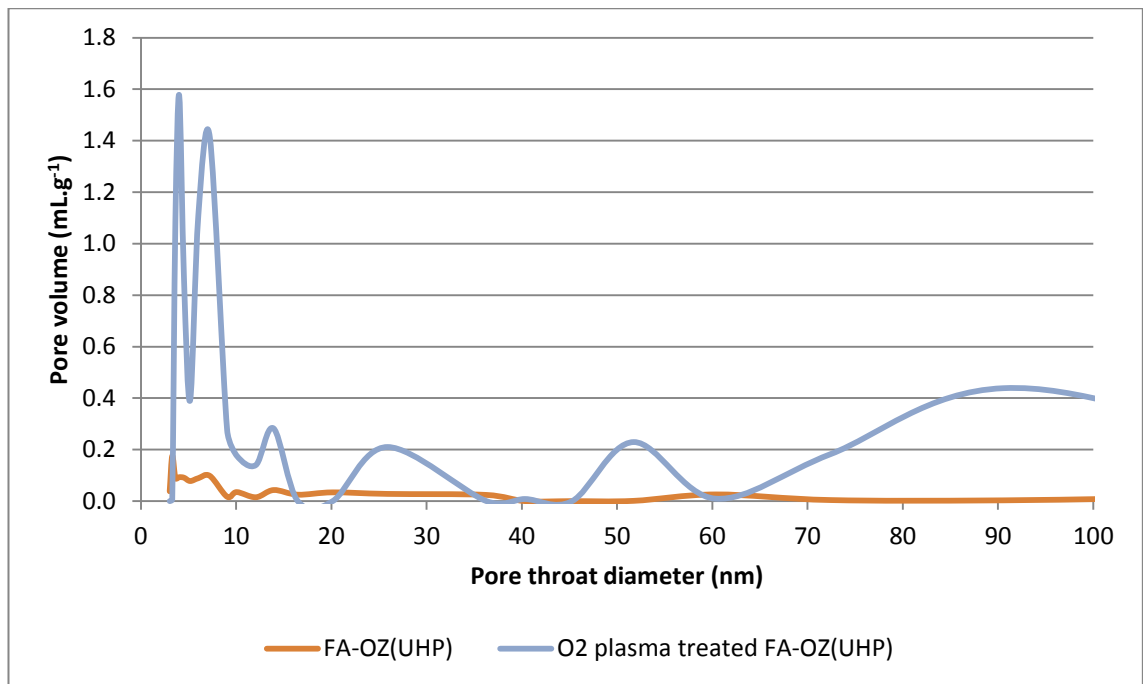
Figure 5.39 - Pore volume distribution (3 - 100 nm) of FA-OZ(UHP) pre-treated wool fibres treated with O₂ plasma

Similar to results obtained in previous studies (Ward and Mao, 2016), the total pore volume reduces by treating the FA pre-treated wool fabrics with UHP and OZ(UHP) (see Figure 5.40), which could be caused by the removal of cuticles or swelling of the fibres. It is well known that UHP is an oxidising agent with swelling properties, which could reduce the size of the pores between and on the wool fibres. Also, the total pore volume of the FA-UHP and FA-OZ(UHP) fibres significantly increases after treating with O_2 plasma. Again, this demonstrates that the combination of chemical pre-treatment and selective degradation technique is capable of forming porous wool fibres.
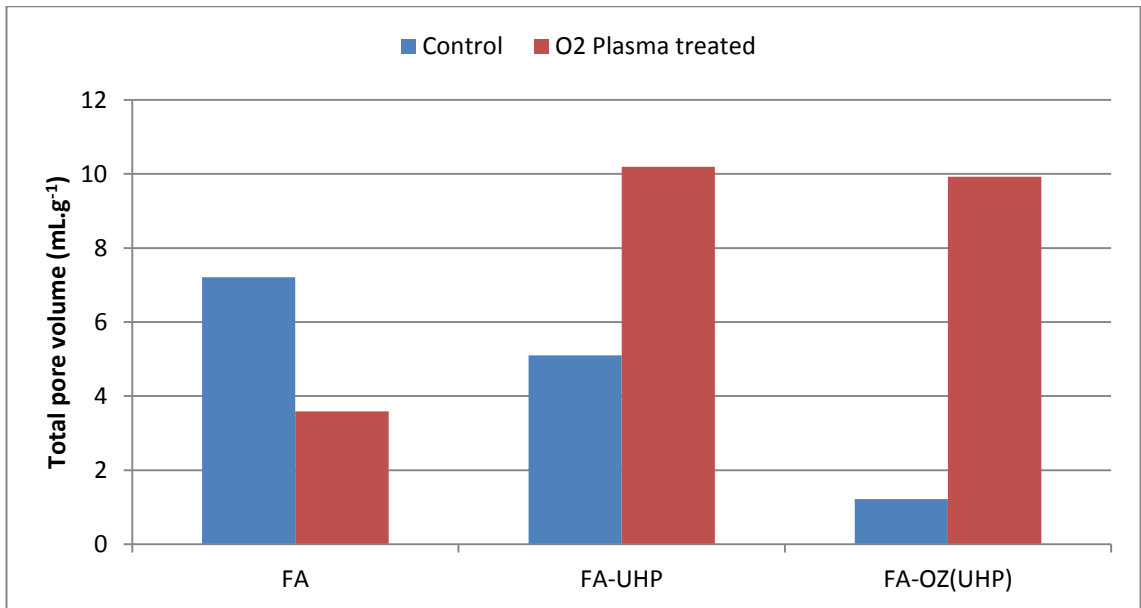
Figure 5.40 - Comparison of total pore volume (3 nm – 1 µm) for chemical pre-treated wool fabrics treated with O_2 plasma

A similar trend is observed when the comparing the total meso-pore volume of chemically pre-treated wool fabrics treated with O_2 plasma (see Figure 5.41). This graph also indicates that a significant proportion of the pore volume formed are from mesopores (<50 nm).
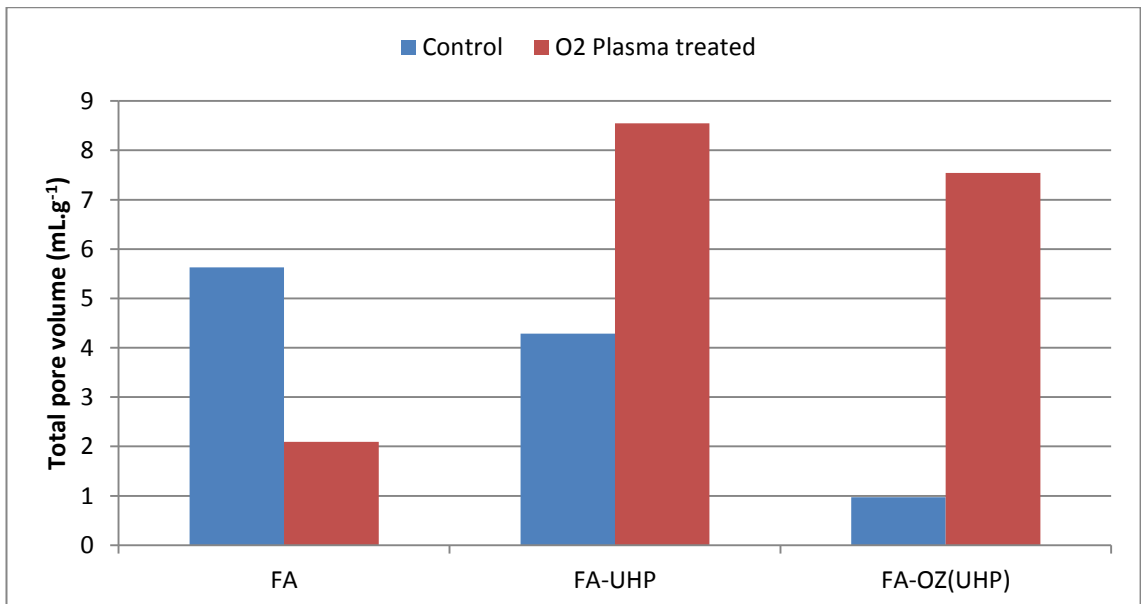
Figure 5.41 - Comparison of total meso-pore volume (3 – 50 nm) for chemical pre-treated wool fabrics treated with O_2 plasma

5.2.2.4.5 Specific surface area

Within this section, the specific surface area of the wool fibre before and after O_2 plasma exposure was analysed. BET surface area was measured using gas adsorption porosimetry. Due to the pore formation evident after the O_2 plasma treatments it is expected that the wool fibre specific surface areas will increase as a result of the treatment. This section explores this hypothesis for chemically pre-treated wool fibre exposed to O_2 plasma.

An increase in BET surface area is evident after treating the various raw and chemical modified wool fabrics with O_2 plasma for 15 min at 5 $cm^3.min^{-1}$ O_2 flow rate (see Figure 5.42).
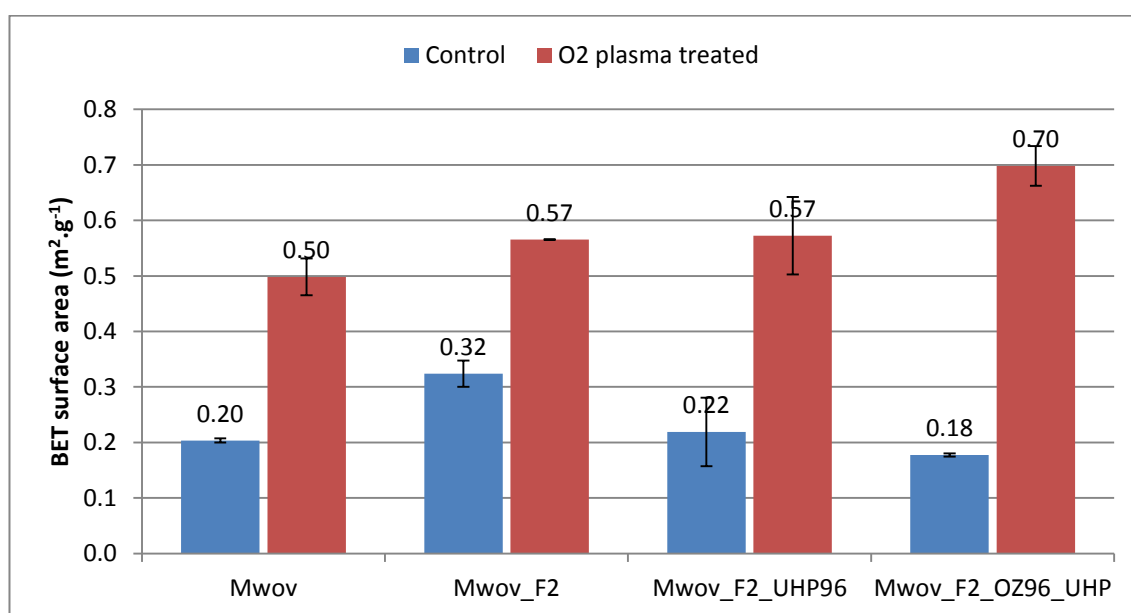
Figure 5.42 - The effect of O_2 plasma treatment on the BET surface area of raw, FA, FA-UHP and FA-OZ(UHP) pre-treated wool fabrics

The BET surface area of the FA-OZ(UHP) fabric appears to increase the most in comparison to the other wool fabrics. This could be caused by increased surface indentations or the formation of a reticulated pore structure (see Figure 5.24).

5.3 Summary

Pore formation is possible using both electron beam irradiation in SEM and plasma irradiation on both raw and chemically pre-treated wool fibres. The electron beam irradiation technique by SEM is capable of degrading selective areas of the wool fibres; however, the plasma treatment is capable of modifying a large population of exposed fibres.

Degradation and pore formation is evident after exposing the wool fibres to selective degradation under high energy electron impacts; however, sufficient electron beam intensity and exposure durations are required to form pores on the chemically modified wool fibres.

A novel technique for forming porous wool fabrics using subsequent chemical pre-treatments and plasma (air and O_2) was determined. These techniques demonstrated the capability of selective degradation and formation of porous wools. Similar morphological features were observed when exposing wool fibres to electron beam radiation. However, this new technique is capable of treating the whole surface of the wool fibres and potentially exposing the inaccessible pores formed by chemical modification.

Macro-pore formation by selective degradation was evident for wool fibres pre-treated with oxidation treatments, suggesting the fibres partially fibrillate after the chemical treatments. However, an additional treatment, such as selective degradation with high electron impact is required to complete the fibrillation of wool fibres. It is possible the consecutive chemical treatments are capable of forming inaccessible pores formations within the fibres; however, an additional physical treatment, such as high energy impact is required to expose these internal features, thus creating porous wool fibres.

Different morphological features are evident after treating the FA-UHP pre-treated wool fabrics for different O_2 plasma exposure durations. Extending the exposure duration

appears to increase the pores to macropores, while reducing the number of pores present, which suggests the pores expand and merge as a result of the extended O_2 plasma exposure. Also, reticulated pore structures are evident after exposing the chemically modified wool fibres to O_2 plasma for a longer duration; however, the depths of the pore matrices are unclear. The specific surface area significantly increases by exposing the chemically modified wool fibres to O_2 plasma, particularly for longer exposure durations.

Moreover, the chemical pre-treatments appear to affect the pore formation within wool fibres using electron beam radiation and plasma selective degradation techniques. When the FA-UHP and the FA-OZ(UHP) treated fibres are exposed to O_2 plasma within the low pressure environments, the fibres appear to fibrillate, and the pore formations and reticulated pore formations are results of the selective degradation.

Different morphological features were evident after treating the wool fabrics with O_2 plasma, by varying the O_2 plasma treatment duration and chemical pre-treatment. Therefore, by varying these parameters, it is possible the porosity of the wool fibres could be tailored depending on the desired function or application. Finally, this technique could be used for forming keratin scaffolds for the incorporation of other functional materials, such as aerogels, activated carbon, metal organic frameworks and zeolites.

Chapter 6 Incorporation of Nanoporous Materials Inside Porous Wool Fibres

While both polymers of intrinsic micro-porosity (PIM) and nanoporous aerogels were successfully synthesised and widely used in various applications (Zhang et al., 2015; Rao et al., 2006), whether they can be formed inside porous wool fibres are still unknown. In this chapter, the incorporation of both polymers of intrinsic micro-porosity (PIM) and nano-porous aerogel materials into macropores of porous wool fibres resultant in Chapters 4 and 5 to advance their adsorption capacities of the wool fibres. The techniques and procedures of how to synthesis nanoporous materials and how to incorporate them into porous wool fibres are detailed in Chapter 3.

6.1 Incorporation of nano-porous materials inside porous wool fibres

The techniques and procedures for incorporating both polymers of intrinsic micro-porosity (PIM) and nano-porous aerogels into various porous wool fibres were detailed in the section 1.1.

6.1.1 Incorporation of PIM polymers into porous wool fibres

Two PIM crude products were obtained according to the procedures described in the section 3.4.1, one was dissolved in Tetrahydrofuran (THF) and the other was dissolved in Chloroform ($CHCl_3$). It is possible these solvents could solubilise components of the wool fibres during the synthesis of wool-PIM composites; however, Aluigi et al. (2014) reported that THF is less degrading solvent than $CHCl_3$ when dissolving keratin powders. Therefore, the incorporation of polymers of intrinsic micro-porosity (PIM) materials inside macropores were investigated during this study. It was found that the

product dissolved in THF had the highest specific surface area (or BET surface area) at 3.59 $m^2.g^{-1}$ in comparison to the DMF dissolved product, which has the value of 1.80 $m^2.g^{-1}$. However, the BET surface area of the two PIM crude products were significantly lower than what was reported in the literature (e.g. 620-850 $m^2.g^{-1}$) (Zhang et al., 2015). Therefore, it is likely that only a fraction of PIM were formed during this experiment.

Two methods for incorporating the PIM into the macropores of the FA treated wool fibres were also investigated (see section 3.4) to determine if PIM could be included into the macropores inside wool fibres without significant coating. The intention of Method 1 was to incorporate the PIM into the macropores only. For this study, FA (2h) treated woven wool fabrics (MWov_F2) were selected as they demonstrated internal pore formation as a result of the chemical treatment (see section 4.2.1). The FA treated wool fibres were saturated with a mixture containing anhydrous potassium carbonate (K_2CO_3), 5,5′,6,6′-Tetrahydroxy-3,3,3′,3′-tetramethyl-1,1′-spirobisindane (TTSBI) and 2,3,5,6-tetrafluoroterephthalonitrile (TFTPN) dissolved in anhydrous N,N-Dimethylformamide. The excess of PIM raw materials on the saturated wool fibres were removed to prevent the formation of a PIM coating on the wool fibres. Water was then introduced to initiate the PIM polymerisation reaction on the saturated wool fibre.

Method 2 involved saturating the wool fibres in the polymerising mixture solution during the PIM synthesis process (see section 3.4.1), and it was expected that excess PIM would be present on the surface of wool fibres after this treatment.

However, it was found that wool fibres produced in both of the two methods having PIM materials coated heavily on the wool fibre surfaces as shown in Figure 6.1 and Figure 6.2 below.
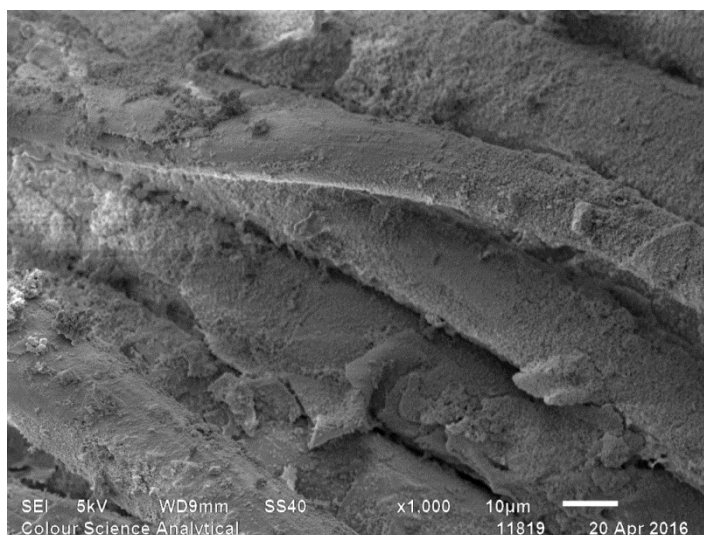
Figure 6.1 - Woven wool fabrics with FA treatment after incorporation of PIM using method 1
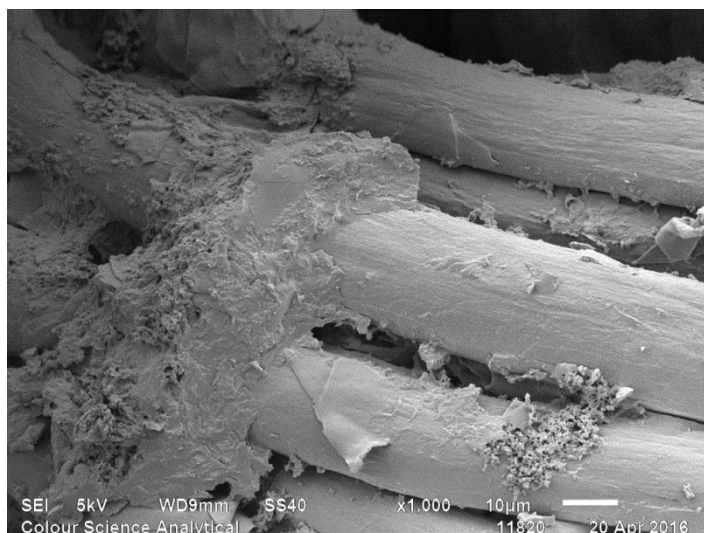
Figure 6.2 - Woven wool fabrics with FA treatment after incorporation of PIM using method 2

Because the BET surface area of the two PIM materials were so low and the incorporation methods can only produce coating morphologies in wool fibres, this study of PIM materials was discontinued and the incorporation of nano-porous aerogels materials into porous wool fibres is the main body of this research.

6.1.2 Incorporation of silicone aerogels into porous wool fibres

The aim of this study was to incorporate aerogels into the macropores formed in the modified wool fibres resultant in Chapters 4 and 5.

In Chapter 5, it was demonstrated that reticulated porous structures and superficial pore formation is evident after chemical treated wool fibres were exposure to low pressure oxygen plasma treatments. Therefore, incorporation of nanoporous aerogel materials into the resultant porous wool fibres is desirable for developing adsorbent materials. To avoid coating the aerogel materials on the surface of wool fibres and to target formation within the voids between wool fibres, porous wool fibres were applied to the sol-gel process in different stages of the aerogel synthesis process to incorporate the aerogel material within the macropores formed in the wool fibres.

The aerogels were made by a sol-gel method described in Figure 2.14 (Hüsing and Schubert, 2000) and detailed in the section 3.4.2.1. The precursor solution is firstly dissolved in an organic solvent that is miscible in water, and then the acid and base catalysts are added separately to speed up the hydrolysis and condensation reactions to obtain the wet gel, which is then aged and strengthened in a solvent. Finally, the strengthened wet gel is dried to form porous aerogels (Du, 2014). When the wet gel was dried using supercritical CO_2 (SCCO$_2$) drying process, the material had BET surface area >450 m^2.g^{-1}; therefore, similar to PIMs, MTMS based silicone aerogels are an attractive material for the application of adsorbing VOCs. The procedures for incorporating aerogels into porous wool fibres are shown in Figure 3.14 (see section 3.4.2.2). Porous wool fibres after a series of chemical treatments and treated with oxygen plasma treatment were saturated with a sol-gel within the various stages of a silicone aerogel condensation reaction. Once saturated the fibres were aged and then dried with the supercritical CO_2 drying method used previously to form the aerogels (Du, 2014; Ward and Mao, 2015). SEM, BET surface area and EDX were used to characterise the modified wool fibres.

In this section, the porous wool fibres exposed to the sol-gel in the different stages of aerogel synthesis process (10 min, 12h and 24 h) to determine whether excess aerogel coating on the wool fibres could be avoided.

6.1.2.1 Formation of aerogel within porous wool fibres after 10 min of exposure in sol-gel process

The experiments to incorporate aerogel within porous wool fibres after 10 min of sol-gel exposure are detailed in Table 6.1.

In this sol-gel process, the sol was prepared by hydrolysing MeOH and MTMS with an aqueous solution of oxalic acid, ammonia solution was added to the sol solution to initiate its condensation reaction. This mixture was then agitated for 1 h to ensure the sol was homogenous before immersing the wool fibres into it. Then, porous wool fibres were saturated with the sol for a short duration of 10 min (see section 3.4.2). After 10 min of exposure to the sol, the wool fibres were removed and placed in a separate jar and methanol was added to submerge the whole wool fabric. The jars were sealed with parafilm to prevent the methanol from evaporating. The wool fabrics were then aged for 88 h and dried using a supercritical CO_2 drying process.

Table 6.1 - Experiment to characterise porous MWov wool fibres after 10 min of exposure in sol-gel treatments

Sample Code	UHP treatment duration (h)	Ozone treatment duration (h)	Sol-gel exposure duration (min)
FA-O2Plasma (Control)	N/A	N/A	N/A
FA-O2Plasma-AG10	N/A	N/A	10
FA-UHP-O2Plasma (Control)	96	N/A	N/A
FA-UHP-O2Plasma -AG10	96	N/A	10
FA-OZ(UHP)-O2Plasma (Control)	N/A	96	N/A
FA-OZ(UHP)-O2Plasma -AG10	N/A	96	10
AG	N/A	N/A	N/A

All the worsted woven fabrics made from merino wool fibres (MWov) were pre-treated with FA for 2 h and were exposed to oxygen plasma with 5 cm^3.min^{-1} oxygen flow rate for 30 min each side.

6.1.2.2 **Formation of aerogel within porous wool fibres after 24 h of**

        exposure in sol-gel process

The porous wool fibres were exposed to the sol-gel process following each procedure described in the section 6.1.2.1 except that the wool fabrics were immersed in the sol solution for 24 h, this is to determine whether the amount of aerogel present within the macropores of porous wool fibres increase with the increases of the time duration of wool fabrics dwelling in sol-gel process.

Similar to experimental plan shown in Table 6.1, the experiments for making various porous wool fibres incorporating aerogel materials in the sol-gel process 24 h are detailed in Table 6.2.

Table 6.2 - Experiment to determine whether porous MWov wool fibres can be incorporated with aerogel after 24 h sol-gel exposure

Sample Code	UHP treatment duration (h)	Ozone treatment duration (h)	Sol-gel exposure duration (h)
FA-O2Plasma (Control)	N/A	N/A	24
FA-O2Plasma -AG24	96	N/A	24
FA-UHP96-O2Plasma (Control)	N/A	N/A	24
FA-UHP96-O2Plasma -AG24	N/A	96	24
FA-OZ(UHP)-O2Plasma (Control)	96	N/A	24
FA-OZ(UHP)-O2Plasma -AG24	N/A	96	24
FA-OZ(UHP)-O2Plasma -AG88	N/A	96	88
AG	N/A	N/A	N/A

All the worsted woven fabrics made from merino wool fibres (MWov) were pre-treated with FA for 2 h and were exposed to oxygen plasma with 5 cm^3.min^{-1} oxygen flow rate for 30 min each side.

6.2 Characteristics of porous wool fibres incorporated with silicone aerogels

The morphologies, element composition and specific surface area of porous wool fibres incorporated with silicon aerogels were examined using SEM, EDX and gas adsorption porosimetry, respectively. The adsorption capacity of the developed wool-aerogel composite material was investigated using Dynamic Vapour Sorption (DVS).

6.2.1 Morphologies of porous wool fibres incorporating aerogels

Morphologies of porous wool fibres incorporating aerogels were examined in SEM images and EDX to determine whether aerogel was present in both external and inner structure of the porous wool fibres. Both external wool fibre features and the fibre cross-sections were analysed.

6.2.1.1 Porous wool fibres after 10 min sol-gel exposure

The effect of treating two types of porous wool fibres incorporated with aerogels after 10 min sol-gel exposure is shown in Figure 6.3. All fibre used were those which were through either FA and UHP or FA and Ozone-UHP chemical treatments followed by the O_2 plasma treatments, they are displayed by the top and bottom rows, respectively. These wool fibres were selected because macro-pore formation was evident after consecutive chemical and O_2 plasma treatments.
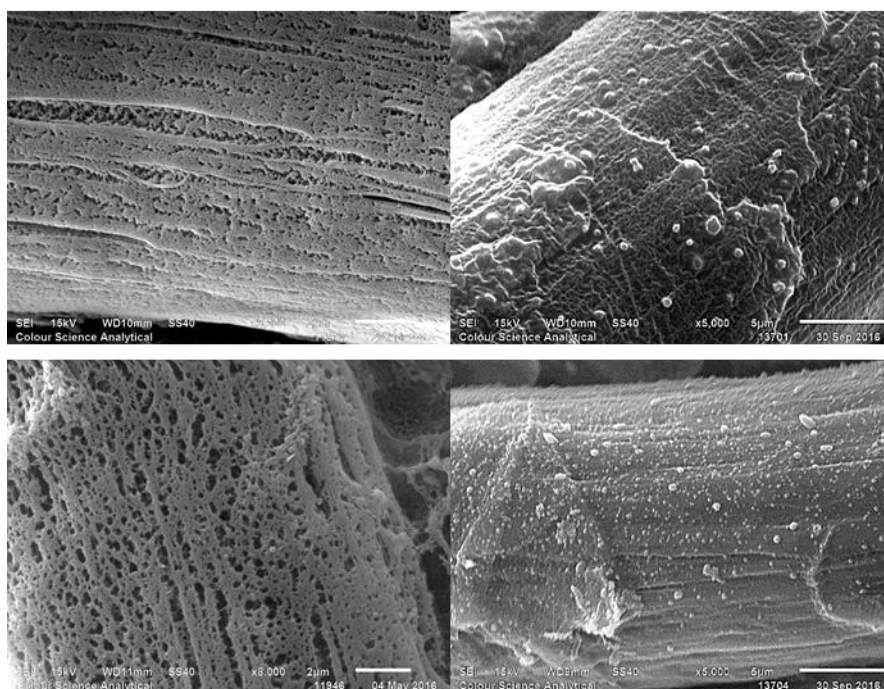
Figure 6.3 - Porous wool fibres incorporated with aerogel. Left: Porous wool fibres (Control, Mag. x8000), Right: incorporated with aerogel (Mag. x5000). Top: FA-UHP-O2Plasma; Bottom: FA-OZ (UHP)-O2Plasma

It is clear when comparing the SEM images of the fibre surfaces before and after aerogel incorporation that the surface morphology has changed. The pattern (FA pre-treated) or pore formation (FA-UHP and FA_OZ (UHP) pre-treated) observed after O_2 plasma treatment appears to disappear as a result of the aerogel incorporation method. However, it is uncertain whether the indentation between patterns (FA pre-treated) or pores (FA-UHP and FA_OZ(UHP) pre-treated) are filled with aerogel or whether the pattern/ pores have been eroded by exposure to sol during the aerogel synthesis.

Remnants of the pores formed after the O_2 plasma treatment are evident for the wool fibres pre-treated with UHP solution (see Figure 6.4); however, the pores volumes appear to be less significant and there is no longer evidence of reticulated pore structures.. The fibres could have swelled or the pore edges could have eroded due to exposure to chemicals within the aerogel synthesis process. It is also possible the pores are filled with aerogel, but this cannot be concluded by the SEM images alone.
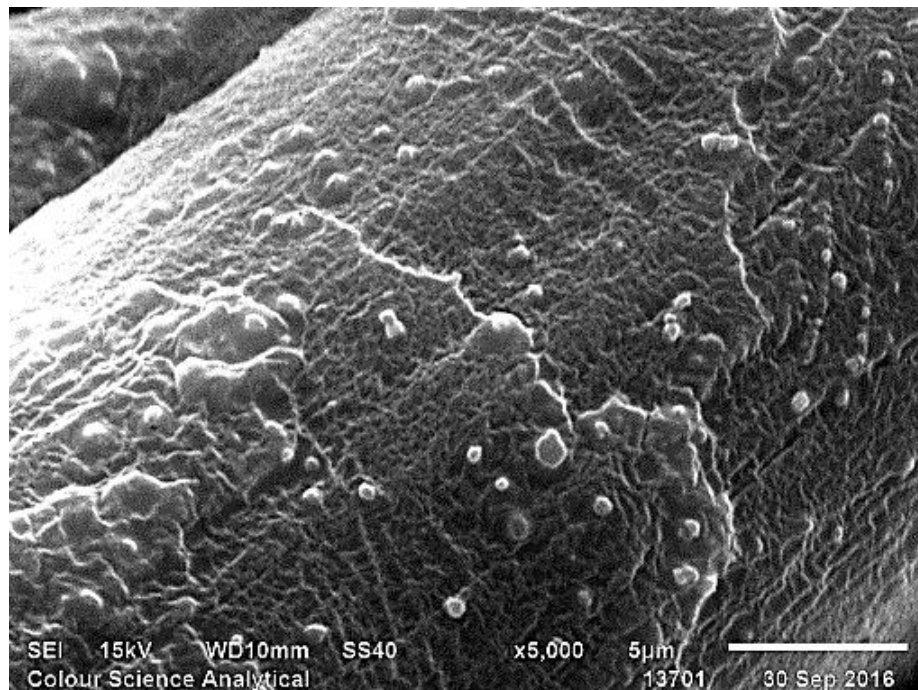
Figure 6.4 - Porous wool fibres pre-treated with FA and O_2 plasma and incorporated with aerogel (FA-UHP-O2Plasma-AG10), Mag. x5000

Also, pores are present within the fibre cross-sections (see Figure 6.5) despite aerogel incorporation; however, it is uncertain whether pores aerogel is present within the porous features of the fibre by SEM analysis.
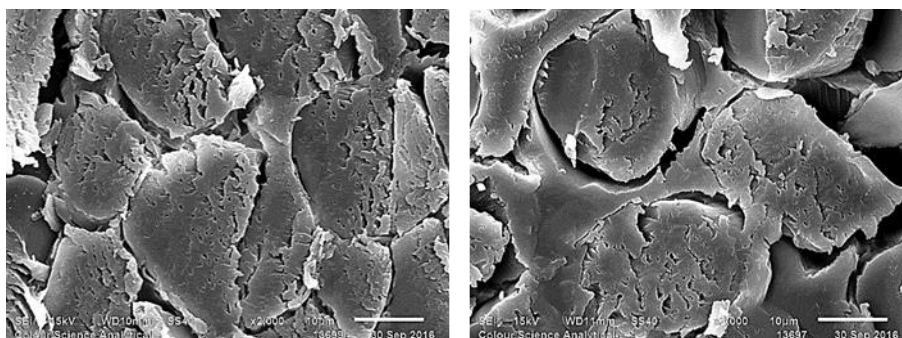
Figure 6.5 - Porous wool fibres incorporated with aerogel (Mag. x2000), Left: FA-UHP pre-treated, Right: FA-UHP pre-treated

From these SEM images, it is difficult to determine whether the macropores formed in the modified wool fibres (see Chapters 4 and 5) have been incorporated with aerogel material. However, the porous wool fibres and porous wool fibres incorporated with aerogel appear different in terms of their surface morphologies. Also, for all wool fibre variations, there is evidence of what appears to be particles scattered on the wool fibres surfaces after the aerogel incorporation methods. It is possible these particles are aerogel materials or nanospots (Tsoi et al., 2010). It is uncertain whether pores, formed by the O_2 plasma treatments, and the fibre cross-sections contain aerogel, so EDX element mapping techniques are employed to investigate this hypothesis and is discussed below.

The element composition mapping of silicon of the areas of interest was analysed for the purpose of identifying aerogel within the wool fibres. Figure 6.6 and Figure 6.7 demonstrates the individual element composition mapping of the porous wool fibres pre-treated with FA-UHP and UHP-OZ(UHP), respectively.
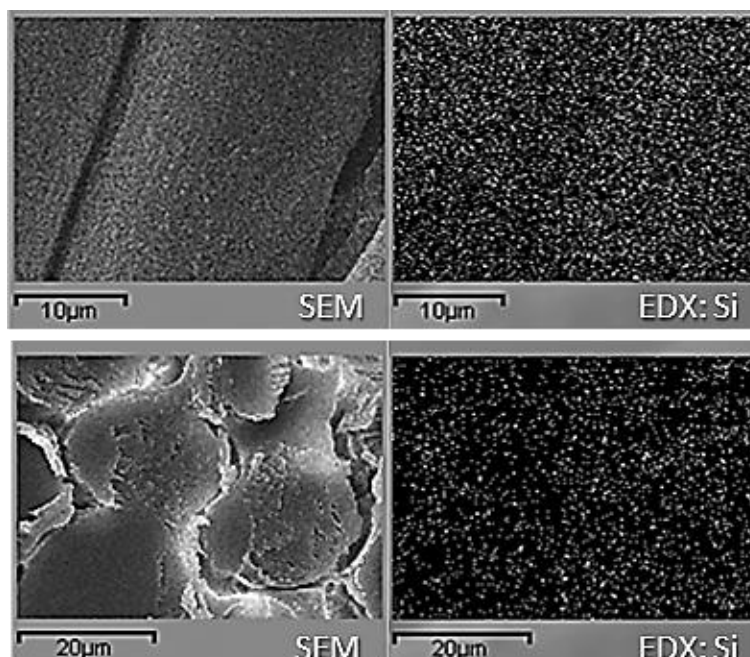
Figure 6.6 - Mapping of Si element distribution in the fibre surface (Top) and cross-section (Bottom) of FA-UHP pre-treated worsted merino wool fibres treated with O$_2$ plasma and exposed to aerogel condensation reaction for 10 min (FA-UHP-O2Plasma-AG10)
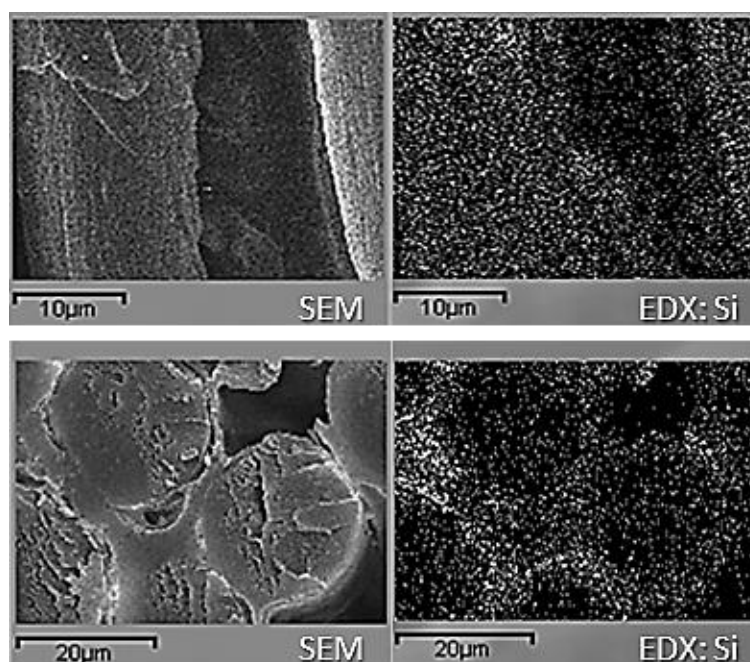
Figure 6.7 - Mapping of Si element distribution in the fibre surface (Top) and cross-section (Bottom) of FA-OZ(UHP) pre-treated worsted merino wool fibres treated with O$_2$ plasma and exposed to aerogel condensation reaction for 10 min (FA-OZ(UHP)-O2Plasma-AG10)

Silicon was evident on the fibre surfaces and within the fibre cross-sections of both wool fibres. Firstly, this indicates that pores are formed inside the cortex. Secondly, it indicates that the silicon has diffused into the pores of cortex despite the limited amount of aerogel used within the treatment process. Interestingly in Figure 6.7, the silicon elements appear to be more concentrated around the edges of fibre cross-sections and gradually reduce towards the centre of the fibre. This indicates that the silicone is accessing pores on the fibre surfaces, as well as, the cavities/ internal pores within the fibres.

The aerogel present within the wool fibres was limited to the amount of sol-gel absorbed by the fibres during the 10 min exposure before initiating the condensation reaction (see Figure 3.14). However, Silicon was present on the surface of both wool fibres and cross-sections appear evenly distributed over the porous wool fibres, despite the limited amount of sol present within the treatment process.

The amount of incorporating silicone aerogels into porous wool fibres could be indicated by BET surface area and the results are shown in Figure 6.8. After incorporating aerogels into the FA-UHP and FA-OZ(UHP) pre-treated wool fibres treated with O_2 plasma, it is evident that its surface area increased by approximately 33 and 25%, respectively. However, it is uncertain whether this is as a result of the specific fibre type or the aerogel content on the surface of the fibre as the aerogel add-on rate was not controllable during the sol-gel treatment process. Therefore, the incorporation of silicone aerogel into porous wool fibres requires refinement.

213
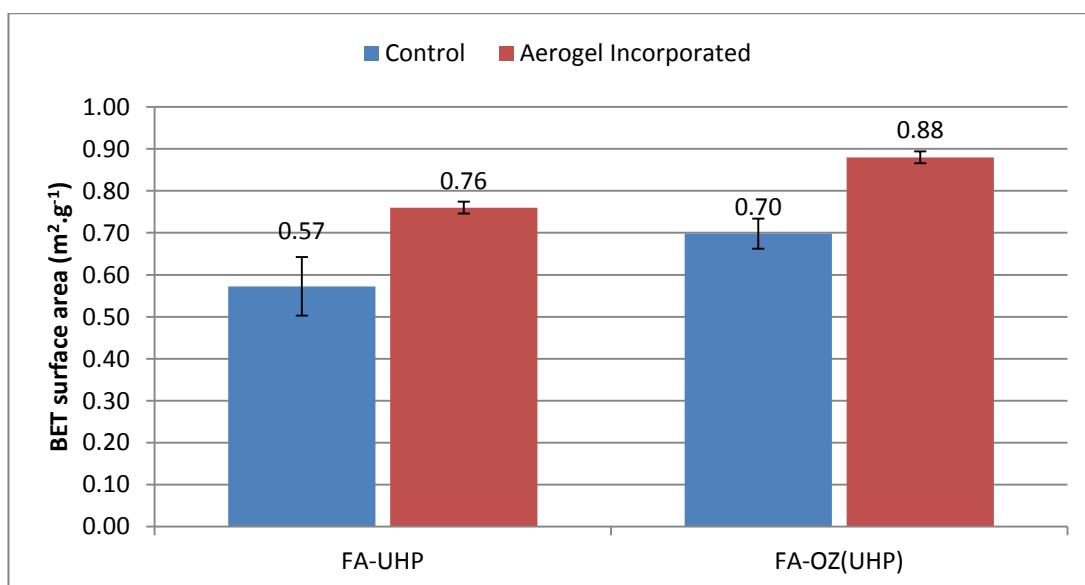
Figure 6.8 - BET surface area of chemically modified wool fibres, porous wool fibres and porous wool fibres incorporating with aerogels (Wool fibres incorporating with aerogels were exposed to Sol-gel process for 10 min and then aged)

The amount of silicon on the fibre surface and within the wool fibres could be influenced by the amount of sol absorbed into porous wool fibres and this could be enhanced by extending the time duration of immersing wool fibres into the sol solutions before initiating the ageing process.

Also, excess methanol added in the ageing process to prevent premature precipitation of the sol-gel could have diluted the sols absorbed on the wool fibres. Therefore, the time duration between the initiation of the gelation process and adding the wool fibres, as well as, the saturation time duration are variables to be further investigated to improve the amount of silicone aerogels on the porous wool fibres.

In summary, it is difficult to differentiate between aerogel and wool when observing the SEM images of the fibre surfaces and cross-sections; however, EDX analysis determined that silicon elements were present within the fibre cross-sections and this indicates that pores exist within the wool fibres and that the sol-gel is capable of diffusing into the cortex layer of various porous wool fibres. Also, the specific surface area increases as a result of incorporating aerogel into the porous wool fibres.

6.2.1.2 **Porous wool fibres after 24 h sol-gel exposure**

The aim of this study was to investigate whether extending the porous wool fibre sol-gel exposure duration, during the incorporation/ aerogel synthesis process enables a greater content of aerogel to be incorporated into the macropores within the porous wool fibres. For this study, FA, FA-UHP and FA-OZ(UHP) treated wool fibres with subsequent O_2 plasma treatment were saturated in the sol-gel for 24 h before initiating the ageing and drying process (see Table 6.2 and 6.3). The full aerogel synthesis process is described within Figure 3.14. Conversely to the UHP and OZ(UHP) pre-treated fibres, this fibre demonstrated pattern formation after O_2 plasma exposure rather than pore formation (see Figure 5.28). Therefore, the FA pre-treated wool fibres were included within this study to determine whether the aerogel is capable of diffusing into the wool fibres without the present of superficial pores or a reticulated pore structure evident after O_2 plasma treatment.

It is clear that the wool-aerogel composite fibres illustrated in Figure 6.9 that when the porous fibres are exposed to the gel for 24 h the aerogel material partially coats the fibres. Also, these fibres show a greater aerogel content to the fibres exposed to the gel for 10 min (see Figure 6.3) during the gelation and ageing process.

The excess aerogel present on the wool fibres is not consistently spread across the wool fibres. This is likely to be caused by the current methodology for removing the aerogel material. Also, SEM imagining is difficult when a high concentration of silicon is present due to its high surface area. Significant charging and saturation distortion is often present when capturing the images, particularly at high magnifications. Consequently, SEM images of the fibre cross-sections were not obtained.
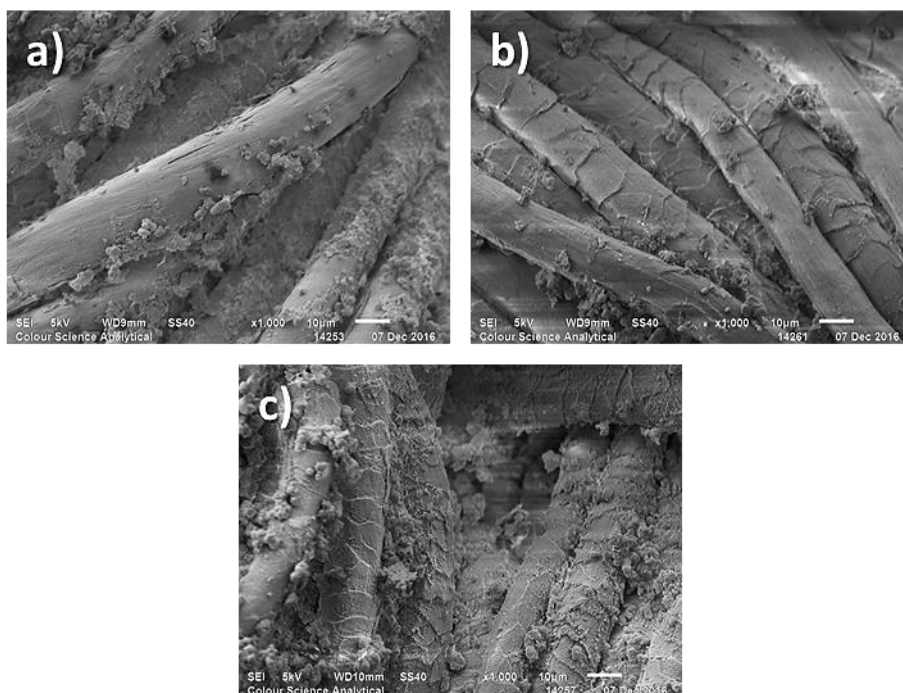
Figure 6.9 - Porous wool fibres incorporated with aerogel. a) FA-O2Plasma-AG24, b) FA-UHP-O2Plasma-AG24 and c) FA-OZ(UHP)-O2Plasma-AG24

All porous wool fibres treated saturated with gel for 24 h show a BET surface area between 17.89 and 22.3 $m^2.g^{-1}$. The increase in aerogel content could be the reason for the considerably higher BET surface area measurements indicated within Figure 6.10. Regardless of whether the BET surface area increase is due to the excess aerogel material on the surface of the wool fibres or a combination of the excess and the aerogel formed within the wool fibres it is possible the adsorption capacity of the material will increase.
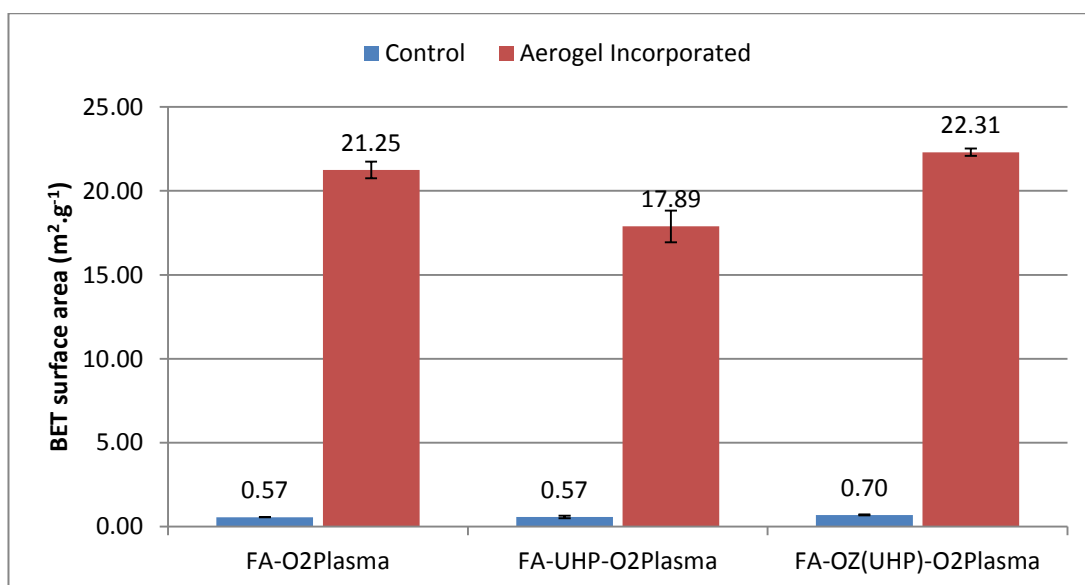
Figure 6.10 - BET surface area of porous wool fibres and porous wool fibres incorporating aerogels

Similar to the fabrics exposed to gel for 10 min, EDX analysis was conducted to investigate whether silicon was present on the surface and within the wool fibres. For all types of porous wool fibres (see Figure 6.11, Figure 6.12 and Figure 6.13) the silicon is clearly distributed over the wool fibre surface and within the fibres cross-sections in particle form. However, the areas of excess aerogel are represented with more concentrated white areas and show that the aerogel aggregates or agglomerates on the fibre surface, which is a common feature of aerogel materials (Du, 2014).
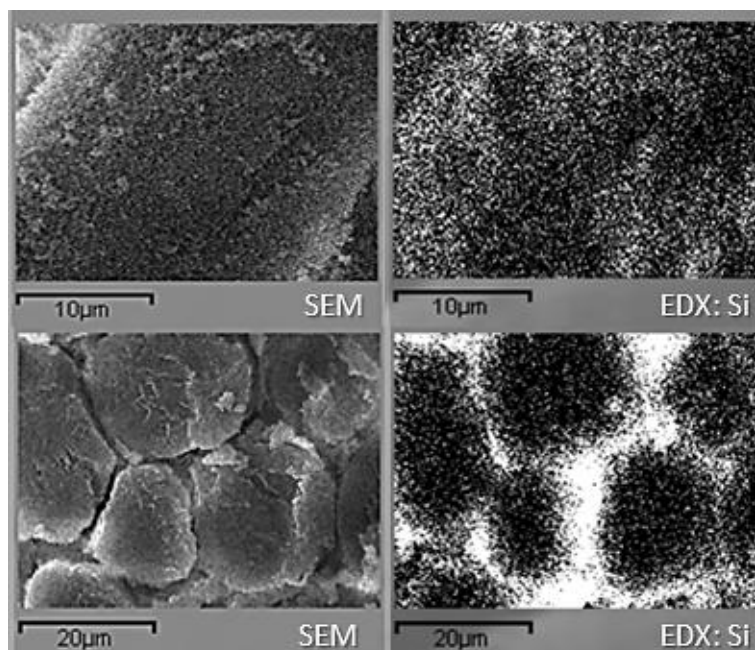
Figure 6.11 - Mapping of Si element distribution in the fibre surface and cross-section of FA pre-treated worsted woven merino wool fabrics treated with O$_2$ plasma and exposed to aerogel condensation reaction for 24 h (FA-O2Plasma-AG24).Top row: fibre surface. Bottom row: fibre cross-sections
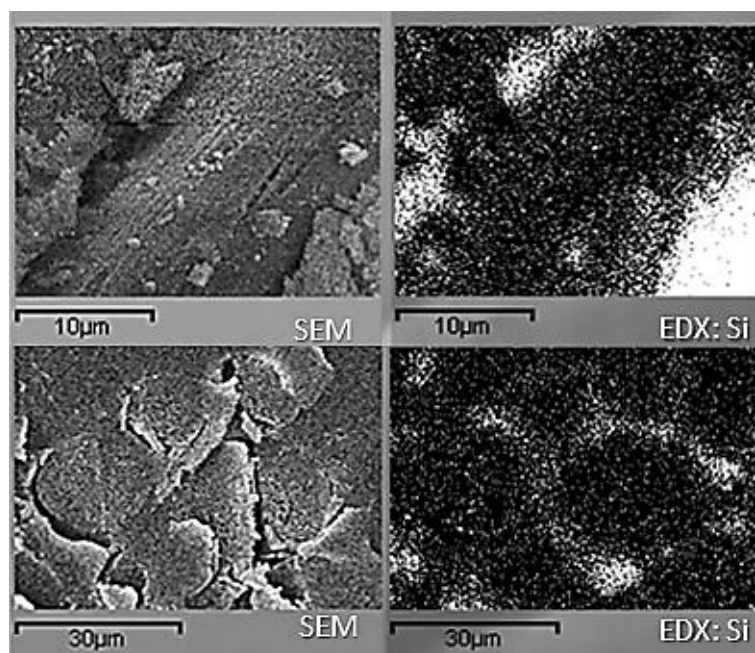
Figure 6.12 - Mapping of Si element distribution in the fibre surface and cross-section of FA-UHP pre-treated worsted woven merino wool fabrics treated with O$_2$ plasma and exposed to aerogel condensation reaction for 24 h (FA-UHP-O2Plasma-AG24). Top row: fibre surface. Bottom row: fibre cross-sections
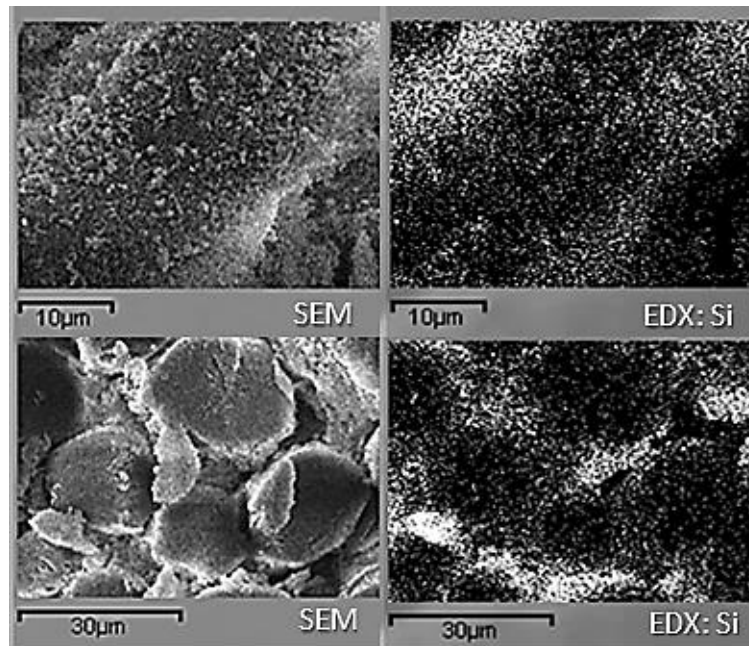
Figure 6.13 - Mapping of Si element distribution in the fibre surface and cross-section of FA-ozone pre-treated worsted woven merino wool fabrics treated with O_2 plasma and exposed to aerogel condensation reaction for 24 h (FA-OZ(UHP)-O2Plasma-AG24). Top row: fibre surface. Bottom row: fibre cross-sections

To investigate whether the BET surface could be increased by extending the gel saturation time, the FA pre-treated wool fibres treated with UHP for 96 hours and then O_2 plasma treated were exposed to both the gelation process caused by the condensation reaction and the ageing process (88h). Essentially, wool fibres were submerged in the sol-gel and aged collectively. Once the ageing process was complete the wool fibres were removed and excess gel was removed using a laboratory spatula before being exposed to the Supercritical CO_2 drying process to form the wool-aerogel composite material. The SEM analysis determined that despite removing the excess gel, aerogel coated the majority of the porous wool fibres (see Figure 6.14).
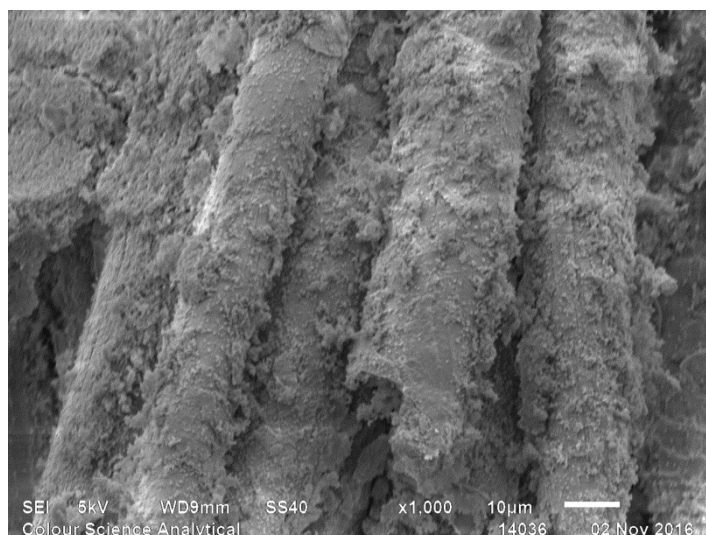
Figure 6.14 - SEM of FA-ozone pre-treated worsted woven wool fabrics treated with O$_2$ plasma and exposed to the whole aerogel gelation and ageing process (FA-OZ(UHP)-O2Plasma-AG24)

For this processing procedure, the BET surface area increased to 33.6 m^2.g^{-1}; however, it is uncertain whether this enhancement is a result of the increased aerogel content or the alternative wool-aerogel composite processing procedure. The BET surface area of the excess aerogel material formed for each sample was measured. The excess aerogel from the porous wool fibres treated for 24 h had a BET surface area of 424.2 m^2.g^{-1}, whereas, the excess aerogel from the porous wool fibres exposed to both the gelation process and the ageing process (88h) had a slightly higher BET surface area of 432.3 m^2.g^{-1}. As the discrepancy between these measurements in marginal, it is likely that the higher BET surface area is due to a greater content of excess aerogel. However, further testing is required to confirm this theory.

EDX analysis was conducted to determine the distribution of silicon on the surface and within the wool fibres (see Figure 6.15). The wool fibres appear to have an even distribution of silicon on the surface of the wool fibres and the excess aerogel is represented by the high concentrated white areas. The EDX analysis of the fibre cross-section demonstrates the effect of excess aerogel present after exposing the wool fibres to both the gelation and the ageing process. This excess aerogel is illustrated by

the highly concentrated white speckles between the wool fibre cross-sections. The white speckles, indicating the presence of silicon, are also displayed within the wool fibre cross-sections. This suggests that the silicon diffuses into the wool fibres and forms aerogel within the pores formed during the chemical modification stages. Interestingly, the wool fibres appear to have a gradient of Si concentration towards the out side surface. The concentration of Si elements appears to reduce towards the centre of the fibres, which could be caused by the diffusion of the sol-gel into the porous wool fibres during the condensation reaction.
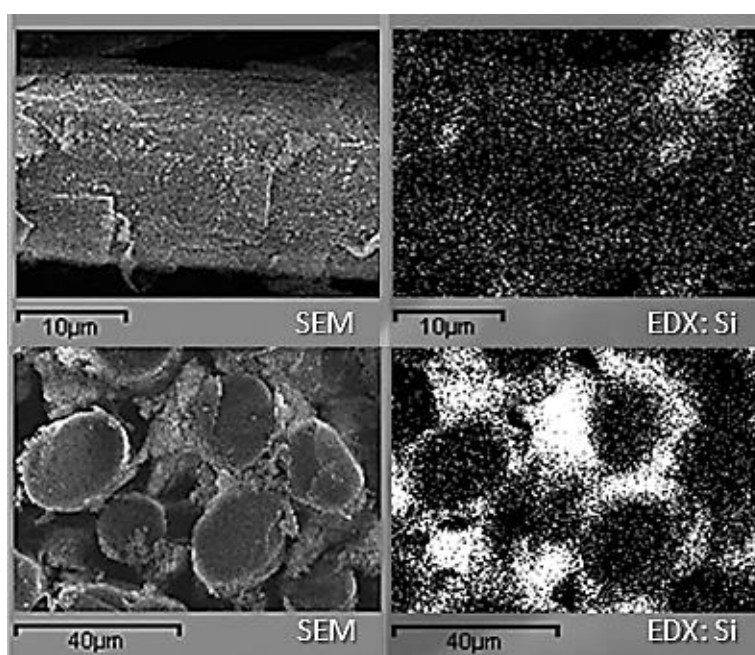
Figure 6.15 - Mapping of Si element distribution in the fibre surface and cross-section of FA-ozone pre-treated worsted woven merino wool fabrics treated with O$_2$ plasma and exposed to the whole aerogel gelation and ageing process (FA-OZ(UHP)-O2Plasma-AG88). Top row: fibre surface. Bottom row: fibre cross-sections

Gravimetric analysis was conducted to investigate the relationship between aerogel content and BET surfaces area for each of the individual fabrics. The porous wool fibres were dried in an oven at 105 °C overnight (circa 16 h) to remove any water residue before being weighed on a balance (accurate to 4 decimal places). After the aerogel treatment the wool fibres were dried again in an oven at 105 °C overnight

before being weighed. The proportion of aerogel within the wool fibres was calculated by the following equation:

$$Proportion\ of\ aerogel = \frac{PWF_{aerogel} - PWF}{PWF_{aerogel}} \times 100$$

$PWF = Mass\ of\ porous\ wool\ fibres\ (g)$

$PWF_{aerogel} = Mass\ of\ porous\ wool\ fibres\ incorporated\ with\ aerogel\ (g)$

The relationship between aerogel content and BET surface area is represented in Table 6.3. It appears that the aerogel content does not directly influence the BET surface area of the material as fabrics FA-O2Plasma-AG24 and FA-OZ(UHP)-O2Plasma-AG24 have much greater aerogel mass proportions than FA-UHP-O2Plasma-AG24 and FA-OZ(UHP)-O2Plasma-AG88; however, their BET surface areas do not vary significantly. Therefore, it is possible that the poor correlation between BET surface area and aerogel content is a result of aerogel quality. The reduction in quality of the aerogel can be caused by aggregation during synthesis (Hüsing and Schubert, 2000), which could reduce the surface area significantly.

One shortfall from this experimental procedure was that the BET surface area was not recorded for the excess aerogels. This would have given an indication of the quality of the aerogel formed for each sample and a better comparison of the different porous wool fibres. Therefore, for further trials and development of wool-aerogel composite materials BET surface areas are required for both the wool-aerogel materials and the excess aerogel for each sample to determine the quality of the aerogel formed.

Table 6.3 - Wool-aerogel composite fabric compositions (24 h exposure to the gelation process) and resultant BET surface areas

Sample code	Proportion of aerogel (%)	BET surface area ($m^2.g^{-1}$)
FA-O2Plasma-AG24	5.13%	21
FA-OZ(UHP)-O2Plasma-AG24	0.45%	18
FA-OZ(UHP)-O2Plasma-AG24	0.60%	22
FA-OZ(UHP)-O2Plasma-AG88	4.03%	32
AG	100 %	424

All the worsted woven fabrics made from merino wool fibres (MWov) were pre-treated with FA for 2 h and were exposed to oxygen plasma with 5 $cm^3.min^{-1}$ oxygen flow rate for 30 min each side.

Despite this shortcoming, it is evident that silicon aerogels can be incorporated into porous wool fibres as well coating the external surface. This novel process for synthesising wool-aerogel composite fibres increases the BET surface area of the fibres, which could improve the adsorption properties of the material. To determine whether these materials are capable of adsorbing VOCs, the DSTL conducted some cyclohexane adsorption testing of the porous wool fibres exposed to the sol-gel for 12 h during the condensation reaction.

6.2.2 Cyclohexane adsorption capacity of porous wool fibres containing silicone aerogels

Cyclohexane is often used as a simulants for VOCs due to its molecular size and extensive use in industrial applications (Wang et al., 2015). The molecular schematic of cyclohexane is detailed within Figure 6.16.
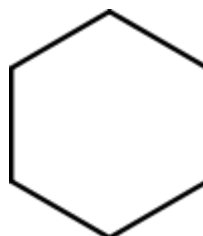
Figure 6.16 - Molecular structure of cyclohexane (C_6H_{12})

To investigate whether the developed wool-aerogel composite material is capable of adsorbing CWA, the cyclohexane adsorption capacity of the fabrics detailed in

Table 6.4 were performed using Dynamic Vapour Sorption (DVS) (Surface Measurement Systems Ltd, Alperton, UK) at the DSTL.

Five plasma treated wool fabrics and their corresponding wool fabric-aerogel composites are detailed in Table 6.4 their aerogel add-on rate and BET surface area were shown.

Table 6.4 - BET surface areas of the wool-aerogel composite fabric composites (12 h exposure to the gelation process)

Sample	Sample code	BET Surface area ($m^2.g^{-1}$)
A	FA-O2Plasma (Control)	0.6
B	FA-O2Plasma-AG12	9.8
C	FA-UHP-O2Plasma (Control)	0.4
D	FA-UHP-O2Plasma -AG12h	3.3
E	FA-OZ(UHP)-O2Plasma (Control)	1.8
F	FA-OZ(UHP)-O2Plasma -AG12h	3.8

All the worsted woven fabrics made from merino wool fibres (MWov) were pre-treated with FA for 2 h and were exposed to oxygen plasma with 5 $cm^3.min^{-1}$ oxygen flow rate for 30 min each side.

Fabrics B, D and F are porous wool fabrics incorporated with aerogels and fabrics A, C and E are control samples without aerogels incorporated. Wool fabric Mwov_F2_O2Plasma_AG12h (sample B) has the greatest BET surface area in comparison with the others two fabrics (D and F) because it has the highest add-on rate of aerogels among these three wool-aerogel composites. It is thus expected to have the greatest cyclohexane adsorption capacity while sample Mwov_F2_UHP96_O2Plasma_AG12h (D) will have lowest one.

Table 6.5 - Aerogel mass percentage composition of porous wool-aerogel composite fabrics

Sample	Sample code	Add-on rate of Aerogels in wool fibres (%)
A	FA-O2Plasma (Control)	-
B	FA- O2Plasma-AG12	5.1
C	FA-UHP-O2Plasma (Control)	-
D	FA-UHP-O2Plasma-AG12	1.1
E	FA-OZ(UHP)-O2Plasma (Control)	-
F	FA-OZ(UHP)-O2Plasma-AG12	1.4

All the worsted woven fabrics made from merino wool fibres (MWov) were pre-treated with FA for 2 h and were exposed to oxygen plasma with 5 $cm^3.min^{-1}$ oxygen flow rate for 30 min each side.

Cyclohexane adsorption isotherms were obtained at 298K, in Dynamic Vapour Sorption (DVS). A small sample (20-30 mg) was loaded into the instrument and heated at 105 °C for 3 hours under nitrogen flow before being cooled back to 298K. The adsorption isotherm was measured by sequentially increasing the relative pressure of cyclohexane. At each relative pressure, the rate of mass uptake was monitored; once it remained below 0.001% / minute for ten minutes, the instrument automatically moved on to the next programmed data point. Cyclohexane BET surface areas were calculated using the instrument software. Also, it is worth noting that cyclohexane BET surface areas will tend to be lower than nitrogen ones obtained in nitrogen adsorption porometry (see Table 6.4). This is because the cyclohexane molecule is larger than nitrogen molecule and therefore cannot access porous morphology as extensively. The shapes of the isotherms indicate a fairly broad pore size distribution.

The cyclohexane isotherms for the three wool fabric-aerogel composites shown in Table 6.5 are detailed in Figure 6.17 to demonstrate the VOC adsorption capability of wool-aerogel composite materials. The three composites incorporated with aerogels demonstrate adsorption capability up to 2.5 w/w% uptake. This indicates that it is possible for one kg of wool fabric-aerogel composite material could adsorb 25 g of cyclohexane. The other three composites without aerogel included showed limited cyclohexane adsorption capability.
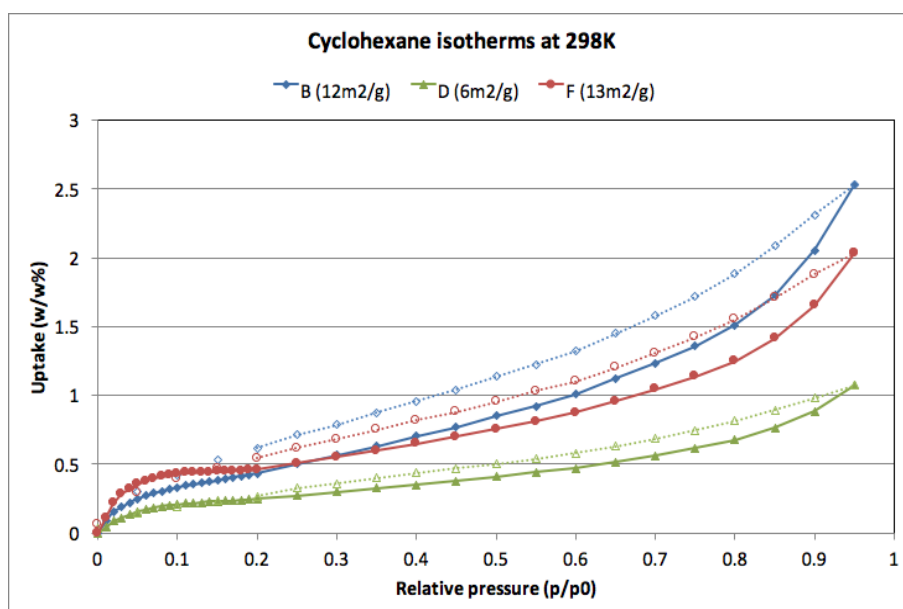
Figure 6.17 - Comparison of cyclohexane isotherms for various wool-aerogel composite fabrics

As expected, the composite FA-O2Plasma-AG12 (B) had the greatest cyclohexane adsorption capacity and FA-UHP-O2Plasma-AG12 (D) had the lowest one. Interestingly, the adsorption capacity of FA-OZ(UHP)-O2Plasma-AG12 (F) was higher than expected as it had a much smaller aerogel add-on rate (1.1 %) in comparison with that of FA-O2Plasma-AG12 (5.1 %). Also, despite having a much lower aerogel add-on rate, FA-OZ(UHP)-O2Plasma-AG12had a greater BET surface area (13 $m^2.g^{-1}$) than FA-OZ(UHP)-O2Plasma-AG12 (12 $m^2.g^{-1}$) measured in DVS. The BET surface area values obtained using DVS are shown in Table 6.6.

Table 6.6 - Aerogel add-on rate in relation to BET surface area for various wool-aerogel composite fabrics

Sample	Sample code	Aerogel mass percentage (%)	BET surface area ($m^2.g^{-1}$)
B	FA-O2Plasma-AG12	5.1	12
D	FA-UHP-O2Plasma-AG12	1.1	6
F	FA-OZ(UHP)-O2Plasma-AG12	1.4	13

FA-OZ(UHP)-O2Plasma-AG12 (sample F) has an apparent enhanced adsorption nature than the other fabrics. As the wool-composite materials were dried in the same

conditions, it is possible that water vapours were adsorbed in the aerogels and have pre-occupied some micropores of the aerogel materials which might cause the discrepancy between the adsorption capacities of the aerogel materials.

As sample FA-O2Plasma-AG12 (B) demonstrated the highest surface area and adsorption capacity measured in a condition of having pre-heated in 105 °C in nitrogen gases for 3 h, its adsorption capacity was measured without any pre-heating to investigate how the composite material would perform in conditions similar to real use in ambient conditions. In order to maintain a stable baseline and to ensure the results are comparable to the pre-heated sample, Mwov_F2_O2P_AG12h (B) was exposed to a passing flow of dry N_2 at ambient temperature, which caused weight loss of the composite materials, suggesting the removal of water residues from the materials.

Outgassing at 25°C results in a slightly lower uptake in adsorption capacity test than that at 105 °C (see Figure 6.18), and the isotherm drops below zero at the end, suggesting some further drying has taken place during the measurement. However, it's worth noting that the outgassing at 25 °C took ~6 hours to stabilise, after which time it had lost just over 6% of its original weight. Therefore, if you use the wool-aerogel composite material without any pre-conditioning, there may be moisture or residual solvent of some kind on the sample, which could reduce the materials capacity to adsorb CWA. Therefore, this demonstrates that wool-aerogel composite fabrics are capable of adsorbing VOCs at conditions similar to environments present during the use of CPC.
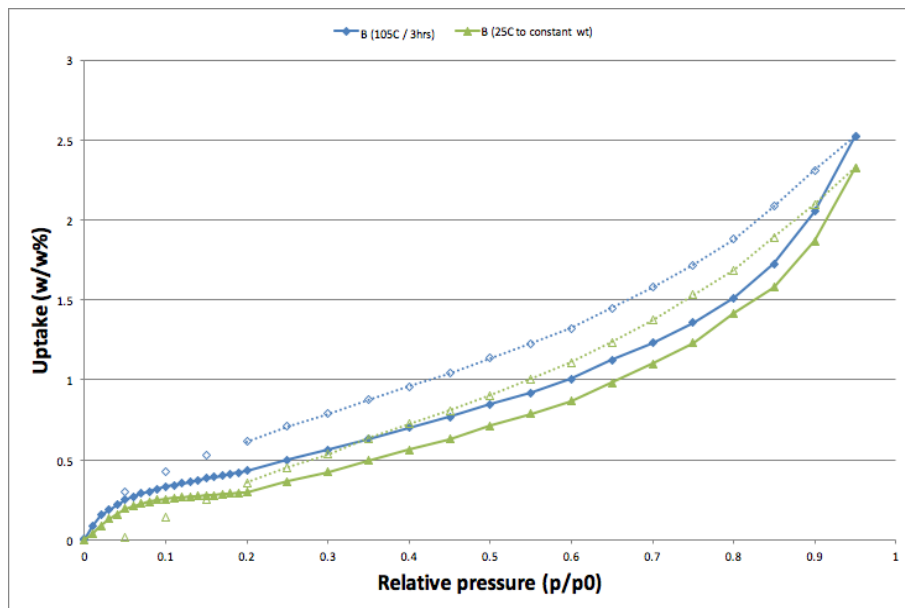
Figure 6.18 - Comparison of cyclohexane isotherms produced by Mwov_F2_O2P_AG12h with outgassing at 25 °C and 105 °C

However, the presence of water residue will be detrimental to the adsorption capacity of the wool-aerogel composite fabrics as the moisture could occupy pore volumes within the materials. Therefore, the DVS instrument was used again to obtain a water isotherm on wool B (see Figure 6.19). This is consistent with the 6-7 % weight loss which was observed after loading the fabrics into the DVS and outgassing them, suggesting they had been in 40-50 % humidity air.
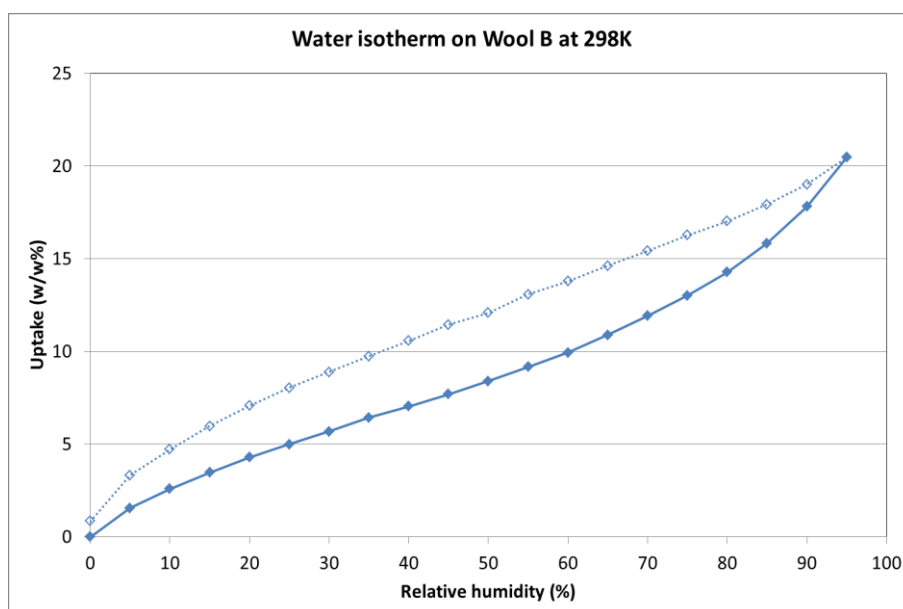
Figure 6.19 - Water isotherm on Mwov_F2_O2Plasma_AG12h at 298K

6.3 Summary

A process for developing and synthesising novel wool-aerogel composite fibres has been investigated. The resultant fibres demonstrated consistent silicon distribution across the external fibre surface and wool fibre cross-sections (EDX), suggesting that aerogel has formed externally and within the internal pores within the chemically modified wool fibres.

Incorporating aerogel into porous wool fibres increased the BET surface area of the wool fibres up to 32 $m^2.g^{-1}$. However, excess aerogel formation was evident on the wool fibre external surfaces after increasing the porous wool fibres exposure duration to the gelation phase (SEM/EDX). It is difficult to differentiate between effectiveness of the different chemically modified wool fibres as the current aerogel incorporation method produces inconsistent aerogel qualities and loadings.

Despite this shortcoming, cyclohexane adsorption capacity testing demonstrated that porous wool fibres containing silicone aerogels are capable of adsorbing VOCs. The three sample variants incorporated within aerogel demonstrated cyclohexane adsorption capability up to 2.5 w/w% uptake, while the control samples without aerogel

did not show any significant adsorption. This indicates that is possible 1 kg of wool-aerogel composite material could adsorb 25 g of cyclohexane (DVS). A similar adsorption capacity was obtained when the DVS testing was conducted without any sample pre-heating process. This demonstrates that wool-aerogel composite fabrics are capable of adsorbing VOCs at conditions similar to environments present during the use of CPC.

Chapter 7 Conclusions and Future Work

7.1 Conclusions

The aim of the study was to develop novel keratin materials with enhanced VOCs adsorption capacities. This was achieved by incorporating nanoporous materials into porous wool fibres, formed by a combination of oxidation treatment and subsequent O_2 plasma treatment. The resultant composite fibres were capable of adsorbing cyclohexane with up to 2.5 w/w% uptake. Also, similar uptakes were evident after testing without any sample pre-heating process. This demonstrates that wool-aerogel composite fabrics are capable of adsorbing VOCs at conditions similar to environments present during the use of CPC.

It is known that keratin is capable of sorption of VOCs; therefore, by partially degrading the complex hierarchical structure of wool fibres to form accessible pore formations, it is possible the adsorption capacity of the material will be enhanced. Degradation techniques investigated included, chemical and physical treatments and their combinations. The individual conclusions from both degradation methodologies and their combinations, as well as, conclusions from the process for developing and synthesising wool-aerogel composite fibres are detailed in the following sections.

Two novel wool fibre products, porous wool fibre and wool-aerogel composite wool fibre, were achieved during this study. Porous wool fibres were developed by a combination of a series of chemical treatments and subsequent selective degradation using either high energy electron beam or oxygen plasma treatments. Wool-aerogel composite fibres having a relatively greater physical adsorption capacities were developed by incorporating silicone aerogels into the internal pores of the above resultant porous wool fibres.

7.1.1 Modification of internal porous structure of wool fibres via various chemical treatments

The effects of several novel chemical treatments and their combinations on the microstructure of wool fibres have been studied in order to improve the adsorption properties of the wool fibres. It was found that meso- and macro-pore formation was evident after wool fibres and fabrics were treated with the following three individual chemical treatments and their consecutive combinations: oxidation (Formic acid treatment, see 4.2.1), oxidation/swelling (Ozone treatment in urea hydrogen peroxide solution, see 4.2.3), and reduction treatments (Sodium hydroxide treatments, section 4.2.4). However, the pore formation after these chemical treatments did not produce significant amount of mesopores and micropores, and the specific surface areas of the resultant keratin materials are not comparable to activated carbon. Despite this shortcoming there was evidence of both accessible and inaccessible pores formed (see objective 1, section 2.2).

1. Internal porous structure of wool fibres were found able to be characterised by using the combination of SEM examination, porosimetry method and pycnometry apparent density measurement (see objective 4, section 2.2). SEM examination of fibre cross-section can determine whether internal pores are formed within the wool fibres; Mercury porosimeter can be used to investigate accessible pore formation. Theoretically, the apparent density of the material should increase if the internal cavities within the fibres become accessible to helium gas molecules used in Pycnometer (Micrometrics Accupyc 1330 Pycnometer). Therefore, the reduction in apparent density could indicate the changes of internal microstructures of the wool fibres and there might be some inaccessible pores (closed pores) created within the wool fibres.

2. Formic acid treatment is found to be an effective method to alter the internal porous structure of wool fibres while formic acid was used to remove the cuticle

layer from wool fibres to expose its cortex layer (see 4.2.1). This research has determined that the FA treatment is capable of introducing macropores within British medium fine hill wool (MFH) and hill wool (H) fibres wool fibres, and the pores appear to be encased by the cuticle or cortex exterior. Macropores formed within cortex is evident within wool fibre cross sections after refluxing in FA at 110 °C for more than 1 hours and the cuticle layer might be some signs of degradation or completely removed (cortex becomes exposed) after 3 hours of treatment. However, extended time duration of FA treatment causes significant fibre shrinkage, brittleness and degradation.

Extensive cortex exposure and internal macro-pore formation within FA treated wool fibres were evident in SEM analysis and demonstrated in the mercury porosimetry analysis.

The two British wool fibres (MFH and H) selected in this study appear to respond differently to the FA treatment. The total pore volume for H wool fibres appears to increase after the 2 h FA treatment, while decreases for the MFH fibres only treated for 1 h.

3. For certain wool fibres, an increase in the number of interstices, inter-fibre segregation and rupture are evident after exposure to urea hydrogen peroxide (**UHP) treatments** (see section 4.2.2). This is believed due to the fact that urea hydrogen peroxide is a swelling-oxidant agent for wool fibres and **UHP treatment** could help breakdown the disulphide bonds between polypeptide chains in the cortical layer of the FA treated wool fibres. The effects of the treatments are inconsistent across the range of wool fibres treated, suggesting that different wool fibres have different reactions to consecutive FA and UHP treatments of identical time durations.

It was also found that the wool fibres after extended time duration of UHP treatment have smaller apparent density; this suggested that there was either a decrease in the amount of accessible pores or an increase of closed pores within

the wool fibres. Interestingly, consecutive FA-UHP treatments have an effect on the wool fibre internal microstructure, apparent density and specific surface area, these fibres demonstrated similar trends for both the apparent density and BET measurements. An increased number of interstices and inter-fibre segregation, and in some cases, fibre rupture are evident after FA-UHP treatment. However, it is unclear whether these changes are due to the FA pre-treatment or a combination of the FA-UHP treatment. Also, the BET results demonstrated a gradual reduction in surface area after each consecutive chemical treatment (i.e. FA and UHP treatment). This suggests the wool fibres swell as a result of the treatment, which could impede the access of the internal pore formation.

For both British MFH and H wool fibres after FA treatment, their apparent density values reduced after UHP treatments; however, their AD is greater than that of the original scoured wool. This suggests that inaccessible pores are created as a result of the treatment novel **ozone treatment** in UHP solution (see section 4.2.3), which has been developed by combining two experimental procedures of UHP treatment and ozone treatment in water (Ward and Mao, 2014). In this study, the effect of swelling/oxidising treatment by using ozone treatment on the porous structure of MFH fibres in both urea hydrogen peroxide and water were discussed and summarised.

It is interestingly noticed that, among all of the ozone treatments of wool fibres, both wool fibres with and without FA pre-treatment after ozone-UHP treatment process for 96 hours demonstrate significant increases in pore volume for macropores between approximately 1.3 – 2 µm in porosimetry results. This suggests that wool fibres swells significantly after the extended durations (i.e. 96 hours) of exposure in ozone-UHP solution, this might be due to the expansion of the smaller pores formed in previous treatments.

When analysed using mercury porosimetry, mesopore (2-50nm) formation in wool fibres without FA pre-treatment appears to be evident after ozone treatment in

water for 24 hours and 96 hours, as well as in UHP for 24 hours. Contrary to this, when examined using SEM, the wool fibres treated with ozone in H_2O for 24 h did not show any evidence of internal pore formation. However, there were signs of slight cuticle separation. Therefore, the increase in meso-pore formation for wool fibres without FA pre-treatment exposed to ozone-water and ozone-water could be attributed to the increase of the volume of the pores between cuticles. It is possible that the pore volumes measured in mercury porosimetry include the changes of the pores existing between cuticles when the cuticles become partially degraded, cleaved or macro-pore formed in cortex become exposed. When this treatment was extended to 96 h, there was evidence of internal pore formation and cuticle degradation. Similar characteristics were observed when the wool fibres were treated with ozone-UHP for 24 h; however, the sizes of internal pores formed were significantly smaller.

This phenomenon is also evident in the ozone treatment of FA pre-treated fibres as both 24 h ozone-water and ozone-UHP treated fibres demonstrate meso-pore formation; whereas, fibres treated in ozone-water solution for 96 h contain little accessible mesopores when analysed using mercury porosimetry. This suggests that wool fibres experienced swelling and meso-pore formation during their extended exposure to the ozone-UHP process.

It is apparent that, regardless of whether the wool fibres are pre-treated with FA higher total pore volumes are evident in all of wool fibres after both ozone-water or ozone-UHP treatments. Also, the total pore volumes increase with the increases of time duration for both ozone-water and ozone-UHP treatments.

Additionally, it is noticed that fibres subjected to ozone-water and ozone-UHP without FA pre-treatments have higher total pore volumes than fibres with FA pre-treatment despite a proportion of the increase of pore volume during the ozone treatment might be due to the increase of the volume of the pores between

235

cuticles. It is also noticed (SEM) that wool fibre cuticles were significantly removed with the extended exposure to the ozone treatment process.

A significant proportion of the total pore volume for wool fibres (without FA pre-treatment) treated with ozone-H_2O for 24 and 96 h, and ozone-UHP for 24 h consists of mesopores (3-50 nm). Similarly, a significant proportion of the total pore volume for FA pre-treated wool fibres treated with ozone-solutions for 24 h consists of pores with throat diameters between 3nm–50 nm. However, by extending the treatment duration to 96 hours for both ozone treatments in water and UHP solutions, the mesopores seem to completely disappear and the total pore volume consists of pores within the range 50 nm – 2 µm in throat diameter. This suggests that the smaller mesopore formed after the 24 h treatment swell into macropores after extending the treatment to 96 h.

4. **Sodium hydroxide treatment** (see section 4.2.4) of raw and FA pre-treated British hill (MFH) wool fibres with a lower (1%) and higher (5%) concentrations for different time durations were conducted to investigate the pore formation within wool fibres. The sodium hydroxide treatment is unique and has been proved to be an effective way of forming macro- and mesopores within the wool fibres, particularly for fibres pre-treated with FA (cuticle removed). It is evident that the NaOH solutions degrade the wool fibres and the concentration and exposure time are key parameters for modifying the pore formation within wool fibres.

For wool fibres without the FA pre-treatment, the fibres treated with alkali solutions of lower concentrations have a greater total pore volume and it is possible that the total pore volume increases with time durations of the treatment; however, further treatments with varying exposure durations would be required to evaluate this theory. The fibres treated with a greater concentrated NaOH solution appear to have a different effect on the wool fibres as increasing the treatment time duration appears to reduce the total pore volumes.

Similar to the wool fibres without FA pre-treatment, the treatment of FA pre–treated wool fibres with lower concentration of NaOH appear to be an effective way of introducing macro- and mesopores within the British hill wool (H) fibres. Fibrillation was also evident for FA pre-treated fibres exposed to NaOH solutions. Both meso- and macropores were evident as the fibrils began to separate. The FA pre-treated wool fibres experienced significant degradation and partial dissolution as a result of exposure to higher concentrated NaOH solutions, particularly beyond 1 min treatment durations. However, macro- and meso-pore formation was evident for FA pre-treated fibres exposed to 0.5 and 1 min treatment durations when analysed using mercury porosimetry. Similar to the lower concentrated treated fibres it was proposed that these pore formations are the result of partial fibre fibrillation.

7.1.2 Formation of porous wool fibres using physical selective degradation processes

To open and expose inaccessible pores formed within wool fibres after various chemical treatments (see Chapter 4), the effect of subsequent selective degradation techniques were investigated. Pore formation in selective degradation of wool fibres were discovered in both using electron beam irradiation in SEM and plasma irradiation using low pressure plasma in air and O_2 gases (see Chapter 5).

It is found that pore formation in wool fibres is possible using both of the two techniques on both raw and chemically pre-treated wool fibres. The electron irradiation technique is capable of degrading limited surface areas of the wool fibres exposed; and sufficient electron beam intensity and exposure durations are required to form pores on the chemically modified wool fibres (see section 5.2). The plasma irradiation technique is capable of forming porous morphological features in wool fibres in a larger scale.

Different porous morphological features were evident after treating the wool fabrics with O_2 plasma, by varying the O_2 plasma treatment duration and chemical pre-treatment (see section 5.2).

Extending the exposure duration appears to increase the pores to macropores, while reducing the number of pores present, which suggests the pores expand and merge as a result of the extended O_2 plasma exposure. Also, reticulated pore structures are evident after exposing the chemically modified wool fibres to O_2 plasma for a longer duration; however, the depths of the pore matrices are unclear. The specific surface area significantly increases by exposing the chemically modified wool fibres to O_2 plasma, particularly for longer exposure durations. Moreover, by varying these parameters, it is possible the porosity of the wool fibres could be tailored depending on the desired function or application.

Macro-pore formation by selective degradation was evident for wool fibres pre-treated with FA and ozone in UHP solution for 24 h and 96 h, suggesting the fibres partial fibrillate after the chemical treatments. However, an additional treatment, such as selective degradation with high electron impact is required to complete the fibrillation of wool fibres. It is possible that the consecutive chemical treatments are capable of forming inaccessible pores formations within the fibres; however, an additional physical treatment, such as high energy impact is required to expose these internal features, thus improving the adsorption capability of the wool fibres.

Finally, this technique could be used for forming keratin scaffolds for the incorporation of other functional materials.

7.1.3 Pore formation on wool fibres using high energy particle impacts

Pore formation and reticulated pore structures are evident after exposing the FA and FA-ozone-UHP pre-treated wool fibres to high frequency electron beams and low pressure plasmas.

The main difference between the treatments is the electron beam used in SEM system degrades smaller areas of the wool fibres exposed, while the plasma treatment process is capable of modifying a much larger population of exposed fibres, producing uniform

surface etching/ pore formation. In addition, the extent of the pore formation or fibrillation caused by the chemical pre-treatment processes are evident after exposing the FA and Ozone-UHP pre-treated wool fibres to both selective degradation treatments.

Selective degradation by SEM is capable of forming pores with diameters < 1 μm. It was determined that system parameters such as voltage, beam size, exposure time duration, spot size and working distance have an effect on the pore formation within the raw and chemically treated wool fibres. Also, it is possible the electron beam is capable of causing internal shrinkage of the wool fibres.

For FA and FA-Ozone-UHP modified wool fibres exposed to low pressure plasma treatments, reducing the oxygen pressure within the system increased the etching intensity/ pore formation in wool fibres. However, increasing oxygen flow increased the pressure within the chamber. Therefore, there is a trade-off between oxygen concentration/ oxygen flow and reduced pressure for having sufficient etching intensity/ pore formation. By extending the treatment duration for the FA pre-treated MWov fabrics and subsequently ozone treated in UHP for 96 h a reticulated macro-porous structure was evident. This combination of chemically treatment, followed by a plasma treatment increased the BET surface area of the fibres to 2.03 $m^2.g^{-1}$ (see objective 2, section 2.2). However, this surface area is significantly lower than common activated carbon adsorbents which have a specific surface area of 800-1500 $m^2.g^{-1}$ (Bansal and Goyal, 2005). Also, Hayes (2002) documented ACF with surface areas as high as 2500 $m^2.g^{-1}$ when measured using the same BET methodology. Therefore, an alternative solution to improving the adsorption capacity of keratin fibres is incorporating nano-porous materials within porous wool fibres.

7.1.4 Incorporation of nano-porous aerogel inside macropores

Novel wool-aerogel porous composite fibres were produced (see objective 3, section 2.2). The wool fibres exposed to either the condensation reaction or the whole

aerogel gelation and ageing process have consistent silicon distribution across the external fibre surface. Also, there is evidence of silicon within the wool fibre cross-sections, suggesting that aerogel has formed within the internal pores formed in the above chemically modified wool fibres although excess aerogel formation was evident on the wool fibre external surfaces after increasing the porous wool fibres exposure duration to the gelation phase.

VOCs adsorption capacity of the porous wool fibres containing silicone aerogels were tested by using cyclohexane adsorption capacity test and Dynamic vapour sorption (DVS) test. It was shown that the three wool-aerogel composite fibres tested have demonstrated adsorption capability up to 2.5 w/w% uptake, while the control samples without aerogel shows little adsorption capacity. A similar adsorption capacity was obtained when the DVS testing was conducted without any sample pre-heating process. This demonstrates that wool-aerogel composite fabrics are capable of adsorbing VOCs at conditions similar to environments present during the use of CPC.

7.2 Future work

7.2.1 Enhancing the adsorption capacity of wool fibres

Although this research demonstrated wool fibres could be modified to adsorb a greater capacity of VOCs. This was ultimately achieved by incorporating a nanoporous material into porous wool fibres. Due to the unique hierarchical structure of wool fibres it is possible the wool fibres could be selectively degraded to form reticulated pore structures, which could enhance the adsorption capacity without the need to introduce nanoporous materials, such as silicon aerogel.

The following sections propose alternative investigations for modifying wool fibres to enhance the adsorption capacity of wool fibres.

7.2.1.1 Sequence of chemical treatments

Within Chapter 4, pore formation was evident when the British wool fibres were exposed to ozone in UHP for both 24 and 96 h treatment durations despite the cuticle remaining intact. Therefore, it might be possible that by then treating the wool fibres with FA after the ozone-UHP treatment, internal pore formations might then be exposed by removing or partially removing the cuticles.

7.2.1.2 Investigate the effect of oxygen plasma on the pore formation within alternative chemical pre-treated wool fibres and fabrics

The selective degradation of wool fibres by electron beam irradiation and low pressure plasma demonstrated some interesting morphological modifications, particularly after oxidation/ swelling chemical treatments (FA-OZ(UHP)).Therefore, the relationship between chemical pre-treatment and selective degradation by high energy particle bombardment could be explored further. For instance, the effect of alternative chemically pre-treatments could be explored, such as reduction treatments (e.g., NaOH treatment) or alternative oxidation treatments.

7.2.1.3 Popping popcorn mechanism using microwave radiation

In section 3.5.1, raw wool fibres, sized fibres and partially gelated fibres were subjected to a microwave treatment to investigate the effect of microwave irradiation on the physical property, chemical structure, and surface morphological structure of wool fibres. This treatment was also applied to determine whether the "popping popcorn" mechanism could be applied to form pores within the wool fibres. Moisture within kernel is superheated, which provides internal pressure. This causes the pericarp to rupture and the pressure forces the internal features of the kernel to expand, forming a reticulated porous structure. Currently, no apparent cracking of cuticle layer has been observed and the porosimetry analytical techniques are unable to detect porous structure of the fibres containing sizing agents. Therefore, investigations using these

methodologies were discontinued; however, this concept could be investigated as further work.

To replicate the popping popcorn mechanism observed by corn pericarps during domestic microwave treatment. The raw, chemically modified or gelatinised or partially-gelatinised wool fibres could be encased within polymers with high melting points. Then the capsule could be subjected to super-heating by microwave radiation to increase the pressure within the enclosed cavity until rupture.

7.2.2 Investigate the moisture management properties of the resultant wool-aerogel composite material

In this study, forming porous structures within wool fibres to enhance the adsorption capacity was the main focus; further investigations are needed to explore the effect of the porous structures formed and the nanoporous materials incorporated on the thermal and moisture management properties of the resultant porous wool fibres and fabrics.

7.2.3 Alternative applications for porous wool fibres and wool-aerogel composite materials

Aerogel materials and wool fabrics are both used as insulation materials, due to their low thermal conductivity properties (Mao and Russell, 2007). Aerogel materials have the lowest thermal conductivity (0.017 $W.m^{-1}.K^{-1}$) properties of any known material, in fact their thermal conductivity is lower than still air (0.025 $W.m^{-1}.K^{-1}$) (Du, 2014). However, commercial textile-aerogel composite materials, including Aspen aerogel blankets (Spaceloft, Cryogel and Pyrogel) and Cobot aerogel blankets (Thermal Wrap) are more suitable for use in construction materials than in clothing. This is due to the fact that the assembly is subject to the mechanical forces during use that break the aerogel component into smaller particles (Du, 2014). Also, textile-aerogel composites are usually composed of glass, ceramic or carbon fibres (Kim, C. et al., 2008; Yuan,

2012; Feng and Zhang, 2012). Therefore, the thermal insulation properties of the resultant wool-aerogel composite material could be investigated for both garment and construction insulation applications.

References

A. Brewer, S., C. Apperley, D. and A. Stone, C. 2007. *Nanoheterogeneity of a Polymer Blend and the Effect of Humidity as Characterized by Solid-State NMR.*

Abbott, W.F. 1962. *USP 3053775.*

Abrams, L. and Corbin, D.R. 1995. Probing Intrazeolite Space. In: Herron, N. and Corbin, D.R. eds. *Inclusion Chemistry with Zeolites: Nanoscale Materials by Design.*   Springer - Science + Business Media, B. V.

AccuPyc 1330 Pycnometer 2001. Operator's Manual V3.03. Micromeritics Instrument Corporation.

Adams, L.B., Hall, C.R., Holmes, R.J. and Newton, R.A. 1988. An examination of how exposure to humid air can result in changes in the adsorption properties of activated carbons. *Carbon.* **26**(4), pp.451-459.

Ahmed, I., Khan, N.A., Hasan, Z. and Jhung, S.H. 2013. Adsorptive denitrogenation of model fuels with porous metal-organic framework (MOF) MIL-101 impregnated with phosphotungstic acid: effect of acid site inclusion. *J. Hazard. Mater.*, pp.37-44.

Alexander, P., Hamilton, L.D.G. and Stacey, K.A. 1960. Irradiation of proteins in the solid state I. Aggregation and disorganization of secondary structure in bovine serum albumin. *Radiation Research.* **12**, pp.510-525.

Alexander, P. and Hudson, F. 1954. Wool - Its Chemistry and Physics. *Chapman & Hall.*

Alexander, P. and Hudson, F. 1963. The Morphological Structure. *Wool its Chemistry and Physics.*   Chapman and Hall Ltd.

Allen, E. and Alexander, P. 1961. An effect of ionizing radiations on the hydrogen bonds in wool. *Radiation research.* **15**, pp.390-399.

Aluigi, A., Tonetti, C., Rombaldoni, F., Puglia, D., Fortunati, E., Armentano, I., Santulli, C., Torre, L. and Kenny, J.M. 2014. Keratins extracted from Merino wool and Brown Alpaca fibres as potential

fillers for PLLA-based biocomposites. *Journal of Materials Science.* **49**(18), pp.6257-6269.

Alzaga, R., Pascual, E., Erra, P. and Bayona, J.M. 1999. Development of a novel supercritical fluid extraction procedure for lanolin extraction from raw wool. *Analytica Chimica Acta.* **381**(1), pp.39-48.

Arai, K., Kameda, T. and Ichikawa, R. 1990. Mechanical properties of regenerated keratin fibres under processing conditions. In: *8th International Wool Textile Research Conference, Christchurch, New Zealand.* Wool Research Organisation of New Zealand (Inc), p.449.

Arifoglu, M., Marmer, W.N. and Carr, C.C. 1989. Effect of Urea on Bleaching Wool with Hydrogen Peroxide Under Alkaline and Acidic Conditions. *Textile Research Institute.* **89**, pp.425-431.

Armadillo. 2017. *ARMATECH: 303 - WHAT IS THE MOST EFFECTIVE BASELAYER SYSTEM FOR SAFETY, PERFORMANCE AND WELLBEING?* [Online]. [Accessed 23rd January]. Available from: https://armadillomerino.com/blogs/armatech/2301-armatech-303-what-is-the-most-effective-baselayer-system-for-safety-performance-and-wellbeing

Ashquith, R.S. 1977. *Chemistry of Natural Protein Fibres.* Belfast, Northern Ireland: John Wiley & Sons.

Astbury, W.T. and Woods, H.J. 1933. X-ray studies of the structure of hair, wool and related fibres. II. The molecular structure and elastic properties of hair keratin. *Phil. Trans. Roy. Soc.* **A232**, pp.333-394.

Atav, R. and Yurdakul, A. 2011. Effect of the ozonation process on the dyeability of mohair fibres. *Coloration Technology.* **127**(3), pp.159-166.

Bajgar, J. 2004. Organophosphates/nerve agent poisoning: Mechanism of action, diagnosis, prophylaxis, and treatment. *Adv Clin Chem.* **38**, pp.151-216.

Bajgar, J. 2005. Complex view on poisoning with nerve agents and organophosphates. *Acta Medica (Hradec Kralove)* **48**, pp.3-21.

Bajgar, J., Fusek, J., Kassa, J., Kuca, K. and Jun, D. 2009. Chemical aspects of pharmacological prophylaxis against nerve agent poisoning. *Curr Med Chem.* **16**, pp.2977–2986.

Bansal, R.C. and Goyal, M. 2005. Activated Carbon and Its Surface Structure. *Activated Carbon Adsorption.* CRC Press, pp.1-65.

Barritt, J. and Elsworth, F.F. 1948. *J. S. D. C.* **64**, p19.

Barthomeuf, D. 1996. Basic Zeolites: Characterization and Uses in Adsorption and Catalysis. *Catalysis Reviews.* **38**(4), pp.521-612.

Bauer, U. 2012. *Method for manufacturing an aerogel-containing composite and composite produced by that method*.

Bellamy, A.J. 1994. Reaction of gaseous sulfur mustard with zeolite 13X. *J. Chem. Soc., .* (Perkin Trans. 2), pp.2325-2328.

Benli, H. and Bahtiyari, M.İ. 2015. Combination of ozone and ultrasound in pretreatment of cotton fabrics prior to natural dyeing. *Journal of Cleaner Production.* **89**(0), pp.116-124.

Biswas, A., Bayer, I.S., Biris, A.S., Wang, T., Dervishi, E. and Faupel, F. 2012. Advances in top–down and bottom–up surface nanofabrication: Techniques, applications & future prospects. *Advances in Colloid and Interface Science.* **170**(1–2), pp.2-27.

Bottani, E.J. and Tascón, J.M.D. 2008. *Adsorption by Carbons - Novel Carbon Adsorbents*. Elsevier. Available from: http://app.knovel.com/hotlink/toc/id:kpACNCA005/adsorption-by-carbons

Boucher, E.A., Cooper, R.N. and Everett, D.H. 1970. Preperation and studies of Sarin-carbon fibres. *Carbon.* **8**(5), pp.597-605.

Bradbury, J.H. 1973. The Structure and Chemistry of Keratin Fibres. In: Anfinsen, C.B., et al. eds. *Advances in Protein Chemistry.* New York: Academic Press, pp.111-211.

Bradbury, J.H. and Peters, D.E. 1972. Method for the Complete Removal of Cuticle from Wool Fibers. *Textile Research Journal.* **42**(4), pp.248-250.

Bradley, R.H., Smith, M.W., Andreu, A. and Falco, M. 2011. Surface studies of novel hydrophobic active carbons. *Applied Surface Science.* **257**(7), pp.2912-2919.

Brewer, S., Stone, C., Willis, C. and Beadle, B. 2004. *Novel uses of polymers*. Google Patents. Available from: https://www.google.com/patents/US20040166350

Brown, R.B. 1928. *J. Soc. Dyers and Colourists.* **44**, p230.

BS ISO 9277. 2010.

BSISO15901-1. 2005. *Pore size distribution and porosity of solid materials by mercury porosimetry and gas adsorption.*

BSISO15901-2. 2006. *Pore size distribution and porosity of solid materials by mercury porosimetry and gas adsorption.*

Buckling, S. 1943. *Medical manual of chemical warfare.* New York: Chemical Publishing Co.

Budd, P.M., Butler, A., Selbie, J., Mahmood, K., McKeown, N.B., Ghanem, B., Msayib, K., Book, D. and Walton, A. 2007. The potential of organic polymer-based hydrogen storage materials. *Phys. Chem. Chem. Phys.* **9**, pp.1802-1808.

Budd, P.M., Elabas, E.S., Ghanem, B.S., Makhseed, S., McKeown, N.B., Msayib, K.J., Tattershall, C.E. and Wang, D. 2004a. Solution-processed, organophilic membrane derived from a polymer of intrinsic microporosity. *Adv. Mater.* **16**, pp.456-459.

Budd, P.M., Ghanem, B.S., Makhseed, S., McKeown, N.B., Msayib , K.J. and Tattershall, C.E. 2004b. Polymers of intrinsic microporosity (PIMs): robust, solution-processable, organic nanoporous materials. *Chem. Commun.*, pp.230-231.

Budd, P.M., McKeown , N.B. and Fritsch, D. 2006. Polymers of Intrinsic Microporosity (PIMs): High Free Volume Polymers for Membrane Applications. *Macromol. Symp.* **245-246**, pp.403-405.

Budd, P.M., Msayib, K.J., Tattershall, C.E., Ghanem, B.S., Reynolds, K.J., McKeown, N.B. and Fritsch, D. 2005. Gas separation membranes from polymers of intrinsic microporosity. *J. Membr. Sci.* **251**, pp.263-269.

BWMB. 2014. *British Sheep Breeds and Their Wool.* [Online]. [Accessed 02/08/2014]. Available from: http://www.britishwool.org.uk/factsheet1.asp?pageid=163

Cameron, D. and Clegg, N. 2010. *A Strong Britain in an Age of Uncertainty: The National Security Strategy.* HM Government.

Causer, S.M. 1993. *Absorption of Nitrogen Dioxide by Carpets.* Christchurch: Wool Research Organisation of New Zealand.

Caven, B. 2010. *Exploring a Textile Route to Mimicking the Adhesion Properties of the Gecko Foot.pdf>.* PhD thesis, University of Leeds.

Cavka, J.H., Jakobsen, S., Olsbye, U., Guillou, N., Lamberti, C., Bordiga, S. and Lillerud, K.P.J. 2008. A new zirconium inorganic building brick forming metal organic frameworks with exceptional stability. *Am. Chem. Soc.* **130**, p13850.

CDC. 2014. *Protective Clothing and Ensembles.* [Online]. Available from: http://www.cdc.gov/niosh/topics/protclothing/

CFW. 2017. *About us.* [Online]. Available from: http://www.campaignforwool.org/about-wool/

Cockett, K.R.F., Kilpatrick, D.J., Rattee, I.D. and Stevens, C.B. 1971. Effect of Urea on the Dyeing of Wool at Low Temperatures. *Appl. Polymer Symp.* **18**(1), pp.409-418.

Cockett, K.R.F., Rattee, I.D. and Stevens, C.B. 1969. Some Observations on the Effect of Urea on the Dyeing Behaviour of Wool at Low Temperatures. *J. Soc. Dyers and Colour.* **85**, pp.461-468.

Cohen, A.C., Johnson, I. and Pizzuto, J.J. 2012. Natural and Manufactured Fibres. *Fabric Science.* Fairchild Books, pp.43-58.

Compton, J.A.F. 1987. Military chemical and biological agents. *The Telford press.* p111.

Croddy, E., Armendariz, C.P. and Hart, J. 2002. *Chemical and biological warfare.* New York: Springer-Verlag.

CSD. 2015. *How many MOFs are there in the CSD?* [Online]. [Accessed 16 Nov]. Available from: http://www.ccdc.cam.ac.uk/support-and-resources/support/case/?caseid=9833bd2c-27f9-4ff7-8186-71a9b415f012

Cucinell, S.A. 1974. Review of the toxity of long-term phosgene exposure. **28**.

Cui, Y., Yue, Y., Qian, G. and Chen, B. 2011. Luminescent functional metal-organic frameworks. *Chem. Rev.* **2**(112), pp.1126-1162.

de Saussure, N.T. 1982. Cited in Gregg SJ, Sing KSW: 2nd ed.; Academic Press, London. *Gilbert's Ann. Physik.* **47**(Adsorption, surface area and porosity), p113.

DeCoste, J.B. and Peterson, G.W. 2014. Metal–Organic Frameworks for Air Purification of Toxic Chemicals. *Chemical Reviews.* **114**(11), pp.5695-5727.

Denby, E.F. 1983. The Effect of Relaxation, Set and Hygral Expansion of Single Wool Fibres on Finishing Wool Fabrics. In: Postle, R., et al. eds. *Objective Evaluation of Apparel Fabrics.* Osaka: Textile Machinery Society of Japan, pp.423-432.

Di Modica, G. and Marzona, M. 1968. Effects of Ionizing Radiations on Wool. Part II: Chemical Modifications of Keratins. *Textile Research Journal.* pp.1208-1209.

Du, M. 2014. *The Thermal Insulation Properties of a Flexible Methyltrimethoxysilane (MTMS) Based Silicon Aerogel and its Application on Aerogel-spacer Fabric Composites*. PhD thesis, University of Leeds.

DuPont. 2014. *Tychem® garments.* [Online]. [Accessed 09/07/2014]. Available from: http://www.dupont.com/products-and-services/personal-protective-equipment/chemical-protective-garments/brands/tychem.html

Duren, T., Bae, Y.S. and Snurr, R.Q. 2009. Using molecular simulation to characterise metal-organic frameworks for adsorption applications. *Chem. Soc. Rev.* **38**, pp.1237-1247.

Eddaoudi, M., Kim, J., Rosi, N., Vodak, D., Wachter, J., O'Keeffe, M. and Yaghi, O.M. 2002. Systematic design of pore size and functionality in isoreticular MOFs and their application in methane storage. *Science.* **5554**(295), pp.469-472.

Egerton, R.F. 2005. *Physical principles of electron microscopy : an introduction to TEM, SEM, and AEM.* Springer.

Everett, D.H. 1972. Manual of Symbols and Terminology for Physicochemical Quantities and Units, Appendix II: Definitions,

Terminology and Symbols in Colloid and Surface Chemistry. *Pure Appl. Chem.* **31**, p577.

Everett, D.H. and Powl, J.C. 1976. Adsorption in slit-like and cylindrical micropores in the henry's law region. A model for the microporosity of carbons. *Journal of the Chemical Society, Faraday Transactions 1: Physical Chemistry in Condensed Phases.* **72**(0), pp.619-636.

Fajula, F. and Plee, D. 1994. Application of molecular sieves in view of cleaner technology. Gas and liquid phase separations. In: J.C. Jansen, M.S.H.G.K. and Weitkamp, J. eds. *Studies in Surface Science and Catalysis.* Elsevier, pp.633-651.

Fan, J., Yu, W.D. and Chem Ind, P. 2007. *A rapid method for complete removal of cuticle from Merino wool fibers.* Beijing: Chemical Industry Press.

Farha, O.K., Eryazici, I., Jeong, N.C., Hauser, B.G., Wilmer, C.E., Sarjeant, A.A., Snurr, R.Q., Nguyen, S.T., Yazaydın, A.Ö. and Hupp, J.T. 2012. Metal-organic framework materials with ultrahigh surface areas: is the sky the limit? *J Am Chem Soc.* **36**(134), pp.15016-15021.

Farha, O.K., Spokoyny, A.M., Mulfort, K.L., Hawthorne, M.F., Mirkin, C.A. and Hupp, J.T. 2007. Synthesis and Hydrogen Sorption Properties of Carborane Based Metal-Organic Framework Materials. *J. Am. Chem. Soc.* **129**, p12680.

Feng, J. and Zhang, C. 2012. Carbon fibre reinforced carbon aerogel composites composites for thermal insulation prepared by soft reinforcement. *Material Letters.* **67**, pp.266-268.

Férey, G., Mellot-Draznieks, C., Serre, C., Millange, F., Dutour, J., Surblé, S. and Margiolaki, I. 2005. A chromium terephthalate-based solid with unusually large pore volumes and surface area. *Science.* **5743**(309), pp.2040-2042.

Férey, G., Serre, C., Mellot-Draznieks, C., Millange, F., Surblé, S., Dutour, J. and Margiolaki, I. 2004. A Hybrid Solid with Giant Pores Prepared by a Combination of Targeted Chemistry, Simulation, and Powder Diffraction. *Angewandte Chemie International Edition.* **43**(46), pp.6296-6301.

Flanigen, E.M. 1980. Molecular sieve zeolite technology - the first twenty-five years. *Pure Appl. Chem.* **52**(9), pp.2191-2211.

Fletcher, A.J., Uygur, Y. and Thomas, K.M. 2007. Role of surface functional groups in the adsorption kinetics of water vapor on microporous activated carbons. *Journal of Physical Chemistry C.* **111**(23), pp.8349-8359.

Fontana, F. 1777. Cited in Gregg SJ, Sing KSW: 2nd ed.; Academic Press, London. *Memorie Mat. Fis. Soc. Ital. Sci.* **1**(Adsorption, surface area and porosity), p679.

Fricke, A. and Fojan, P. 2014. *Polymer fibres comprising aerogel and method for production.*

Furukawa, H., Cordova, K.E., O'Keeffe, M. and Yaghi, O.M. 2013. The chemistry and applications of metal-organic frameworks. *Science.* **6149**, p341.

Ganesan, K., Raza, S.K. and Vijayaraghavan, R. 2010. Chemical warfare agents. *J Pharm Bioallied Sci.* **3**, pp.166-178.

Ghosh, A., Clerens, S., Deb Choudhury, S. and Dyer, J. 2013. Thermal effects of ionic liquid dissolution on the structures and properties of regenerated wool keratin. *Polym. Degrad. Stab.*

Ghosh, A. and Collie, S.R. 2014. Keratinous Materials as Novel Absorbent Systems for Toxic Pollutants. *Defence Science Journal.* **64**(3), pp.209-221.

Giesche, H. 2006. Mercury Porosimetry: a General (Practical) Overview. *Part. Part. Syst.* **23**, pp.1-11.

Glass, W.I., Harries, W.E. and Whitlock, R.M. 1971. Phosgene poisoning: A case report. *N Z Med J.* **74**, pp.386-389.

Glover, T.G., P., G.W., Schindler, B.J., Britt, D. and Yaghi, O. 2011. MOF-74 building unit has a direct impact on toxic gas adsorption. *Chemical Engineering Science.* **66**, pp.163-170.

Goldstein, J. 2003. *Scanning electron microscopy and x-ray microanalysis.* Kluwer Adacemic/Plenum Pulbishers.

Graham, W.G. 2007. The physics and chemistry of plasmas for processing textiles and other materials. In: Shishoo, R. ed. *Plasma*

technologies for textiles. Cambridge: Woodhead Publishing Limited, pp.3-24.

Gregg, S.J. and Sing, K.S.W. 1982. *Adsorption, Surface Area and Porosity.* London: Academic Press Inc. (London).

Gültekin, I. and Ince, N.H. 2006. Degradation of aryl-azo-naphthol dyes by ultrasound, ozone and their combination: Effect of α-substituents. *Ultrasonics Sonochemistry.* **13**(3), pp.208-214.

Haly, A.R. 1974. Thermal analysis and flame resistance of wool. *Textile Research Journal.* **44**(8), pp.636-637.

Han, S.S., Mendoza-Cortes, J.L. and Goddard III, W.A. 2009. Recent advances on simulation and theory of hydrogen storage in metal–organic frameworks and covalent organic frameworks. *Chem. Soc. Rev. .* **28**, pp.1460-1476.

Hayes, J.S.J. 1994. Activated Carbon Fibers and Textiles. *Kynol Europa GmbH.* pp.1-20.

Hayes, J.S.J. 2002. Nanostructure of Activated Carbon Fibres and Kinetics of Adsorption/ Desorption. *Air & Waste Management Association, 95th Annual Conference and Exhibition.*

Hearle, J.W.S. 2000. A critical review of the structural mechanics of wool and hair

fibres. *International Journal of Biological Macromolecules.* **27**, pp.123- 138.

Hearle, J.W.S. 2002. Physical Properties of Wool. In: Simpson, W.S. and Crawshaw, G.H. eds. *Wool: Science and Technology.* Woodhead Publishing pp.80- 129.

Henry, B.K., Russell, S.J., Ledgard, S.F., Gollnow, S., Wiedemann, S.G., Nebel, B., Maslen, D. and Swan, P. 2015. LCA of Wool Textiles and Clothing. In: Muthu, S.S. ed. *Handbook of Life Cycle Assessment (LCA) of Textiles and Clothing.* Elsevier, pp.217-254.

Ho, W.S.W. and Sircar, K.K. 1992. *Membrane Handbook.* New York: Van Nostrand Reinhold.

Höcker, H. 2002. Fibre Morphology. In: Simpson, W.S. and Crawshaw, G.H. eds. *Wool: Science and Technology.* Woodhead Publishing pp.60- 79.

Hoenig, S.L. 2007. *Compendium of chemical warfare agents.* New York, USA: Springer Science.

Hüsing, N. and Schubert, U. 2000. Aerogels. *Ullmann's Encyclopedia of Industrial Chemistry.* Wiley-VCH Verlag GmbH & Co. KGaA.

Idris, A., Vijayaraghavan, R., Rana, U.A., Fredericks, D., Patti, A.F. and MacFarlane, D.R. 2013. Dissolution of feather keratin in ionic liquids. *Green Chemistry.* **2**(15), pp.525-534.

ISPO. 2016. *Sustainability: Some Sports Brands Already Have Close Ties to Nature.* [Online]. [Accessed 24th January]. Available from: http://www.ispo.com/en/trends/id_79418458/sustainability-sports-brands-need-close-ties-to-nature.html

Ito, H., Sakabe, H., Miyamoto, T. and Inagaki, H. 1984. Fibrillation of the Cortex of Merino Wool Fibers by Freezing-Thawing Treatment. *Textile Research Journal.* **54**(6), pp.397-402.

IUPAC. 1997. *Compendium of Chemical Terminology.* Oxford: Blackwell Scientific Publications.

IWTO. 2013. *IWTO Wool Market Information 2013 Edition; Statistics for the Global Wool Production and Textile Industry.*

IWTO. 2017a. *History of Wool.* [Online]. [Accessed 24th January]. Available from: http://www.iwto.org/history-wool

IWTO. 2017b. *Wool Fact Sheets.* [Online]. [Accessed 24th January]. Available from: http://www.iwto.org/resources/fact-sheets

IYNF. 2009. *Natural Fibres.* [Online]. [Accessed 19/12/2016]. Available from: http://www.naturalfibres2009.org/en/index.html

J Rosseinsky, M., Smith, M. and Timperley, C. 2015. *Metal–organic frameworks: Breaking bad chemicals down.*

JEOL. 2009. *Scanning Electron Microscope A to Z.*

Johnson, P.J., Setsuda, D.J. and Williams, R.S. 1999. Activated Carbon for Automotive Applications. In: Burchell, T.D. ed. *Carbon Materials for Advanced Technologies.* Elsevier.

JSLIST Military Specification, M.-D.-. 2002. Joint Service Lightweight Integrated Suit Technology (JSLIST) Coat and Trouser, Chemical Protective.

Karasik, T. 2002. *Toxic Warfare; RAND.* Santa Monica, CA.

Kazuo, F. 2008. Nanofabrication by advanced electron microscopy using intense and focused beam. *Science and Technology of Advanced Materials.* **9**(1), p014110.

Kendall, R.J., Presley, S.M., Austin, G.P. and Smith, P.N. 2008. *Advances in Biological and Chemical Terrorism Countermeasures.* Boca Raton: CRC Press.

Kim, C., Lee, J. and Kim, B. 2008. Synthesis and pore analysis of serogel-glass fiber composites by ambient drying method. *Colloids and Surfaces A: Physicochemical and Engineering Aspects.* **313-314**, pp.179-182.

Kim, K.C., Yu, D. and Snurr, R.Q. 2013. Computational Screening of Functional Groups for Ammonia Capture in Metal–Organic Frameworks. *Langmuir.* **5**(29), pp.1446-1456.

Klobes, P., Meyer, K. and Munro, R.G. 2006. Porosity and Specific Surface Area Measurements for Solid Materials. *National Institute of Standards and Technology (US).*

Koros, W. and Fleming, G. 1993. *Journal of Membrane Science.* **83**(1).

Kozlowski, R.M. 2012. *Handbook of Natural Fibres, Volume 2 - Processing and Applications*. Woodhead Publishing. Available from: http://app.knovel.com/hotlink/toc/id:kpHNFVPA04/handbook-natural-fibres

Kreno, L.E., Leong, K., Farha, O.K., Allendorf, M., Van Duyne, R.P. and Hupp, J.T. 2011. Metal-organic framework materials as chemical sensors. *Chem. Rev.* **2**(112), pp.1105-1125.

Kuhl., G. 1999. Fundamentals and Applications. In: Weitkamp, L. and Puppe, L. eds. *Catalysis and Zeolites.* New York: Spinger-Verlag, pp.81-197.

Kynol Europa GmbH Prospectus. 2014. [Leaflet].

Lamprou, D., Smith, J., Nevell, T., Barbu, E., Stone, C., Willis, C., Ewen, R. and Tsibouklis, J. 2010. *Self-assembled alkanethiol structures on gold: A further insight into the origins of structural rearrangement phenomena.*

Lee, J., Farha, O.K., Roberts, J., Scheidt, K.A., Nguyen, S.T. and Hupp, J.T. 2009. Metal-organic framework materials as catalysts. *Chem. Soc. Rev.* **5**(38), pp.1450-1459.

Li, J.R., Kuppler, R.J. and Zhou, H.C. 2009. Selective gas adsorption and separation in metal-organic frameworks. *Chem Soc Rev.* **5**(38), pp.1477-1504.

Li, J.R., Sculley, J. and Zhou, H.C. 2012. Metal-organic frameworks for separations. *Chem Rev.* **2**(112), pp.869-932.

Li, J.Y. 2001. *Chemical and Mechanical Treatment of Wool Fabric.* PhD thesis, University of Leeds.

Li, R. and Wang, D. 2013. Preparation of regenerated wool keratin films from wool keratin-ionic liquid solutions. *J. Appl. Polym. Sci.* **4**(127), pp.2648-2653.

Lippens, P. 2007. Low-pressure cold plasma processing technology. In: Shishoo, R. ed. *Plasma technologies for textiles.* Cambridge: Woodhead Publishing Limited, pp.64-78.

Liu, J., Thallapally, P.K., McGrail, B.P., Brown, D.R. and Liu, J. 2012. Progress in adsorption-based CO2 capture by metal-organic frameworks. *Chem. Soc. Rev.* **6**(41), pp.2308-2322.

López-Muñoz, F., Alamo, C., Guerra, J.A. and García-García, P. 2008. The development of neurotoxic agents as chemical weapons during the National Socialist period in Germany. *Rev Neurol.* **47**, pp.99-106.

Lordgooei, M., Carmichael, K.R., Kelly, T.W., Rood, M.J. and Larson, S.M. 1996. Activated carbon cloth adsorption-cryogenic system to recover toxic volatile organic compounds. *Gas Separation & Purification.* **10**(2), pp.123-130.

Maffei, A.V., Budd, P.M. and McKeown, N.B. 2006. Adsorption studies of a microporous phthalocyanine network polymer. *Langmuir.* **22**, pp.4225-4229.

Mao, N. 2013. *The Development Absorbent Keratin Materials having Thermo-Physiological Comfort Properties for Chemical Protective Clothing.* Centre for Technical Textiles: University of Leeds.

Mao, N. and Russell, S.J. 2007. The thermal insulation properties of spacer fabricswith a mechanically integrated wool fibre surface. *Textile Research Journal.* **77**(12), pp.914-922.

Mather, R.R. and Wardman, R.H. 2011. Protein Fibres. *Chemistry of Textile Fibres.* Royal Society of Chemistry.

McKeown, N.B., Budd, P.M., Msayib, K.J., Ghanem, B.S., Kingston, H., Tattershall, C.E., Makhseed, S., Reynolds, K.J. and Fritsch, D. 2005. Polymers of Intrinsic Microporosity (PIMs): Bridging the void between microporous and polymeric materials. *Chem. Eur. J.* **11**, pp.2610-2620.

McKeown, N.B., Ghanem, B., Msayib, K.J., Budd, P.M., Tattershall, C.E., Mahmood, K., Tan , S., Book, D., Langmi, H.W. and Walton, A. 2006. Towards polymer-based hydrogen storage materials: engineering ultramicroporous cavities within polymers of intrinsic microporosity. *Angew. Chem. Int. Ed.* **45**, pp.1804-1807.

Mcphee, J.R. and Shaw, T. 1984. The Chemical Technology of Wool Processing. *Rev. Prog. Color.* **14**, pp.58-68.

McPherson, M., Morris, R., Smith, M., A. Stone, C., McCormick, L. and Peterson, G. 2015. *Enhanced Ammonia Uptake and Stability in Humid Conditions in Metal-Organic Frameworks.*

Mehta, P.N. 1980. Engineered Wool Industrial Protective Clothing'. *Textile Research Journal.* **50**(3), pp.185-193.

Meng, Q., Doetschman, D.C., Rizos, A.K., Lee, M.-H., Schulte, J.T., Spyros, A. and Kanyi, C.W. 2011. Adsorption of Organophosphates into Microporous and Mesoporous NaX Zeolites and Subsequent Chemistry. *Environmental Science & Technology.* **45**(7), pp.3000-3005.

Metha, P.N. 1980. Engineered Wool Industrial Protective Clothing. *Textile Research Journal.* **50**(3), pp.185-193.

Meyer, K., Klobes, P. and Röhl-Kuhn, B. 1997. Certification of Reference Material with Special Emphasis on Porous Solids. *Crystal Research and Technol. .* **32**

pp.173-183.

Micromeritics. 2014a. [Online]. Available from: http://www.micromeritics.com/repository/files/gas_adsorption_theory_poster.pdf

Micromeritics. 2014b. *Mercury Intrusion Porosimetry Theory*. Micromeritics Instrument Corporation.

Misaelides, P., Macasek, F., Pinnavaia, T.J. and Coletta, C. 1999. Natural Microporous Materials in Environmental Technology. Dordrecht: Kluwer Academic.

Mitscherich, E. 1843. Cited in Gregg SJ, Sing KSW: 2nd ed.; Academic Press, London. *Pogg. Ann.* **59**(Adsorption, surface area and porosity), p94.

Moncrieff, R.W. 1953. *Wool Shrinkage and its Prevention*. London: National Trade Press Ltd.

O'Connell, R.A. and Waldne, M.K. 1957. Influence of ionizing radiations on wool fibre properties. *Textile Research J.* **27**, pp.516-518.

OPCW. 1993. *Convention on The Prohibition of the Development, Production, Stockpiling and use of Chemical Weapons and on their Destruction.*

OPCW. 2014. *Types of chemical agent.* [Online]. [Accessed 04/08/2014]. Available from: http://www.opcw.org/about-chemical-weapons/types-of-chemical-agent/

Payra, P. and Dutta, P.K. 2003. Zeolites: Primer. In: Auerbach, S.M., et al. eds. *Handbook of zeolie science and technology.* New York: Marcel Dekker.

Perincek, S., Bahtiyari, M.I., Körlü, A.E. and Duran, K. 2008. Ozone treatment of Angora rabbit fiber. *Journal of Cleaner Production.* **16**(17), pp.1900-1906.

Perincek, S., Bahtiyari, M.İ., Körlü, A.E. and Duran, K. 2011. Effect of ozone and ultrasound on the fiber properties of angora rabbit. *Journal of Applied Polymer Science.* **120**(6), pp.3119-3125.

Perincek, S.D., Duran, K., Korlu, A.E. and Bahtiyari, İ.M. 2007. An Investigation in the Use of Ozone Gas in the Bleaching of Cotton Fabrics. *Ozone: Science & Engineering.* **29**(5), pp.325-333.

Peterson, G., DeCoste, J., Willis, C., Smith, M. and Stone, C. 2012. *258927 Enhanced Stability of Metal-Organic Frameworks Via Plasma-Enhanced Chemical Vapor Deposition.*

Peterson, G.W., Wagner, G., Balboa, A., Mahle, J., Sewell, T. and Karwacki, C.J. 2009. Ammonia Vapor Removal by Cu(3)(BTC)(2) and Its Characterization by MAS NMR. *J Phys Chem C Nanomater Interfaces. .* **31**(113), pp.13906-13917.

Platzman, R. and Franck, J. 1958. A physical mechanism for the inactivation of proteins by ionizing radiations. *Symposium of Information Theory Biol.*, pp.262-275.

Plowman, J.E., Flanagan, L.M., Paton, L.N., Fitzgerald, A.C., Joyce, N.I. and Bryson, W.G. 2003. The effect of oxidation or alkylation on the separation of wool keratin proteins by two-dimensional gel electrophoresis. *Proteomics.* **6**(3), pp.942-950.

Poole, A.J., Church, J.S. and Heudson, M.G. 2009. Environmentally sustainable fibres from regenerated protein. *Biomacromolecules.* **10**(1), pp.1-8.

Postle, R., Carnaby, G.A. and Jong, S.d. 1988. The Wool Fibre. *The Mechanics of Wool Structures.* Chichester: Ellis Horwood Limited.

Prabaharan, M. and Rao, J.V. 2001. Study on ozone bleaching of cotton fabric – process optimisation, dyeing and finishing properties. *Coloration Technology.* **117**(2), pp.98-103.

Ramaseshan, R. and Ramakrishna, S. 2007. Zinc Titanate Nanofibers for the Detoxification of Chemical Warfare Simulants. *Journal of the American Ceramic Society.* **90**(6), pp.1836-1842.

Ramkumar, S.S., Sata, U. and Hussain, M. 2008. Personnel Protective Fabric Technologies for Chemical Countermeasures. In: Kendall, R.J., et al. eds. *Advances in Biological and Chemical Terrorism Countermeasures.* CRC Press.

Rao, A.V., Bhagat, S.D., Hirashima, H. and Pajonk, G.M. 2006. Synthesis of flexible silica aerogels using methyltrimethoxysilane

(MTMS) precursor. *Journal of Colloid and Interface Science.* **300**, pp.279-285.

Raza, S.K. and Jaiswal, D.K. 1994. Mechanism of cyanide toxicity and efficacy of its antidotes. *Def Sci J.* **44**, p331.

Reimer, L. 1998. *Scanning electron microscopy : physics of image formation and microanalysis.* Springer.

Renes, S. 1985. An Evaluation of SInk Terms in Removing NO2 and SO2 from Indoor Air. *Proceedings of Clima.*

Rennie, R. 2016. *Oxford Dictionary of Chemistry.* [Online]. Available from:
//www.oxfordreference.com/10.1093/acref/9780198722823.001.0001/acref-9780198722823-e-9

Rippon, J.A. 2013. The Structure of Wool. In: Lewis, D.M. and Rippon, J.A. eds. *The Coloration of Wool and Other Keratin Fibres.* Wiley.

Rocha, J., Carlos, L.D., Paz, F.A.A. and Ananias, D. 2011. Luminescent multifunctional lanthanides-based metal–organic frameworks. *Chem. Soc. Rev.* **40**, pp.926-940.

Rosi, N.L., Kim, J., Eddaoudi, M., Chen, B., O'Keeffe, M. and Yaghi, O.M. 2005. Rod Packings and Metal−Organic Frameworks Constructed from Rod-Shaped Secondary Building Units. *J. Am. Chem. Soc.* **5**(127), pp.1504-1518.

Roswell, J. and Yaghi, O.M. 2006. Effects of functionalization, catenation, and variation of the metal oxide and organic linking units on the low-pressure hydrogen adsorption properties of metal-organic frameworks. *J. Am. Chem. Soc. Rev.* **128**, pp.1304-1315.

Ruthven, D.M. 1984. *Principles of Adsorption and Adsorption Processes.* Wiley.

Sambur, J.B., Doetschman, D.C., Yang, S.-W., Schulte, J.T., Jones, B.R. and DeCoste, J.B. 2008. Multiple effects of the presence of water on the nucleophilic substitution reactions of NaX Faujasite zeolite with dimethyl methylphosphonate (DMMP). *Microporous and Mesoporous Materials.* **112**(1-3), pp.116-124.

Schrooven, P.M.M., Dijkstra, P. and Feijen, J. 1998. Biodegradable films from selectively modified feather keratin dispersions. *Polymer Reprints.* **2**(39), p160.

Shakarjian, M.P., Heck , D.E., Gray, J.P., Sinko, P.J., Gordon, M.K., Casillas, R.P., Heindel, N.D., Gerecke, D.R., Laskin, D.L. and Laskin, J.D. 2010. Mechanisms mediating the vesicant actions of sulfur mustard after cutaneous exposure. *Toxicol Sci.* **1**(114), pp.5-19.

Shishoo, R. 2007. Introduction - The potential of plasma technology in the textile industry. In: Shishoo, R. ed. *Plasma technologies for textiles.* Cambridge: Woodhead Publishing Limited, pp.xv-xxx.

SING, K.S.W., EVERETT, D.H., HAUL, R.A.W., MOSCOU, L., PIEROTTI, R.A., ROUQUÉROL, J. and SIEMIENIEWSKA, T. 1985. IUPAC Recommendations 1984. Reporting Physisorption Data for Gas Solid Systems with Special Reference to the Determination of Surface Area and Porosity. *Pure & Appl. Chem. Biol.* **57**, pp.603-319.

Slauson, S.D., Miller, B. and Rebenfeld, L. 1984. Physicochemical Properties of Sized Yams Part I: Initial Studies. *Textile Research Journal.* **54**, pp.655-664.

Somani, S.M. 1992. *Chemical Warfare Agents.* USA: Academic Press Inc.

Sou, B.Y., McMillan, R.C. and Causer, S.M. 2001. *Absorption of Formaldehyde by Carpets.* Christchurch: Wool Research Organisation of New Zealand.

Spafford, R.B. 1996. *The Development of a Reactive Sorbent for Immediate Decontamination.* U.S. Army ERDEC: Aberdeen Proving Ground.

Spicer, C.W., Coutant, R.W., Ward, G.F., Joseph, D.W., Gaynor, A.J. and Billick, I.H. 1989. Rates and Mechanisms of NO2 Removal from Indoor Air by Residential Materials. *Environment International.* **15**(1-6), pp.643-654.

Stachewicz, U., A Stone, C., Willis, C. and Barber, A. 2012. *Charge assisted tailoring of chemical functionality at electrospun nanofiber surfaces.*

Stoeckli, F. 1974. The Gas-Solid Interface Calculations of Adsorption Potentials in Slot-Like Pores of Molecular Dimensions. *HCA.* **57**, pp.2195-2199.

Stoves, J.L. 1949. Symposium of Fibrous Proteins. *Bradford: Society of Dyers and Colourists.* p58.

Suh, M.P., Park, H.J., Prasad, T.K. and Lim, D.W. 2011. Hydrogen storage in metal-organic frameworks. *Chem. Rev.* **2**(112), pp.782-835.

Sumida, K., Rogow, D.L., Mason, J.A., McDonald, T.M., Bloch, E.D., Herm, Z.R., Bae, T.-H. and Long, J.R. 2012. Carbon dioxide capture in metal-organic frameworks. *Chem. Rev.* **2**(112), pp.724-781.

Sun, P., Liu, Z.-T. and Liu, Z.-W. 2009. Particles from bird feather: A novel application of an ionic liquid and waste resource. *J. Hazard. Mater.* **2-3**(170), pp.786-790.

Szinicz, L. 2005. History of chemical and biological warfare agents. *Toxicology.* **214**(3), pp.167-181.

Szostak, R. 1992. *Handbook Of Molecular Sieves.* Springer Science & Business Media.

T Wilcox, O., Fateeva, A., Katsoulidis, A., Smith, M., A Stone, C. and J Rosseinsky, M. 2015. *Acid loaded porphyrin-based metal-organic framework for ammonia uptake.*

Talbot, T.B., Lukey, B. and Platoff, G.E. 2008. *Medical Aspects of Chemical Warfare.* Washington, DC.

Thorsen, W.J. 1965. New Aspects on the Ozonization of Wool. *Textile Research Journal.* **35**(7), pp.638-647.

Truong, Q. and Rivin, D. 1996. *Testing and Evaluation of Waterproof/Breathable Materials for Military Clothing Applications.* US Army Natick RD&E Center, Natick: NATICK/TR-96/023L.

Truong, Q. and Wilusz, E. 2005. Chemical and biological protection. In: Scott, R.A. ed. *Textiles for Protection.* Woodhead Publishing.

Truong, Q. and Wilusz, E. 2006. Materials technologies for next generation chemical and biological protective clothing. In: *Internationa Nonwovens Technical Conference, Housten.*

Tsarkov, S., Khotimskiy, V., Budd, P.M., Volkov, V., Kukushkina, J. and Volkov, A. 2012. Solvent nanofiltration through high permeability glassy polymers: Effect of polymer and solute nature. *Journal of Membrane Science.* **423-424**, pp.65-72.

Tschernich, R.W. 1992. *Zeolites of the World.* [Press release]. Available

Tsoi, W.Y.I., Kan, C.W., Yuen, C.W.M. and Tang, T.B. 2010. Achieving nanoscale surface structure on polyester film by atmospheric pressure plasma treatment *AMER CHEMICAL SOC.* **240**.

Wagner, G.W. and Bartram, P.W. 1999. Reactions of VX, HD, and Their Simulants with NaY and AgY Zeolites. Desulfurization of VX on AgY. *Langmuir.* **15**(23), pp.8113-8118.

Walsh, M., Black, A. and Morgan, A. 1977. Sorption of SO2 by Typical Indoor Surfaces Including Wool Carpets, Wallpaper and Paint. *Atmospheric Environment.* **1**(1), pp.1107-1111.

Wan, A. and Yu, W. 2011. Effect of wool fiber modified by ecologically acceptable ozone-assisted treatment on the pilling of knit fabrics. *Textile Research Journal.* **82**(1), pp.27-36.

Wang, G., Dou, B., Zhang, Z., Wang, J., Liu, H. and Hao, Z. 2015. Adsorption of benzene, cyclohexane and hexane on ordered mesoporous carbon. *Journal of Environmental Sciences.* **30**, pp.65-73.

Ward, R.R. and Mao, N. 2014. *Year 1 Interim Report: Development of Keratin Adsorbent Material for Chemical Protective Clothing.* University of Leeds.

Ward, R.R. and Mao, N. 2015. *Year 2 Interim Report: Development of Keratin Adsorbent Material for Chemical Protective Clothing.* University of Leeds.

Ward, R.R. and Mao, N. 2016. *Year 3 Interim Report: Development of Keratin Adsorbent Material for Chemical Protective Clothing.* University of Leeds.

Watanabe, T., Manz, T.A. and Sholl, D.S. 2011. Accurate Treatment of Electrostatics during Molecular Adsorption in Nanoporous

Crystals without Assigning Point Charges to Framework Atoms. *J. Phys. Chem. C.* **11**(115), pp.4824-4836.

Weikart, C.M. and Yasuda, H.K. 2000. Modification, degradation, and stability of polymeric surfaces treated with reactive plasmas. *J. Polym. Sci. A Polym. Chem.* **38**, pp.3028-3042.

Weitkamp, J. 2000. Zeolites and catalysis. *Solid State Ionics.* **131**, pp.175-188.

Wilusz, E. 1996. In: Salamone, J.C. ed. *Polymeric Materials Encyclopedia.* Boca Raton: CRC Press.

Wilusz, E. 2007. Breaking with tradition. *CBRNe World Spring 2007.*

Wilusz, E. 2008. *Military Textiles.* Cambridge: Woodhead Publishing in Textiles.

Wortmann, F.J. 2009. The structure and properties of wool and hair fibres. In: Eichhorn, S.J., et al. eds. *Handbook of Textile Fibre Structure, Volume 2 - Natural, Regenerated, Inorganic and Specialist Fibres.* Woodhead Publishing, pp.108- 145.

Wu, H., Gong, Q., Olson, D.H. and Li, J. 2012. Commensurate adsorption of hydrocarbons and alcohols in microporous metal organic frameworks. *Chem. Rev. .* **2**(112), pp.836-868.

Xie, H., Li, S. and Zhang, S. 2005. Ionic liquids as novel solvents for the dissolution and blending of wool keratin fibers. *Green Chemistry.* **7**, pp.606-608.

Yamauchi, K., Yamauchi, A., Kusunoki, T., Kohda, A. and Konishi, Y. 1996. Preparation of stable aqueous solution of keratins, and physiochemical and biodegradational properties of films. *J. Biomed. Mater. Res. A.* **4**(31), pp.439-444.

Yang, Q., Liu, D., Zhong, C. and Li, J. 2013. Development of computational methodologies for metal-organic frameworks and their application in gas separations. *Chem Rev.* **10**(113), pp.8261-8323.

Yang, S.-W., Doetschman, D.C., Schulte, J.T., Sambur, J.B., Kanyi, C.W., Fox, J.D., Kowenje, C.O., Jones, B.R. and Sherma, N.D. 2006. Sodium X-type faujasite zeolite decomposition of dimethyl methylphosphonate (DMMP) to methylphosphonate: Nucleophilic

zeolite reactions I. *Microporous and Mesoporous Materials.* **92**(1-3), pp.56-60.

Yildiz, O., Stano, K., Faraji, S., A Stone, C., Willis, C., Zhang, X., S Jur, J. and Bradford, P. 2015. *High Performance Carbon Nanotube – Polymer Nanofiber Hybrid Fabrics.*

Yoon, M., Srirambalaji, R. and Kim, K. 2011. Homochiral Metal–Organic Frameworks for Asymmetric Heterogeneous Catalysis. *Chem. Rev.* **2**(112), pp.1196–1231.

Yu, D., Ghosh, P. and Snurr, R.Q. 2012. Hierarchical modeling of ammonia adsorption in functionalized metal–organic frameworks. *Dalton Trans.* **41**, pp.3962-3973

Yuan, B. 2012. Heat insulation properties of silica aerogel/glass fibre composites fabricated by press forming. *Material Letters.* **75**, pp.204-206.

Zahn, H., Fritze, E.R., Pfannmuller, H. and Satlow, G. 1959. The effect of high-energy radiation on wool keratin and polyamide and polyester fibres. *Proc. 2nd Intern. Conf. Peaceful Uses Atomic Energy.* **29**, pp.233-237.

Zhang, J., Jin, J., Cooney, R.P. and Zhang, S. 2015. Synthesis of polymers of intrinsic microporosity using an AB-type monomer. *Polymer.* **57**, pp.45-50.

Zhou, H.C., Long, J.R. and Yaghi, O.M. 2012. Introduction to metal-organic frameworks. *Chem Rev.* **2**(112), pp.673-674.

Appendix

Consistence of mercury porosimetry in characterising resultant porous fibres in wool fabrics

In this project, the consistency of mercury porosimetry in characterising resultant porous fibres was investigated. The effect of several chemical treatments and their combinations on the microstructure of wool fibres will be studied. These techniques include cuticle removal process by using formic acid treatment, swelling/oxidising treatment by using both urea hydrogen peroxide and ozone-UHP treatment. The worsted woven merino wool fabrics were cut into strips with 50 mm by 5 mm dimensions (for the purpose of filling the mercury penetrometer sealed sample cup) and then conditioned in a vacuum oven overnight (circa. 16 h) at 105 °C to remove any atmospheric contaminants, such as water vapour and adsorbed gas.

Previous work determined that mercury porosimetry is capable of measuring accessible pores ranging from 3 nm to 400 μm within keratin wool fibres. In this study, trials were conducted to investigate the accuracy, repeatability and consistency of the developed porosity measurement procedure. Worsted woven merino wool fabrics with and without consecutive chemical treatments (MWov, MWov_F2 and MWov_F2_UHP96), as well as, knitted Nylon 66 (PA66) filaments (PA66 knitted) and woven polyethylene terephthalate (PET) filaments (PET woven) were used for this testing procedure. The mean total pore volumes for pores between 3nm-2μm, 3nm-50nm and 50nm-2μm for each of the fibre types are detailed in Figure 0.1. The mean and standard deviation data was collected from 3 repeat samples for each fibre type.

All fibres demonstrate the presence of mesopores, this was not the case for the study conducted in year 2 on single fibres cut into staple fibres (Ward and Mao, 2015). This could be due to the fact that the current study analyses fabrics; therefore, it is possible

a proportion of the mesopores recorded could be fibre intersects within the fabric structure. Generally, there is evidence to suggest that the material and/or fabric structures have a greater proportion of mesopores than micropores in terms of total volumes, though this trend is not consistent for the worsted woven merino wool fabrics pre-treated with FA for 2 h (Ward and Mao, 2015) . Section 0, indicated that a 2h FA pre-treatment was capable of exposing the cortex within the wool fibres; however, the cleavage of the cuticles was not consistent despite the majority of the cuticles being removed (Ward and Mao, 2015). This could explain why there was a discrepancy between the pore volumes within the 3nm-50nm range for the worsted woven merino wool fabrics pre-treated with FA and the rest of the fabrics. This inconsistency is also represented by the standard deviation errors bars, which demonstrated that the total pore volumes recorded (3nm-50nm range) for worsted woven merino wool fabrics pre-treated with FA are significantly dispersed from the mean value.
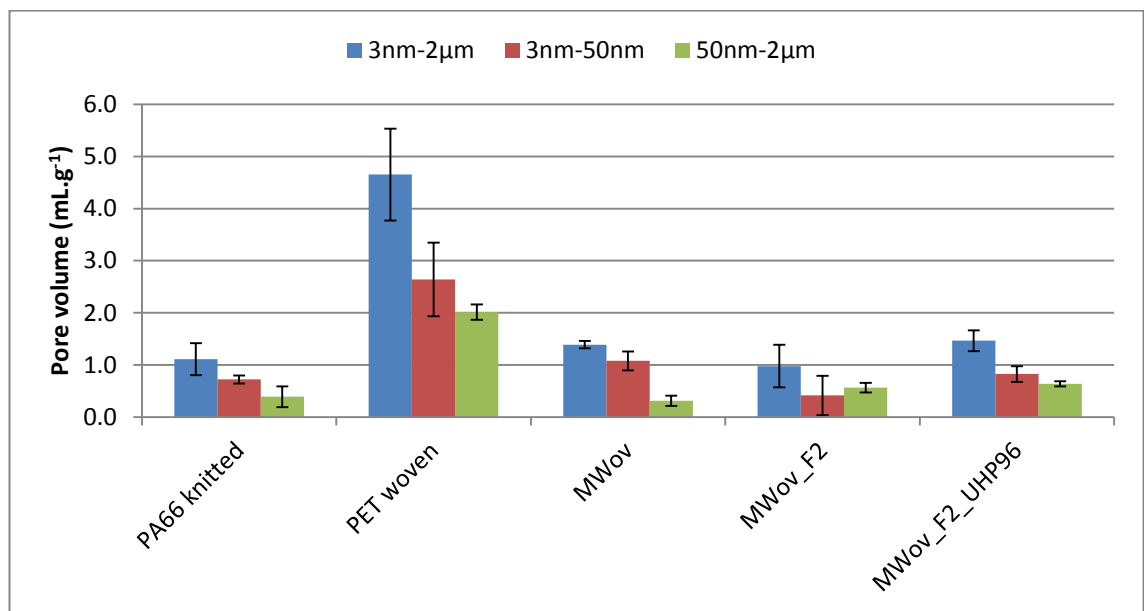
Figure 0.1 - Total pore volume of fibres using mercury porosimetry

Interestingly, the FA pre-treated wool fibres treated with UHP for 96 h demonstrated a greater consistency of pore volumes between the repeated samples than the FA pre-treated wool fibres. By observing the SEM images of both the FA pre-treated wool fibres and the FA pre-treated wool fibres treated with UHP for 96 h, it is evident that

there are far fewer cuticles intact. This could explain the greater consistency of pore volumes amongst the repeated FA pre-treated wool fibres treated with UHP for 96 h. Therefore, it is possible the mercury porosimetry characterisation technique is more affective at quantifying and differentiating between pore formations for fabrics chemical modified post FA treatment, as there are fewer cuticles intact.

The mercury porosimetry data of the PA66 knitted and PET woven fabrics were measured to investigate whether the pore volume data was comparable with trends observed after measuring the raw and chemically modified wool fibres. The PA66 knitted (see Figure 0.2 and Figure 0.3) and PET woven fabrics (see Figure 0.4 and Figure 0.5) demonstrate similar trends to the raw wool fibres; however, the total pore volumes for both macro and mesopores appear greater for the PET woven fabric (see Figure 0.1). This could be caused by the unique porous structure of this material and/or the construction of the fabric. However, the characteristics associated with this increase in total pore volume were not investigated as the aim was determine whether the trends observed after mercury porosimetry for different fibre types were comparable. Also, the variations between total pore volumes of the tested fabrics are relatively low.
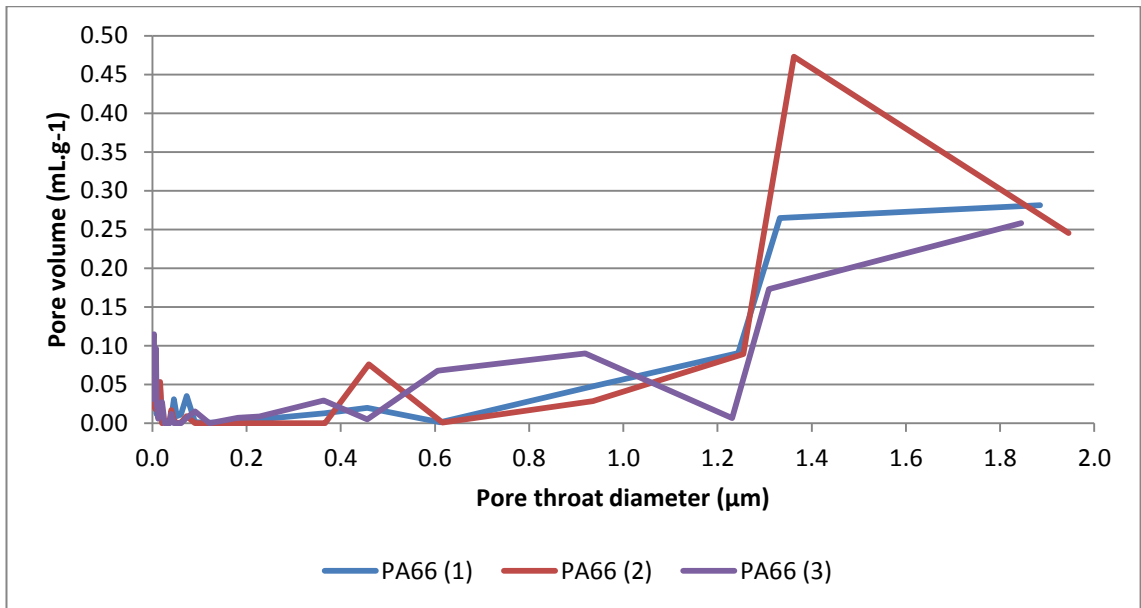
Figure 0.2 - Pore volume distribution of knitted Nylon 66 (PA66) filaments, maximum pore throat diameter 2 μm
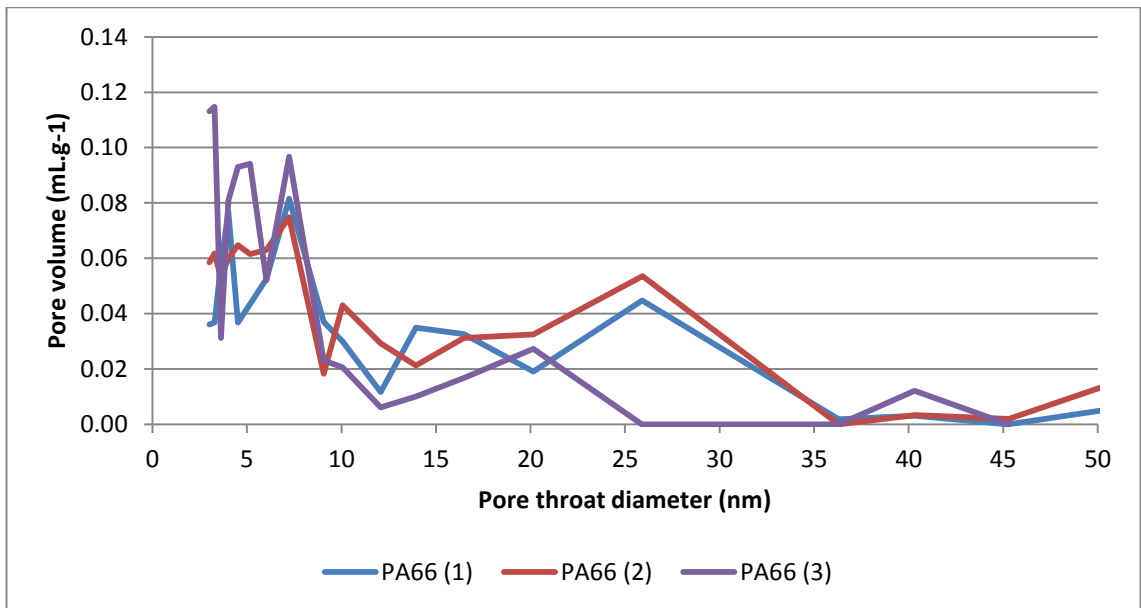
Figure 0.3 - Pore volume distribution of knitted Nylon 66 (PA66) filaments, maximum pore throat diameter 50 nm
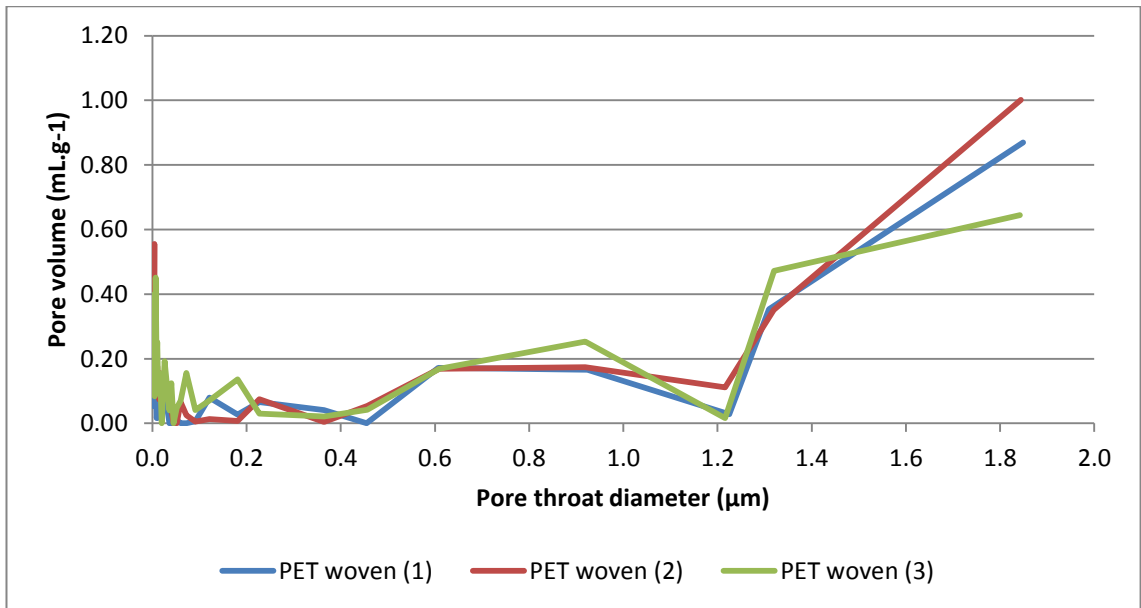
Figure 0.4 - Pore volume distribution of woven polyethylene terephthalate (PET) filaments, maximum pore throat diameter 2 µm
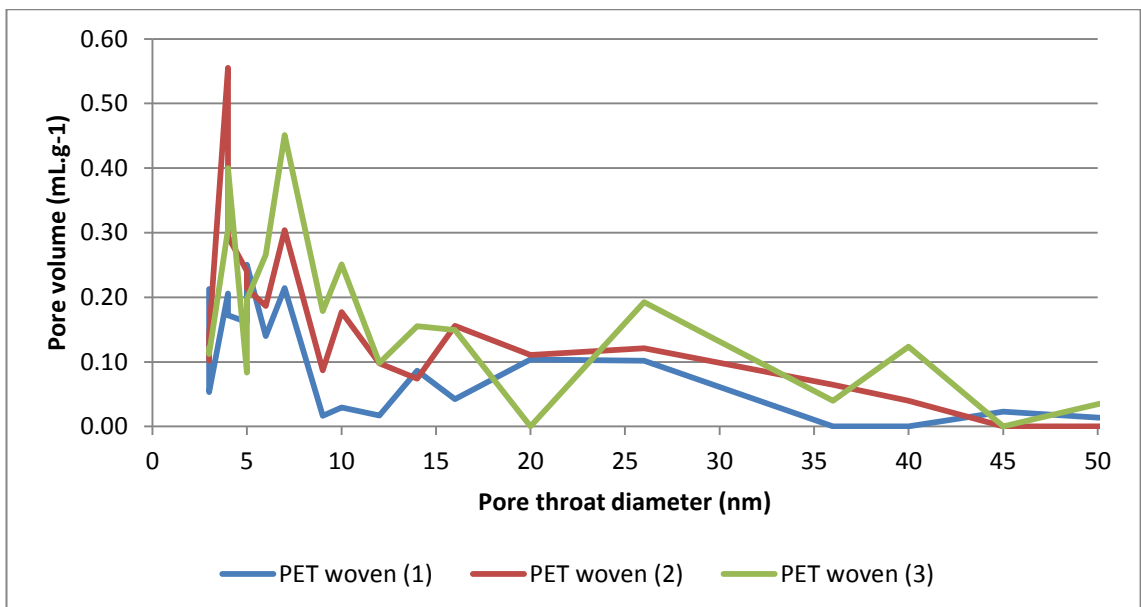
Figure 0.5 - Pore volume distribution of woven polyethylene terephthalate (PET) filaments, maximum pore throat diameter 50 nm

Similar to the total pore volume analysis (Figure 0.1), the pore volume distributions demonstrate that the repeat samples for each fabric type exhibit similar trends for both macro and mesopores. The only inconsistent results were the meso-pore volume distributions for the repeated FA pre-treated worsted woven merino wool fibres (see

269

Figure 0.11 and Figure 0.12). Again, this could be caused by the inconsistent amount cuticles present on the wool fibres.

Therefore, the mercury porosimetry technique is capable of analysing the following characteristics of fibres:

- Pore volume distributions in terms of superficial pore throat diameters for accessible pores and fibre intersects.

- Total pore volume for accessible pores and fibre intersects.

- Proportion of meso-pore to macropores for a single fibre/ fabric type.

- Trend analysis of the proportion of meso-pore to macropores for different fibre/ fabric types.

However, the analytical procedure has some limitations when measuring the porous structure of wool fibres, which are detailed below:

- Not suitable for characterising all porous materials (Giesche, 2006).

- Process measures both accessible pores and fibre intersects, but is not capable of differentiating between the two where they co-exist. This could be problematic for measurements for both wool fibres and fabrics as spaces between fibres could be misinterpreted as pores.

- Does not measure inaccessible pores; although it is likely the VOCs will only come into contact with accessible pores.

- Does not provide a full representation of the porosity of a material as the system only measures external pore throat diameter data. This could be problematic if a pore has a large cavity, but a small superficial pore throat or vice versa.

- Calculations assume the pore shapes are cylindrical, where in reality they can have complex internal features, with high surface areas. The system limitation is represented as a schematic within Figure 0.6.

Measures superficial pore throat diameter
Ø (µm or nm)

Mercury porosimetry assumes pores are cylindrical

Wool fibre
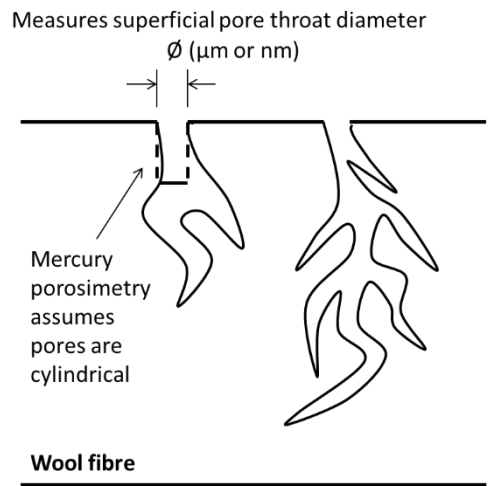
Figure 0.6 - Cylindrical pore measurement of mercury porosimetry and its limitation for measuring pore volumes

Consequently, additional measurement techniques, such as BET surface area, SEM and helium pycnometry should be applied to gain a greater understanding of material fibre morphology.
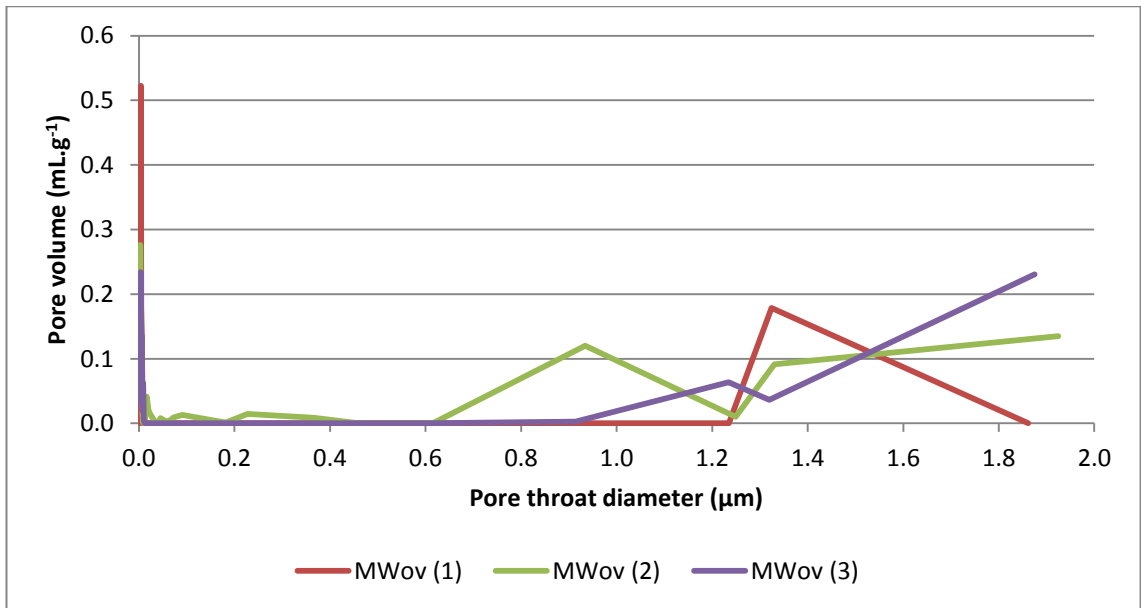
Figure 0.7 - Pore volume distribution of worsted woven merino wool fabrics without pre-treatment, maximum pore throat diameter 2 µm
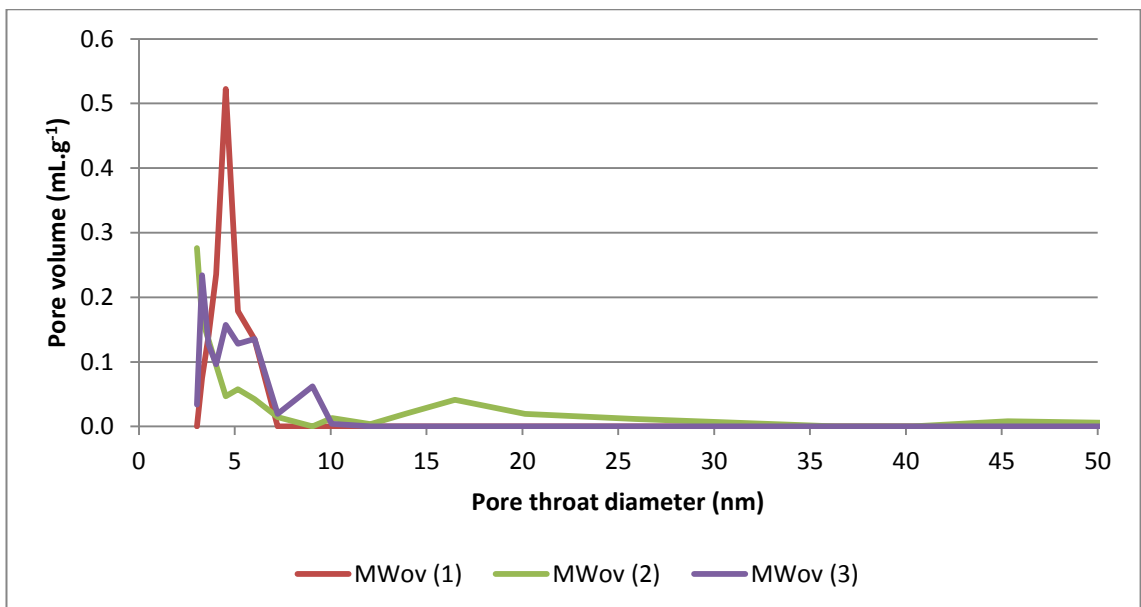
Figure 0.8 - Pore volume distribution of worsted woven merino wool fabrics without pre-treatment, maximum pore throat diameter 50 nm
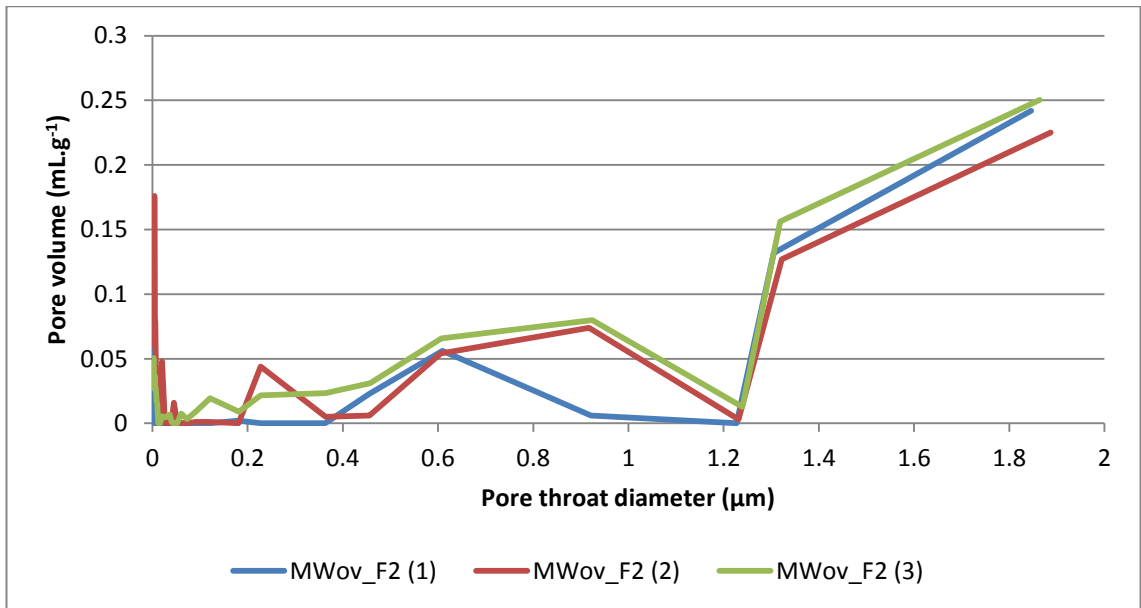
Figure 0.9 - Pore volume distribution of worsted woven merino wool fabrics with FA pre-treatment, maximum pore throat diameter 2 µm
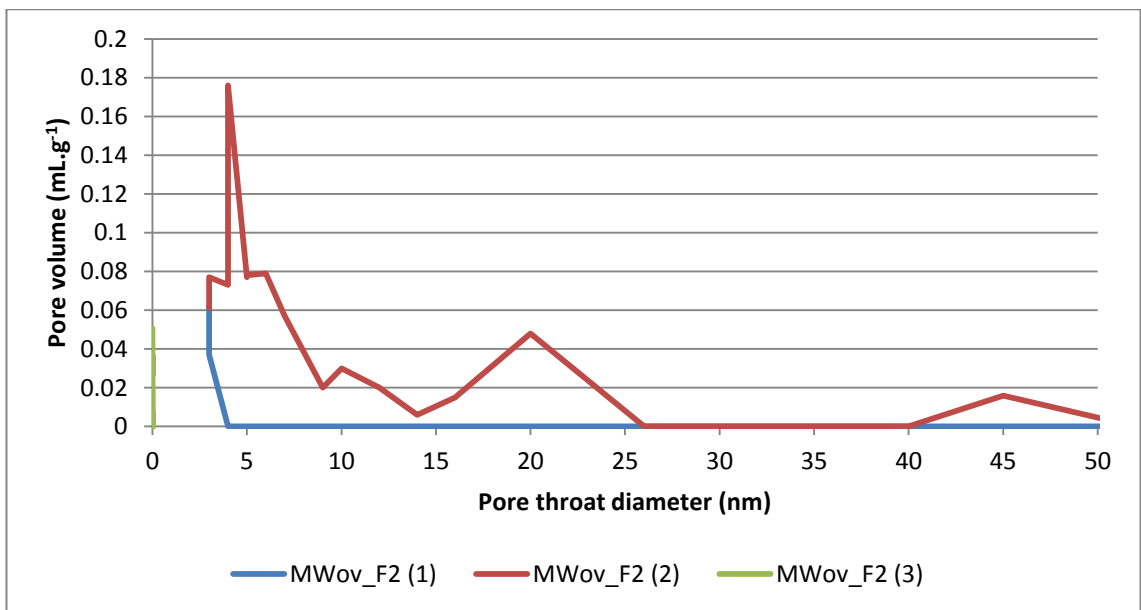
Figure 0.10 - Mercury porosimetry analysis (Pore volume distribution) of worsted woven merino wool fabrics with FA pre-treatment, maximum pore throat diameter 50 nm
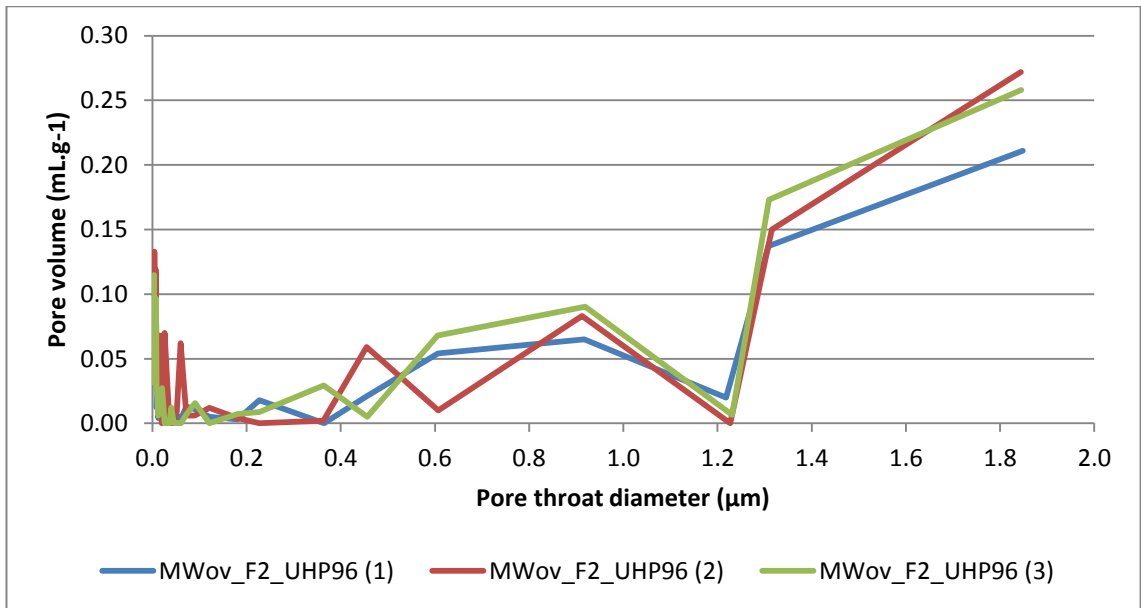
Figure 0.11 - Pore volume distribution of FA pre-treated worsted woven merino wool fabrics with Ozone-UHP, maximum pore throat diameter 2 μm
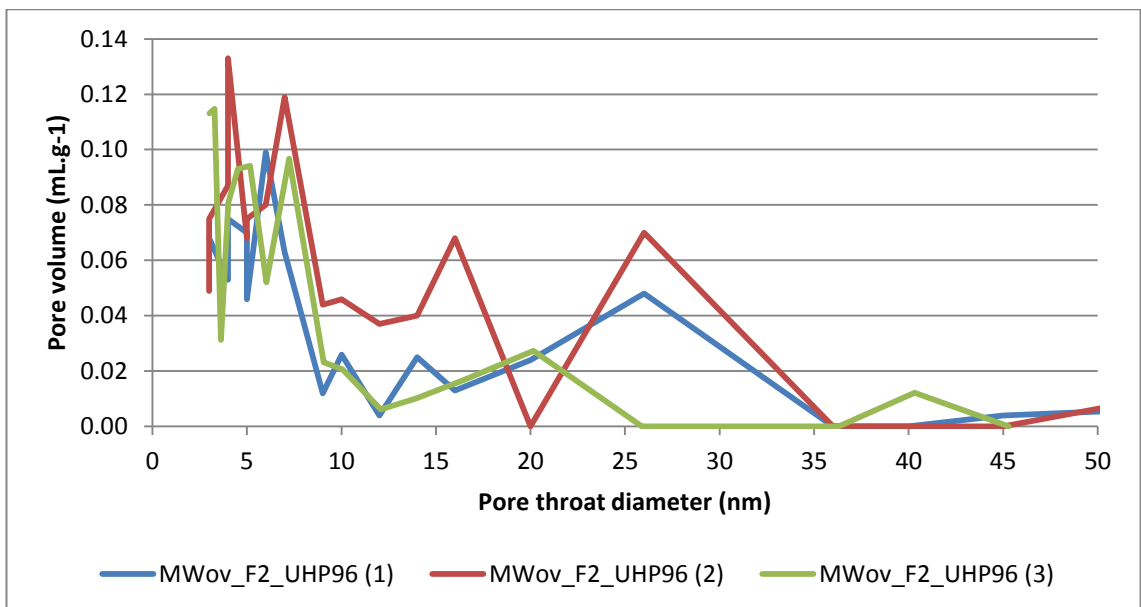
Figure 0.12 - Pore volume distribution of FA pre-treated worsted woven merino wool fabrics with Ozone-UHP, maximum pore throat diameter 50 nm

This research has provided a comprehensive understanding of the changes of microstructures of British wool fibres after various chemical and physical treatments associated with developing keratin adsorbent materials for CPC. The structural characteristics, including their cross-sectional microstructures, AD and surface areas of

274

scoured wool before and after chemical treatments were examined using SEM, Helium Pycnometry, porosimetry and BET.

Chemical treatments included formic acid treatment, ozone treatment in water and UHP solution and sodium hydroxide treatment. Although this study demonstrated that pore formation after individual and consecutive chemical treatments was possible. The porous morphology formed was insufficient for the CWA adsorption application. Also, in many cases pore formed within the wool fibres were not necessarily accessible. Therefore, additional treatments may be required in order to produce or expose internal pore formation and enhance the adsorption capacity of wool fibres.